QC
1
.P5812
v.56
no.11

THE PHYSICAL REVIEW

VOLUME 56 | Second Series | NUMBER 11

DECEMBER 1, 1939

Published for the

AMERICAN PHYSICAL SOCIETY

by the

AMERICAN INSTITUTE OF PHYSICS

Incorporated

LANCASTER, PA., AND NEW YORK, N. Y.

UNIVERSITY OF MICHIGAN LIBRARIES

THE PHYSICAL REVIEW

A journal of experimental and theoretical physics established by E. L. Nichols in 1893

Published by the American Institute of Physics for the

American Physical Society

OFFICERS

President

JOHN T. TATE
University of Minnesota
Minneapolis, Minnesota

Vice President

JOHN ZELENY
Yale University
New Haven, Connecticut

Secretary

W. L. SEVERINGHAUS
Columbia University
New York, New York

Treasurer

G. B. PEGRAM
Columbia University
New York, New York

Local Secretary for the Pacific Coast

PAUL KIRKPATRICK
Stanford University
California

Editor

JOHN T. TATE
University of Minnesota
Minneapolis, Minnesota

BOARD OF EDITORS

JOHN T. TATE, *Editor* J. W. BUCHTA, *Assistant Editor*

Associate Editors

K. T. BAINBRIDGE	A. L. HUGHES	W. BLEAKNEY
H. P. ROBERTSON	T. H. JOHNSON	G. BREIT
H. B. WAHLIN	F. A. JENKINS	D. M. DENNISON

Manuscripts for publication should be submitted to John T. Tate, University of Minnesota, Minneapolis, Minnesota.

Proof and all correspondence concerning papers in the process of publication, should be addressed to the Publications Manager, American Institute of Physics, 175 Fifth Avenue, New York, New York.

Subscription Price

United States and Possessions and Canada $15.00
Foreign $16.50

Back Numbers

Complete set: Series 2,[1] Vol. 1, 1913–Vol. 54, 1938—$990.00
Yearly rate: $16.50
Single copies: $1.50 each prior to July, 1929; $.75 each after July, 1929.

Subscriptions and orders for back numbers should be addressed to Prince and Lemon Streets, Lancaster, Pennsylvania, or to the American Institute of Physics, 175 Fifth Avenue, New York, New York.

Advertising is not accepted for the *Physical Review* but attention is called to the *Review of Scientific Instruments* and the *Journal of Applied Physics* companion publications of the Institute, and media through which the field of physics can be reached most effectively. Rates and other information will be furnished on request.

Changes of address in the case of members of the American Physical Society, should be addressed to the Treasurer; in the case of other subscribers, to the Publications Manager.

[1] For Series 1 inquire of Physics Department, Cornell University, Ithaca, N. Y.

The Physical Review is published semi-monthly at Prince and Lemon Streets, Lancaster, Pennsylvania.

Entered at the Post Office at Lancaster, Pennsylvania, as second class matter.

Acceptance for mailing at special rate of postage provided for in section 1103, Act of October 3, 1917, authorized September 6, 1926.

Physics
Physics-USA
Johnson
Kaplan

THE
PHYSICAL REVIEW

A Journal of Experimental and Theoretical Physics Established by E. L. Nichols in 1893

VOL. 56, No. 11 DECEMBER 1, 1939 SECOND SERIES

An Experimental Test of Schremp's Theory of Cosmic-Ray Fine Structure*

H. S. RIBNER†
Wayman Crow Hall of Physics, Washington University, St. Louis, Missouri
(Received August 8, 1939)

From a consideration of geomagnetic and absorptive effects upon the energy spectra of primary cosmic rays, Schremp some years ago inferred the existence of an anomalous directional intensity pattern in the sky, the analysis of which might be expected to yield detailed information concerning the identity of the primary cosmic rays, their energy spectra at infinity, and their interaction with absorbing matter. An east-west directional intensity survey has recently been carried out at Washington University, St. Louis, to test these predictions with apparatus of high angular resolution. In the curve of directional intensity *vs.* zenith angle z, the present results indicate the existence of symmetrical prominences at $z=\pm 20°$ and further suggest that other symmetrically disposed prominences may exist in the neighborhood of $z=\pm 10°$ and $z=\pm 40°$. This symmetry, in the light of the theory, carries implications concerning the character of the primary cosmic rays.

1. INTRODUCTION

A BRIEF summary of the Schremp fine structure theory is given in another paper.[1] An important case of such a fine structure occurs when the intensity $I(z)$ recorded by a coincidence counter telescope is plotted against the zenith angle z in the east-west plane. The well-known empirical relation is

$$I(z)=I(0)\cos^2 z. \qquad (1)$$

The fine structure, susceptible of resolution by telescopes of small angular aperture, consists of prominences and depressions in the smooth curve of Eq. (1). The theory further contemplates an east-west positional symmetry of these irregularities under certain circumstances.[1] The present investigation was undertaken to establish the existence or non-existence of this fine structure and, if such exists, the presence or absence of positional symmetry.

2. THE COSMIC-RAY TELESCOPE

The coincidence counter array is somewhat over two meters high and comprises three triple-coincidence Geiger-Müller trains in parallel planes. The cathodes of the counter tubes are 9 cm in diameter and 71 cm long. The large scale of the apparatus affords an appreciable counting rate under the condition of small angular aperture for the array. The steel framework supporting the counter boxes has a cross section 95 cm by 114 cm and is extensible in the long direction. It was set for the survey at 207 cm. At this extension each triple-train subtends an angle of 5° in the plane in which it can rotate and 38° in the plane of the counter wires.[2] The framework is equipped to turn about a horizontal axis, and a goniometer reads the angular setting to one minute of arc.

* The investigation here reported forms the subject of a doctoral dissertation submitted to the Board of Graduate Studies of Washington University.

† Now with Gravity Service Corporation, Houston, Texas.

[1] E. J. Schremp and H. S. Ribner, a paper read at the Chicago Cosmic-Ray Symposium, June 27–30, 1939, to appear in *Reviews of Modern Physics*, July–October, 1939.

[2] Half of the rays counted, however, traverse the center 30 percent of each of these angular ranges.

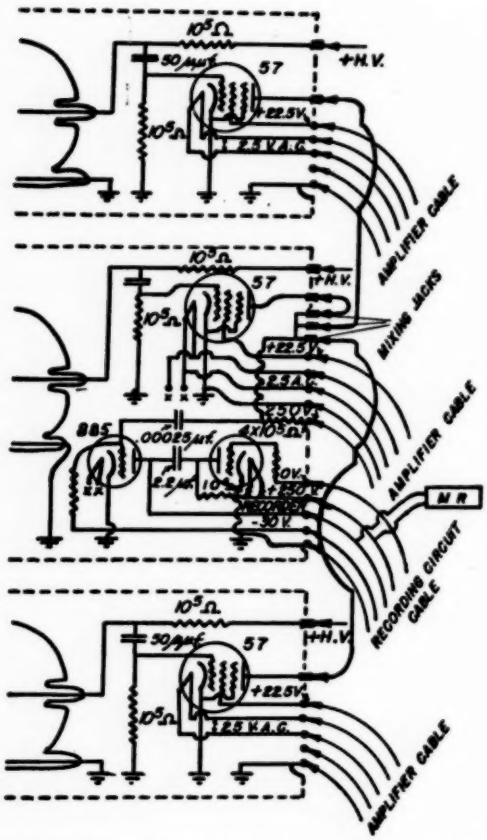

FIG. 1. Schematic circuit for one triple-train. Power supplies not shown. Top box: G-M tube and amplifier. Middle box: G-M tube, amplifier (above), and recording circuit (below). Bottom box: G-M tube and amplifier. The grid leaks of the recording circuit 885 tubes are each 5×10^6 ohms. "MR" signifies "message register."

The coincidence and recording circuit of each triple train is located in its center counter box. There is provision for external change-over from triple-coincidences to double-coincidences between any pair of counters or single pulses from any one counter. The circuit diagram for one triple-train, with power supplies omitted, is shown in Fig. 1. The counter quenching circuit employs straight resistance quenching[3] and is conventionally coupled to the amplifier of the Rossi coincidence circuit.[4] The recording circuit was designed by Mouzon.[5] The power supply includes a high voltage unit for the counters, employing the circuit of Schmitt,[6] which is stabilized against input and load fluctuation, a low voltage unit for the amplifiers of the conventional unstabilized type, and a separate low voltage RCA type TMV-118-B stabilized unit for the recording circuits. The recording assembly consists of three message registers to count the triple-coincidences of their respective trains, and a high speed stopwatch type recorder, used in testing, to count the pulses from a single counter.

The Geiger-Müller tubes are of a type which quench satisfactorily with a resistance of only 10^5 ohms. Hence resistance quenching[3] is used instead of the usual vacuum tube circuit.[7] With the constants shown the pulse length is 2×10^{-5} second. The method of construction, due to Neher,[8] involves oxidation of the cathode and filling with argon in the presence of xylol.[9] The tubes were filled to a pressure at which the threshold, at 20°C, was in the neighborhood of 1400 v. With the 5-mil tungsten anode wires initially used the counter pressure was 9 cm, while with the 10-mil wires finally used the pressures range from 4 to 8 cm. In most cases the plateau extends to 2000 volts.

Tests on the discrimination of the Rossi coincidence circuit against partial coincidences were conducted as follows: a triple train was connected for normal operation, but with the high voltage disconnected from one of the three counters. Under this circumstance single pulses and double-coincidences were incident on the mixing circuit, but no triple-coincidences. If the discrimination between partial and total coincidences were imperfect some counts would be recorded. None was recorded in tests lasting at least forty-five minutes.

From the oscillograph value of the pulse length (2×10^{-5} second) and the measured twofold accidental counting rate[10] (1.8 ± 0.2 counts per

[3] Cf. John Strong, *Procedures in Experimental Physics*, p. 276.
[4] B. Rossi, Nature **125**, 636 (1930).
[5] J. C. Mouzon, Rev. Sci. Inst. **7**, 467 (1936).
[6] O. H. A. Schmitt, Rev. Sci. Inst. **5**, 435 (1934).
[7] For vacuum tube quenching methods cf. Strong, reference 3, p. 277ff.
[8] Cf. H. V. Neher's discussion of construction methods for fast counters in Strong, reference 3, pp. 269–270.
[9] It has been observed that the optimum xylol content is rather critical: with too little, the threshold voltage is low and the plateau very short; while with an excess, the vapor pressure dependence on temperature leads to a marked temperature dependence of the counter characteristic curve.
[10] Obtained by subtracting from the twofold horizontal rate, which includes both accidentals and showers, the threefold horizontal rate, which consists almost wholly of showers. The twofold accidental rate then furnishes a reliable estimate of the true single counting rates, which was not available otherwise because our single pulse recorder missed an appreciable fraction of the counts at high single rates.

minute) the threefold accidental rate was computed[11] to be one count in eleven hours.

3. Experimental Procedure

The cosmic-ray telescope was set up on a portion of the roof of the Wayman Crow Hall of Physics of Washington University which provides a clear view of the eastern horizon and to within 15° of the western horizon. The axle of the framework was oriented north and south so the rotation would be in the local magnetic east-west plane.

The exploration of the east-west plane was carried out by what we shall call the "method of cycles." This method consists in the exploration of a section of the east-west intensity curve, consisting usually of six or seven distinct angles z. If each angle is exposed just once, in any order, for ten minutes, then in a period of a little over one hour the whole section will be exposed. The complete exposure of these six or seven points, in any order, at the rate of ten minutes per point, constitutes one cycle. The method of cycles then consists in recording the counting rate $I(z)$ and internally normalized values of $I(z)$ (cf. below), as primary data, and in averaging the latter for a large number of cycles. By describing each cycle in random order any secular drift of sensitivity of the apparatus within a single cycle is converted into random fluctuations about some mean sensitivity. The latter may vary from one cycle to the next but is canceled out in the normalization process, which involves only ratios of intensities. Hence only changes of sensitivity within a cycle remain effective, but these are converted into random fluctuations the only effect of which is to augment the probable error of the average of the normalized $I(z)$'s somewhat. This probable error can, of course, be computed by the method of residuals from the normalized $I(z)$'s for the complete set of cycles.

Table I. *Results for separate sections.*

1 Section Number	2 Number of Cycles	3 Zenith Angle z Degrees	4 Total Counts N	5 Deviation $\Delta(z)$	6 Probable Error $\sigma_r(z)$ from Residuals	7 Probable Error $\sigma_c(z)$ from Counts
I	20	0E	2974	+0.002	0.011	0.012
		5E	2965	+ .003	.012	.012
		10E	2902	+ .007	.013	.013
		15E	2736	− .013	.011	.013
		20E	2671	+ .024	.013	.013
		25E	2392	− .025	.012	.014
II	21	0W	2205	+ .012	.014	.014
		5W	2222	+ .028	.014	.014
		10W	2116	+ .003	.014	.015
		15W	2037	+ .003	.014	.015
		20W	1907	− .011	.014	.015
		25W	1742	− .035	.016	.016
III	18	15E	1493	+ .015	.020	.017
		20E	1376	− .011	.020	.018
		25E	1282	− .009	.018	.019
		10W	1548	+ .012	.019	.017
		15W	1415	− .026	.014	.018
		20W	1420	+ .028	.014	.018
IV	27	0	2381	+ .044	.012	.014
		30E	1652	− .035	.017	.017
		40E	1319	− .014	.016	.019
		50E	942	− .002	.019	.022
		30W	1698	− .008	.014	.016
		40W	1352	+ .014	.023	.018
		50W	940	− .008	.019	.022

[11] By means of the formula for accidentals given by $A_{123}=3N^3\tau^2$, where N is the single counting rate and τ is the resolving time.

4. Results and Discussion

Table I presents the individual results of each of the separate sections surveyed during the course of this investigation. In all, four sections in the east-west plane were explored. The zenith angles comprised within the separate sections are indicated in column 3 of this table. The total number of cycles in each section and the total number of counts[12] are indicated in columns 2 and 4, respectively. The quantities $\Delta(z)$ in column 5 constitute a measure of the deviation of the observed east-west distribution curve $I(z)$ from the empirical $\cos^2 z$ distribution. In column 6 are given the probable errors $\sigma_r(z)$ of $\Delta(z)$ as computed from residuals. These probable errors include any fluctuations in the over-all efficiency of the counter telescope. For comparison, we give in column 7 the probable errors $\sigma_c(z)$ of $\Delta(z)$ as computed from the total number of counts (column 4). The relative magnitudes of the two sets of probable errors provide a criterion for judging the reliability of the counter telescope. Of these two sets of values, the probable errors from residuals are the more significant.

Table II presents the final results, obtained

[12] The total counts here indicated may be used to form a reliable intensity curve for the angles within a single section, but not for all angles and all sections. Thus in Table II, we may not compare intensities at two angles by means of their total counts unless both angles are covered throughout in the same sections.

from an appropriate superposition at each zenith angle, of the data of the four sections of Table I. The column headings of Table II are identical with those of Table I, but they refer in this case to superposed values of the quantities designated.

The following relations serve to define the several quantities involved and to indicate the method of superposition used. The first ten relations suffice to form Table I. The last four relations tie together the entries of Tables I and II.

(1) $I(z)$ = the number of counts per 10 minutes at zenith angle z, for a given cycle.

(2) $I_0(z) = I(z) \sec^2 z$.

(3) $\bar{I}_0$ = the average, over z, of the $I_0(z)$'s for a given cycle.

(4) $I_0(z)/\bar{I}_0$ = the value of $I_0(z)$, normalized with respect to $\bar{I}_0$ for the purpose of reducing the given cycle to a basis comparable with all other cycles of the same section, when similarly reduced.

(5) $\langle I_0(z)/\bar{I}_0\rangle_{Av}$ = the average of $I_0(z)/\bar{I}_0$, over all cycles of a given section.

(6) $\Delta(z) = \langle I_0(z)/\bar{I}_0\rangle_{Av} - 1$ = the fractional deviation, at z, of the observed distribution from the $\cos^2 z$ distribution.

(7) $\delta(z)$ = the deviation of $I_0(z)/\bar{I}_0$ from $\langle I_0(z)/\bar{I}_0\rangle_{Av} \equiv$ the residual.

(8) $\bar{\delta}(z)$ = the average of $\delta(z)$, over all cycles of a given section.

(9) $\sigma_r(z) = 0.845\ \bar{\delta}(z)/(\text{no. cycles})^{\frac{1}{2}}$ = the probable error of $\Delta(z)$ computed from residuals.[13]

(10) $\sigma_c(z) = 0.675/(\text{no. counts})^{\frac{1}{2}}$ = the probable error of $\Delta(z)$ computed from total counts.

(11) $\Delta_i(z) = \Delta(z)$ for section i (i = I, II, III, or IV).

(12) $\Delta_0(z) = (w_i/w_0)\Delta_i(z) + (w_j/w_0)\Delta_j(z)$ = the weighted mean of $\Delta(z)$ for two superposed sections i and j.

(13) $w_i = k/\sigma_i^2$ = the weight of $\Delta_i(z)$, in terms of its probable error σ_i, where k is an arbitrary constant.

(14) $w_0 = k/\sigma_0^2 = w_i + w_j$ = the weight of $\Delta_0(z)$, which defines the probable error σ_0 of $\Delta_0(z)$.

TABLE II. *Combined results.*

1 Section Number	2 Number of Cycles	3 Zenith Angle z Degrees	4 Total Counts N	5 Deviation $\Delta(z)$	6 Probable Error $\sigma_r(z)$ from Residuals	7 Probable Error $\sigma_c(z)$ from Counts
IV	27	50W	940	−0.043	0.019	0.022
IV	27	40W	1352	− .022	.023	.018
IV	27	30W	1698	− .043	.014	.016
II	21	25W	1742	− .035	.016	.016
II, III	39	20W	3327	+ .007	.010	.012
II, III	39	15W	3452	− .011	.009	.011
II, III	39	10W	3664	+ .006	.011	.011
II	21	5W	2222	+ .028	.014	.014
I, II, IV	68	0	7560	+ .006	.008	.009
I	20	5E	2965	+ .003	.012	.012
I	20	10E	2902	+ .007	.013	.013
I, III	38	15E	4229	− .007	.009	.010
I, III	38	20E	4047	+ .014	.011	.011
I, III	38	25E	3674	− .020	.010	.011
IV	27	30E	1652	− .070	.017	.017
IV	27	40E	1319	− .049	.016	.019
IV	27	50E	942	− .037	.019	.022

The $\Delta_i(z)$'s contemplated in relations 11–14 should in general be adjusted to give the same average over z for those portions of any two superposed sections which overlap. Sections I and II, strictly speaking, overlap only in the zenith direction. However, it is known from measurements of the east-west effect[14] that the means of these two sections must agree to within less than one percent. Hence it was considered preferable to retain the original $\Delta_i(z)$'s for these two sections. The resulting superposition of Sections I and II yields the modified zenith value in Table II. In superposing Section III upon the combined Sections I and II, again it was found possible to retain the original $\Delta_i(z)$'s. In the case of Section IV, however, the only point which overlaps the combined Sections I, II, III is the zenith, and here the difference of the zenith values was too large to neglect. Accordingly, the $\Delta(z)$'s for Section IV were adjusted to effect an equality of the zenith values. This readjustment practically amounts to a rigid displacement of the curve for Section IV sufficient to bring the zenith values into coincidence.

The results of Table II are plotted in the top graph of Fig. 2. The ordinates indicate the absolute deviation[15] of the observed distribution from

[13] We here make use of a simplified formula for the probable error, based upon the normal law. That this simplification is sufficiently accurate has been ascertained by forming frequency polygons for each angle, and comparing them with the normal distribution.

[14] Cf. T. H. Johnson, reference 17; and T. H. Johnson and E. C. Stevenson, reference 18.

[15] As may be seen from the foregoing definition (6) of the fractional deviation $\Delta(z)$, the absolute deviation is, in effect, $\Delta(z)\cos^2 z = [I(z)/I_0] - \cos^2 z$. The latter quantity

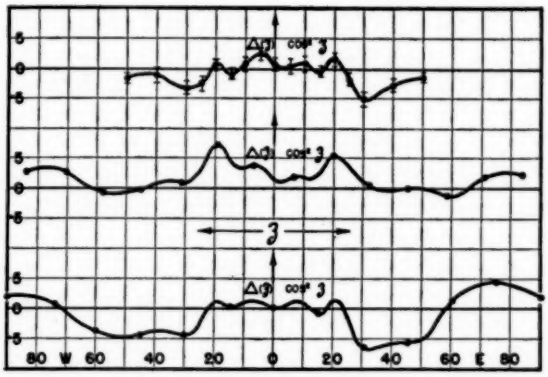

FIG. 2. East-west section of the cosmic-ray directional intensity pattern. z is the zenith angle in degrees. $\Delta(z)\cos^2 z$ is the absolute deviation, in percent of the zenith value, of the observed intensity from that given by the $\cos^2 z$ relation. Top graph: results of the present investigation. Middle graph: pattern deduced from the data of Johnson, reference 17, interpolated between experimental points. Bottom graph: pattern deduced from the data of Johnson and Stevenson, reference 18, likewise interpolated between experimental points.

the $\cos^2 z$ distribution, in percent of the zenith value. The probable errors are indicated for each experimental point. As a matter of additional interest, we have reproduced in the lower two graphs the earlier, less closely spaced data[16] of Johnson[17] and of Johnson and Stevenson,[18] respectively. The two curves interpolated between their experimental points are so drawn as to agree, qualitatively with respect to their form, and quantitatively with respect to the location of peaks, with our own curve. Since the interpolations have been effected without violation of any experimental points, there is no evidence of a discrepancy among the several surveys.

Our own curve, taken alone, indicates the existence of a pair of peaks, symmetrically disposed about the zenith, at angles $z=\pm 20°$. There are suggested also additional pairs of peaks near $z=\pm 10°$ and $z=\pm 40°$. The second curve confirms the peaks at 20°.

The east-west positional symmetry of the prominences in our own curve confirms the symmetry which was earlier pointed out[16, 19] to exist in the data from which the lower two curves were derived. The implications of this symmetry are discussed elsewhere.[19]

The existence of such peaks constitutes the sought-for Schremp effect.

The present evidence has been corroborated by recent independent results of Cooper,[20] and, in combination with the latter, seems to have securely established the above-mentioned effect. However, as has been pointed out elsewhere,[19] much additional experimental information remains to be found from an extension of this type of survey to other azimuths and localities, and from the development of cosmic-ray telescopes of sufficient aperture to permit a study of time variations in the directional intensity pattern.

In conclusion, the writer wishes to take this opportunity to express his appreciation to Dr. E. J. Schremp, who conceived this problem, for the very considerable extent to which his assistance and advice contributed to its completion.

is to be identified with Cooper's $\Delta(\theta)$ (cf. reference 20 below).

[16] These reduced data do not appear in the original articles quoted, but form a part of certain unpublished calculations of Dr. E. J. Schremp which he kindly made available to the writer. Since these data are based on total counts, the question arises as to the extent to which they may reflect sensitivity fluctuations in the apparatus. In general, a reduction of data based on total counts should agree closely with one based on ratios of intensities, provided that the primary data are obtained by a method involving frequent interchanges of directions, properly distributed over the whole angular range. We have verified this conclusion by comparing the two methods of reduction of our own primary data. Apparently the data of Johnson (reference 17) satisfy this condition, but those of Johnson and Stevenson (reference 18) do not. The possibility that the prominences in Johnson's curve are spurious instrumental effects would therefore seem quite remote. The experimental points of Johnson and Stevenson's curve, on the other hand, might be expected to show a spurious instrumental effect. However, they exhibit in themselves no prominences susceptible of such an interpretation. Instead, they straddle the prominences of the other two curves and otherwise agree fairly well with corresponding points of the latter.

[17] T. H. Johnson, Phys. Rev. **48**, 287 (1935).

[18] T. H. Johnson and E. C. Stevenson, Phys. Rev **44**, 125 (1933).

[19] Cf. E. J. Schremp and H. S. Ribner, reference 1; also E. J. Schremp, Phys. Rev. **53**, 915A (1938).

[20] D. M. Cooper, Phys. Rev. **55**, 1272 (1939). Subsequent results privately communicated to us by Professor N. S. Gingrich and Mr. Cooper continue to show three symmetrical pairs of prominences in the east-west plane, approximately at $z=\pm 7°$, $\pm 20°$, $\pm 35°$. These positions agree closely with the approximate positions given above by us, at $z=\pm 10°$, $\pm 20°$, $\pm 40°$. The ratios of the magnitudes of these prominences to their probable errors, in the light of all results up to date, are in excess of 7, 7, 3, respectively.

World-Wide Variations of the Earth's Magnetic Field and the Intensity of Cosmic Radiation

O. GODART*
Massachusetts Institute of Technology, Cambridge, Massachusetts
(Received September 28, 1939)

The observational data show that changes in the intensity of cosmic radiation are correlated with fluctuations of the magnetic field of the earth. It is suggested that the principal part of these fluctuations is due to variations in the intensity of the ionospheric currents. A rough schematic representation of these currents is assumed, as well as of their diurnal variations, and used to find the variation of the intensity of cosmic radiation caused by variations of the magnetic force due to these currents. A change of 0.4 percent in the intensity of cosmic rays in equatorial regions is thus obtained, in good agreement with experiment. At high latitudes discrepancies appear which, however, seem to be satisfactorily accounted for by the influence of the sun's magnetic field. Nonperiodic variations seem to be accounted for by the same mechanism, except in the case of magnetic storms.

I

THE parallelism between the variations of the earth's magnetic field and the fluctuations of the intensity of cosmic radiation has been pointed out by a great many investigators.[1] The action of the magnetic field on charged particles forming the most important part of primary cosmic rays seems to account for this correlation. A quantitative theory requires then the knowledge of the earth's magnetic field along the entire trajectories of the primary particles. Unfortunately we know only the terrestrial magnetism on the surface of the earth and our incomplete knowledge of the ionosphere obliges us to consider what is probably only a rough approximation to the magnetic field outside the earth.

In the absence of electric currents the earth's magnetic field has a potential which may be expanded in terms of spherical harmonics and at very large distances the dipole term in $1/r^2$, where r is the distance from the dipole, predominates. We may then consider long range variations of the earth's magnetism—and consequently of the cosmic radiation—as due to variations of the position, direction or strength of the earth's magnetic dipole. At shorter ranges the higher order terms and the magnetic field due to electric currents in the ionosphere are no longer negligible and give rise to short range perturbations.

II

We are concerned in this section with the diurnal variation of the earth's magnetic field and its influence on cosmic radiation. The variations of the magnetic potential observed on the earth can be split up into two parts $\Delta\Omega=\Delta\Omega_I+\Delta\Omega_E$, the first arising from the variation of the internal magnetic field and the second from the variation of the external one. These potentials may be expanded in spherical harmonics, the former in powers of $1/r$ valid everywhere, and the latter in powers of r valid only under the ionospheric layers; at larger distances $\Delta\Omega_E$ can be also expanded in powers of $1/r$ but the coefficients of this expansion depend on the shape and current distribution in the ionospheric layers. Neglecting the polar regions we may adopt as a representation of the source of the external field the two currents suggested by Vestine and Chapman,[2] *viz.*

(a) Uniform circular currents along the parallels of a sphere of radius a at a mean height of about 180 km above the surface of the earth. If i is the density of these currents and λ is assumed to be the geomagnetic latitude, the expression for the magnetic potential is:

$$\begin{aligned}&(4\pi i/3)(r/a)\sin\lambda \quad (r<a)\\ &-(2\pi i/3)(a^2/r^2)\sin\lambda \quad (r>a).\end{aligned}$$

If now the center of the sphere and the axis per-

* Fellow of the Belgian American Educational Foundation.

[1] For a comprehensive survey together with full references see T. H. Johnson, Rev. Mod. Phys. **10**, 222 (1938).

[2] E. H. Vestine and S. Chapman, Terr. Mag. and Atmos. Elec. **43**, 351 (1938).

pendicular to the parallels are displaced there results a variation of potential:

$$\Delta\Omega_I' = (4\pi i a^2/r^3)\sin\lambda\cdot\Delta r - (2\pi i/3)(a^2/r^2)\cos\lambda\cdot\Delta\lambda$$
$$\Delta\Omega_E' = 0+(4\pi i/3)(r/a)\cos\lambda\cdot\Delta\lambda.$$

A change of only the height of this current will have no magnetic effect under the ionosphere but will have one at large distance; we assume that these permanent currents remain at the same

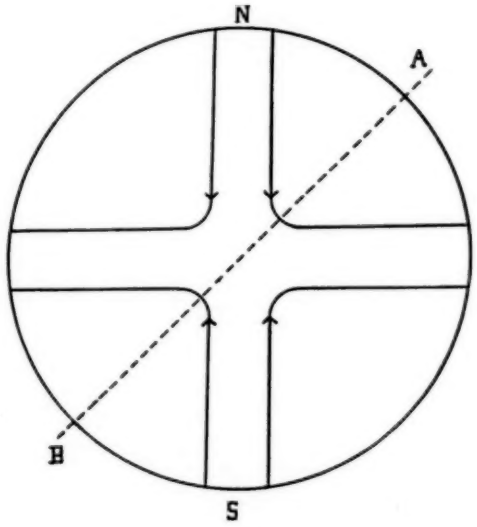

FIG. 1. Diagram of perturbing ionospheric currents.

height but that the axis oscillates periodically so that $\Delta\lambda = l_1\cos(t+\varphi')$.

(b) Perturbing currents going along the meridian plane passing through the sun and then along the equator at a mean height of 300 km. We have along the axis of symmetry AB (Fig. 1) the potential

$$\Omega \cong k a_1^2/(a_1^2+r^2)^{\frac{1}{2}},$$

where k is a function of the intensity and breadth of the current, a_1 is radius of the sphere containing the current. Everywhere,

$$\Delta\Omega_E'' = (k/a_1)[1-3(r/a_1)^2\sin\lambda\cos\lambda\cos(t+\varphi)-\cdots] \quad (r<a)$$
$$\Delta\Omega_I'' = (k a_1^2/r^3)2\sin\lambda\cos\lambda\cos(t+\varphi)+\cdots \quad (r>a),$$

where t is the local Greenwich time in hours and φ is the longitude.

III

Using Chapman's notation[3] we may write

$$\Delta\Omega_I = I_1'(\cos\lambda/r^2)\cos(t+\varphi_0) + I_2'(\sin\lambda\cos\lambda/r^3)\cos(t+\varphi_1)$$
$$\Delta\Omega_E = E_1' r\cos\lambda\cos(t+\varphi_0') + E_2' r^2\sin\lambda\cos\lambda\cos(t+\varphi_1'),$$

where I_2', E_2'; $\varphi_1 \leqq \varphi_1'$ are coefficients which are constant with respect to the season, while I_1', E_1'; $\varphi_0 \leqq \varphi_0'$ change with the season. The amplitudes I_1' and E_1' have their maximum value during the solstices and their minimum during the equinoxes, the phase angle increasing all the time. Comparing with the theory outlined in Section II we find

$$(4\pi i/3a)l_1 = E_1' \quad -(3k/a^3) = E_2'.$$

The expression for the increment of potential at large distances now becomes

$$\Delta\Omega = [I_1' - (a^3/2)E_1'](\cos\lambda/r^2)\cos(t+\varphi_0) + [I_2' - (2a_1^5/3)E_2'](\sin\lambda\cos\lambda/r^3)\cos(t+\varphi_1).$$

These terms may be interpreted as a circular motion of the dipole in the equatorial plane with a radius (M is the earth's dipole moment)

$$p = (-I_2' + 2a_1^5 E_2'/3)/2M$$

and an oscillation of amplitude

$$l = (I_1' - a^3 E_1'/2)/M$$

maximum at the equinox. The radius p is constant throughout the year but the phase of the motion is such as if the dipole were repelled by the sun.[4] The residues

$$I_1' - (a^3/2)E_1' = -2.8\times10^{-6},$$
$$I_2' - (2a_1^5/3)E_2' = -1.9\times10^{-6}$$

however, are so small as to be negligible. This seems to corroborate Schuster's assumption[5] that the variation of the internal field is induced by the variation of the external one.

A similar study of the seasonal variation, based, however, on much more incomplete data, suggests that we may also neglect in this case the variation of the terrestrial field at large distances.

[3] S. Chapman, Phil. Trans. Roy. Soc. **218**, 2 (1919).
[4] The coupling of the sun's and earth's dipoles was suggested to me by Professor M. S. Vallarta as an explanation of this motion.
[5] O. Schuster, Phil. Trans. Roy. Soc. **180**, 467 (1889).

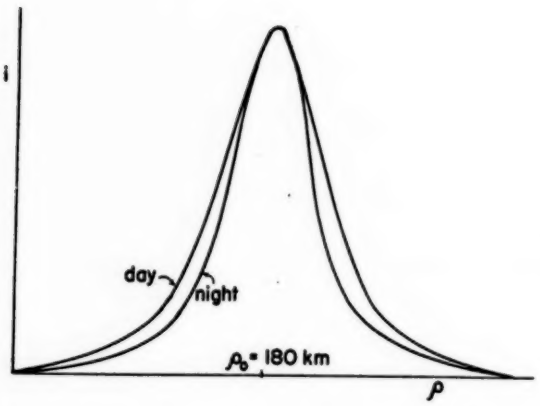

FIG. 2. Schematic representation of ionospheric currents and their diurnal variation.

IV

The short range perturbations are thus produced mainly by ionospheric current variations. We represent these ionospheric currents schematically by assuming a current parallel to the earth's surface of intensity variable with the distance ρ from the earth's center (Fig. 2). From the magnetic point of view we may replace these currents by spherical magnetic shells of thickness $d\rho$. The law of intensity of magnetization is assumed to be roughly

$$dI = I_0 e^{-h^2(\rho-\rho_0)^2} d\rho,$$

where ρ_0 is the height of the permanent currents considered in Section II(a). Then ρ_0 and I_0 are assumed to be constants in time, but h decreases during the day so that the ionization is then greater in the lower Kennelly-Heaviside layer and also greater in the more distant layers, thus taking into account the supplementary currents supposed by Vestine and Chapman[2] to exist in the F layer around noon. The values of I_0 and h have been so chosen that they give the correct external magnetic field and in such a way that the mean value of h gives for I on the earth's surface the value $I_0 \times 10^{-3}$. The total field of these magnetic shells at a point of polar geomagnetic coordinates r, λ, φ, is

$$H_r = \frac{4\pi}{3} I_0 \sin\lambda \left[\int_r^\infty e^{-h^2(\rho-\rho_0)^2} d\rho + (1/r^3) \int_0^r e^{-h^2(\rho-\rho_0)^2} \rho^3 d\rho \right]$$

$$H_\lambda = \frac{4\pi}{3} I_0 \cos\lambda \left[\int_r^\infty e^{-h^2(\rho-\rho_0)^2} d\rho - (1/2r^3) \int_0^r e^{-h^2(\rho-\rho_0)^2} \rho^3 d\rho \right],$$

$$H_\varphi = 0.$$

The resulting perturbing force on charged particles due to this subsidiary magnetic field does not change the symmetry around the magnetic axis. In the notation of Lemaître and Vallarta[6] we find the integral

$$r\cos\lambda\, d\varphi/ds = \sin\theta = 2\gamma_1/r\cos\lambda - \cos\lambda/r^2 + k\left[(r\cos\lambda/2) \int_r^\infty e^{-h^2(\rho-\rho_0)^2} d\rho + (\cos\lambda/2r^2) \int_0^r e^{-h^2(\rho-\rho_0)^2} \rho^3 d\rho \right],$$

where

$$k = (4\pi I_0 e/3m_0 v)(1-v^2/c^2)^{\frac{1}{2}} = (\alpha Me/m_0 v)(1-v^2/c^2)^{\frac{1}{2}}$$

and α is a constant of dimensions L^{-4}. Taking as a unit of length the Störmer unit

$$(Me/mv)^{\frac{1}{2}} \quad [m = m_0/(1-v^2/c^2)^{\frac{1}{2}}],$$

we find

$$\alpha = 0.0815/r_0^4,$$

where r_0 is the radius of the earth measured in Störmer units. If h changes we have, differentiating with respect to h and neglecting in the integrals the contribution coming from the internal field,

$$\Delta \sin\theta = -\pi^{\frac{1}{2}} kR \cos\lambda \Delta h/2h^2,$$

where R is the earth's radius. Introducing Störmer units we find

$$\Delta \sin\theta = -10^{-3} \cos\lambda / r_0^2.$$

V

Liouville's theorem remains valid for our present case and thus the intensity of cosmic radiation of energy E is still proportional to the solid angle of the cone of allowed directions. A first approximation to this allowed cone is the Störmer cone[6] and we assume that as a first approximation the Störmer cone and the allowed

[6] See for example M. S. Vallarta's *An Outline of the Theory of the Allowed Cone of Cosmic Radiation* (Univ. of Toronto Press, 1938).

cone vary proportionately. The solid angle of the former is given by $2\pi(1+\sin\theta_1)$, where the subscript of θ means that in the expression for $\sin\theta$, γ_1 has the value one. $2\pi\Delta\sin\theta$ will then be the change in solid angle. Now if we assume that the distribution of the primary particles with respect to their energy is given by $n(E)=\text{const.}/E^{2.8}$, as suggested by many investigators, and integrate graphically following the method used by Vallarta[7] we obtain the results shown in Table I. As seen in this table the agreement between the present theory and experiment[8] is satisfactory at low latitudes. The progressively increasing discrepancies at high latitudes are largely accounted for by the influence of the sun's magnetic field on primary cosmic rays.[9]

VI

A more precise model of the ionosphere would throw additional light on the intensity variations of cosmic radiation. It seems already probable that many of the aperiodic variations are also correlated in a similar way with changes in the ionosphere. The relations between cosmic rays and solar phenomena thus appear to be partly indirect through the medium of ionization of the atmosphere by ultraviolet light emitted from the sun. What appears to be most important is that observations of the intensity of cosmic radiation ought to be able to yield valuable information on the structure of the ionosphere.

An important exception to this correlation appears to exist in the case of magnetic storms, where the correlation factor $(\Delta I/I)/(\Delta H/H)$ is either 15 or 0, instead of agreeing with the prediction derived from a theory similar to the present that it ought to be positive and have a value about 4. But as some authors,[10] including the writer,[11] have pointed out, magnetic storms can be explained by the existence of ring currents at distances from the earth of the order of magnitude of a few earth's radii. From these premises we may infer three important magnetic perturbations: (a) at large distances an increase of the strength of the earth's magnetic dipole, (b) at shorter distances perturbations by the currents themselves,[12] and (c) perhaps a decrease of ionization in the ionosphere by partial absorption of the solar ultraviolet radiation. This decrease of ionization seems to be connected with the long time echoes[13] observed during magnetic storms. Radio waves are then able to pierce the ionosphere but are turned back by the ring currents.

All these three factors tend to decrease the intensity of cosmic rays. The quantitative development of the theory, however, still offers some difficulties, particularly the fact that certain magnetic storms seem to have no influence whatever on the intensity of cosmic rays.

I wish to express my indebtedness to Professor M. S. Vallarta, under whose direction this work was carried out, for his inspiring advice and kind encouragement.

TABLE I. *Comparison of calculated and observed values of* $\Delta I/I$.

Geomag. lat. λ	Calc. $\Delta I/I$ (in tenths of one percent) Ampl.	Phase	Obs. $\Delta I/I$ (in tenths of one percent) Ampl.	Phase
0°	2	11 h.	2	14 h.
20°	1.9	11 h.	2	14 h.
30°	1.8	11 h.	2	13 h.
40°	0.4	11 h.	3	12 h.
50°	—	—	3	13 h.

[7] M. S. Vallarta, Phys. Rev. **47**, 647 (1935).
[8] J. L. Thompson, Phys. Rev. **54**, 93 (1938); S. E. Forbush, Terr. Mag. and Atmos. Elec. **42**, 1 (1937).
[9] A paper by M. S. Vallarta and O. Godart presented at the University of Chicago's symposium on cosmic rays (June, 1939), including a study of the influence of the sun's dipole field and a summary of the present results, appears in Rev. Mod. Phys. **11**, 180 (1939).
[10] For example C. Störmer, Arch. de Sci. Phys. et Nat. **32**, 277 (1911); S. Chapman, Nature **140**, 423 (1937).
[11] O. Godart, Phys. Rev. **55**, 875 (1939).
[12] S. Kusaka, S. M. Thesis, M. I. T., 1938.
[13] H. R. Mimno, Rev. Mod. Phys. **9**, 1 (1937).

The Scattering of Protons by Protons. III

N. P. HEYDENBURG, L. R. HAFSTAD AND M. A. TUVE
Department of Terrestrial Magnetism, Carnegie Institution of Washington, Washington, D. C.

(Received October 9, 1939)

Our work of 1936 on the anomalous scattering of protons by protons in the energy region 600 to 900 kv was repeated during 1938 with an entirely new scattering apparatus designed for better angular measurements. Particular care was taken in order to know the energy (velocity) of the protons at the scattering volume with accuracy. The number of protons in the primary beam during each observation was determined by counting the protons scattered backward from a gold foil placed in the path of the proton-beam beyond the hydrogen-scattering volume. The scattering of protons by spectroscopically pure argon for several voltages and various angles was found to obey the Rutherford-Darwin formula. These measurements with argon provided a calibration of the voltage-scale in absolute units which was found to agree with our standard voltage-scale within about one percent. On the latter scale the midpoint of the gamma-ray resonance for protons on lithium is at 440 kv, the molecular ions thus giving a calibration point at 880 kv. A strong resonance for protons on fluorine occurs at 867 kv. The scattering anomaly arises from the failure of the Coulomb law of repulsion for very close distances of approach, because of the existence of a strong attraction of very short range which is the nuclear force between two protons. The newer measurements are in good agreement with our results in 1936, which were shown by Breit and his colleagues to correspond in the wave mechanics to a simple s wave scattering. They also agree well with the data of Herb and his colleagues where the measurements overlap at about 860 kv. No clear-cut evidence for higher order scattering is found in our newer data, although the Mott ratios for angles from 20° to 30° are higher than would be predicted from the values for angles from 40° to 45° on the basis of s wave scattering only. The departures are from five to ten percent, whereas from the internal consistency of the data one would hardly expect statistical errors of this magnitude. The discussion indicates that systematic errors affecting the scattering at 20° to 30°, although unlikely, cannot definitely be excluded. These observed systematic deviations are of the type which would be contributed by a small amount of p wave scattering superposed on the spherically symmetrical s wave scattering.

I. INTRODUCTION AND DISCUSSION

DURING 1936 we made a series of measurements on the scattering of protons by protons in the energy range 600 to 900 kv,[1] which demonstrated the existence of a scattering anomaly caused by the nuclear force acting between two protons at close distances. These measurements were shown by Breit, Condon and Present[2] to correspond to a simple s wave scattering arising from a potential well representing an attraction between two protons very nearly equal in magnitude to the attraction between a proton and a neutron. Their analysis of our measurements showed that the range of these proton-proton forces could not be much above 4×10^{-13} cm, although a lower limit on the range could not be set by the measurements over this restricted region of energies. During 1937 we carried out measurements on proton-proton scattering in the region 200 to 600 kv, using the more sensitive but less quantitative Geiger point-counter instead of the usual linear-amplifier arrangement.[3] These measurements gave added and unequivocal proof that the anomaly is due to an attraction superposed on the Coulomb repulsion and not an added repulsion, since the scattering at 45° falls to less than five percent of the Coulomb value at a voltage of 400 kv. This is because of the opposing effects of the electrical forces of repulsion and the nuclear forces of attraction.

These measurements were subject to several sources of error which made a repetition seem desirable. The major features of the results could not be called into question, but it appeared that if the measurements could be made more reliable in detail, important quantitative improvements in the theoretical deductions might become possible. By an oversight the original apparatus was disassembled before the alignment was checked, and it appeared that an error in the angular measurements of as much as 1° conceivably might have been present. A second source of error was the fact that the number of protons in

[1] M. A. Tuve, L. R. Hafstad and N. P. Heydenburg, Phys. Rev. **50**, 806–825 (1936).
[2] G. Breit, E. U. Condon and R. D. Present, Phys. Rev. **50**, 825-845 (1936).
[3] L. R. Hafstad, N. P. Heydenburg and M. A. Tuve, Phys. Rev. **53**, 239–246 (1938).

the primary beam, measured by using the scattering chamber as a Faraday cage, could not be checked continuously during the observations, but was measured before and after each observation and was assumed to be constant during the intervening period. A third source of error was an uncertainty regarding our voltage-scale, which had been determined by reference to ordinary standards at lower voltages. Finally, the scattering observations for individual values of voltage and angle were not sufficiently extensive to reduce the statistical fluctuations as far as seemed desirable.

For the measurements of 1938 reported in this paper, these sources of error were considerably reduced. An entirely new scattering chamber was constructed, with careful mechanical checks to insure that the axes of the beam-diaphragm and the detector-slit system, and also the axis of rotation of the detector, intersected in one point. Careful measurements were made of the defining slits and diaphragms, and an accurately centered circle of good quality was used for the angular measurements. Provision was made for continuous measurement of the proton beam-current by counting protons recoiling at 135° from a gold foil larger than the whole beam, placed beyond the gas-scattering volume. These gold-foil counts as a function of voltage were reduced to microcoulombs of protons by Faraday-cage measurements made before and after the scattering observations. The 10,000-megohm voltmeter-resistor was dismantled and rechecked thoroughly, and then recalibrated at 440 and 880 kv against the proton-lithium resonance. The accuracy of our standard voltage-scale, defined by this resonance, was checked in absolute units by measuring the scattering of protons by spectroscopically pure argon gas as a function of voltage and of angle. The argon scattering agreed within one percent with the expected Coulomb scattering, indicating that our measurements of voltage, and corrections for stopping power of window and gas in the path of the proton-beam, were satisfactory. The proton-scattering measurements in this series were restricted to three voltages (specified at the scattering volume), namely, 867, 776 and 680 kv. The first value, 867 kv, coincides with one of the strong gamma-ray resonances for protons on fluorine, and was so selected and specified in order to provide an accurately repeatable voltage-point for the intercomparison of results with other laboratories. Comparisons made at this resonance-voltage are obviously independent of voltmeter-scales. The statistical fluctuations of our observations in this series are considerably better than in the earlier measurements. They are not as satisfactory as we might have desired, because the high humidity conditions of Washington summer set in before we had quite finished the observations, putting an end to accurate work. The observations with argon, in particular, are less extensive than they would have been except for this difficulty. A third series of measurements with hydrogen was similarly limited to a few points.

The results of this series of proton-scattering measurements do not differ in any very important way from the measurements of 1936, and the conclusions then drawn are not significantly altered. Our experimental data are also in close agreement, even on an absolute basis, with the values obtained by Herb and his colleagues[4] in the voltage-region (near 860 kv) common to both investigations. As shown by the analysis made by Breit, Thaxton and Eisenbud,[5] the major features of the observations are accounted for as an *s* wave scattering by a potential well which is very nearly the same as that for the proton-neutron attraction, provided the Coulomb force between two protons is not "cut off" at the edge of the well but is assumed to exist also for shorter distances, superposed on the nuclear attraction. One feature of the measurements which is not entirely in accord with this picture is the fact that the scattering observed for angles from 20° to 30° is higher than would be computed from our observations for angles from 40° to 45° on the basis of simple *s* wave scattering, by an amount considerably in excess of the apparent accuracy of the measurements as judged by their internal consistency (about two percent). The deviations in the scatterings at 20° to 30° are as large as six to ten percent for some voltages and angles. Although they are not entirely consistent, they might be due to a small amount of *p* wave scatter-

[4] R. G. Herb, D. W. Kerst, D. B. Parkinson and G. J. Plain, Phys. Rev. **55**, 998–1017 (1939).

[5] G. Breit, H. M. Thaxton and L. Eisenbud, Phys. Rev. **55**, 1018–1064 (1939).

ing superposed on the spherically symmetrical s wave contribution; a repulsive p wave term would give rise to added scattering at these angles without affecting the values at 45°. Since the scattering values obtained by Herb and his colleagues[4] in the range from 880 to 2400 kv are in substantial agreement with simple s wave scattering, it does not appear reasonable to accept these deviations as sufficient evidence for p wave scattering, and it seems most interesting to examine this possibility by a search for p wave scattering in the range from 650 down to 400 kv. Our survey of 1937, in which a Geiger point-counter was used in this region, was not sufficiently quantitative to test for a small amount of p wave contribution to the scattering.

Instead of being due to a p wave contribution, the possibility cannot be excluded that the excess scattering at 20° to 30° is caused by systematic errors which affect the values at these angles more strongly than at 45°. Several types of error have this characteristic, especially because Coulomb scattering is predominantly into the forward angles. Multiple scattering in the gas and slit-edge scattering would tend to give high values at low angles, and so would the finite angular width of the slit-systems, since the excess of particles scattered through one-half degree less than the average angle will more than compensate for the diminished scattering of particles through one-half degree more than the average angle. An error in determining the zero of the angular scale for the detector of the scattered protons (when the axis through the detector slit-system is in line with the incident beam) also is more important at small angles. All of these sources of error were recognized and experimentally examined, and we satisfied ourselves that they did not contribute large effects. However, one source of difficulty in connection with the zero of the angular scale was not obvious until the experiments were completed, and this may have contributed part of the excess scattering observed at 20° to 30°. The scattering chamber was not directly beneath the high voltage tube since magnetic analysis was used, the magnet being adjusted to deflect the beam (through about 17°) until it was centered on the aluminum-foil window just preceding the diaphragm-system of the scattering chamber. A shift of the beam by five or eight mm due to focusing readjustment would be immediately obvious if the motion were at right-angles to the plane of the magnetic deflection, and would be compensated for by adjusting the position of the ion-source. However, a similar motion in the plane of the magnetic deflection would escape notice, being compensated for by a change in the magnet current. This would result, however, in a slight change in the initial direction of the beam entering the diaphragm-system, with a correspondingly different correct position for the zero-setting of the angular scale. The latter was determined by scattering observations to each side of zero during the initial calibration of the apparatus, after which a slit-guard was installed and observations were made to one side of zero only, as discussed below. It is our impression that an error from this cause should fluctuate from day to day, and it appears unlikely that the excess observed at 20° to 30° is to be explained entirely on this basis.

II. Computations

In order to be completely independent of our earlier work, the theoretical Coulomb-law values of the scattering were recomputed from Mott's formula[6] for each voltage and angle used in this series of observations. The same values were obtained independently by two computers and are given in Table I. We used the older set of Birge's constants (1929), as follows: Electronic charge: $e=4.770\times10^{10}$ e.s.u.; Energy of 1000-kv proton: $(\frac{1}{2})\ mv^2=1.5911\times10^{-6}$ erg; Avogadro's number: $N=6.06436\times10^{23}$ atoms per mole; Perfect gas volume: $R=22{,}415$ cc per mole at 0°C. With these constants we have $N_0=3.7710\times10^{14}$ protons in our beam per microampere-minute (6.285×10^{12} per microcoulomb), and 6.5888×10^{16} hydrogen atoms per cc in our scattering volume at 22°C under a pressure of 1 mm of mercury (15.7 mm of Apiezon oil).

If N_0 is the number of protons per second in the incident beam having kinetic energy T, then the numbers of primary particles N_s scattered per second into a solid angle ω at an angle θ with respect to the initial beam by a target having N_t hydrogen nuclei are as follows according

[6] N. F. Mott, Proc. Roy. Soc. **A126**, 259–267 (1930).

to Mott:

$$N_s = N_0 N_t \omega (e^4/T^2) \cos\theta \{\csc^4\theta + \sec^4\theta - \csc^2\theta \sec^2\theta \cos[n \log((1+\cos 2\theta)/(1-\cos 2\theta))]\},$$

where $n=(1/137)(c/v)=0.161$ for $T=1000$ kv, $N_0 N_t \omega (e^4/T^2)=2.04498$ for $N_0 N_t \omega = 10^{26}$ and $T=1000$ kv.

The values of N_0, N_t, and ω, calculated from the dimensions of the slit-systems of our scattering chamber (see next section) are: $N_0=3.7710\times10^{14}$ protons per microampere minutes; $N_t=1.37047\times10^{16}\times(1/\sin\theta)$ hydrogen nuclei, at one mm pressure of mercury and 22°C (the $1/(\sin\theta)$ factor is included to take into account the variation with angle of the target-thickness as discussed in reference 1); $\omega=0.869202\times10^{-4}$ steradian. With these values, and with a hydrogen pressure at the target of 12 mm of mercury at 22°C

$$N_0 N_t \omega (e^4/T^2) = 110.2334 \times (1/\sin\theta) \quad \text{for} \quad T=1000 \text{ kv}.$$

For the convenience of experimentalists we have listed in Table I the numerical factors required for quick computation of the Mott values for various angles at different voltages. Our values for the "Mott function" agree, where angles coincide, with those computed by Breit and his colleagues for this series,[5] but our numerical values for the theoretical number of scattered protons from our scattering volume are 0.43 percent lower than theirs, due to the slightly different values adopted for the fundamental constants.

In Table I, columns 2, 3 and 4 give the functions of angles occurring in Mott's formula. For most uses one needs cot θ instead of cos θ because of the factor $(1/\sin\theta)$ occurring in N_t to take account of the change in our scattering volume with angle. Column 5 gives the angular function for $n=0$, that is, for an "infinite velocity" of the incident protons. The absolute value of $N_s(\theta)$ is given in column 6 for $n=0$, $T=1000$ kv, and $N_0 N_t \omega = 10^{26}$. Columns 7 and 8 show the effect of taking into account the factor n, which depends on the velocity, at a proton-energy 685 kv. At this energy the correction is about one percent and at higher energies it will be correspondingly smaller. The values of $N_s(\theta)$ in these two columns were those used to compare directly with the experimental data from our apparatus, for which the coefficient of the Mott function is

$$N_0 N_t \omega (e^4/T^2) = 110.2334 \times (1/\sin\theta)(1000 \text{ kv}/685 \text{ kv})^2.$$

III. Apparatus and Technique

The requirements for an apparatus to measure accurately the scattering of protons by gases are evident from the Mott formula given in Section II. It is necessary to know the number and energy

Table I. *Tabulation of angle functions used in calculating scattering values from Mott's formula, also $N_s(\theta)$ at 1000 kv and at 685 kv for $n=0$ and $n=0.191$.*

θ	$A+B$ ($A=\csc^4\theta$, $B=\sec^4\theta$)	D ($\csc^2\theta \sec^2\theta$)	cot θ	$(A+B-D)\cot\theta$ $n=0$	$N_s(\theta)$ $n=0$ $N_0N_t\omega=10^{26}$ 1000 kv	$N_s(\theta)$ $n=0$ 685 kv	$N_s(\theta)$ $n=0.191$ 685 kv
15°	224.000	16.0000	3.73205	776.266	410.863	182,367	184,980
20	74.3616	9.68110	2.74747	177.708	124.293	41,748	42,210
22.5	48.0000	8.00000	2.41421	96.5684	75.5726	22,687	22,940
25	32.8300	6.81636	2.14451	55.7864	48.2131	13,106	13,251
27.5	23.6131	5.96116	1.92098	33.9089	32.0191	7966.2	8049.6
30	17.7777	5.33333	1.73205	21.5543	21.9273	5063.7	5111.3
32.5	13.9751	4.86977	1.56969	14.1513	15.5489	3324.6	3384.4
35	11.4602	4.52990	1.42815	9.89748	11.6092	2325.2	2339.3
37.5	9.80560	4.28719	1.32704	7.19176	8.95302	1689.6	1696.3
40	8.76166	4.12437	1.19175	5.52649	7.26453	1298.33	1300.9
42.5	8.18464	4.03062	1.09131	4.53332	6.26308	1065.0	1065.6
45	8.00000	4.00000	1.00000	4.00000	5.78407	939.72	939.72
50	8.76166	4.12437	0.83910	3.89115	6.09566	914.14	916.40
55	11.4602	4.52990	0.70021	4.85265	8.12888	1140.0	1146.9
60	17.7777	5.33333	0.57735	7.18477	12.7243	1687.9	1703.8
65	32.8300	6.81636	0.46631	12.1304	22.4821	2849.8	2881.2
70	74.3616	9.68110	0.36397	23.5418	45.2390	5530.7	5591.5

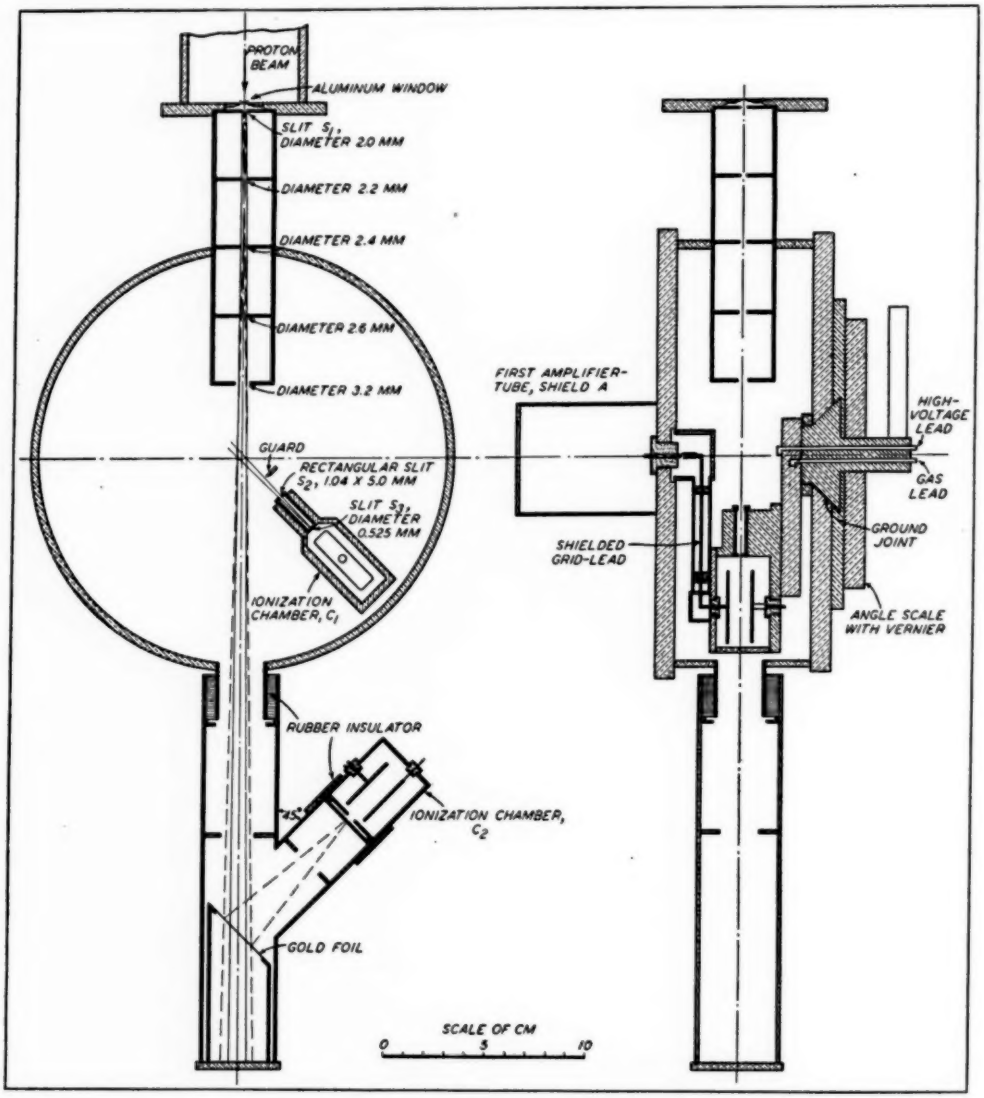

FIG. 1. Proton-scattering apparatus.

of the protons entering the scattering volume, the pressure of the gas scatterer, and the solid angles defining the scattering volume. With these quantities known, the number of protons scattered is measured at different voltages as a function of the scattering angle. Angular dispersion must be kept as small as possible and precautions must be taken to prevent spurious counts. The scattering apparatus used in this work was entirely distinct from our first scattering apparatus and was designed to overcome the difficulty of measuring the number of incident protons, which was experienced in our first work, and to give greater accuracy throughout. (This new chamber with its carefully aligned slit and rotational axes was also used in our second series of observations, made with Geiger counters.)

A diagram of the scattering apparatus is given in Fig. 1. The magnetically analyzed homogeneous proton beam from the 1200-kv electrostatic generator entered the scattering chamber through the thin aluminum window and was defined by the first diaphragm S_1, diameter 2 mm. The succeeding diaphragms were each 0.2 mm larger in diameter than the preceding one. The detector of the protons from the scattering volume of gas defined by this diaphragm-system and that of the movable detector was the ionization-chamber C_1,

the plates of which were parallel to the path of the entering protons. This chamber and the defining system attached to it could be rotated, allowing the scattering angle to be varied at will. The connection from the collector plate of the chamber passed through an insulator and a shielding tube to the grid of the first amplifier-tube located in the shielding box A outside the gas chamber. This tube was an "acorn type" (954), which was found to be very satisfactory because of its low microphonic characteristics and compactness. However, the input capacity on the grid was still too large to measure protons scattered at 45° below 650 kv.

Angular measurements

The incident proton-beam defined by the diaphragm-system and the solid angle defined by the detector slit-system intersect in space to form a "scattering volume" from which the protons may be scattered to the detector. This volume varies with the scattering angle θ and is proportional to the csc θ (neglecting very small second-order corrections). The dimensions and spacings of the detector slit-system are given in Fig. 1. The rectangular slit S_2 was accurately machined and was found to be 1.04×5.0 mm by direct comparison on a measuring engine with a standard meter bar. The hole S_3 into the detector was 0.525 mm in diameter, and the distance from the center of the scattering volume to the slit S_3 was 50,116 mm and from S_2 to S_3 was 25.024 mm. The resolution of the slit-system was approximately 2°. The thickness of the scattering volume is determined by the width of the slit S_2, and is given by (aR/S_2S_3) when the detector slit-axis is perpendicular to the incident beam, where a is the width of slit S_2 and S_2S_3 is the distance between slits S_2S_3 and R is the distance from S_3 to the center of the beam. The thickness for any angle is then given by $(aR/S_2S_3)\csc\theta=0.208\csc\theta$ for the above dimensions. This value neglects the small second-order corrections due to the slight divergence of the incident beam and the finite size of the hole S_3.

The detector and its slit-system could be rotated on a ground joint about an axis passing accurately through the center of the scattering volume. The accurate intersection of these axes at right-angles also was insured by the method of construction, using a good milling machine. A vernier scale which permitted readings of 0.1° was attached to the arm controlling the setting of the scattering angle. The zero-angle of the detector was first set by eye-observations with a beam of light passing through the diaphragm-systems of the incident beam and of the detector. It was then checked by observing the scattering from air at a scattering angle of 25° on either side of zero. It was found necessary to shift the zero-setting by $\frac{3}{6}$° to make the scattering from the two sides equal.

Later, when much of the data on the scattering in hydrogen had been taken, a more careful check of the zero-position was made and a residual error of $\frac{1}{6}$° was found. Since it was desirable to use the same angle-settings throughout the measurements, it seemed preferable to correct the results for the true zero-position. This was done by calculating the percentage change in scattering for each angle in the case where the results were in good agreement with the classical theory, and by finding the percentage change for $\frac{1}{6}$° graphically for each angle by plotting the scattering curve for all angles and taking increments on the tangent at each angle, when there was an observed anomaly. These corrections are given in percentages in Table II. The second column gives the percentage correction for shift of $\frac{1}{6}$° in zero, calculated from the Rutherford scattering law. The next three columns apply to the proton-proton scattering angles, and the percentages were obtained graphically from the slopes of the experimental scattering curves. The observed counts were in all cases reduced by these percentages since with an angle-setting of 20°, for example, the true scattering angle was actually $19\frac{5}{6}$°.

TABLE II. *Percentage excess scattering due to zero-correction (the last three columns are corrections for the experimental proton-proton scattering curve).*

θ	CLASSICAL $R-D$ SCATTERING	670 KV	776 KV	867 KV
20°	4.19	4.00	4.00	4.00
25	3.31	2.97	2.90	1.84
27.5	2.97	2.76	2.00	1.82
30	2.73	2.16	1.60	1.05
32.5	2.47	1.67	1.18	0.88
35	2.29	1.11	1.11	0.83
37.5	2.10	0.88	1.02	0.77
40	1.98	0.81	0.62	0.61
42.5	1.82	0.75	0.52	0.47
45	1.71	0.70	0.42	0.40

Gas pressure

The mercury manometer used to measure the gas pressure in the scattering chamber in the earlier work was replaced by an Apiezon-oil manometer. This manometer has a sensitivity 15.7 times greater than that of a mercury manometer and has the added advantage of being easier to read because of the transparency of the oil. The vacuum-arm of the manometer was continuously pumped.

It was important to be sure that no foreign gas entered the scattering chamber during the measurements. The rate of leakage was determined by pumping the chamber to the best possible vacuum, isolating it and noting the time which elapsed before appreciable scattering was observed. A check was also made on each set of measurements by repeating an observation of the scattering at 20° at the conclusion of the run. Before using a continuous-flow procedure the gas was always pumped out and renewed after 50 or 60 minutes of observation—during this time the scattering would not change by more than one or two percent. In the later series of measurements the apparatus was arranged so that a hydrogen flow was maintained through the chamber continuously during the observations. This was done by pumping on the chamber through a needle-valve which was adjusted to give the same rate of flow as the hydrogen leak into the chamber through the palladium tube. It was found in practice that a given pressure could be maintained to within a tenth of a mm of mercury, or better than one percent, with an adjustment of the needle-valve about once every five minutes. The rate of flow was adjusted to give a complete change of hydrogen every ten minutes, so that the necessity of stopping the observations to renew the gas was avoided. Tank hydrogen, purified by passing through palladium (palladium tube not contaminated with deuterium), room air, spectroscopically pure argon from Linde, and purified Linde nitrogen were used as scattering gases in this work.

Current measurement

The second ionization chamber (C_2) served to detect protons scattered at about 135° to the beam from the gold foil located in the chamber beyond the scattering volume. The number of protons scattered from the gold foil was of course proportional to the number of particles passing through the scattering volume. It was therefore possible to know the relative number of protons in the incident beam during a given measurement of the gas scattering by simultaneously counting the protons scattered from the gold foil throughout the same period. A calibration of the scattering from the gold foil when a known current impinged upon it with a vacuum in the scattering chamber permitted the calculation of absolute numbers of protons in the incident beam during the scattering experiments. This arrangement circumvented the objection to our previous work that it was impossible to measure the current in the beam simultaneously with the gas-scattering observations, because of the production of secondary electrons in the Faraday cage.

An important item which had to be taken into account for each measurement was the change in the energy of the protons between the scattering volume and the gold leaf due to the stopping power of the intervening gas. The number of protons scattered from the gold per microampere-minute with a vacuum in the scattering chamber was determined over the range of voltage to be encountered, using the insulated lower part of the scattering chamber as a Faraday cage. (Tests with a magnetic field showed that the current-readings were correct to one-half percent or less.) In any later observation with gas in the chamber the energy of the protons at the gold foil was then known from the voltage and stopping powers of windows and gas, and the proton-current passing through the scattering volume was taken directly from the curve of the vacuum Faraday-cage observations. No correction was made for the negligible proton-current lost from the beam by scattering in the gas in the chamber or the negligible gas-scattering into the gold counter. Inhomogeneity in the gold leaf could give rise to an error due to the spreading of the beam over a larger area of the gold when gas was present than when the current calibrations were made, with a vacuum in the chamber. This was checked by measuring the number of protons scattered from the gold foil (under steady conditions of beam current and voltage) first with a vacuum and then again with 1.5 mm of air in the scattering chamber. The decrease in the energy of the protons of

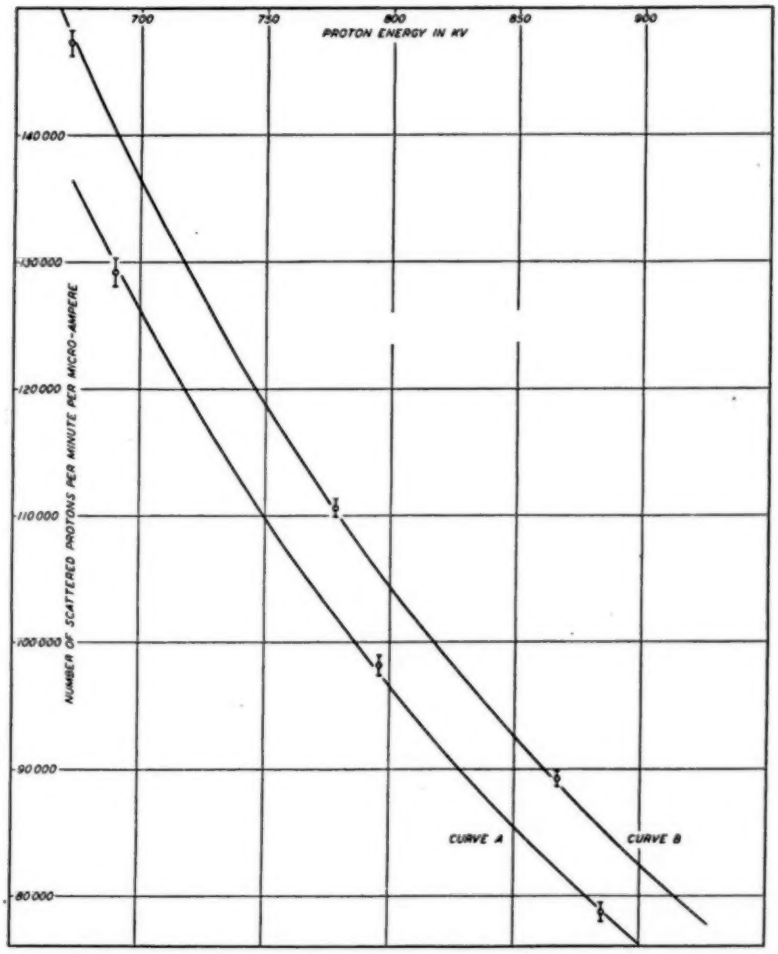

FIG. 2. Current-calibration curves, gold-foil scattering.

23 kv due to the stopping power of the added air should increase the scattering by 6.25 percent according to the classical theory of scattering. It was found that the number of counts actually did increase by 6.2 percent when the gas was added, in agreement with the theory, and indicating that the spread of the beam due to the pressure of the gas did not affect the counting rate from the gold leaf.

The gold leaf, which had a stopping power for protons of less than one mm, was mounted on a brass ring. The ionization chamber C_2 was placed to observe protons scattered at approximately 135°. The opening into the chamber was 0.5 mm in diameter, covered with a thin collodion window. The size of this hole was chosen to give a counting rate of about 2000 protons per minute with the current used in the scattering observations. As any single observation lasted for five minutes or longer, the statistical error introduced by counting only the small fraction of the total beam scattered by the gold was one percent or less. An independent amplifier and counting unit was used for the gold-foil scattering, and counts were recorded simultaneously with the counts from the gaseous scatterer.

The calibration-curves for the gold-foil scattering are shown in Fig. 2. The number of scattered protons per minute per microampere beam current is plotted as the ordinate and the energy of the proton as the abscissa. The length of the lines through the points indicates the probable error, each point representing about 25,000 counts. According to the Rutherford scattering law, which should be obeyed by gold for protons of these energies, the number of scattered par-

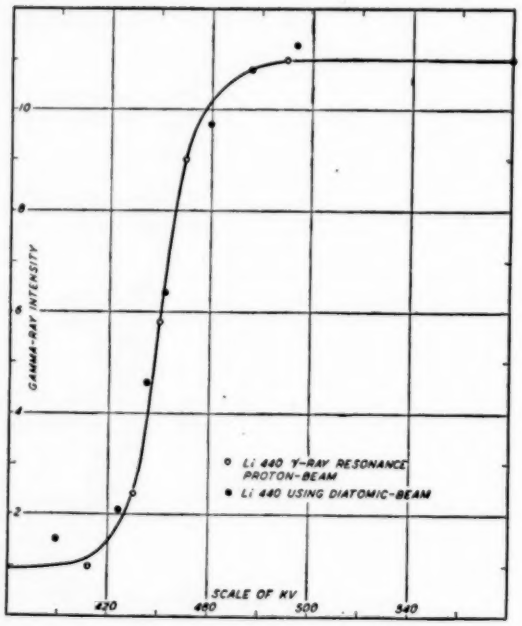

FIG. 3. Lithium gamma-ray resonance at 440 kv, using proton monatomic and diatomic beams.

ticles from the gold should vary as $1/V^2$, where V is the voltage of the incident protons. The curves in Fig. 2 are proportional to $1/V^2$ and represent the best adjustment to the points. These curves were calculated by taking the average value of the product of the square of the voltage by the observed counts at that voltage.

Curve A is the calibration curve used during the second series of scattering measurements. After this series was completed it was noticed that the counter, recording protons scattered from the gold leaf, missed an appreciable, but constant, fraction (eight percent) of the counts, due to excessive bias. This condition was corrected by adjusting the amplifier to give much larger pulses which were assuredly counted by the Thyratron-unit. Curve B was taken after this correction had been made and was used for the third series of the scattering observations. No error is introduced in the second series of measurements provided that the fraction of the counts missed remained the same during the calibration and during the measurements. Fortunately, all adjustments of the amplifier and of the Thyratron-unit remained unchanged during the calibration of curve A and the second series of scattering measurements, and evidence obtained from the series itself shows that any error introduced was very small.

At all times the counting rates of both Thyratron-units were sufficiently low that the number of counts missed through failure to resolve simultaneous counts was negligible (less than one percent). To insure that this was the case a test was made by counting with much larger currents and observing the resultant decrease in the number of counts per minute per microampere. With very large currents the number missed was proportional to the square of the counting rate so that it was possible to extrapolate back to determine safe counting rates.

Voltage measurements

In any experiment dealing with scattering of particles it is important that the energy of the incident particle be known as accurately as possible. When dealing with Coulomb scattering, an error of one percent in the voltage measurement is sufficient to introduce an error of two percent in the final result. The situation is even more serious when observing the anomalous scattering of protons by protons around 45°, where an error of one percent in voltage can cause a final error of four or five percent, due to the rapid change of the scattering anomaly with voltage. The greatest feasible precautions have therefore been taken to insure a minimum contribution from this source of error. In these experiments it is necessary to know the energy (velocity) of the proton at the scattering volume and at the gold foil. This necessitates measuring the voltage applied to the accelerating tube, the stopping power and uniformity of the aluminum window of the scattering chamber, and the stopping power of the gas traversed in the chamber before reaching the small scattering volume defined by the diaphragm-systems.

Calibration of resistance voltmeter

The accelerating voltage was measured by observing the current which passed through the corona-free high resistance unit (10,000 megohms) previously described.[7] The 440-kv gamma-ray resonance in lithium was used as the nominal standard of voltage. The measured voltage of 440

[7] L. R. Hafstad, N. P. Heydenburg and M. A. Tuve, Phys. Rev. **50**, 504–514 (1936).

kv originally assigned by us was considered to be accurate to within two percent as it was measured immediately after the original calibration of the resistance unit of the voltmeter in 200-kv sections at the National Bureau of Standards. It was necessary for the present work to recalibrate the high resistance unit and to recheck its performance in respect to the absence of corona, because the rubber tubing in which the individual unit resistors were originally enclosed had been replaced by varnished cambric tubing since the first calibration. This was accomplished by again assigning the value 440 kv to the voltage at which the lithium resonance occurred; the voltage at which the same resonance was observed when bombarding with molecular hydrogen ions was correspondingly assigned the value 880 kv. These points do not lie quite on a straight line through the origin, possibly because of heating effects in the voltmeter resistor, so a parabola drawn through these points and zero was taken as the correct calibration curve of the voltmeter. Fig. 3 shows the measurement of the lithium resonance used in the recalibration of the voltmeter. The equation of the calibration curve is

$$V=9.85\ I-0.00766\ I^2,$$

where V is in kv and I is in microamperes. The correction term in I^2 is presumably due to the heating of the resistors. To obtain strictly consistent results it was necessary that the voltage be applied to the voltmeter for about 45 minutes to insure thermal equilibrium before any measurements were made. This effect was observed directly by measuring the 867-kv fluorine gamma-ray resonance at five-minute intervals after first applying the voltage. The equilibrium reading of the current through the voltmeter resistor at the resonance voltage corresponded to a voltage approximately 20 kv lower than the initial reading. The same effect was also observed in bench measurements on individual resistor units. In all calibrations and scattering measurements the voltage was turned on at least 45 minutes previous to any observations to preclude any errors of this sort. Because of a peculiar construction of our apparatus the total accelerating voltage is measured in two parts, the voltage applied to the first two focusing gaps and the voltage applied to the rest of the tube. The agreement of the calibration of the two voltmeters was checked by observing the extremely sharp 334-kv fluorine resonance first with 100 kv applied to the first two gaps and later with 20 kv. The corresponding change in the voltage applied to the rest of the tube showed that the calibrations of the two sections were in good agreement.

The fluorine gamma-ray resonance at 867 kv is a more useful voltage reference point for the higher voltage range than the 880-kv point of lithium because of the greater intensity of the gamma-radiation. The voltage at which this resonance occurred was therefore measured in comparison with the 880-kv point of the lithium resonance and thereafter was used as a reference point. Some difficulty was encountered in this measurement due to the charging up of the CaF_2 crystal used as a target. This effect was called to our attention by Drs. Herb and Breit. It was found that the displacement of the resonance was proportional to the bombarding current and was due to the IR potential drop across the target. For one microampere of impinging protons the displacement was approximately 15 kv. The effect was avoided by covering the crystal target with a fine gauze, otherwise by using a low resistance target composed of a pasty mixture of calcium fluoride powder, water, and phosphoric

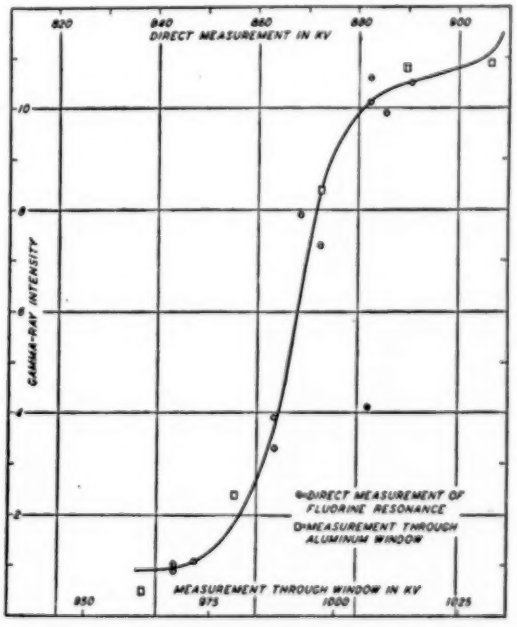

FIG. 4. Fluorine 867-kv gamma-ray resonance before and after passing through aluminum window.

acid. Our previously published[7] voltage for this resonance is accordingly too high because of this error. Using a thin target Herb and colleagues[8] assigned the voltage 862 kv to this resonance, but the best value from our thick target observations seemed to be 867 kv. Fig. 4 shows a typical determination of this resonance voltage. Throughout the scattering measurements frequent observations were made of this resonance to insure that there was no change in the calibration of the

[8] E. J. Bernet, R. G. Herb and D. B. Parkinson, Phys. Rev. **54**, 398–408 (1938).

TABLE III. *Observed scattering of protons by protons, second and third series, Washington, D. C., spring of 1938, voltage-scale based on lithium gamma-ray resonance at 440 kv.*

θ	Ratio $\times 10^3$, hydrogen to gold	Probable error, from fluctuations among data	Observed N_θ from hydrogen per μa minute	N_θ corrected for zero-angle and strays	Total counts	Calculated N_θ per μa minute	Ratio N_θ observed to N_θ Mott	Probable error of ratio
Second series: Five runs; scattering at 867 kv; 843 kv at Au foil; total tube voltage 1011 kv								
20°	235.48	±1.33	20,439	19,434	11,511	26,285	0.74	±0.004
25	83.489	2.18	7246.8	7028.8	2852	8251.5	0.85	0.02
27.5	63.252	2.18	5490.3	5379.5	2415	5013.2	1.07	0.035
30	50.569	0.85	4389.4	4340.5	2942	3184.0	1.36	0.024
32.5	43.136	0.16	3744.2	3711.8	2051	2108.8	1.76	0.03
35	40.230	0.60	3492.0	3462.6	2820	1459.0	2.37	0.04
37.5	34.969	0.30	3035.3	3013.0	2093	1058.0	2.85	0.04
40	31.583	0.11	2741.4	2725.8	2735	811.81	3.36	0.05
42.5	29.324	0.42	2545.3	2533.8	2125	665.00	3.81	0.06
45	27.232	0.41	2363.7	2354.7	2801	586.59	4.01	0.06
Second series: Four runs; scattering at 776 kv; 752 kv at Au foil; total tube voltage 924 kv								
20°	225.95	±1.46	24,674.	23,276	11,669	32,841	0.71	±0.005
25	72.412	0.45	7907.3	7574.5	3352	10,310	0.73	0.008
27.5	51.828	1.59	5659.6	5508.8	2092	6263.7	0.87	0.03
30	40.230	0.60	4393.1	4324.1	1935	3977.9	1.09	0.016
32.5	32.847	0.31	3586.9	3546.2	1874	2634.3	1.35	0.02
35	26.636	0.65	2908.7	2877.0	2074	1821.4	1.58	0.04
37.5	23.330	0.30	2547.6	2521.7	1931	1341.3	1.88	0.03
40	21.639	0.22	2362.9	2349.3	1936	1013.5	2.31	0.03
42.5	19.527	0.56	2132.3	2122.7	1878	830.25	2.55	0.07
45	18.474	0.23	2017.4	2009.0	1985	732.24	2.75	0.04
Second series: Three runs; scattering at 670 kv; 640 kv at Au foil; total tube voltage 827 kv								
20°	205.13	±3.40	30,934	29,437	8134	44,119	0.67	±0.011
25	58.068	2.47	8756.6	8493.8	2376	13,850	0.61	0.008
30	27.428	0.16	4136.1	4032.6	1016	5342.5	0.75	0.014
32.5	20.866	0.67	3146.6	3099.4	967	3537.5	0.87	0.02
35	16.356	0.20	2466.5	2440.4	1439	2445.1	0.99	0.02
37.5	13.807	0.28	2082.1	2064.9	1451	1773.0	1.17	0.02
40	12.095	0.05	1823.9	1809.4	1474	1359.7	1.33	0.02
42.5	11.347	0.06	1711.1	1699.3	1445	1113.8	1.52	0.03
45	9.844	0.19	1484.5	1474.9	1330	982.22	1.50	0.03
Third series: One run; scattering at 867 kv; 843 kv at Au foil; total tube voltage 1011 kv								
20°	215.1	....	....	19,276	17,822	....	0.73	....
25	78.95	....	....	7220	4048	....	0.87	....
30	48.26	....	....	4498	2760	....	1.41	....
35	36.29	....	....	3388	1806	....	2.32	....
40	28.75	....	....	2694	1673	....	3.32	....
45	24.73	....	....	2321	1503	....	3.96	....
Third series: One run, scattering at 776 kv; 752 kv at Au foil; total tube voltage 924 kv								
20°	204.7	....	....	22,991	15,944	....	0.70	....
45	16.81	....	....	1982	503	....	2.71	....
Third series: One run; scattering at 670 kv; 640 kv at Au foil; total tube voltage 827 kv								
20°	193.3	....	....	30,956	6288	....	0.68	....
45	8.81	....	....	1468.6	110	....	1.46	....

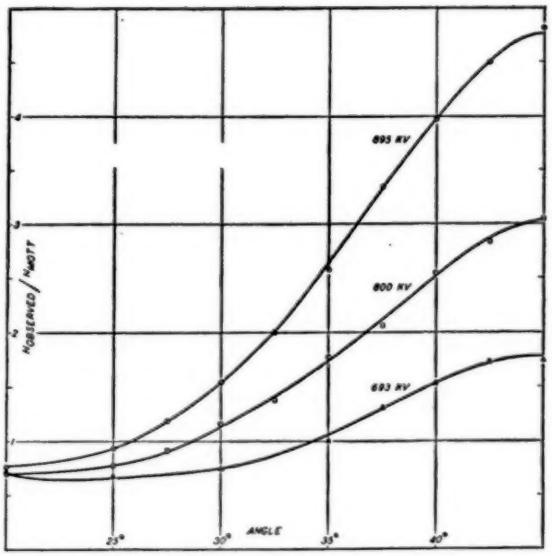

FIG. 5. Proton-proton scattering, first series of observations.

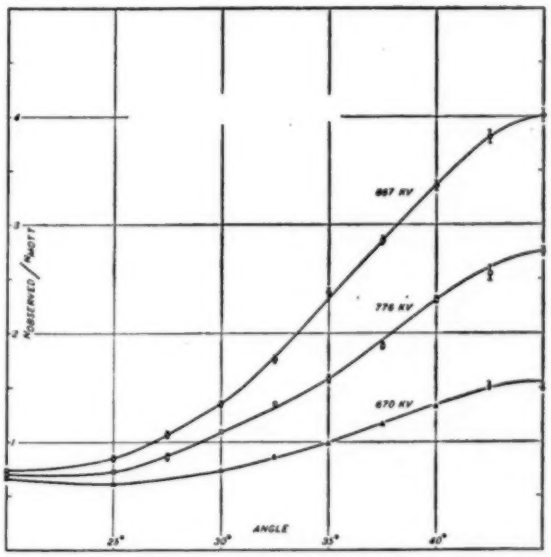

FIG. 6. Proton-proton scattering, second series of observations.

voltmeter unit. All values of voltage in this paper refer to the nominal voltage scale based on assigning the value 440 kv to the lithium resonance but, as will be noted below, the absolute calibration of this voltage scale in terms of the Coulomb scattering of protons by spectroscopically pure argon gas shows that our nominal scale is correct to within about one percent.

Stopping power of window and gas

The stopping power of the aluminum foil through which the protons entered the scattering chamber was measured by further observations of the fluorine resonance. For this purpose a calcium-fluoride crystal was placed inside the scattering chamber and bombarded by protons which passed through the aluminum window. The difference in the observed resonance voltages as measured inside and outside the scattering chamber, with due precautions to avoid charging up of the crystal, is due to the stopping power of the window. The range-curve of Parkinson and associates[9] for protons in aluminum was then used to determine the thickness of the aluminum window. When using protons of any other energy the same range curve was used to give the stopping power of the window at the other voltage. This measurement had to be repeated from time to time to measure the change in the stopping power of the window due to accumulation of carbon. As this deposit of carbon never became greater in thickness than 15-kv stopping power and the aluminum windows were approximately 100-kv stopping power, it was not necessary to calculate the stopping powers separately. The current reaching the CaF_2 target at the bottom of the scattering chamber was always so small that the charging effect of the crystal previously mentioned was not observable. Fig. 4 shows fluorine resonance curves as observed inside and outside of the scattering chamber.

The stopping power of the gas in the scattering chamber was calculated from the known pressure and length of path. Herb's range curve for protons in air and Bethe's[10] data for the relative stopping powers of the various gases were used. For the stopping power of hydrogen we used 0.24 times the stopping power of air, for nitrogen and oxygen the same as air, and for argon 1.92 times that of air. In obtaining the voltages at the scattering volume and at the gold foil some inaccuracy is introduced because of the difficulty in reading the voltages from the range curve. This could introduce an over-all error in the final scattering results of about one percent.

[9] D. B. Parkinson, R. G. Herb, J. C. Bellamy and C. M. Hudson, Phys. Rev. **52**, 75–79 (1937).

[10] M. S. Livingston and H. A. Bethe, Rev. Mod. Phys. **9**, 272 (1937).

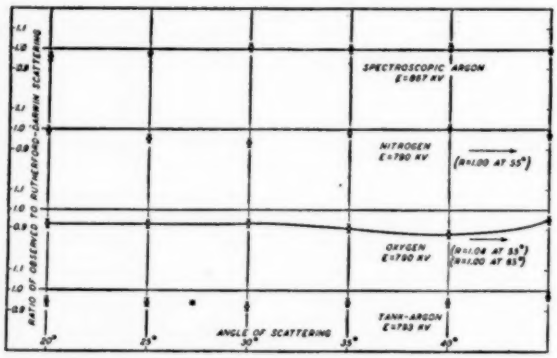

FIG. 7. Proton scattering in argon, nitrogen and oxygen.

Method of reduction of experimental data

The experimental data consist of a certain number N_H of scattered protons from the gas target for a given number N_G of scattered protons from the gold foil, the latter being a measure of the incident beam current. The ratio (N_H/N_G), if multiplied by the conversion factor from gold-scattering counts per minute to microamperes (Fig. 2), will then give the number which can be compared to the Mott value N_s as given in Table III. This conversion factor is read directly from the gold foil calibration curves in Fig. 2. The voltage to be used at the gold foil is lower than that at the scattering volume, of course, by the loss of voltage due to the intervening gas.

V. RESULTS

After the first set of observations of this group were made on proton-proton scattering, it was discovered that the microammeter used to measure the current through the voltmeter resistor between the concentric spheres of the electrostatic generator had changed its calibration some time during the period the data were being taken. When recalibrated, the meter read 12 percent low. This would amount to a correction of a little over one percent in the total voltage on the tube. This meter had not been properly protected against transients when sparking occurred on the generator. We are, therefore, uncertain as to the exact energy at which these curves were taken and hence the absolute values of the ratios of the observed counts to the Mott-theory scattering do not quite agree with the data taken later. However, the curves, as shown in Fig. 5, have the same general contour and therefore add weight to the later observations. Each curve is the average of from two to three independent runs. The probable error based on the spread of the data is given by the lines through the points on the curves.

After the first set of observations described above, the aluminum window and gold foil were accidentally damaged due to a sudden burst of air into the scattering chamber. New aluminum and gold foils were then installed and calibrated. This aluminum window had a stopping power of 113 kv. The calibration curve for the scattering of protons from this gold foil is given in Fig. 2; curve A has been used for the second series of observations and curve B for the third series as discussed in Section II. The gold foil curve for the first series is not shown.

Table III gives rather completely the data for the second and third series of observations on proton-proton scattering. In this table we have included the initial voltages of the protons, their voltage at the scattering volume and at the gold foil.

The observed ratio of hydrogen to gold scattering given in column 2 of Table III is the average of three to five independent runs; a new filling of

TABLE IV. *Proton scattering in oxygen and nitrogen.*

θ	Ratio $\times 10^3$, gas to gold	N_s corrected for zero-angle	Total counts	Calculated $N_s(R-D)$	Ratio N_s observed to $N_s(R-D)$	Probable error (statistical)
		Oxygen: 790 kv; 780 kv at Au foil				
20°	1792.4	177,700	7,144	190,518	0.93	0.014
25	594.2	59,470	14,672	63,880	0.93	0.014
30	245.0	24,680	2,565	26,406	0.93	0.014
35	113.7	11,500	1,662	12,632	0.91	0.014
40	58.59	5,943	1,115	6,735.7	0.88	0.02
45	36.41	3,705	971	3,906.9	0.95	0.02
55	16.13	1,652	278	1,581	1.04	0.03
65	7.59	777	187	777.1	1.00	0.04
		Oxygen: 684 kv; 669 kv at Au foil				
25°	601.3	80,540	18,480	85,212	0.95	0.014
		Oxygen: 882 kv; 870 kv at Au foil				
25°	629.6	50,540	21,656	51,247	0.99	0.014
		Nitrogen: 684 kv; 669 kv at Au foil				
20°	1454	144,200	6,184	145,864	0.99	0.014
25	461.9	46,220	13,900	48,908	0.95	0.014
30	185.9	18,720	3,353	20,217	0.93	0.014
35	93.31	9,435	1,980	9,672.0	0.98	0.014
40	50.98	5,169	1,442	5,157.1	1.00	0.02
45	28.45	2,894	885	2,991.1	0.97	0.02
55	11.79	1,208	343	1,211.0	1.00	0.03
		Nitrogen: 790 kv; 780 kv at Au foil				
25°	445.3	59,630	14,568	65,240	0.91	0.014
		Nitrogen: 882 kv; 870 kv at Au foil				
25°	485.5	38,960	13,816	39,236	0.99	0.014

hydrogen was used for each run. In column 5 labeled "Observed N_s, corrected for zero-angle and strays" we have applied the percentage correction for the shift in the zero position as discussed in Section III and given in Table II. The stray-count correction, due to the counting rate when the scattering chamber is evacuated, amounted to about one percent of the counting rate with the hydrogen in the chamber. The ratios of the observed N_s to that calculated from the Mott formula of Section II are given in column 8 and are plotted in Fig. 6.

After completion of the second group of observations, some improvements were made on the amplifier which counted the protons scattered from the gold foil. The oscillograph then showed that the pulses were about five times the noise level, thus removing any doubt of their being recorded on the Thyratron counter. At this stage it was decided to recalibrate the gold foil and to repeat some points on the proton-proton scattering curves. The results on this third set of observations are given in Table III. It is seen that the agreement with the second series is good. The entire curve at 876 kv was checked but only the points at 20° and 45° for the other two voltages. This agreement with the results of the second series indicates that they were reliable even though the gold-foil scattering counter was missing a few counts (eight percent). The number missed must have remained approximately constant during the calibration of the foil and the scattering measurements. This is reasonable since the amplifier gain was adjusted, by means of a gain control, before (and checked after) each run to give the same grid bias setting on the selector tube of the scale-of-eight counter for the amplifier noise level. The grid bias was then set a fixed amount above this noise level.

During the course of the second series of observations we tried the scattering of protons from nitrogen and oxygen. If the scattering from these gases proved to behave classically it could be used as a check on the absolute calibration of the scattering apparatus and voltage scale. These data are given in Table IV and the ratio of the observed scattering to that predicted from the Coulomb scattering law is plotted in Fig. 7. The

TABLE V. *Proton scattering in spectroscopically pure argon.*

θ	Ratio $\times 10^3$, argon to gold, $p=1.00$ mm	N_s corrected for zero-angle	Total counts	Calculated $N_s(R-D)$ per μa minute	Ratio N_s observed to $N_s(R-D)$	Probable error (statistical)
			867 kv, 858 kv at Au foil			
20°	4404	383,250	2,960	397,951	0.96	0.018
25	1487	130,503	77,530	133,438	0.98	0.004
30	630	55,581	10,800	55,160	1.01	0.01
35	300	26,561	6,504	26,388	1.00	0.012
40	160	14,239	4,040	14,070	1.01	0.016
45	90.5	8,075	1,544	8,161	0.99	0.026
			781 kv, 773 kv at Au foil			
25	1531	166,287	17,128	164,435	1.00	0.01
			683 kv, 673 kv at Au foil			
25	1505	215,539	17,902	215,019	1.00	0.01

deviations of these ratios are larger than can be accounted for by experimental errors. Oxygen shows an appreciable dip in the variation of the scattering with angle at 40°. The variation of both oxygen and nitrogen scattering with energy is not strictly in agreement with classical theory and at present is not explained except as a true scattering anomaly. The scattering from argon was then tried. It is of course much more to be expected that argon gives rise only to Coulomb scattering, because of the larger nuclear charge. The ratios of the observed to Rutherford-Darwin scattering for tank argon and spectroscopically pure Linde argon are given in Table V and are plotted in Fig. 7. The scattering for spectroscopic argon agrees in absolute value with the classical theory using the voltage scale discussed above in Section III, in which the lithium gamma-ray resonance was given the value 440 kv. The tank argon is seen to be about five percent lower than the spectroscopic argon; this is probably due to air contamination because this argon had been stored for some time in a laboratory tank at about atmospheric pressure.

The theoretical significance and discussion of our results has already been given by Breit, Thaxton and Eisenbud.[5]

We wish to express our indebtedness to Dr. J. A. Fleming for his continued support of this program. We also want to acknowledge the important part taken in this work by R. C. Meyer, who designed and constructed the scattering apparatus.

Deuteron-Deuteron, Proton-Helium, and Deuteron-Helium Scattering

N. P. HEYDENBURG AND R. B. ROBERTS
Department of Terrestrial Magnetism, Carnegie Institution of Washington, Washington, D. C.
(Received October 9, 1939)

Measurements have been made on deuteron-deuteron scattering at angles between 20° and 45° for incident deuteron energies of 832, 720, and 614 kv. In this range of angles and energies the ratio of the observed scattering to that predicted by classical theory, as modified according to Mott to take account of the identity of the particles, is always greater than unity. At 832 kv the ratio increases from 1.28 at 15° to 3.98 at 45°. This anomaly is of the type to be expected if there is present a short range repulsive force between the particles in addition to the Coulomb force. The scattering of protons in helium was in agreement with the Rutherford-Darwin scattering formula for 994-kv protons in the angular range from 20° to 45°. The scattering of deuterons in helium showed an anomaly which increased from about unity at 20° to 4.4 at 75°. This anomaly also indicates an additional repulsive nuclear force between the deuteron and helium particles.

INTRODUCTION AND TECHNIQUE

WHILE making the proton-proton scattering measurements described in the preceding paper, we also made some observations on the scattering of deuterons on deuterons and of protons and deuterons in helium. These measurements were confined to the region 600 to 1000 kv for the energy of the incident particles. The apparatus and technique were the same as used for the proton-proton scattering, and has already been discussed in detail in the preceding paper. The gold-foil scattering technique was used as the current monitor and integrator for the incident beam. The ratio of the number of scattered particles, N_H, from the gas to the number, N_G, from the gold foil was recorded, and the number of scattered particles, N_S, from the gas per minute per microampere of beam-current was then given by $N_S=N_H n/N_G$, where n is the number of counts from the gold foil per minute per microampere. The value of N_S was then compared to the predicted classical scattering as calculated from the constants of the apparatus, the pressure of the gas target, and the energy of the initial particles.

Deuterium of purity better than 99 percent, obtained from the Stuart Oxygen Company, was used throughout the experiments on deuteron-deuteron scattering both in the ion-source and for the scattering gas. The deuterium was introduced into the scattering chamber through a palladium tube. It was found that very careful outgassing of the palladium tube, which had previously been used for ordinary hydrogen, was necessary to eliminate hydrogen contamination of the deuterium. The palladium tube was heated to a dull red heat in a vacuum for some time, then deuterium was passed through it for several hours. After this treatment the hydrogen contamination was negligible. For the deuteron-deuteron scattering the presence of ordinary hydrogen in the scattering volume was readily detectable from the scattering results. In the scattering of deuterons in light hydrogen (protium) the classical Rutherford-Darwin theory predicts that there will be no scattered deuterons beyond a 30° angle. This results from the fact that in the general formula for the scattering cross section

$$q=Qnt\omega\left(\frac{ZeE}{Mv^2}\right)^2 \csc^3\theta \times\frac{\{\cot\theta\pm[\csc^2\theta-(M/m)^2]^{\frac{1}{2}}\}^2}{[\csc^2\theta-(M/m)^2]^{\frac{1}{2}}},$$

the radical in the denominator becomes negative for $\theta>30°$. The presence of ordinary hydrogen can be recognized by a sharp increase in the number of scattered deuterons at 30° in going from larger to smaller angles. Preliminary observations made before the palladium tube was well outgassed showed this effect very clearly; after careful outgassing it disappeared. Any hydrogen contamination in the magnetically analyzed deuteron-beam would be in the form of diatomic hydrogen ions, each proton having only half the energy of the deuterons, and therefore would not be recorded by our ionization-chambers. We used a deuterium pressure of 12 mm of mercury in the scattering chamber for these experiments.

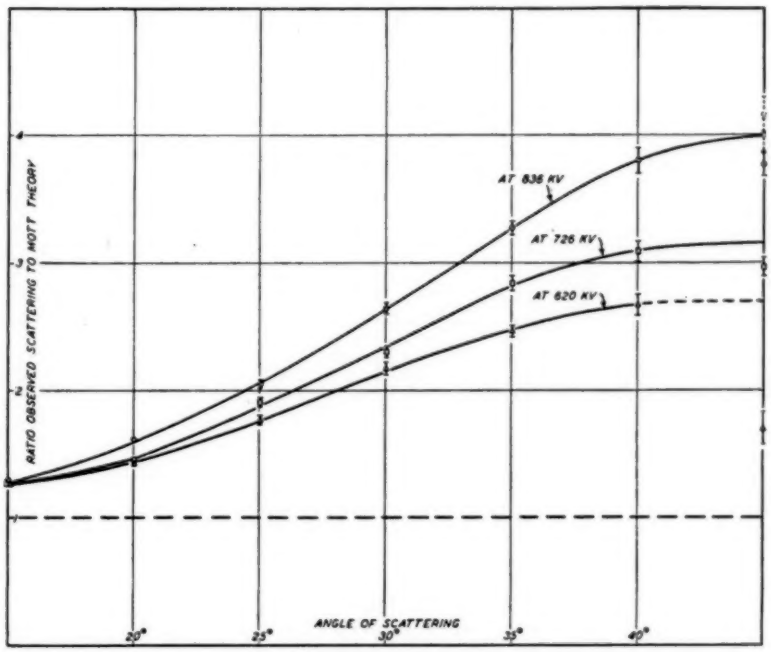

FIG. 1. Scattering of deuterons in deuterium.

For the scattering in helium we used 10-mm mercury pressure of commercial helium (98 percent), which was purified somewhat by passing through a liquid-air-cooled charcoal trap.

For proton-helium and deuteron-helium scattering there will be two groups of particles at a given angle, the scattered incident particle and the recoil helium or alpha-particle. It can easily be shown by calculating the range of the recoil alpha-particle that the recoils will not have sufficient energy to be counted in the case of the proton-helium scattering. For the deuteron-helium scattering the recoil alpha-particles entering the detector at an angle of 35° or less might perhaps have sufficient energy to be counted. The recoils at 35° are the result of collisions in which the deuteron is scattered at about 80°. The deuterons scattered at 80° and hence the recoil alphas at 35° would amount to only 2.5 percent of the number of deuterons scattered at 35° on the basis of the Rutherford-Darwin theory, and to about five times this or ten percent if one takes into account the observed scattering anomaly. Hence the effect of the recoil alpha-particles on the scattering curves would be small even if they were counted. The observed curves in Fig. 2 give no indication of their presence.

TABLE I. *Results on proton-helium, deuteron-helium scattering.*

θ	Ratio D to Au (corrected)	N observed (corrected)	N Mott	Ratio N observed to N Mott	Total count	Probable error (statistical)
			V = 832 kv			
15°	1776.3	176,919	138,052	1.28	29,750	..
20	564.20	56,194	34,996	1.61	12,930	0.01
25	257.39	25,636	12,651	2.02	4,410	0.03
30	153.70	15,309	5,844.7	2.62	7,270	0.04
35	106.77	10,634	3,281.2	3.24	2,170	0.07
40	82.52	8,219.0	2,182.5	3.77	2,080	0.09
45	63.73	6,347.5	1,698.2	3.74	1,930	0.09
(45)	(67.83)	6,755.9		(3.98)		
			V = 720 kv			
15	1703.2	232,487	184,340	1.26	16,804	0.01
20	489.74	66,850	46,730	1.43	5,860	0.02
25	233.05	31,811	16,892	1.88	7,940	0.03
30	129.56	17,685	7,804.4	2.27	3,341	0.04
35	89.72	12,247	4,381.3	2.80	3,011	0.05
40	64.95	8,865.7	2,914.3	3.04	2,925	0.06
45	48.47	6,616.2	2,267.6	2.92	1,037	0.09
			V = 614 kv			
15	1684.1	321,663	253,484	1.27	16,794	0.01
20	470.57	89,879	64,257.4	1.40	8,392	0.02
25	211.30	40,358	23,227.7	1.74	4,579	0.03
30	119.71	22,865	10,731.7	2.13	2,115	0.05
35	75.98	14,512	6,024.6	2.41	2,098	0.05
40	55.01	10,507	4,007.4	2.62	1,727	0.06
45	27.37	5,227.7	3,118.2	1.68	910	0.06

RESULTS AND DISCUSSION

In the deuteron-deuteron scattering we are concerned with identical particles, so instead of comparing our results with the Rutherford-Darwin scattering law we have used the following

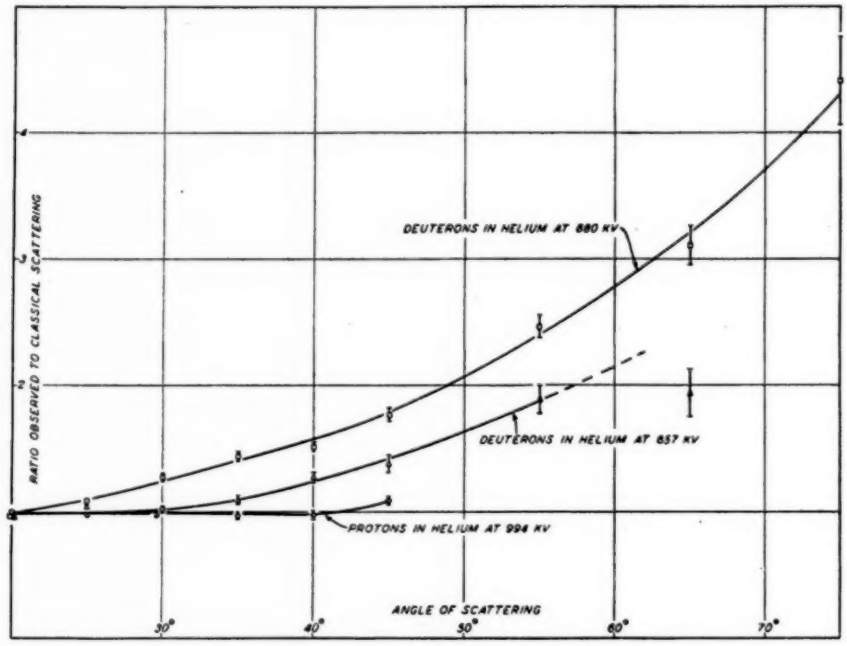

FIG. 2. Scattering of deuterons and protons in helium.

scattering cross section for Coulomb interaction, which takes into account the interference effect for identical particles:

$$q=(e^4/m^2v^4)(\csc^4\theta+\sec^4\theta+\tfrac{2}{3}\Phi\csc^2\theta\sec^2\theta)\times 4\cos\theta, \quad (1)$$

where $\Phi=\cos[(2\pi e^2/hv)\log\tan^2\theta]$. This equation includes both scattered and recoil deuterons since they are indistinguishable and was obtained directly from the equations and discussions given, by Mott and Massey.[1]

Our results are given in Table I for deuteron energies 832, 720, and 614 kv, for scattering angles between 15° and 45°. The number of scattered deuterons observed per minute per microampere of the incident beam has been compared to the number to be expected according to Eq. (1) for our apparatus constants, the number and energy of the incident deuterons, and the pressure of the scattering gas; this number we have called the Mott value. The ratio of the observed scattering to the Mott value has been plotted in Fig. 1. There is a definite disagreement with the scattering cross section calculated from the above equation. The anomaly thus indicated is of the same order as that which has been found for proton-proton scattering although it differs in its dependence on the energy of the incident deuterons and also in the dependence on angle. The deuteron-deuteron ratio remains above unity even down to an angle of 15° while the ratio for proton-proton scattering was 30 percent below

[1] N. E. Mott and H. S. W. Massey, *The Theory of Atomic Collisions* (Cornell University Press, 1933), pp. 73–77.

TABLE II. *Results on deuteron-deuteron scattering.*

θ	Ratio $\times 10^3$ He to Au scatterer, He pressure = 10 mm	N_S corrected for zero angle	$N_S(R-D)$	Ratio	Total count	Probable error (statistical)
	H–He, *994 kv, 978 kv at* Au *foil (gold counts 696)*					
20°	568.8	3792.2	3766.4	1.01	18,100	0.01
25	183.4	1239.3	1263.4	0.98	1,900	0.016
30	77.65	537.60	521.97	1.03	1,000	0.021
35	36.78	251.04	249.38	1.01	800	0.024
40	20.15	137.64	132.93	1.04	500	0.03
45	13.47	92.24	77.057	1.20	425	0.03
	D–He, *880 kv, 850 kv at* Au *foil (gold counts 904)*					
20	528.5	4569.0	4821.5	0.95	13,177	0.006
25	197.8	1741.9	1616.3	1.08	2,101	0.02
30	94.30	835.0	667.2	1.25	2,184	0.03
35	50.86	453.0	318.3	1.42	1,002	0.03
40	28.23	252.0	169.1	1.49	746	0.04
45	19.20	171.7	97.96	1.75	577	0.05
55	10.67	96.02	39.32	2.44	324	0.09
65	6.50	58.57	19.05	3.07	191	0.15
75	5.11	46.05	10.54	4.37	73	0.35
	D–He, *657 kv, 623 kv at* Au *foil (gold counts 1676)*					
20	510.0	8173.0	8680.8	0.94	7,986	0.01
25	182.4	2975.0	2910.1	1.02	2,774	0.01
30	71.2	1166.0	1201.2	0.97	1,440	0.02
35	37.49	617.1	573.1	1.08	804	0.03
40	22.97	380.6	304.5	1.25	515	0.04
45	14.40	239.4	176.4	1.36	200	0.07
55	7.89	131.6	70.78	1.86	116	0.11
65	3.93	65.5	34.31	1.91	57	0.19

unity at 20°. This anomaly for deuteron-deuteron scattering is of the type to be expected if there is present, in addition to the Coulomb interaction, a short range repulsive force between the deuterons. An additional repulsive force would give an increase in scattering even at small angles (15° to 30°), while an attractive force would give a reduction in scattering at small anlges due to a cancellation-effect between the Coulomb repulsive force and the assumed attractive force.

The results for the scattering of protons and deuterons in helium are summarized in Table II. We have given the number of scattered particles to be expected from the Rutherford-Darwin scattering formula; the ratio of the observed scattering to this calculated number has been plotted as a function of angle in Fig. 2. At 700 kv the proton scattering in helium from 20° to 45° was in agreement with the inverse-square law of scattering (curve and data not given). However, there appears to be a slight excess of scattering at 45° for 994-kv protons. This is probably a real effect.

The scattering of deuterons in helium was investigated at two energies, 657 and 880 kv, and for scattering angles up to 75°. Beyond this angle at 880 kv the range of the scattered deuterons is too small to count reliably in our detector; for 657 kv some of the scattered deuterons were missed at 65°. At 880 kv the scattering at 75° is 4.4 times the expected value from the inverse-square scattering law. The slope of these curves against angle is similar to those for deuteron-deuteron scattering, indicating that one also has an additional repulsive force entering here between the two particles.

DECEMBER 1, 1939 PHYSICAL REVIEW VOLUME 56

Nuclear Isomerism in Zinc

J. W. KENNEDY, G. T. SEABORG AND E. SEGRÈ
Radiation Laboratory, Department of Physics, and Department of Chemistry, University of California, Berkeley, California

(Received October 6, 1939)

Zn^{69} has two isomeric states differing by 0.47 Mev in energy. The upper state decays into the lower with a half-life of 13.8 hours, emitting a gamma-ray which has an internal conversion coefficient less than 0.1. The lower isomeric state decays to Ga^{69} with a half-life of 57 minutes. The most probable value for the spin difference between the isomeric states is five.

IN a systematic study of the radioactive zinc isotopes, Livingood and Seaborg[1] found two beta-emitters, with half-lives of 13.8 hours and 57 minutes, respectively, both of which were assigned to Zn^{69}. These isomers were found to have very similar beta-spectra, but the 13.8-hour period was accompanied by gamma-radiation whereas no gamma-rays were associated with the 57-minute period. These results suggest at once that the 13.8-hour activity decays to Ga^{69} passing through the isomeric state of 57 minutes half-life. Since this case is fairly simple and experimentally accessible, we have investigated the situation in more detail.

The radioactivities were produced by the reaction Zn^{68} (d, p) Zn^{69} as the result of bombardment of zinc with about 50 microampere-hours of 8-Mev deuterons in the Berkeley cyclotron. The measurements were made upon chemically separated samples. The gallium and copper, primary transmutation products, were removed by ether extraction and with hydrogen sulfide in acid solution, respectively.[2] Zinc was precipitated last by the addition of sodium carbonate.

The measurements were made with an aluminum ionization chamber connected to a vacuum tube electrometer system. The chamber and its calibration have already been described.[3]

If the upper isomeric state decays by means of a gamma-ray with a life of 13.8 hours to a

[1] J. J. Livingood and G. T. Seaborg, Phys. Rev. **55**, 457 (1939).

[2] A. A. Noyes and W. C. Bray, *Qualitative Analysis for the Rare Elements* (Macmillan Company, 1927).

[3] W. Gentner and E. Segrè, Phys. Rev. **55**, 814 (1939); G. T. Seaborg and E. Segrè, Phys. Rev. **55**, 808 (1939).

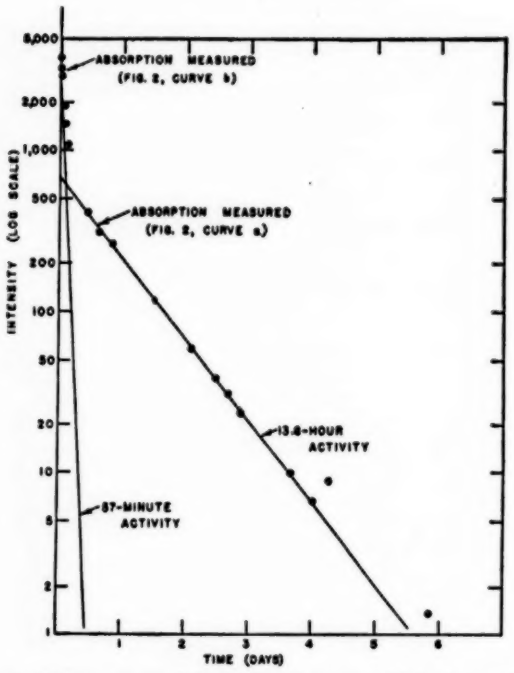

FIG. 1. Decay curve of Zn^{69}. The times at which absorption measurements were made are indicated.

lower state from which the beta-rays are emitted with a period of 57 minutes, it is obvious that the beta-spectra associated with the two activities should be identical. In fact, the apparent beta-spectrum of the 13.8-hour activity is then the spectrum of the 57-minute activity in equilibrium with it.

In order to check this point, we have taken an absorption curve shortly after the end of the bombardment, when the activity was overwhelmingly due to the primarily formed 57-minute activity, and again on the same sample twelve hours later, when the 13.8-hour activity was practically the only one present. Fig. 1 shows a composite decay curve with indications of the times when the two absorption curves were taken. Fig. 2 shows the absorption curves (*a*) of the 13.8-hour activity and (*b*) of the 57-minute activity. Curve (*a*) is corrected for the very weak 250-day activity (Zn^{65}, which is also formed during the bombardment) and curve (*b*) is corrected for both the 13.8-hour and 250-day activities. The two beta-spectra are indeed identical, confirming under improved conditions the previous work. Incidentally, the method described by Feather[4] gives an end-point for the beta-rays of 0.41 g/cm² which corresponds, according to the formula of Feather, to an upper energy limit of 1.05 Mev.

Curve (*a*) in Fig. 2 shows that there is a gamma-ray associated with the 13.8-hour period. Absorption measurements in lead, which covered a factor of ten in intensity, showed a half-value thickness of 3.6 g/cm² for this gamma-ray. This corresponds, according to Gentner's data[5] and our calibration[3] of the chamber, to an energy of 0.47 Mev.

In our picture, then, this gamma-ray must be interpreted as corresponding to the transition from the upper to the lower isomeric state. We have further checked this interpretation by making coincidence measurements on the beta- and gamma-rays. If the gamma-ray transition precedes the beta-particle emission, no coincidences are expected.

A search for coincidences was conducted by placing a sample of the 13.8-hour activity between two Geiger-Müller counters connected in a coincidence arrangement. One of the counters had a thin wall in order to count the beta-particles, and the other was screened with 1.5 g/cm² of paraffin so that only gamma-rays were counted. The effectiveness of the arrangement for counting beta-gamma coincidences was proved by detecting the coincidences between the beta- and gamma-rays of ThB. The 13.8-hour zinc activity gave no coincidences above the accidental rate. A ThB sample gave a net coincidence rate of 5.3 ± 0.8 per minute whereas samples of the 13.8-hour Zn^{69}, with strengths ranging as high as ten times that of the ThB, gave an average net rate of -0.3 ± 0.8 per minute.

It is interesting to investigate the extent of the internal conversion of this 0.47-Mev gamma-ray which we have assigned to the transition between the two isomeric states. The absence of any anomaly at the beginning of the absorption curve of the beta-particles from the 13.8-hour activity shows that very few internal conversion electrons can be present. The same conclusion is reached by comparing the intensities of the gamma-rays and the disintegration electrons in curve (*a*) of Fig. 2. The ratio of the ionization produced by the gamma-rays and the disintegration electrons, as measured in our calibrated

[4] N. Feather, Proc. Camb. Phil. Soc. **34**, 599 (1938).

[5] W. Gentner, Physik. Zeits. **38**, 836 (1937).

chamber, corresponds to approximately one quantum per disintegration. (The chamber was calibrated[3] for this purpose with the radiations from Cu^{61}, which have practically the same energies as the ones considered here.) From these results we may conclude that the ratio of internal conversion electrons to transition gamma-rays is less[6] than 0.1.

We attempted to separate these genetically related isomers by the chemical method. In one experiment the 13.8-hour radioactive zinc was converted into zinc acetyl acetonate in benzene solution. We shook this solution with water but could extract no 57-minute activity. In another attempt the zinc was synthesized into zinc diethyl. This compound was kept as a vapor in a glass bulb for several hours in the hope that any zinc atoms which might escape from the organic molecule by recoil would collect on the walls. The zinc diethyl was then removed and the walls washed with hydrochloric acid. No separated isomer was found in the hydrochloric acid solution. Since there may be many possible reasons for the failure of such experiments, it does not seem safe to conclude that these isomers could not be separated chemically under other conditions.

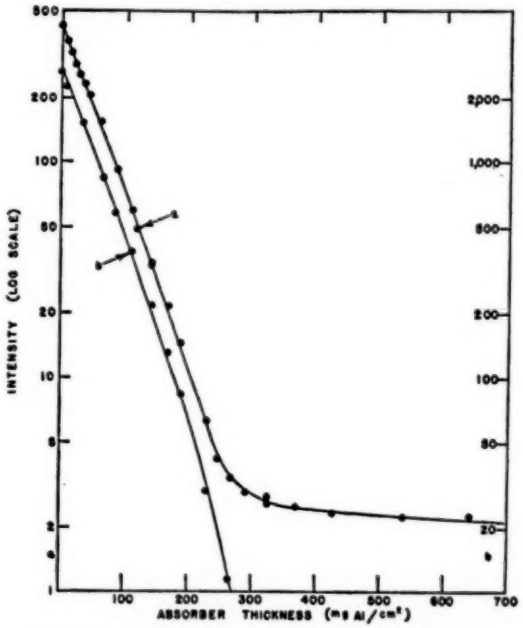

FIG. 2. Absorption curves (in aluminum) of Zn^{69}. (*a*) 13.8-hour activity. (*b*) 57-minute activity.

It is possible to compare the data concerning this isomeric transition, i.e., the energy difference between the states, the half-life of the upper one and the conversion coefficient of the gamma-ray, with theory. The spin difference between the two isomeric states can be deduced from the energy difference and half-life using a formula of Hebb and Uhlenbeck[7] based upon the Weizsäcker[8] theory of nuclear isomerism. This spin change seems to be five and from the spin change and the energy the conversion coefficient can be calculated.[7, 9] One finds $N_e/N_\gamma=0.13$, where N_e is the number of internal conversion electrons and N_γ the number of gamma-rays. The theoretical figures are to be considered as very rough due to well-known uncertainties in the theory. Our experiments show that the internal conversion coefficient is certainly not higher than this but, since experimentally we cannot set a lower limit, it is impossible to say that the coefficient is not less than that predicted by theory.

It is a pleasure to thank Professor Ernest O. Lawrence for his interest in this work. Our thanks are also due to the Research Corporation and the Rockefeller Foundation for financial support.

[6] L. A. DuBridge, in a private communication, tells us that he has searched for conversion electrons in a magnetic spectrograph in this energy region and has failed to find any.

[7] M. H. Hebb and G. E. Uhlenbeck, Physica **5**, 607 (1938).

[8] W. Weizsäcker, Naturwiss. **24**, 813 (1936).

[9] S. M. Dancoff and P. Morrison, Phys. Rev. **55**, 122 (1939).

Some Features of an Electrostatic Generator and Ion Source for High Voltage Research

I. A. GETTING,* J. B. FISK,* AND H. G. VOGT
Harvard University, Cambridge, Massachusetts

(Received July 17, 1939)

A compact generator of the Van de Graaff type is described in which several new features have been incorporated. Short-circuit current of one milliampere is available. When operating at 600 kv as voltage supply for accelerating protons or deutersons, 130μa of charged particles at the target have been obtained from an unusual low voltage capillary arc source. In normal operation as a neutron generator, the equivalent of 15 curies of radon-beryllium is readily produced by the reaction Li+D, and 60 curies by the D on D reaction.

IN the past few years a number of articles have appeared in various journals[1, 2] in which electrostatic, belt-type generators have been described in considerable detail. The present article describes a generator which has been in use in the Harvard Laboratory for some time and which incorporates certain new features. The fundamental ideas concerning such voltage sources, and many practical considerations for carrying them out are well known. However, inasmuch as generators incorporating recent developments are either in construction or being studied in several laboratories, it seems desirable to make readily available information concerning these developments and details on the performance which may be expected. With the apparatus herein described a continuous current of 130 μa of deuterons can be maintained with the high voltage terminal at a positive potential of 600 kv above ground. This is not the maximum to be expected either of current or of voltage. The voltage can be increased by using gases of high dielectric strength, as is well known, while the current limitation lies in the ion source itself, not at present in the accelerating tube. A useful low voltage capillary arc has been developed giving 250 μa total ion current of which 60 percent is atomic. This ion source requires no liquid cooling. It is, therefore, well suited for operation in a confined space at high potential.

The major portion of the apparatus is shown in Fig. 1. The generator itself, which stands 8½ ft. (about 2.5 m) high, is at the left. The adjoining equipment consists of a high voltage body, housing the ion source and power supplies; a resistance voltmeter; and the acceleration tube suspended from the ceiling. The remaining apparatus (vacuum pumps, target chamber, all of the controls and measuring instruments) is contained within the room above, with no direct mechanical connection to the high speed machinery below.

GENERATOR

The generator was designed to produce a maximum of current in a restricted space. In order to accomplish this the principles sketched in Fig. 2 were applied.[2, 3] In *A*, a single isolated belt can be charged to a value σ e.s.u. per cm², such that its gradient of potential, $2\pi\sigma$, on each side corresponds to about 25,000 volts per cm. The charge which can be put on the belt is thus limited by this gradient which corresponds approximately to the "breakdown strength" of air. In *B* a common belt arrangement is shown. Here the lines of force are inward, between the positively and negatively charged portions of the belt. If now $2\pi\sigma$ is the maximum field intensity, then $\sigma/2$ will be the maximum charge per cm². In *C* is shown a two-belt system. Here the outer belt may carry a charge of $\sigma/2$ e.s.u. per cm² while the inner belt may carry σ e.s.u. per cm². In our design a three-belt system is used, similar to the arrangement of *C*. The pulleys, 3, 4, and 5 inch in diameter, are centered one above the other, making the spacing between belts equal to ½ in. Table I shows the charging current

* Society of Fellows.

[1] R. J. Van de Graaff, K. T. Compton, L. C. Van Atta, Phys. Rev. **43**, 149 (1933).

[2] Trump, Merril and Safford, Rev. Sci. Inst. **9**, 389 (1938).

[3] J. B. Fisk and I. A. Getting, Phys. Rev. **53**, 916A (1938).

carried by each of the three belts when the total charging current happened to be 880 μa.

It is evident that considerable improvement is obtained by such an arrangement of belts. One might ask why the belts on the 3-in. and 4-in. pulleys do not carry twice the theoretical maximum for a single belt, rather than 97 percent and 124 percent, respectively. The reasons for this are that a single belt does not in general approach its theoretical limit because of "edge" effects or inhomogeneities of the field, and because the fabric of the belt will only sustain a certain gradient through it as it leaves the pulley without burning or excessive sparking. Hence, any improvement should be measured with respect to currents actually obtained in practice with a single belt.

When running in air at normal pressure and temperature, the maximum "short-circuit" current which the generator will deliver is 980 μa

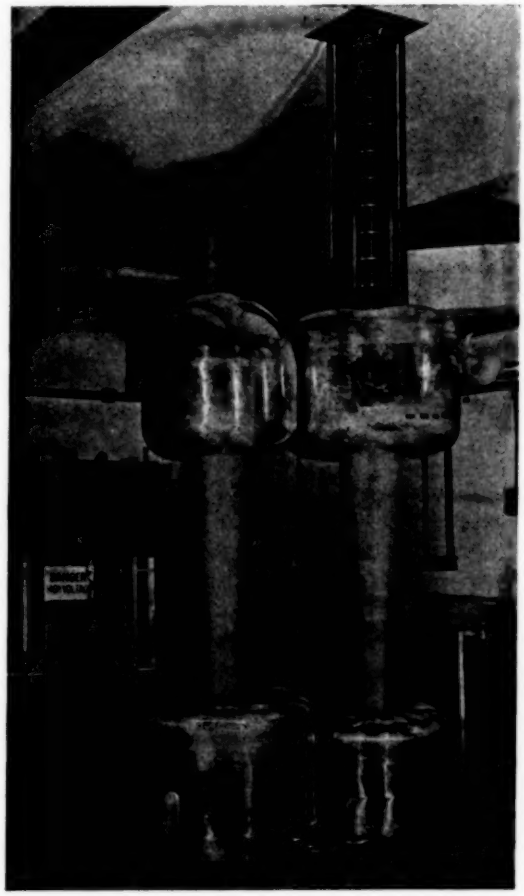

FIG. 1. Generator (left), high voltage body and acceleration tube.

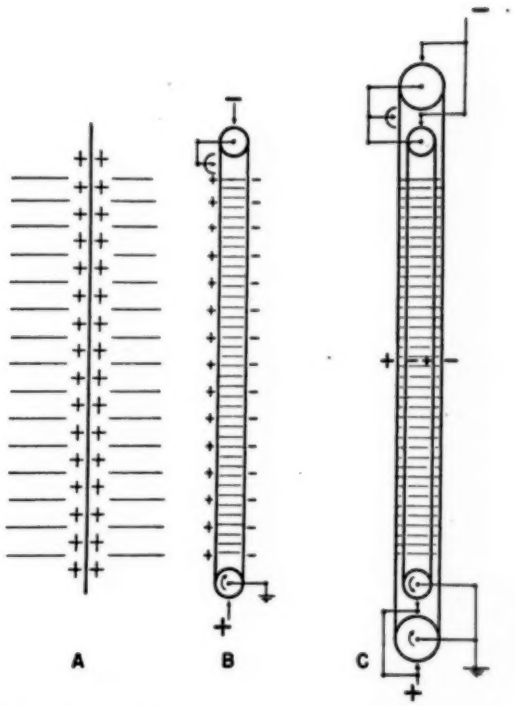

FIG. 2. Lines of force in various belt arrangements.

with the terminal positive, 1000 μa with the terminal negative. The spacing between adjacent belts, carrying charge of opposite sign, should be small compared to the belt width, as pointed out by Trump.[2] This is borne out by the results quoted in Table I, where one compares a current of 372 μa (carried by a belt spaced midway between two other belts carrying opposite charges, $\frac{1}{2}$ in. (1.25 cm) from each) with 278 μa (carried by a belt spaced $\frac{1}{2}$ in. from one adjacent belt, 3 in. (7.5 cm) from the other). Other factors may influence these values, such as the effect of greater or less spacing between upper pulleys, etc., but these things are not critical and the numbers quoted would be only slightly altered.

Even though the belts were but $\frac{1}{2}$ in. (1.25 cm) apart, no difficulty was experienced in their successful operation. Windage and flexure losses depend markedly on the type of belt used. Tilton endless woven cotton fabric belts required 1 hp more to drive in this arrangement than Goodyear rubberized Zeppelin fabric. However, with Tilton belts 1000 μa were available compared with 600 μa with Zeppelin fabric belts. This was due in part to the low dielectric breakdown strength of the thin fabric belts prohibiting high voltage

on the corona points. Furthermore, with slightly crowned pulleys the thin fabric belts tend to rip.

Positive or negative charge is "sprayed" on belts at the bottoms of the lower pulleys, as indicated at *Q* in Fig. 3. The spray points (phonograph needles) are mounted uniformly about $\frac{1}{2}$ in. apart and kept at 15,000 volts or less. Each group of spray points is fed from the Kenotron rectifier through an adjustable ballast resistor which takes about one-fourth the total voltage drop. The resistors were adjusted for maximum short-circuit current while the generator was running.

The self-induction scheme for charging the upper terminal is used. This is shown in Fig. 3. The shielded spray "comb," *E*, is connected directly to the pulleys, while the spray combs, *D*, are connected in parallel to the aluminum shell, *A*. The upper pulley assembly, *C*, is insulated from the high voltage terminal, *A*, by means of eight canvas-Bakelite screws, *G*. The position of *E* along the outer belt, and the position of each spray comb with respect to its pulley, are critical, and adjustment should be made while the generator is running.

Following Trump,[2] re-entrant electrodes were used. The discontinuity between the conducting shell, *A*, and the dielectric column, *J*, is made much less abrupt by this means, and the high voltage terminal behaves very nearly as one might expect a charged, isolated sphere to behave. Breakdown at maximum voltage occurs usually as a "spray" of corona from the outer portion of the high voltage electrode where the cylinder joins the re-entrant shape, and not, in general, as damaging sparks down the supporting column.

The supporting column is Textolite, 12 in. (30.5 cm) outside diameter $\frac{3}{16}$-in. (48 mm) wall. Apparently "Textolite" is available with several

TABLE I. *Charging current on the belts.*

Radius of Pulley in Inches	R.P.M. of Pulley	Linear Speed of Belt ft./min.	Width of Belt in Inches	Current in μa (Measured)	Ratio of Current Carried to Theoretical Maximum for Single Belt
5	4280	5610	8.75	230	0.74
4	5240	5500	9.75	372	1.24
3	6860	5560	9.75	278	0.97

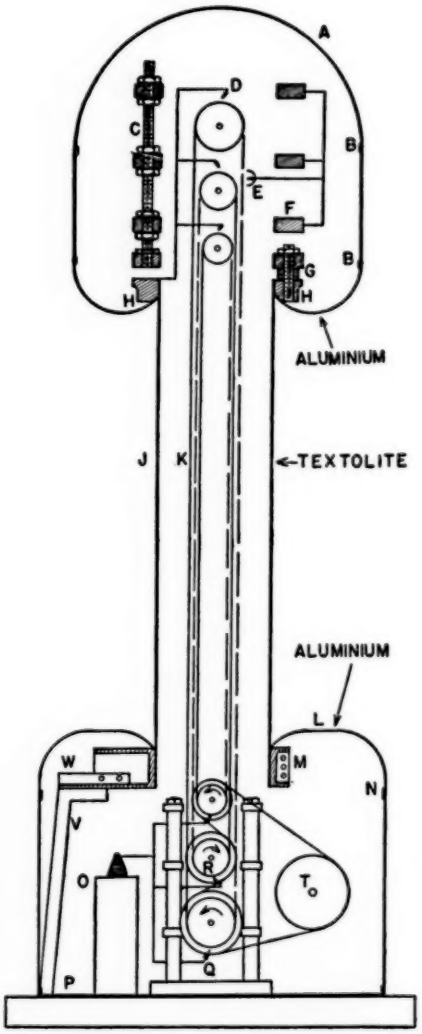

FIG. 3. Schematic diagram of generator.

binders: shellac and Bakelite among them. The columns supplied for this work were bound with Bakelite and were found to be very hygroscopic, and to possess a high negative temperature coefficient of resistance. Considerable difficulty was at first encountered in maintaining a high resistance (i.e., greater than 10^{11} ohms). To prevent absorption of moisture the following procedure was used: The columns, after being scraped to remove dirt and wax, were baked at 110°C for 48 hours. They were then given two coats of glyptal lacquer No. 1202, inside and out, followed by 4 hours baking after each coat. Finally a thin coating of ceresin wax was applied while the columns were still warm. The resistance was then greater than 10^{13} ohms at room temperature. To

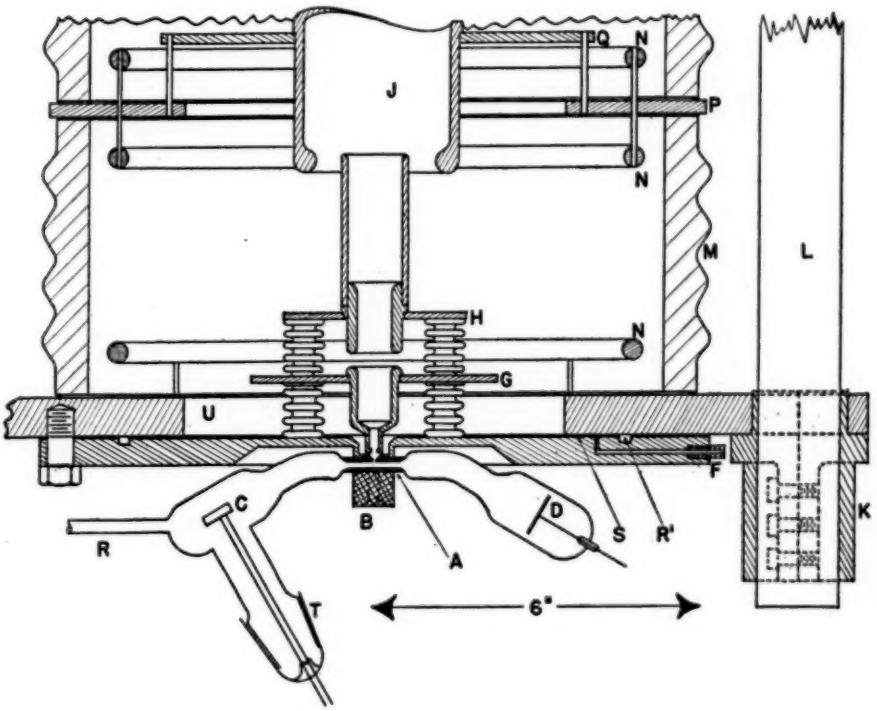

FIG. 4. Diagram of source end of tube showing ion source, endplate, electron-optical system, first tube section and method of holding tube together.

prevent undue heating of the column the temperature of the air within the generator is maintained at about room temperature by means of a small water-cooled radiator and circulating fan in the base of the generator.

The base of the generator is shown in Fig. 3. Three column supports, *V*, are welded to the steel flange, *P*, which, together with the clamp, *M*, form a very rigid structure. The 1.5-hp driving motor has recently been replaced by a 5-hp motor which has been mounted outside the aluminum shield, *L*. The belt for driving the pulleys is an HT4 Tilton endless woven and operates at a linear speed of 7000 ft. per minute. Rockwood paper pulleys are used with this driving belt. The three pairs of charging belt pulleys, upper and lower, were dynamically balanced and mounted in self-aligning bearings.

In order to reduce vibration the upper pulleys are mounted on separate cushion pads, each being isolated from the others, and each being independently adjustable. All charging belt adjustments are made at the upper end.

VOLTMETER

The resistance voltmeter consists of four IRC type MVR resistor units, 10,000 megohms each, total length 80 in. (203.2 cm). The resistors are mounted in series along the axis of a 4 in. (10.2 cm) diameter Pyrex tube which is filled and coated with ceresin. The complete unit stands vertically inside the column shown to the right in Fig. 1. The voltmeter can be shown to be free from corona by comparing meter readings at grounded and high voltage ends of the resistor. To prevent possible corona pick-up on the cable to the instrument panel, both leads are separately shielded. A neon glow lamp bypass to ground is used to protect the microammeter from surges.*

ION SOURCE

A number of different types of ion sources have been described in the literature, among which the

* *Note added in proof.*—The resistor units failed at a peak voltage of 600 kv after several months of use. A new generating voltmeter of a type to be described by Trump has been installed and found to be extraordinarily dependable.

low voltage capillary arc[4] is particularly suitable for present application. This type of source has the advantage that the ions, drawn from the plasma of the discharge, are monokinetic as compared to other types of sources (e.g., canal ray) in which the source potential may be as high as 50,000 volts. The positive ion density in the capillary part of the arc (i.e., the constricted portion between *C* and *D* in Fig. 4) may be made very high and it is from this region that the ions are withdrawn. Metal, glass and quartz capillaries have been used. Metal and quartz walls encourage recombination; while glass, having low heat conductivity, must be cooled if any appreciable power is to be dissipated from the arc. Even with water cooling the temperature between the inside and outside of a Pyrex capillary may be as much as several hundred degrees when 100 watts is being dissipated in the arc. Hence, either very thin, fragile capillaries must be used or an upper limit must be set to the arc current and voltage.

In the present design this difficulty, and the difficulty occasioned by wearing away of the edge at the small, beveled hole in the capillary wall, is largely overcome by using a "Kovar" capillary lined with Corning 706J glass as suggested by Professor K. T. Bainbridge. The glass lining is but 0.002 in. (0.0051 cm) thick, which gives rise to a temperature drop of less than 10° under fairly severe conditions. Fig. 4 shows the ion source, mounted in position on the plate capping off the high voltage end of the porcelain vacuum tube; the first few focusing electrodes; and some detail of the method of assembly of the acceleration tube. The cathode, *C*, is oxide-coated, wound in a flat spiral, mounted on a grind, *T*, and takes 10 amperes at 2.5 volts. Anode, *D*, is a flat, circular piece of nickel, although several types of anodes have been used with equal success. The anode is made large enough to prevent excessive anode drop and, hence, undue heating in that region. The Kovar capillary is soldered to the end plate, *F*, and to the copper clamping block, *B*. Heat is then dissipated from the entire endplate assembly by air convection. The arc operates satisfactorily with the hydrogen pressure between 10^{-2} and 10^{-1} mm Hg. At 10^{-1} mm the arc current may vary from 0.2 ampere at 125 volts to 1.0 ampere at 170 volts through an $\frac{1}{8}$ in. (3.2 mm) capillary 1 in. (2.54 cm) long. There seems to be no simple dependence of useful ion current on total arc current. With a 0.75-mm diameter outlet from a 3.2-mm diameter capillary a current of 250 μa was obtained, 60 percent being protons. Fig. 5 shows an analysis of the ion beam for this source. The effect of a small quantity of water vapor on the relative yields of monatomic and diatomic ions is indicated (cf. Lamar, Buechner and Compton[4]).

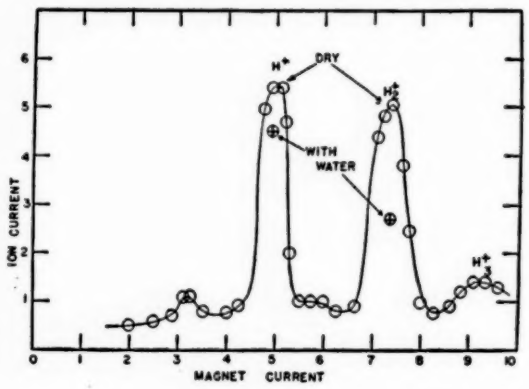

FIG. 5. Mass-spectrographic analysis of ion source.

A source of this description allows a considerable flow of gas into the acceleration tube. The acceleration tube, however, was designed (following Van Atta, etc.[5]) to have high speed of exhaust. Used in conjunction with a 4-in. (10.2 cm) diameter, stainless-steel Hg diffusion pump (of pumping speed 400 l/sec. for H_2) no difficulty was had in maintaining the pressure at the target better than 5×10^{-5} mm Hg. At this pressure there is very little scattering of ions out of the focused beam for this 6-ft. (183 cm) tube, and no difficulty is encountered because of electrical breakdown.

FOCUSING

A number of methods for focusing the ions at the source were tried. The electron-optical lens system which has proven most successful for this purpose is sketched in Fig. 4. The probe, *G*,

[4] E. S. Lamar and O. Luhr, Phys. Rev. **46**, 87 (1934). Tuve, Dahl and Van Atta, Phys. Rev. **48**, 315 (1935). Lamar, Buechner and Compton, Phys. Rev. **51**, 936 (1937). W. H. Zinn, Phys. Rev. **52**, 655 (1937).

[5] Hill, Buechner, Clark and Fisk, Phys. Rev. **55**, 463 (1939).

is held at about −5000 volts, while the electrode, *H*, is held at about −10,000 volts with respect to the end plate, *F*. The entire assembly of *G* and *H* can be adjusted externally for alignment although details of the mechanism are not shown. Electrode *J* is at a potential determined by the over-all voltage on the acceleration tube and is controlled by corona.* An ion beam of 130 μa on the target was focused to a spot $\frac{1}{8}$ in. in diameter by means of this arrangement. The diameter and length of electrode *H* were so chosen that the solid angle subtended from the outlet hole in the capillary source was approximately that subtended by the last tube electrode at the same origin. Hence, under normal operating conditions, few ions strike the tube electrodes, and secondary electrons from the metal surface of these electrodes do not constitute a problem. Secondary electrons from the electrodes *G* and *H* are not troublesome, while secondaries from the target and target chamber are prevented from entering the tube by a large cylindrical electrode near the target which is maintained at a retarding potential of −90 volts.

The Generator as a Neutron Source

To have a measure of the output of the unit, neutrons from a lithium target bombarded by deuterons were used to activate a sheet of rhodium. This activity was then compared with that produced by a calibrated radon-beryllium neutron source. The lithium was forced into a water-cooled copper receptacle by means of an arbor-press. A current of 130 μa of unresolved deuterons bombarded the lithium from a potential of 475 kv. A sheet of rhodium was put between two 1-pound blocks of paraffin placed to one side of the target. Artificial radioactivity induced in the rhodium by the neutrons from the lithium-deuteron reaction was then recorded by a beta-ray counter and taken as a measure of the "neutron producing" efficiency of the unit. A multivibrator circuit[6] and vacuum tube, scale-of-eight counter,[7] were used for the measurements. Use was made of the 4.2-minute period only. The counting rate was much too great to be recorded accurately by this means in the first few minutes.

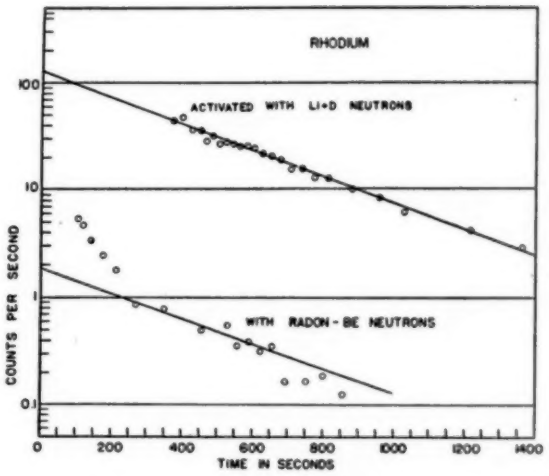

FIG. 6. Decay curves of rhodium activated by: (*a*) 190 mC Rn-Be 20 min. (*b*) neutrons from Li-D reaction for 20 min.

This activity was compared with that induced in the same sample of rhodium by a 190-millicurie radon-Be source, kindly prepared for us by Dr. Cramer Hudson. In this case, however, both the Rn-Be source and the rhodium were completely surrounded by paraffin. The beta-ray counter sensitivity was standardized for the measurements by checking with a radium source held at a fixed distance from the counter before and after each measurement. Fig. 6 gives the results of these measurements. The activity induced by the Li-D reaction neutrons in the rhodium sample was equivalent to at least that which would have been produced by 16.5 curies of Rn-Be. (No allowance was made for the fact that the geometry favored the Rn-Be source.)

This compares reasonably with the datum of Amaldi, Hafstad and Tuve[8] that at 475 kv the Li-D reaction gives 0.380 curie Rn-Be equivalent per μa of deuterons. If their figure is correct we can assume that our ion beam contained at least 36 percent deuterons.

Generator Housing

Recently that part of the apparatus shown in Fig. 1, namely: generator, h.v. body, voltmeter

* To prevent sparking along the tube, the corona points on the successive electrodes of the acceleration tube are arranged to point toward the next more positive electrode —never toward the more negative electrode.

[6] I. A. Getting, Phys. Rev. **53**, 103 (1938).

[7] E. C. Stevenson and I. A. Getting, Rev. Sci. Inst. **8**, 414 (1937).

[8] Amaldi, Hafstad and Tuve, Phys. Rev. **51**, 896 (1937).

and tube, has been enclosed in an air-tight, copper-lined room. A ¾-hp refrigerating unit has been installed which keeps the humidity below 20 percent in the most humid summer weather. With the introduction of freon at a partial pressure[9] of 5 lb./in.^{2} one might expect to obtain a potential of 1000 kv with a corresponding increase in charging current. If, at the same time, the ion current can be maintained, an increase in neutron yield of from 10- to 100-fold may be expected.

[9] Hudson, Hoisington and Royt, Phys. Rev. **52**, 664 (1937).

ACKNOWLEDGMENTS

The authors wish to express their indebtedness to Professor K. T. Bainbridge, who has advised on many difficult points; to Professors J. C. Street and J. G. Trump; and to Mr. A. Grant for considerable technical assistance. They wish to express their thanks to Mr. H. Leighton who is responsible for developing the technique of lining the Kovar capillaries for the ion source.

These developments were supported in part by grants in aid from the Milton Fund and from the Society of Fellows.

DECEMBER 1, 1939 PHYSICAL REVIEW VOLUME 56

Search for a Short Range Group of Protons in the D−D Reaction

F. E. MYERS, R. D. HUNTOON, C. G. SHULL, AND C. M. CRENSHAW
Department of Physics, New York University, University Heights, New York, New York

(Received October 2, 1939)

A thorough search for short range protons arising from the D−D reaction has been made at bombarding energies up to 300 kev, and at angles of 36°, 97°, and 142° to the incident deuteron beam. No evidence for such a group is found. The energy released in the reaction has been rechecked and is found to be in agreement with previous observations.

INTRODUCTION

BONNER'S recent confirmation[1] of previous experiments[2] indicates strongly the presence of a low energy group of neutrons in the reaction $H^2+H^2\rightarrow He^3+n^1$. The tentative explanation of this group is that the He^3 nucleus is left in an excited state about 1.9 Mev above the ground state. Such an excited state cannot readily be accounted for theoretically,[3] and a search for gamma-rays,[4] internal conversion electrons and positrons[5] has led to negative results within an experimental error far below the expected intensities. In spite of these difficulties, the evidence for a low energy neutron group appears strong, and further study of the D−D reaction is desirable.

If one assumes that the only difference between the neutron emitting reaction and the proton emitting reaction is the Coulomb barrier encountered in the latter case, then there should be a corresponding short range group of protons, presumably accompanied by an H^3 nucleus in an excited state. These protons would be expected to have a range of about 5 cm at 90° to an incident beam of 200-kev deuterons. Myers and Langer,[6] and Hudspeth and Bonner[7] found none ejected in a small solid angle approximately at right angles to the beam of incident deuterons.

Since the angular distribution of the protons and neutrons is not spherically symmetrical[8] there must be in some of these nuclear reactions one or more quanta of orbital angular momentum and as has been pointed out to one of us by Ellett[9] there is a possibility that these inter-

[1] T. W. Bonner, Nature **143**, 681 (1939).
[2] T. W. Bonner, Phys. Rev. **53**, 711 (1938); Phys. Rev. **52**, 685 (1937); Baldinger, Huber and Staub, Helv. Phys. Acta **11**, 245 (1938).
[3] Simon S. Share, Phys. Rev. **53**, 875 (1938) and L. I. Schiff, Phys. Rev. **54**, 92 (1938).
[4] Arthur J. Ruhlig, Phys. Rev. **54**, 308 (1938); H. Kallmann and E. Kuhn, Naturwiss. **26**, 106 (1938).
[5] M. H. Kanner and W. T. Harris, Bulletin of Am. Phys. Soc., Princeton Meeting (June, 1939).
[6] F. E. Myers and L. M. Langer, Phys. Rev. **54**, 90 (1938).
[7] E. Hudspeth and T. W. Bonner, Phys. Rev. **54**, 308 (1938).
[8] Kempton, Browne and Maasdorp, Proc. Roy. Soc. **157**, 386 (1936). H. Neuert, Physik. Zeits. **38**, 122 (1937). Haxby, Allen and Williams, Phys. Rev. **55**, 140 (1939).
[9] A. Ellett, private communication to R.D.H.

actions might be the ones to give rise to the excited H^3. Further if the reaction responsible for the excited H^3 were of the p type or higher odd order there would be no short range protons ejected at 90° and the negative result for measurements at 90° becomes inconclusive.

From these considerations and because of the fundamental nature of any information about the simplest of the nuclear reactions it seemed advisable to extend the search for short range protons to other angles and to higher bombarding energies.

Apparatus

The search for short range protons has been extended to 200 and 300 kev at angles of 36°, 97°, and 142° with respect to the direction of motion of the incident beam. The essential part of the equipment is shown schematically in Fig. 1. It is practically the same as previously reported[6] except for the addition of a monitor ionization chamber and amplifier to measure accurately a constant fraction of the total number of disintegrations produced in the target during each individual counting period. The differential chamber was equipped with a screw feed of about 15 mm to vary the path in air of the disintegration particles, and provision was made for the insertion of aluminum foils previously calibrated with polonium alpha-particles. The stopping power of the foils was assumed to be the difference in extrapolated range from air to air plus foil as measured with an ionization chamber 1.1 mm deep. The foils were placed close to the source of alpha-particles.

The geometry was such that all disintegrations produced in an area of about four times that of the spot of resolved deuterons would be counted. The spot was always kept at least 1 mm from the edges of the effective target area. A liquid-air-cooled heavy ice target was used in all measurements.

In all the counting the background and pulses were separated by biased rectifiers on the output of the monitor amplifier and the differential chamber amplifier. The maximum pulse height was held constant to within 10 percent and the bias voltage constant to 1 percent. The recorded data in each case were the ratio of the number of counts recorded by the differential chamber to the counts recorded by the monitor, as counted by scale-of-8 counters. With this arrangement extrapolated range measurements agreed to about one millimeter for runs on different days and individual points on single runs checked within statistical error for counting rates of 4000 to 8000 per minute. Each of the experimental points represents 5000 to 10,000 counts on the monitor with the corresponding number on the differential chamber.

In order to make absolute range measurements the thin Celluloid window and differential chamber assembly were calibrated by putting a source of polonium alpha-particles in place of the target and introducing air into the target chamber as a stopping medium. Pulse heights and rectifier biases were set the same as for the proton measurements.

Results

Figure 2 shows a typical curve taken at 36° to the 200-kev deuteron beam. Similar curves were taken at 97° and 142° to a 200-kev beam and 36° and 142° to a 300-kev beam, and 36° to a 100-kev beam (Mass 4 spot, 200 kv). From such curves we estimate a short range proton

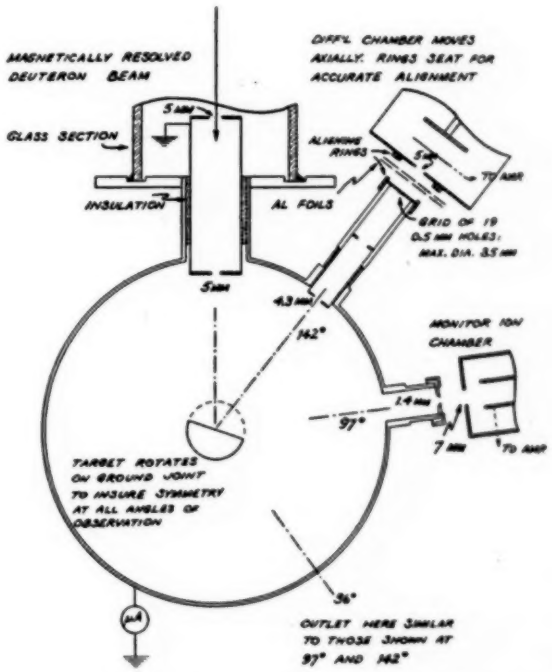

FIG. 1. Schematic diagram of the target chamber and ionization chambers. Scale of cut 1:2.80.

group with an intensity of 2 percent of that of the main group could have been easily detected. This is about $\frac{1}{5}$ the number to be expected upon the basis of Bonner's results and the assumed similarity of the reactions.

The short range peak is evidently the H^3 group. It must be remarked that if the short range protons fall within this group our measurements cannot separate them. Unfortunately our equipment would not measure the complete low range peak.

As a check upon the consistency of our measurements we have calculated the Q of the reaction using the extrapolated ranges in each case with the foil corrections indicated in Livingston and Bethe's paper.[10] In the forward direction and at 97° the full value of the bombarding energy was used in the calculation of Q. In the backward direction it is evident that the longest range protons come from disintegrations produced by deuterons that have been slowed down in the target. This necessitates making estimates of the effective bombarding energy and of the energy lost by the ejected protons in getting out of the target. Accordingly the Gamow disintegration function for deuterons was plotted and the almost linear portion was extrapolated to zero. The bombarding energy of 60 kev thus obtained was used for the calculation of Q. While this approximation is obviously crude, an error of about ±30 kev here does not change the value of Q by more than the indicated experimental error. The observed range of the ejected protons was increased by an amount equal to the range lost by the incident deuterons in slowing down to 60 kev.

TABLE I. *Extrapolated ranges of the protons and calculated values of Q as a function of angle and bombarding energy.*

Energy kev	Angle	Al Foils Air Equiv. 15°C	Air Path 15°C	Corr. Range	Q Mev
200	142	9.81	2.25	12.18	3.96
200	142	9.65	2.28	12.05	3.93
300	142	9.55	2.28	12.10	3.94
200	36	15.35	2.50	17.87	3.90
300	36	16.78	2.50	19.36	3.93
200	36	15.35	2.36	17.73	3.89
100	36	13.92	2.36	16.23	3.88
200	97	11.70	2.48	14.17	4.03*

* This value is slightly less reliable than the others due to minor difficulties with the apparatus while the data were being taken.

[10] M. S. Livingston and H. A. Bethe, Rev. Mod. Phys. **9**, 245 (1937).

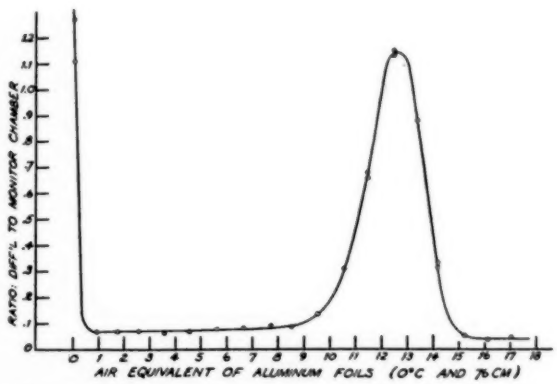

FIG. 2. Differential range curve of the protons ejected at 36° to the 200-kev beam of incident deuterons. The protons pass through 2.37 cm of air (0° and 76 cm) in addition to the aluminum foils indicated in the diagram.

Table I shows the observed extrapolated ranges of the protons as a function of angle and bombarding energy. The last column gives the corresponding calculated values of Q. From these we arrive at $Q=3.93\pm0.10$ Mev.

Rumbaugh, Roberts and Hafstad[11] show that one or more of the four values of Q in the reactions

$$(1)\quad H^2+H^2=H^3+H^1+Q_1$$

$$(2)\quad H^2+H^2=He^3+n^1+Q_2$$

$$(3)\quad Li^6+n^1=He^4+H^3+Q_3$$

$$(4)\quad Li^6+H^1=He^4+He^3+Q_4$$

must be in error since $Q_1-Q_2=Q_3-Q_4$ whereas experimentally they differ by 0.5 Mev. The Q_1 herein obtained appears to rule out the possibility of a large error in Q_1 previously reported as 3.98.[10]

Our thanks are due to Dr. Lawrence M. Langer for his cooperation in the early part of this work, and to Mr. Henry P. Manning, Jr. for his able technical assistance and help in taking data.

[11] Rumbaugh, Roberts and Hafstad, Phys. Rev. **54**, 657 (1938).

The Binding Energy of H^3

FREDERICK W. BROWN
California Institute of Technology, Pasadena, California
(Received October 2, 1939)

A calculation has been made of the constants in the meson type of potential by fitting the scattering data for the scattering of slow neutrons by protons and the binding energies of H^2 and H^3. Assuming the interaction between any two particles to be $(P_{ij}+gP_{ij}Q_{ij})(Ce^{-\lambda r_{ij}}/r_{ij}\lambda)$ one gets $C=49.54\ mc^2$, $g=0.2667$, $\lambda=1.536\ (mc^2/e^2)$. This potential gives results which will be very little different from those given by the spherically symmetrical parts of the interaction obtained from meson field theory. The use of the coordinates introduced by James and Coolidge allows sufficient simplification so that the results can be easily modified to take account of other types of spin dependence. The possibility of λ and C being different for different particle interactions may also be taken into account.

I

THE increasing importance of the potential $Ce^{-\lambda r}/r\lambda$ obtained from the meson field theory gives interest to an accurate determination of the interaction constants. Such an accurate determination has been made by Rarita and Present[1] for the potential $Ce^{-\lambda r}$. In this paper a similar determination is made for the meson type of potential, but the system of coordinates[2] used below allows considerable simplification in the calculations.

The interaction between any pair of particles (ij) is assumed to be given by

$$V_{ij}=(P_{ij}+gP_{ij}Q_{ij})Ce^{-\lambda r_{ij}}/\lambda r_{ij}, \qquad (1)$$

where P_{ij} interchanges the particle coordinates and Q_{ij} interchanges their spins. To be consistent one should use the spin dependence obtained from the meson field theory,[3] but since the spherically symmetrical parts of the interaction thus obtained will give results which differ very little from those obtained from (1) and since the non-spherically symmetrical spin-spin interaction involves an arbitrary cut-off at some distance, a practical procedure is to calculate with the type of interaction (1). There is also an ambiguity in the spherically symmetrical parts of the interaction obtained from the meson field theory, since they depend on whether one allows heavy particles to interact only with neutral mesons or whether they are also allowed to interact with charged mesons.

The use of the coordinate system introduced by James and Coolidge[2] for their discussion of the helium atom makes the calculation sufficiently simple so that these results can be easily modified when the spin dependence of the interaction becomes more definite.

II

In the interaction (1) there are three constants g, C, λ to be determined. The binding energies of H^2 and H^3 and the scattering of thermal neutrons by protons give the three conditions necessary for their determination. The interaction constants are assumed to be the same for all pairs of particles. In this paper the binding energies of H^2 and H^3 are determined by a variational calculation and the scattering is determined by numerical integration of the deuteron equation for zero energy. The scattering could also be obtained by a variational calculation but the work would be tedious.

For the S states of H^3 it is convenient to introduce the coordinates

$$\begin{aligned} x&=\lambda(r_1+r_2-r)\\ y&=\lambda(r_2+r-r_1)\\ z&=\lambda(r_1+r-r_2). \end{aligned} \qquad (2)$$

If one labels the proton particle number 1 and the neutrons 2 and 3, respectively, then r is the distance between the neutrons, r_1 is the distance between particles 1 and 2 and r_2 is the distance

[1] W. Rarita and R. Present, Phys. Rev. **51**, 788 (1937).
[2] H. M. James and A. S. Coolidge, Phys. Rev. **51**, 860 (1937).
[3] N. Kemmer, Proc. Camb. Phil. Soc. **34**, 299 (1938); J. Schwinger, Phys. Rev. **55**, 235 (1939).

between particles 1 and 3. In these coordinates the integral over the volume of a sphere of radius r_0 is

$$(1/4\lambda^6)\int_0^{2\lambda r_0}\int_0^{2\lambda r_0-x}\int_0^{2\lambda r_0-x}(x+y)(x+z)\times(y+z)dxdydz. \quad (3)$$

For the infinite sphere the upper limits become infinite.

In the coordinates (1) the wave equation for an S state of H^3 is

$$\{4/(x+y)(x+z)(y+z)\}\{\psi_{xx}(x^2y+xy^2+x^2z+xz^2+xyz)+\psi_{yy}(x^2y+xy^2+y^2z+yz^2+xyz)+\psi_{zz}(x^2z+xz^2+y^2z+yz^2+xyz)-\psi_{xy}(x^2y+xy^2)-\psi_{xz}(x^2z+xz^2)-\psi_{yz}(y^2z+yz^2)+\psi_x(-x^2+y^2+z^2+xy+xz+yz)+\psi_y(x^2-y^2+z^2+xy+xz+yz)+\psi_z(x^2+y^2-z^2+xy+xz+yz)\}+\{2b_{12}/(x+z)\}\exp\{-(x+z)/2\}P_{12}\psi+\{2b_{13}/(x+y)\}\exp\{-(x+y)/2\}P_{13}\psi+\{2b_{23}/(y+z)\}\exp\{-(y+z)/2\}P_{23}\psi+a'\psi=0; \quad (4)$$

where $a'=(EM/h^2\lambda^2)$ and b_{12}, b_{13}, b_{23} depend on the spin and are given below.

For the ^3S state of the deuteron the value of $a=(EM/h^2\lambda^2)$ for a given value of $b=(CM/h^2\lambda^2)$ is determined by minimizing a with the function

$$\phi=\sum_1^\infty C_k x^k e^{-\alpha z} \quad (x=r\lambda). \quad (5)$$

This value of a together with the known binding energy of H^2 then determines the corresponding value of λ. The value of $b(^1S)$ is then determined by numerical integration to give the proper cross section for the scattering of thermal neutrons by protons.

From the values of $b(^1S)$, $b(^3S)$ and λ for the deuteron one calculates by a variational principle the binding energy of H^3. The values of $b(^1S)$, $b(^3S)$ and λ are adjusted until the calculated binding energy of H^3 equals the experimental energy.

To determine a' of H^3 one minimizes a' with a function

$$\psi=S_A\phi_1+S_S\phi_2, \quad (6)$$

where S_A is a spin function antisymmetric for an exchange of neutron spins, ϕ_1 is a function of (xyz) symmetric for interchange of neutron coordinates and S_S is symmetric for exchange of spins and ϕ_2 is antisymmetric for exchange of coordinates. Using the same spin functions as Rarita and Present,[1] one gets after summing over the spins

	$b_{12}(h^2\lambda^2/MC)$	$b_{13}(h^2\lambda^2/MC)$	$b_{23}(h^2\lambda^2/MC)$
$\phi_1\phi_1$:	$(1+g/2)$	$(1+g/2)$	$(1-g)$
$\phi_1\phi_2+\phi_2\phi_1$:	$(g\sqrt{3}/2)$	$(-g\sqrt{3}/2)$	0
$\phi_2\phi_2$:	$(1-g/2)$	$(1-g/2)$	$(1+g)$.

For ϕ_1 and ϕ_2 one uses the variational functions

$$\phi=\sum C_{klm}x^k y^l z^m \exp\left[-\alpha x/2-\beta(y+z)/2\right], \quad (7)$$

where ϕ_1 must be symmetric for exchange of y and z and ϕ_2 correspondingly antisymmetric. The general matrix elements of a' are easily calculated (cf. appendix). One first minimizes with only the first term of ϕ_1 by varying α and β; then using these values of α and β one varies the coefficients in ϕ_1; finally using this ϕ_1 one varies the coefficients in ϕ_2. A relativistic correction calculated by the method of Feenberg[4] is also included.

The variation of the coefficients was carried out as follows: one writes

$$a'=(A/N)a_0', \quad (8)$$

where a_0' is the value of a' obtained by the previous minimizing process, A is the energy integral (cf. appendix) divided by the energy integral of the previous minimizing process and N is the normalization integral divided by the normalization integral of the previous minimization. Minimizing (8) gives

$$\frac{dA}{dC_{klm}}-\frac{A}{N}\frac{dN}{dC_{klm}}=0 \quad (klm)=0, 1, 2\cdots. \quad (9)$$

By estimating the percent reduction in energy to be obtained from varying the coefficients one can solve the set of linear equations (9) for the C_{klm}, then recalculate (A/N) and readjust the C_{klm} for the new (A/N). A small error in the estimate makes little difference in the calculated value of (A/N).

III

Using the experimental values, $E(^3S\,H^2)=-4.25(0)\,mc^2$, σ (thermal neutrons by protons $=18.3(0)\times10^{-24}$ cm^2, and $E(H^3)=-16.3(0)\,mc^2$,

[4] E. Feenberg, Phys. Rev. **50**, 674 (1936).

one obtains $C=49.54\ mc^2$, $\lambda=1.536\ (mc^2/e^2)$ and $g=0.2667$.

The variational function for the deuteron ^3S state is

$$e^{-0.9175x}(x-0.2363\,x^2+0.07266\,x^3),\quad N=0.2519$$

which gives $a(^3S)=-0.1760$. For a slightly different value of $b(^3S)$ inclusion of five terms in the series gives only 0.06 percent reduction of a below the value obtained with three terms, hence it is certainly sufficiently accurate to take $a(^3S)=-0.1761$. Inclusion of the x^2 and x^3 terms gives a reduction of 11.69 percent below the value obtained by using only the first term. Using $b(^1S)=1.505$, $b(^3S)=2.600$, $\lambda=1.536$ one gets a scattering cross section of thermal neutrons by protons of 18.30×10^{-24} cm^2.

For H^3 the variational functions are

$$\phi_1=[1-0.1087x-0.07112(y+z)+0.03669\times x(y+z)]\exp[-0.8333x-0.7500(y+z)],$$

$$\phi_2=[0.04222(y-z)-0.004793x(y-z)]\times\exp[\cdots],\quad N=0.6284.$$

Adding further second degree terms and third degree terms in ϕ_1 gives only about 0.05 percent reduction in the energy, and adding other terms in ϕ_2 gives a negligible reduction.

The exponential term alone gives $a'=-0.6293$; further terms in ϕ_1 produce a reduction of 1.81 percent; the inclusion of ϕ_2 causes a reduction of 3.74 percent; and the relativistic correction ($0.267\ mc^2$) produces 1.75 percent reduction, giving $a'=-0.6752$ compared to the experimental value of $-0.675(6)$.

The difference in the binding energies of He^3 and H^3, determined by considering the Coulomb interaction as a perturbation, is

$$E(He^3)-E(H^3)=1.671\ mc^2.$$

The experimental value of this difference is uncertain, values of $1.35\ mc^2$ and $2.35\ mc^2$ having been obtained.[5]

The above value of λ gives the mass of the meson as 211 m. The fact that the above value of λ is considerably different from that determined by Share, Hoisington and Breit[6] from proton-proton scattering has been discussed elsewhere,[7]

Use of the spherically symmetrical parts of the potential obtained from meson field theory can cause but little modification in the above values since one would get the same results as above if the wave function $\psi(H^3)$ had the same dependence on x, y and z. The small deviation which one has from this symmetry condition cannot cause more than a few percent change in the calculated energy of H^3. The spin-spin terms of the meson field theory which give rise to a quadripole moment of the deuteron will modify the above values, but one could not calculate the modification in an unambiguous manner because of the arbitrary cut-off necessary to get convergence. From the calculations of Bethe[8] on the quadripole moment of the deuteron it seems likely that the singular spin-spin terms would make the value of λ even less than that given in this paper.

The accuracy of the above results is also dependent on the accuracy of the experimental values used. As an indication of the modifications caused by a change in the binding energy of H^3 or in the scattering cross section, it may be stated that for $E(H^3)=-16.48\ mc^2$ one would have

$$C=50.49\ mc^2,\quad \lambda=1.552(mc^2/e^2),\quad g=0.2643,$$

and for $\sigma=13.1\times10^{-24}$ cm^2 one would have (approximately)

$$C=55.4\ mc^2,\quad \lambda=1.64(mc^2/e^2),\quad g=0.264.$$

In conclusion the author wishes to express his appreciation for being allowed the use of the facilities of the California Institute of Technology.

Appendix

Matrix elements of the H^3 energy terms.

If one puts $a'=A/N=(A_k-b_{12}A_{12}-b_{13}A_{13}-b_{23}A_{23})/N$ one gets for the matrix elements $[(\alpha x)^\kappa(\beta y)^\lambda(\beta z)^\mu|(\alpha x)^k(\beta y)^l(\beta z)^m]$, taking account of the exchange operations

$$P_{12}: x\rightleftarrows z \quad y\rightleftarrows y$$
$$P_{13}: x\rightleftarrows y \quad z\rightleftarrows z$$
$$P_{23}: y\rightleftarrows z \quad x\rightleftarrows x,$$

[5] L. H. Rumbaugh, R. B. Roberts and L. R. Hafstad, Phys. Rev. **54**, 675 (1938).
[6] S. S. Share, L. E. Hoisington and G. Breit, Phys. Rev. **55**, 1130 (1939).
[7] F. W. Brown and M. S. Plesset, Phys. Rev. **56**, 841 (1939).
[8] H. A. Bethe, Phys. Rev. **55**, 1261 (1939).

$$A_k=(1/\beta^4)\{2(131)+2(113)+2(122)-(213)$$
$$-(231)-(222)+4k[(131)+(113)+(122)]$$
$$-4k^2[(031)+(013)+(022)]\}$$
$$+(1/\alpha\beta^3)\{2(221)+2(212)+4(122)+(231)$$
$$+(213)-(321)-(312)-(132)-(123)$$
$$+4k[(221)+(212)-\tfrac{1}{2}(131)-\tfrac{1}{2}(113)]$$
$$+4l[-\tfrac{1}{2}(221)+\tfrac{1}{2}(113)+\tfrac{1}{2}(122)+(121)]$$
$$+4m[-\tfrac{1}{2}(212)+\tfrac{1}{2}(131)+\tfrac{1}{2}(122)+(112)]$$
$$-4k^2[(121)+(112)]-4l^2[(112)+(103)]$$
$$-4m^2[(121)+(130)]+4kl(121)+4km(112)$$
$$+4lm[(121)+(112)]\}$$
$$+(1/\alpha^2\beta^2)\{4(221)+4(212)-2(311)$$
$$-2(222)+(321)+(312)-(231)-(213)$$
$$+4k[(211)-\tfrac{1}{2}(221)-\tfrac{1}{2}(212)]+4l[(221)$$
$$+(212)-\tfrac{1}{2}(311)]+4m[(221)+(212)$$
$$-\tfrac{1}{2}(311)]-4l^2[(211)+(202)]$$
$$-4m^2[(211)+(220)]+4kl(211)+4km(211)\}$$
$$+(1/\alpha^3\beta)\{4(311)-(321)-(312)+4l(311)$$
$$+4m(311)-4l^2(301)-4m^2(310)\},$$

$$N=(1/\alpha\beta^5)[(132)+(123)]+(1/\alpha^2\beta^4)[(231)$$
$$+(213)+2(222)]+(1/\alpha^3\beta^3)[(321)+(312)],$$

where $(123)=\Gamma(\kappa+k+1)\Gamma(\lambda+l+2)\Gamma(\mu+m+3)$;

$$A_{12}=(\alpha/\gamma)^{\kappa+k}(\beta/\gamma)^{\mu+m}\{(1/\beta\gamma^4)2(212)$$
$$+(1/\beta^2\gamma^3)2[(221)+(122)]$$
$$+(1/\beta^3\gamma^2)2(131)\},$$

where $\gamma=(\alpha+\beta+1/2)$ and $(123)=\Gamma(\kappa+m+1)\times\Gamma(\lambda+l+2)\Gamma(\mu+k+3)$;

$A_{13}=A_{12}$ with μ replaced by λ and m replaced by l;

$$A_{23}=(\beta/\delta)^{\lambda+\mu+l+m}\{(1/\alpha\delta^4)2(122)$$
$$+(1/\alpha^2\delta^3)2[(221)+(212)]$$
$$+(1/\alpha^3\delta^2)2(311)\},$$

where $\delta=(\beta+\frac{1}{2})$ and $(123)=\Gamma(\kappa+k+1)\Gamma(\lambda+m+2)\Gamma(\mu+l+3)$. Their numerical evaluation for given values of α and β is a matter of simple arithmetic.

DECEMBER 1, 1939 PHYSICAL REVIEW VOLUME 56

The Spectra of Y V and Zr VI

F. W. PAUL AND W. A. RENSE*
Mendenhall Laboratory of Physics, Ohio State University, Columbus, Ohio

(Received September 29, 1939)

The Br I isoelectronic sequence has been extended to Y V and Zr VI. Spectrograms covering the region from 150A to 1000A were obtained with a three-meter grazing incidence vacuum spectrograph having a dispersion of 1.0A/mm at 500A. The separations of the ground doublets $4s^24p^5$ were predicted by the regular doublet law and observed to be 12,068 cm^{-1} for Y V and 15,600 cm^{-1} for Zr VI. With the aid of the irregular doublet law and Moseley diagram curves, most of the expected $4s4p^6$, $4s^24p^44d$ and $4s^24p^45s$ levels with $j\leq 5/2$ were found. Forty-two lines of the spectrum of Y V and forty-six lines of the spectrum of Zr VI have been classified. The absolute term values of the $^2P^0_{3/2}$ ground levels of Y V and Zr VI were estimated to be 620,000 cm^{-1} and 798,000 cm^{-1}, respectively.

THE spectra of Br I,[1] Kr II,[2] Rb III[3] and Sr IV[3] have been analyzed to the extent that in each case the term values for nearly all the important lower lying levels are known. The ground state of a member of this sequence is determined by the configuration $4s^24p^5$ which gives rise to two odd levels: $^2P^0_{1\frac{1}{2}}$ and $^2P^0_1$, of which the former lies the deeper. The strongest emission lines in this sequence should arise from transitions between the ground state doublet and the configurations $4s4p^6$, $4s^24p^44d$ and $4s^24p^45s$. These lines should exhibit, except when j is $\geqslant 2\frac{1}{2}$, a constant frequency difference equal to the doublet separation of the ground state.

The analysis of Rb III and Sr IV was based on spectrograms made with a vacuum spectrograph covering the extreme ultraviolet region from 250A to 1200A. Only transitions into the ground doublet were considered. In the present

* Now at Louisiana State University.
[1] C. C. Kiess and T. L. de Bruin, Nat. Bur. Stand. J. Research **4**, 667 (1930).
[2] De Bruin, Humphreys and Meggers, Nat. Bur. Stand. J. Research **11**, 409 (1933).
[3] D. H. Tomboulian, Phys. Rev. **54**, 350 (1938).

work a similar analysis was undertaken of the spectra of Y V and Zr VI, the next two members in the sequence. The important lines needed to establish the higher lying odd levels fall outside the range covered by the spectrograms upon which this analysis is based.

Experimental

The spectrograms were obtained with a grazing incidence vacuum spectrograph designed to cover the region below 1000A, and equipped with a 3-meter grating having 30,000 lines per inch. The dispersion is 1.0A/mm at 500A. A condensed spark discharge was used as the source of radiation. Power was supplied to the electrodes at 50 kv from a circuit consisting of a 5-kw transformer, a Kenetron rectifier and a system of condensers having a total capacitance of 0.1 μf.

Aluminum, copper and carbon rods cored with yttrium oxide were used to obtain three sets of spectrograms of yttrium covering the region from 150A to 1000A. In the case of zirconium a similar procedure was followed, the salts being ZrO and $ZrOCl_2$, but in addition, a set of spectrograms was obtained by using electrodes of zirconium metal in carbon. The exposure times varied from one to three hours. Ilford type Q-II plates were used.

Wave-lengths of carbon, oxygen and nitrogen lines taken from a list compiled by Boyce and Robinson,[4] and of copper and chlorine lines from lists by Kruger and Cooper,[5] and I. S. Bowen,[6] respectively, were used as standards. It is estimated that the wave-lengths obtained are accurate to 0.01A.

The lines classified as belonging to the spectrum of Y V are listed in Table I and those of Zr VI in Table III. In these tables the first column gives the intensity; the second the wavelength in angstroms; the third the frequency in cm^{-1}, and the fourth the transition to which this line has been assigned. The symbols used to designate line characteristics in the intensity columns are those used in the *M.I.T. Wavelength Tables*.[7]

The Spectrum of Y V

The screening constant for Y V was found by extrapolating the results given in Tomboulian's paper.[3] By the regular doublet law, the separation of the two ground levels was then computed to be 12,100 cm^{-1}. From the data, a frequently occurring constant difference of 12,068 cm^{-1} was

Table II. *Relative term values for* Y V.

Term Symbol	Relative Term Value	Term Symbol	Relative Term Value
$4s^24p^5\ ^2P^0_{1\frac{1}{2}}$	0	$4s^24p^4(^1D)4d\ ^2D_{2\frac{1}{2}}$	289,836
$4s\ 4p^5\ ^2P^0_{\frac{1}{2}}$	12,068	$4s^24p^4(^1D)4d\ ^2D_{1\frac{1}{2}}$	297,072
$4s4p^6\ ^2S_{\frac{1}{2}}$	170,936	$4s^24p^4(^1D)4d\ ^2F_{2\frac{1}{2}}$	291,052
$4s^24p^4(^3P)4d\ ^4D_{3\frac{1}{2}}$	202,902	$4s^24p^4(^1D)4d\ ^2P_{\frac{1}{2}}$	299,567
$4s^24p^4(^3P)4d\ ^4D_{2\frac{1}{2}}$	213,254	$4s^24p^4(^1D)4d\ ^2P_{1\frac{1}{2}}$	300,217
$4s^24p^4(^3P)4d\ ^4D_{\frac{1}{2}}$	219,116	$4s^24p^4(^1S)4d\ ^2D_{1\frac{1}{2}}$	318,885
$4s^24p^4(^3P)4d\ ^4P_{\frac{1}{2}}$	247,473	$4s^24p^4(^3P)5s\ ^4P_{2\frac{1}{2}}$	280,932
$4s^24p^4(^3P)4d\ ^4P_{1\frac{1}{2}}$	248,352	$4s^24p^4(^3P)5s\ ^4P_{1\frac{1}{2}}$	287,205
$4s^24p^4(^3P)4d\ ^4P_{2\frac{1}{2}}$	250,406	$4s^24p^4(^3P)5s\ ^4P_{\frac{1}{2}}$	290,911
$4s^24p^4(^3P)4d\ ^2D_{1\frac{1}{2}}$	253,678	$4s^24p^4(^3P)5s\ ^2P_{1\frac{1}{2}}$	296,745
$4s^24p^4(^3P)4d\ ^2D_{2\frac{1}{2}}$	263,524	$4s^24p^4(^3P)5s\ ^2P_{\frac{1}{2}}$	306,349
$4s^24p^4(^3P)4d\ ^2P_{\frac{1}{2}}$	258,518	$4s^24p^4(^1D)5s\ ^2D_{2\frac{1}{2}}$	315,430
$4s^24p^4(^3P)4d\ ^2P_{1\frac{1}{2}}$	258,567	$4s^24p^4(^1D)5s\ ^2D_{1\frac{1}{2}}$	317,192
$4s^24p^4(^3P)4d\ ^2F_{2\frac{1}{2}}$	274,254		

[4] J. C. Boyce and H. A. Robinson, J. Opt. Soc. Am. **26**, 133 (1936).

[5] P. Gerald Kruger and F. S. Cooper, Phys. Rev. **44**, 826 (1934).

[6] I. S. Bowen, Phys. Rev. **45**, 401 (1934).

[7] G. R. Harrison, *Wavelength Tables* (John Wiley and Sons, 1939).

Table I. *Classified lines of* Y V.

I	$\lambda(A)$	$\nu(cm^{-1})$	Classification	I	$\lambda(A)$	$\nu(cm^{-1})$	Classification
2	629.478	158,862	$4s^24p^5\ ^2P^0_{\frac{1}{2}} - 4s4p^6\ ^2S_{\frac{1}{2}}$	10	355.958	280,932	$4s^24p^5\ ^2P^0_{1\frac{1}{2}} - 4s^24p^4(^3P)5s\ ^4P_{2\frac{1}{2}}$
20	584.995	170,942	$4s^24p^5\ ^2P^0_{1\frac{1}{2}} - 4s4p^6\ ^2S_{\frac{1}{2}}$	2	351.273	284,679	$4s^24p^5\ ^2P^0_{\frac{1}{2}} - 4s^24p^4(^3P)5s\ ^2P_{1\frac{1}{2}}$
10	497.069	201,179	$4s^24p^5\ ^2P^0_{\frac{1}{2}} - 4s^24p^4(^3P)4d\ ^4D_{1\frac{1}{2}}$	5	350.877	285,000	$4s^24p^5\ ^2P^0_{\frac{1}{2}} - 4s^24p^4(^1D)4d\ ^2D_{1\frac{1}{2}}$
2	492.848	202,902	$4s^24p^5\ ^2P^0_{1\frac{1}{2}} - 4s^24p^4(^3P)4d\ ^4D_{2\frac{1}{2}}$	15	348.188	287,201	$4s^24p^5\ ^2P^0_{1\frac{1}{2}} - 4s^24p^4(^3P)5s\ ^4P_{1\frac{1}{2}}$
60	482.973	207,051	$4s^24p^5\ ^2P^0_{\frac{1}{2}} - 4s^24p^4(^3P)4d\ ^4D_{\frac{1}{2}}$	( )	347.827	287,499	$4s^24p^5\ ^2P^0_{\frac{1}{2}} - 4s^24p^4(^1D)4d\ ^2P_{\frac{1}{2}}$
1	468.911	213,260	$4s^24p^5\ ^2P^0_{1\frac{1}{2}} - 4s^24p^4(^3P)4d\ ^4D_{1\frac{1}{2}}$	2	347.039	288,152	$4s^24p^5\ ^2P^0_{\frac{1}{2}} - 4s^24p^4(^1D)4d\ ^2P_{1\frac{1}{2}}$
100	456.384	219,114	$4s^24p^5\ ^2P^0_{1\frac{1}{2}} - 4s^24p^4(^3P)4d\ ^4D_{\frac{1}{2}}$	5	345.023	289,836	$4s^24p^5\ ^2P^0_{1\frac{1}{2}} - 4s^24p^4(^1D)4d\ ^2D_{2\frac{1}{2}}$
40	424.796	235,407	$4s^24p^5\ ^2P^0_{\frac{1}{2}} - 4s^24p^4(^3P)4d\ ^4P_{\frac{1}{2}}$	1	343.749	290,910	$4s^24p^5\ ^2P^0_{1\frac{1}{2}} - 4s^24p^4(^3P)5s\ ^4P_{\frac{1}{2}}$
15	423.210	236,289	$4s^24p^5\ ^2P^0_{\frac{1}{2}} - 4s^24p^4(^3P)4d\ ^4P_{1\frac{1}{2}}$	1	343.581	291,052	$4s^24p^5\ ^2P^0_{1\frac{1}{2}} - 4s^24p^4(^1D)4d\ ^2F_{2\frac{1}{2}}$
1	413.898	241,605	$4s^24p^5\ ^2P^0_{\frac{1}{2}} - 4s^24p^4(^3P)4d\ ^2D_{1\frac{1}{2}}$	1	339.812	294,280	$4s^24p^5\ ^2P^0_{\frac{1}{2}} - 4s^24p^4(^3P)5s\ ^2P_{\frac{1}{2}}$
5w	405.787	246,435	$4s^24p^5\ ^2P^0_{\frac{1}{2}} - 4s^24p^4(^3P)4d\ ^2P_{\frac{1}{2}}$; $^2P_{1\frac{1}{2}}$	1	336.991	296,744	$4s^24p^5\ ^2P^0_{1\frac{1}{2}} - 4s^24p^4(^3P)5s\ ^2P_{1\frac{1}{2}}$
10	404.086	247,472	$4s^24p^5\ ^2P^0_{1\frac{1}{2}} - 4s^24p^4(^3P)4d\ ^4P_{\frac{1}{2}}$	40	336.613	297,077	$4s^24p^5\ ^2P^0_{1\frac{1}{2}} - 4s^24p^4(^1D)4d\ ^2D_{1\frac{1}{2}}$
1	402.660	248,348	$4s^24p^5\ ^2P^0_{1\frac{1}{2}} - 4s^24p^4(^3P)4d\ ^4P_{1\frac{1}{2}}$	30	333.815	299,567	$4s^24p^5\ ^2P^0_{1\frac{1}{2}} - 4s^24p^4(^1D)4d\ ^2P_{\frac{1}{2}}$
40	399.352	250,406	$4s^24p^5\ ^2P^0_{1\frac{1}{2}} - 4s^24p^4(^3P)4d\ ^4P_{2\frac{1}{2}}$	40	333.095	300,215	$4s^24p^5\ ^2P^0_{1\frac{1}{2}} - 4s^24p^4(^1D)4d\ ^2P_{1\frac{1}{2}}$
5	394.191	253,684	$4s^24p^5\ ^2P^0_{1\frac{1}{2}} - 4s^24p^4(^3P)4d\ ^2D_{1\frac{1}{2}}$	2	327.731	305,128	$4s^24p^5\ ^2P^0_{\frac{1}{2}} - 4s^24p^4(^1D)5s\ ^2D_{1\frac{1}{2}}$
5	386.821	258,518	$4s^24p^5\ ^2P^0_{1\frac{1}{2}} - 4s^24p^4(^3P)4d\ ^2P_{\frac{1}{2}}$	1	326.424	306,350	$4s^24p^5\ ^2P^0_{1\frac{1}{2}} - 4s^24p^4(^3P)5s\ ^2P_{\frac{1}{2}}$
5	386.747	258,567	$4s^24p^5\ ^2P^0_{1\frac{1}{2}} - 4s^24p^4(^3P)4d\ ^2P_{1\frac{1}{2}}$	5	325.928	306,816	$4s^24p^5\ ^2P^0_{\frac{1}{2}} - 4s^24p^4(^1S)4d\ ^2D_{1\frac{1}{2}}$
20	379.472	263,524	$4s^24p^5\ ^2P^0_{1\frac{1}{2}} - 4s^24p^4(^3P)4d\ ^2D_{2\frac{1}{2}}$	1	317.028	315,430	$4s^24p^5\ ^2P^0_{1\frac{1}{2}} - 4s^24p^4(^1D)5s\ ^2D_{2\frac{1}{2}}$
1	364.626	274,254	$4s^24p^5\ ^2P^0_{1\frac{1}{2}} - 4s^24p^4(^3P)4d\ ^2F_{2\frac{1}{2}}$	2	315.269	317,189	$4s^24p^5\ ^2P^0_{1\frac{1}{2}} - 4s^24p^4(^1D)5s\ ^2D_{1\frac{1}{2}}$
5	363.450	275,141	$4s^24p^5\ ^2P^0_{\frac{1}{2}} - 4s^24p^4(^3P)5s\ ^4P_{1\frac{1}{2}}$	1	313.593	318,885	$4s^24p^5\ ^2P^0_{1\frac{1}{2}} - 4s^24p^4(^1S)4d\ ^2D_{1\frac{1}{2}}$
5w	358.624	278,844	$4s^24p^5\ ^2P^0_{\frac{1}{2}} - 4s^24p^4(^3P)5s\ ^4P_{\frac{1}{2}}$				

TABLE III. *Classified lines of* Zr VI.

I	λ(*A*)	ν(CM⁻¹)	CLASSIFICATION
300	568.277	175,971	$4s^24p^5\ ^2P^0_{\frac{3}{2}} - 4s4p^6\ ^2S_{\frac{1}{2}}$
300	522.007	191,568	$4s^24p^5\ ^2P^0_{\frac{1}{2}} - 4s4p^6\ ^2S_{\frac{1}{2}}$
15	434.027	230,400	$4s^24p^5\ ^2P^0_{\frac{3}{2}} - 4s^24p^4(^3P)4d\ ^4D_{1\frac{1}{2}}$
2*w*	428.571	233,334	$4s^24p^5\ ^2P^0_{\frac{3}{2}} - 4s^24p^4(^3P)4d\ ^4D_{\frac{1}{2}}$
70	414.768	241,099	$4s^24p^5\ ^2P^0_{\frac{3}{2}} - 4s^24p^4(^3P)4d\ ^4D_{2\frac{1}{2}}$
200	406.481	246,014	$4s^24p^5\ ^2P^0_{\frac{1}{2}} - 4s^24p^4(^3P)4d\ ^4D_{1\frac{1}{2}}$
130	401.698	248,943	$4s^24p^5\ ^2P^0_{\frac{1}{2}} - 4s^24p^4(^3P)4d\ ^4D_{\frac{1}{2}}$
25	365.332	273,724	$4s^24p^5\ ^2P^0_{\frac{3}{2}} - 4s^24p^4(^3P)4d\ ^4P_{\frac{1}{2}}$
50	362.237	276,062	$4s^24p^5\ ^2P^0_{\frac{3}{2}} - 4s^24p^4(^3P)4d\ ^4P_{1\frac{1}{2}}$
90	356.430	280,560	$4s^24p^5\ ^2P^0_{\frac{3}{2}} - 4s^24p^4(^3P)4d\ ^2D_{1\frac{1}{2}}$
50	352.938	283,336	$4s^24p^5\ ^2P^0_{\frac{3}{2}} - 4s^24p^4(^3P)4d\ ^2P_{\frac{1}{2}}$
60	352.293	283,855	$4s^24p^5\ ^2P^0_{\frac{3}{2}} - 4s^24p^4(^3P)4d\ ^2P_{1\frac{1}{2}}$
20	346.493	288,606	$4s^24p^5\ ^2P^0_{1\frac{1}{2}} - 4s^24p^4(^3P)4d\ ^4F_{2\frac{1}{2}}$
20	346.404	288,680	$4s^24p^5\ ^2P^0_{1\frac{1}{2}} - 4s^24p^4(^3P)4d\ ^4F_{1\frac{1}{2}}$
90*w*	345.636	289,322	$4s^24p^5\ ^2P^0_{1\frac{1}{2}} - 4s^24p^4(^3P)4d\ ^4P_{\frac{1}{2}}$
40	342.869	291,657	$4s^24p^5\ ^2P^0_{1\frac{1}{2}} - 4s^24p^4(^3P)4d\ ^4P_{1\frac{1}{2}}$
80	337.930	295,919	$4s^24p^5\ ^2P^0_{1\frac{1}{2}} - 4s^24p^4(^3P)4d\ ^4P_{2\frac{1}{2}}$
90	337.668	296,149	$4s^24p^5\ ^2P^0_{1\frac{1}{2}} - 4s^24p^4(^3P)4d\ ^2D_{1\frac{1}{2}}$
70	334.520	298,923	$4s^24p^5\ ^2P^0_{1\frac{1}{2}} - 4s^24p^4(^3P)4d\ ^2P_{\frac{1}{2}}$
100	333.945	299,451	$4s^24p^5\ ^2P^0_{1\frac{1}{2}} - 4s^24p^4(^3P)4d\ ^2P_{1\frac{1}{2}}$
250	326.282	306,483	$4s^24p^5\ ^2P^0_{1\frac{1}{2}} - 4s^24p^4(^3P(4d\ ^2D_{2\frac{1}{2}}$
100	317.982	314,483	$4s^24p^5\ ^2P^0_{1\frac{1}{2}} - 4s^24p^4(^3P)5s\ ^4P_{2\frac{1}{2}}$
180	313.392	319,089	$4s^24p^5\ ^2P^0_{\frac{1}{2}} - 4s^24p^4(^3P)5s\ ^4P_{1\frac{1}{2}}$
40	312.993	319,496	$4s^24p^5\ ^2P^0_{1\frac{1}{2}} - 4s^24p^4(^3P)4d\ ^2F_{2\frac{1}{2}}$
250	302.347	330,746	$4s^24p^5\ ^2P^0_{\frac{1}{2}} - 4s^24p^4(^1D)4d\ ^2D_{1\frac{1}{2}}$
60	302.103	331,013	$4s^24p^5\ ^2P^0_{\frac{3}{2}} - 4s^24p^4(^3P)5s\ ^4P_{\frac{1}{2}}$
200	298.779	334,696	$4s^24p^5\ ^2P^0_{1\frac{1}{2}} - 4s^24p^4(^3P)5s\ ^4P_{1\frac{1}{2}}$
60	298.039	335,527	$4s^24p^5\ ^2P^0_{1\frac{1}{2}} - 4s^24p^4(^1D)4d\ ^2D_{2\frac{1}{2}}$
50	297.314	336,345	$4s^24p^5\ ^2P^0_{1\frac{1}{2}} - 4s^24p^4(^1D)4d\ ^2F_{2\frac{1}{2}}$
200	294.398	339,676	$4s^24p^5\ ^2P^0_{\frac{1}{2}} - 4s^24p^4(^1D)4d\ ^2P_{\frac{1}{2}}$
50	294.117	340,003	$4s^24p^5\ ^2P^0_{\frac{1}{2}} - 4s^24p^4(^1D)4d\ ^2P_{1\frac{1}{2}}$
60	290.193	344,598	$4s^24p^5\ ^2P^0_{\frac{1}{2}} - 4s^24p^4(^1S)4d\ ^2D_{1\frac{1}{2}}$
100	288.732	346,342	$4s^24p^5\ ^2P^0_{1\frac{1}{2}} - 4s^24p^4(^1D)4d\ ^2D_{1\frac{1}{2}}$
100	288.501	346,619	$4s^24p^5\ ^2P^0_{1\frac{1}{2}} - 4s^24p^4(^3P)5s\ ^4P_{\frac{1}{2}}$
90	282.397	354,111	$4s^24p^5\ ^2P^0_{1\frac{1}{2}} - 4s^24p^4(^3P)5s\ ^2P_{1\frac{1}{2}}$
60	281.466	355,283	$4s^24p^5\ ^2P^0_{1\frac{1}{2}} - 4s^24p^4(^1D)4d\ ^2P_{\frac{1}{2}}$
100	281.217	355,606	$4s^24p^5\ ^2P^0_{1\frac{1}{2}} - 4s^24p^4(^1D)4d\ ^2P_{1\frac{1}{2}}$
200	277.630	360,192	$4s^24p^5\ ^2P^0_{1\frac{1}{2}} - 4s^24p^4(^1S)4d\ ^2D_{1\frac{1}{2}}$
100	274.588	364,182	$4s^24p^5\ ^2P^0_{\frac{1}{2}} - 4s^24p^4(^3P)5s\ ^2P_{\frac{1}{2}}$
180	270.862	369,192	$4s^24p^5\ ^2P^0_{\frac{3}{2}} - 4s^24p^4(^1D)5s\ ^2D_{1\frac{1}{2}}$
200	270.474	369,721	$4s^24p^5\ ^2P^0_{1\frac{1}{2}} - 4s^24p^4(^3P)5s\ ^2P_{1\frac{1}{2}}$
200	263.312	379,778	$4s^24p^5\ ^2P^0_{1\frac{1}{2}} - 4s^24p^4(^3P)5s\ ^2P_{\frac{1}{2}}$
50	262.919	380,383	$4s^24p^5\ ^2P^0_{1\frac{1}{2}} - 4s^24p^4(^1D)5s\ ^2D_{2\frac{1}{2}}$
160	259.884	384,787	$4s^24p^5\ ^2P^0_{1\frac{1}{2}} - 4s^24p^4(^1D)5s\ ^2D_{1\frac{1}{2}}$
150	245.327	407,619	$4s^24p^5\ ^2P^0_{\frac{1}{2}} - 4s^24p^4(^1S)5s\ ^2S_{\frac{1}{2}}$
70	236.288	423,212	$4s^24p^5\ ^2P^0_{1\frac{1}{2}} - 4s^24p^4(^1S)5s\ ^2S_{\frac{1}{2}}$

observed, and the lines involved were examined as those possibly due to Y V. The term table resulting from this analysis is given in Table II.

Lines from the transition $4s^24p^5(^2P^0_{1\frac{1}{2}}, {}^2P^0_{\frac{1}{2}}) - 4s^24p^44d$ were considered first. The wave-lengths of these lines were predicted by a linear extrapolation of the data on Rb III and Sr IV in accordance with the irregular doublet law. In nearly every case it was found that of the observed lines on the list, only one would fall near a predicted position, so that the classification was readily established. In a similar manner the two resonance lines $4s^24p^5(^2P^0_{1\frac{1}{2}}, {}^2P^0_{\frac{1}{2}}) - 4s4p^6\ ^2S_{\frac{1}{2}}$ were easily identified. The Moseley diagram drawn from Tomboulian's data was helpful in locating lines resulting from the $4s^24p^45s$ transitions. There is some doubt concerning the relative assignment of the levels $4s^24p^4(^3P)5s\ ^2P_{1\frac{1}{2}}$ and $4s^24p^4(^1D)4d\ ^2D_{1\frac{1}{2}}$, for they fall so close together that the criteria used here are not sufficient to distinguish between them. The brighter pair of lines was assigned to the $4d^2D_{1\frac{1}{2}}$ transition in accordance with the observation that the $4d$ transitions give rise to more intense lines than the $5s$ transitions in the other members of this isoelectronic sequence.

Pairs of lines from transitions to the ground doublet from the levels $4s^24p^4(^3P)4d\ ^2P_{\frac{1}{2}}$, $^4F_{1\frac{1}{2}}$, $4s^24p^4(^1D)4d\ ^2P_{\frac{1}{2}}$ and $4s^24p^4(^1S)4d\ ^2D_{1\frac{1}{2}}$ were not observed by Tomboulian for Rb III and Sr IV. Of these levels only the $^4F_{1\frac{1}{2}}$ is known for both Br I and Kr II, so that predicted positions for the levels would not be very reliable. It was observed, however, that one of the two lines of the pair tentatively classified as $4s^24p^5(^2P^0_{1\frac{1}{2}}, {}^2P^0_{\frac{1}{2}}) - 4s^24p^4(^3P)4d\ ^2P_{1\frac{1}{2}}$ was a close double, and the other line, very broad. Furthermore, both lines of the pair tentatively classified as $4s^24p^5(^2P^0_{1\frac{1}{2}}, {}^2P^0_{\frac{1}{2}}) - 4s^24p^4(^1D)4d\ ^2P_{1\frac{1}{2}}$ were close doubles of approximately equal separation. Accordingly, the view was taken that in both cases the $^2P_{\frac{1}{2}}$ and $^2P_{1\frac{1}{2}}$ levels were very close, and the classification here given was made on this basis. The order is taken to be inverted because the corresponding terms in the one member of the sequence for which they were known are listed as inverted. The $4s^24p^4(^1S)4d\ ^2D_{1\frac{1}{2}}$ level was known for only Kr II, but by using the irregular doublet law and extrapolating along a straight line parallel to the available curves of the $(^1D)4d$ levels, it was possible to estimate roughly the wave-lengths of the lines $4s^24p^5(^2P^0_{1\frac{1}{2}}, {}^2P^0_{\frac{1}{2}}) - 4s^24p^4(^1S)4d\ ^2D_{1\frac{1}{2}}$. The lines here classified fall near their predicted positions. The lines from the $^4F_{1\frac{1}{2}}$ level were not

TABLE IV. *Relative term values for* Zr VI.

TERM SYMBOL	RELATIVE TERM VALUE	TERM SYMBOL	RELATIVE TERM VALUE
$4s^24p^5\ ^2P^0_{1\frac{1}{2}}$	0	$4s^24p^4(^3P)4d\ ^2F_{2\frac{1}{2}}$	319,496
$4s^24p^5\ ^2P^0_{\frac{1}{2}}$	15,600	$4s^24p^4(^1D)4d\ ^2D_{2\frac{1}{2}}$	335,527
$4s4p^6\ ^2S_{\frac{1}{2}}$	191,570	$4s^24p^4(^1D)4d\ ^2D_{1\frac{1}{2}}$	346,344
$4s^24p^4(^3P)4d\ ^4D_{2\frac{1}{2}}$	241,099	$4s^24p^4(^1D)4d\ ^2F_{2\frac{1}{2}}$	336,345
$4s^24p^4(^3P)4d\ ^4D_{1\frac{1}{2}}$	246,007	$4s^24p^4(^1D)4d\ ^2P_{\frac{1}{2}}$	355,280
$4s^24p^4(^3P)4d\ ^4D_{\frac{1}{2}}$	248,938	$4s^24p^4(^1D)4d\ ^2P_{1\frac{1}{2}}$	355,604
$4s^24p^4(^3P)4d\ ^4F_{2\frac{1}{2}}$	288,606	$4s^24p^4(^1S)4d\ ^2D_{1\frac{1}{2}}$	360,195
$4s^24p^4(^3P)4d\ ^4F_{1\frac{1}{2}}$	288,680	$4s^24p^4(^3P)5s\ ^4P_{2\frac{1}{2}}$	314,483
$4s^24p^4(^3P)4d\ ^4P_{\frac{1}{2}}$	289,323	$4s^24p^4(^3P)5s\ ^4P_{1\frac{1}{2}}$	334,692
$4s^24p^4(^3P)4d\ ^4P_{1\frac{1}{2}}$	291,660	$4s^24p^4(^3P)5s\ ^4P_{\frac{1}{2}}$	346,616
$4s^24p^4(^3P)4d\ ^4P_{2\frac{1}{2}}$	295,919	$4s^24p^4(^3P)5s\ ^2P_{1\frac{1}{2}}$	369,716
$4s^24p^4(^3P)4d\ ^2D_{1\frac{1}{2}}$	296,155	$4s^24p^4(^3P)5s\ ^2P_{\frac{1}{2}}$	379,780
$4s^24p^4(^3P)4d\ ^2D_{2\frac{1}{2}}$	306,483	$4s^24p^4(^1D)5s\ ^2D_{2\frac{1}{2}}$	380,383
$4s^24p^4(^3P)4d\ ^2P_{\frac{1}{2}}$	298,923	$4s^24p^4(^1D)5s\ ^2D_{1\frac{1}{2}}$	384,790
$4s^24p^4(^3P)4d\ ^2P_{1\frac{1}{2}}$	299,453	$4s^24p^4(^1S)5s\ ^2S_{\frac{1}{2}}$	423,215

found, probably because they were too faint to show on the spectrograms.

Transitions from even levels with $j=2\frac{1}{2}$ can occur only to the $^2P_{1\frac{1}{2}}$ level of the ground doublet, so that but one line instead of a pair can be associated with these levels. The lines fixing the $4s^24p^4(^3P)4d\ ^4D_{2\frac{1}{2}}$, $^4P_{2\frac{1}{2}}$ and $4s^24p^4(^3P)5s\ ^4P_{2\frac{1}{2}}$ levels were identified on the basis of the Lande interval rule which was assumed to hold approximately for this spectrum. The lines from the levels $4s^24p^4(^3P)4d\ ^2D_{2\frac{1}{2}}$, $^2F_{2\frac{1}{2}}$ and $4s^24p^4(^1D)4d\ ^2D_{2\frac{1}{2}}$, $^2F_{2\frac{1}{2}}$ were identified by their proximity to positions calculated by extrapolating the data on Br I and Kr II. The wave-length of the line $4s^24p^5\ ^2P^0_{1\frac{1}{2}} - 4s^24p^4(^1D)5s\ ^2D_{2\frac{1}{2}}$ was predicted by extending a Moseley diagram curve through the two known points for Br I and Kr II, and making it parallel to the corresponding curve through the $(^1D)5s\ ^2D_{1\frac{1}{2}}$ points.

The ionization potential of Y V was estimated to correspond approximately to 620,000 cm^{-1}, since it was found that this value gave the smoothest and most nearly parallel curves (for the same n) on the Moseley diagram.

The Spectrum of Zr VI

In the analysis of Zr VI, the wave-lengths of the two resonance lines $4s^24p^5(^2P^0_{1\frac{1}{2}}, ^2P^0_{\frac{1}{2}}) - 4s4p^6\ ^2S_{\frac{1}{2}}$ were predicted by means of the irregular doublet law. Two intense lines were found very near to these positions. The observed frequency difference of 15,597 cm^{-1} agrees well with a separation of 15,200 cm^{-1} computed from the regular doublet law. An examination of the data revealed the presence of almost a score of pairs of lines having a frequency difference equal to 15,600 cm^{-1} to within the accuracy of measurement. A procedure similar to that used in the analysis of Y V lead to the results given in Table III and Table IV.

A few terms not found for Y V were observed in the spectrum of Zr VI, namely the terms $4s^24p^4(^3P)4d\ ^4F_{2\frac{1}{2}}$, $^4F_{1\frac{1}{2}}$ and $4s^24p^4(^1S)5s\ ^2S_{\frac{1}{2}}$. Of these, the first two are somewhat doubtful because of the absence of the line $4s^24p^5\ ^2P_{\frac{1}{2}} - 4s^24p^4(^3P)4d\ ^4F_{1\frac{1}{2}}$ on the spectrograms. The observed lines fall very near the predicted positions, however. There is also some doubt concerning the relative assignments of the terms $4s^24p^4(^1D)4d\ ^2D_{1\frac{1}{2}}$ and $4s^24p^4(^3P)5s\ ^4P_{\frac{1}{2}}$, which fall very nearly together.

A study of the Moseley diagram curves leads to an estimate of 798,000 cm^{-1} for the ionization potential of Zr VI.

The authors wish to express their gratitude to Professor L. L. Quill of this University for making available to them samples of yttrium and zirconium of high purity.

DECEMBER 1, 1939 PHYSICAL REVIEW VOLUME 56

The Fundamental Rotation-Vibration Band of Nitric Oxide

R. H. Gillette, *Department of Chemistry, University of Michigan, Ann Arbor, Michigan*

AND

Eugene H. Eyster,* *Department of Physics, University of Michigan, Ann Arbor, Michigan*

(Received October 9, 1939)

The fundamental rotation-vibration band of nitric oxide has been measured with the high dispersion of an echellette grating spectrometer, and has been subjected to a complete analysis. The resulting constants have been carefully combined with those derived from the existing electronic data to yield the following molecular constants for the normal state of the molecule: $\omega_e = 1904.03\ (^2\Pi_{1/2}), 1903.68\ (^2\Pi_{3/2})$ cm^{-1}, $\omega_e x_e = 13.97$ cm^{-1}, $\omega_e y_e = -1.20\times10^{-3}$ cm^{-1}, $B_e = 1.7046$ cm^{-1}, $I_e = 16.423\times10^{-40}$ g cm^2, $r_e = 1.1508$A.

Introduction

ALTHOUGH nitric oxide is one of the relatively few diatomic molecules which is chemically stable under ordinary conditions, the values of its molecular constants are still somewhat uncertain. The β and γ electronic band systems of this molecule have been extensively in-

* National Research Fellow in Chemistry.

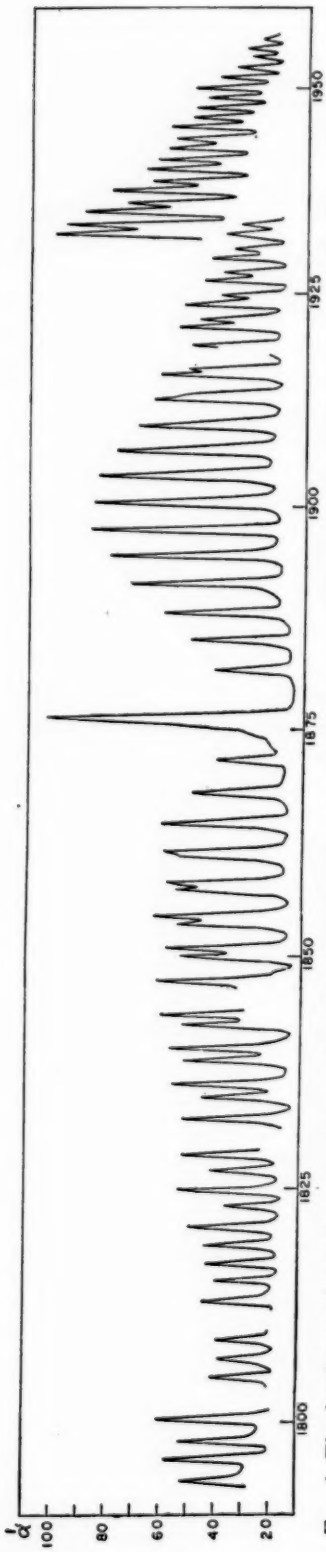

FIG. 1. The fundamental rotation-vibration band of NO. The ordinate, α', is defined as: $\alpha' = 100 \log_{10} D^0/D$, where D is the galvanometer deflection with the cell in the beam, and D^0 the deflection with the cell out of the beam. For the significance of the quantity α see footnote 5.

vestigated,[1] both in their rotational and vibrational structures, and since both systems arise from transitions to the normal state, each should yield constants for the ground state. However, the accepted vibrational constants[2] have been obtained by an unsuitable extrapolation from data which do not include the first four vibrational levels.[1a] Furthermore, the rotational constants determined from two sets of internally consistent data[1a, b] are not in agreement. Direct observation of the rotation-vibration bands should clear up this situation, but unfortunately the existing measurements of the fundamental and its first overtone[3] were made with insufficient dispersion and sensitivity for precision measurements. Consequently it was felt worth while to investigate the fundamental band under the highest available dispersion, and critically to reexamine the electronic data.

EXPERIMENTAL

The nitric oxide used in this work was prepared in two different ways: by treating a mixture of potassium nitrate and concentrated sulfuric acid with metallic mercury, and by the action of copper metal on concentrated nitric acid. In each case the gas was absorbed in a solution of ferrous sulfate to remove the N_2O_4 which always contaminated the product. The solution thus obtained was heated to decompose the $Fe(NO)^{++}$ complex ion, the gas, after discarding the first few liters, being collected over water. The product so obtained, which showed no color even in thick layers, was conducted into a large storage bulb through a drying tube filled with Dehydrite, and from there was withdrawn as needed. The gas from the two sources displayed no observable differences in absorption.

The grating spectrometer, provided with a rocksalt foreprism, has been described in essen-

[1] β system: (a) Jenkins, Barton, and Mulliken, Phys. Rev. **30**, 150 (1927); (b) Schmid, Koenig, and Farkas, Zeits. f. Physik **64**, 84 (1930). γ system: (c) M. Guillery, Zeits. f. Physik **42**, 121 (1927); (d) R. Schmid, Zeits. f. Physik **49**, 428 (1928); see also reference (b).

[2] W. Jevons, *Report on the Band Spectra of Polyatomic Molecules* (Cambridge University Press, 1932), p. 288, and H. Sponer, *Molekülspektren*, Vol. I, p. 36.

[3] Snow, Rawlins, and Rideal, Proc. Roy. Soc. **A124**, 460 (1929); C. P. Snow and E. K. Rideal, Proc. Roy. Soc. **A126**, 356 (1930).

tially its present condition by Barker and Meyer.[4] In this region of the spectrum an echellette grating of 4800 lines per inch gave the best results. Because of the excellence of the optical system and thermocouple, it was possible to obtain background deflections of about 350 mm, while working well below the practical limit of amplification of the Moll thermorelay, even though the effective slit width was only 0.45 cm^{-1}. An ordinary Nernst glower served as a source of radiation.

An 18-cm glass absorption cell, fitted with potassium bromide windows, was so arranged that it could be readily moved into and out of the light beam. The absorption measurements were made in the conventional manner by reading the galvanometer deflection with the cell in the beam and again with the cell out, and then immediately plotting the logarithm of the ratio of the latter to the former[5] against the circle reading. This method has the advantage of detecting large accidental errors at once, so that an offending point can be rechecked before the circle has been moved. With the aid of a divided head tangent screw, the circle could be accurately moved through intervals of 10 seconds of arc (0.15 cm^{-1}). Each absorption line measured in this way has been determined by from eight to twelve points, and except for a slight rounding off at peak and base, the sides of the lines have proved to be accurately linear. Successive determinations of the position of a given line never varied by more than 5 seconds, and in general new points fell upon the same curve as older ones. Consequently, it is believed that the maximum error in locating the relative positions of lines is 0.07 cm^{-1}, and that the probable error is somewhat smaller. In order to minimize the absolute errors in line frequencies, the grating was carefully recalibrated on the helium doublet at 1.083012μ, this being the center of gravity of the two lines measured by Ignatieff[6] by interferometer methods. The third, fourth, and fifth orders were measured, readings being taken every 5 seconds of arc, and led to independent values of the grating constant which were identical to five significant figures, with a mean deviation of three in the sixth place. This is consistent with our estimated accuracy in angle determinations, and indicates that the absolute errors have been reduced to the order of magnitude of the relative errors. The measured wave-lengths in air have been reduced to frequencies in the usual way, using the data of Rusch[7] for the dispersion of air.

The results of this investigation are shown in Fig. 1. In the center of the band, where the ab-

TABLE I.* *Line frequencies and combinations in the fundamental* NO *band.*

$J-\frac{1}{2}$	$R_1(J)$	$P_1(J)$	$R_1(J-1)-P_1(J+1)$	$R_1(J)-P_1(J)$	$\frac{1}{2}[R_1(J-1)+P_1(J)]$
0	1880.91	—	—	—	—
1	1884.43	1870.79	13.67	13.64	1875.85
2	1887.41	1867.24	20.72	20.17	1875.84
3	1890.73	1863.71	26.66	27.02	1875.56
4	1893.91	1860.75	33.35	33.16	1875.74
5	1896.92	1857.38	40.24	39.54	1875.64
6	1900.06	1853.67	46.65	46.39	1875.30
7	1903.18	1850.27	53.48	52.91	1875.16
8	1905.93	1846.58	60.16	59.35	1874.88
9	1908.92	1843.02	66.56	65.90	1874.48
10	1912.08	1839.37	73.40	72.71	1874.14
11	1915.07	1835.52	80.24	79.55	1873.80
12	—	1831.84	87.06	—	1873.46
13	1920.65	1828.01	—	92.64	—
14	1923.29	1824.30	100.20	98.99	1872.48
15	1926.09	1820.45	106.68	105.64	1871.87
16	1928.83	1816.61	113.43	112.22	1871.35
17	1931.73	1812.66	120.24	119.07	1870.74
18	1934.42	1808.59	126.84	125.83	1870.16
19	1937.00	1804.89	133.77	132.11	1869.66
20	1939.51	1800.65	140.45	138.86	1868.82
21	1942.04	1796.55		145.49	1868.03
22	1944.76				
23	1947.03				
24	1949.56				
25	1952.12				
26	1954.43				

$J-\frac{1}{2}$	$R_2(J)$	$P_2(J)$	$R_2(J-1)-P_2(J+1)$	$R_2(J)-P_2(J)$	$\frac{1}{2}[R_2(J-1)-P_2(J)]$
3	(1890.73)				
4	(1893.91)	(1860.27)	(34.09)	(33.64)	(1875.50)
5	(1896.92)	1856.64	(41.06)	(40.28)	(1875.28)
6	(1900.06)	1852.85	(47.54)	(47.21)	(1874.89)
7	—	1849.38	—	—	(1874.72)
8	—	—	—	—	—
9	—	1841.97	—	—	—
10	—	1838.03	—	—	—
11	1915.74	1834.04	—	81.70	—
12	—	—	89.54	—	—
13	1921.48	1826.20	—	95.28	—
14	1924.36	1822.54	102.99	101.82	1872.01
15	1927.08	1818.49	109.55	108.59	1871.43
16	1929.92	1814.81	—	115.11	1870.95
17	1932.98	—	123.18	—	—
18	1935.66	1806.74	—	128.92	1869.86
19	1938.34	—	137.28	—	—
20	1940.86	1798.38	144.03	142.84	1868.36
21	1943.40	1794.31		149.09	1867.59
22	1945.93				
23	1948.39				
24	1950.84				
25	1953.48				
26	1955.54				

Maximum of unresolved Q_1 and Q_2 branches at 1875.52

* Lines and combinations enclosed in parentheses have been rendered uncertain by the overlapping of the two sub-bands near the center.

[4] E. F. Barker and C. F. Meyer, Trans. Faraday Soc. **25**, 912 (1929).

[5] This quantity, owing to the finite slit width of the spectrometer, is proportional to the absorption coefficient only for low absorption, becoming proportional to its square root where absorption is high.

[6] Ignatieff, Ann. d. Physik **43**, 73 (1914). The position of his reference helium line has not been significantly changed by later measurements.

[7] M. Rusch, Ann. d. Physik **70**, 373 (1923).

sorption was found to be relatively strong, the cell was filled to a pressure of 18 cm, while for the weaker wings of the band, a pressure of one-third atmosphere was used. The gaps in the band occur in regions where atmospheric water lines were found to be so strong that absorption measurements by this method become very uncertain. The important features of this graph will be discussed in the next section. The frequencies of the individual lines, as well as their arrangement in branches, are given in Table I.

Molecular Constants

It has been well established by the analyses of the β and γ band systems[1] of NO that the $^2\Pi$ ground state of the molecule is intermediate between Hund's cases a and b ($A/B=73.3$), and that it has a Λ-type doubling much too small to be observed in the fundamental rotation-vibration band even with the high dispersion of our grating instrument. Consequently the energy levels will be given by the Hill and Van Vleck equation for doublet states intermediate between cases a and b,[8] which can be written, neglecting the small term $f(K, J-K)$, as:

$$T_i(J,v)=T_e+G_i(v)+B_v\{(J+\tfrac{1}{2})^2-1+(-1)^i[(J+\tfrac{1}{2})^2-A/B_v+A^2/4B_v]^{\frac{1}{2}}\}+D_vJ^2(J+1)^2+\cdots. \quad (1)$$

When $i=1$ the above equation gives the energy levels comprising the $^2\Pi_{1/2}$ substate, and when $i=2$, those of the $^2\Pi_{3/2}$ substate. The subscript i is also added to the vibrational energy term, $G(v)$, in recognition of the fact that this need not be identical in the two substates. Since the observed A/B is rather large, it is to be expected that the following approximate expressions for the energies of the two substates will be valid:

$$T_1=T_e-A/2+G_1(v)+B^*_{v1}/4+B^*_{v1}J(J+1)+D^*_{v1}J^2(J+1)^2+\cdots$$
$$T_2=T_e+A/2+G_2(v)-7B^*_{v2}/4+B^*_{v2}J(J+1)+D^*_{v2}J^2(J+1)^2+\cdots. \quad (2)$$

The constants of Eqs. (2) are related to those of Eq. (1) by:

$$B_v=(B^*_{v1}+B^*_{v2})/2; \quad D_v=(D^*_{v1}+D^*_{v2})/2. \quad (3)$$

[8] R. S. Mulliken, Rev. Mod. Phys. 2, 109 (1930).

Eqs. (2) display the simple J dependence of the limiting case a equation, so with their aid, and the application of the appropriate selection rules, the structure of the observed infra-red band may be easily understood. The band of Fig. 1 consists of two sets of P and R branches, the P_1 and R_1 branches arising from transitions between the $^2\Pi_{1/2}$ substates, and the P_2 and R_2 branches arising from transitions between the $^2\Pi_{3/2}$ substates. In addition, the unresolved Q_1 and Q_2 branches are to be found at the center of the band. The P_1 and P_2 branches begin to separate at about $J=4\frac{1}{2}$, and the R_1 and R_2 branches at somewhat higher quantum numbers. The lines may be numbered unambiguously since the first lines, $R_1(\frac{1}{2})$ and $P_1(1\frac{1}{2})$, are unmistakable. The R_1 and P_1 branches, originating on the ground state of the doublet, are of course to be identified by their greater intensity.

Vibrational energy

In order to evaluate $\Delta G_i(0)$, where $\Delta G_i(v)=G_i(v+1)-G_i(v)$, with the greatest possible precision, the following combination relations have been employed:

$$\tfrac{1}{2}\{R_1(J-1)+P_1(J)\}=\Delta G_1(0)-\alpha_1(M+\tfrac{1}{4});$$
$$\tfrac{1}{2}\{R_2(J-1)+P_2(J)\}=\Delta G_2(0)-\alpha_2(M-\tfrac{7}{4});$$
$$\alpha_i=B^*_{0i}-B^*_{1i}; \quad M=J^2. \quad (4)$$

The experimental values of these combinations, given in the last column of Table I, are shown plotted against $M-\frac{1}{4}$ in Fig. 2. To these points equations linear in $M-\frac{1}{4}$ were fitted by the method of least squares, yielding the following values for the constants of Eqs. (4):

$$\Delta G_1(0)=1876.102\ \text{cm}^{-1}; \quad \alpha_1=0.01733\ \text{cm}^{-1}$$
$$\Delta G_2(0)=1875.636\ \text{cm}^{-1}; \quad \alpha_2=0.01736\ \text{cm}^{-1}.$$

These constants differ appreciably from the values $\Delta G_1(0)=1877.734$ and $\Delta G_2(0)=1877.481$, given by the equation which fits the vibrational levels from $v=4$ to 14.[1a] That the error does not lie in the infra-red data may be demonstrated by a consideration of two bands from the γ system.[1d] The numbering and identification of branches in the (0, 0) and (0, 1) $^2\Pi_{1/2}$ sub-bands have been carefully rechecked, and data from these bands have been used to calculate the following combinations, which, for the low values of J involved, depend only upon the ground electronic state,

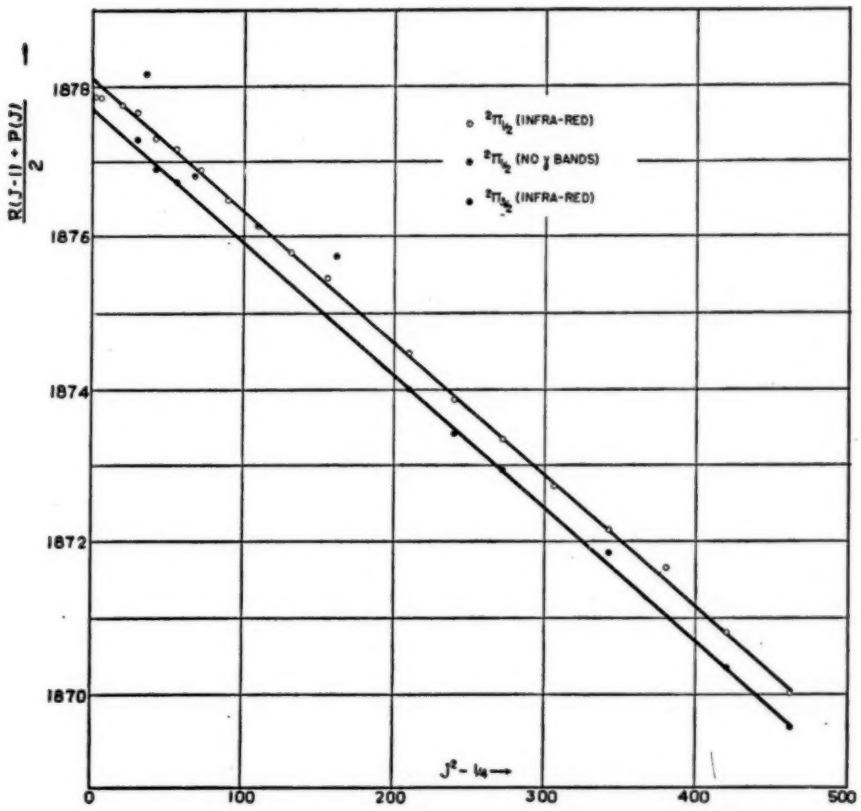

FIG. 2. Combinations from the fundamental rotation-vibration band of NO and from the (0,0) and (0,1) $^2\Pi_{\frac{1}{2}}$ sub-bands of the γ system of NO, which determine the quantities $\Delta G_i(0)$. The ordinates of this figure should be uniformly decreased by two units.

and have the same form as the first of Eqs. (4):

$$\tfrac{1}{2}\{P_1(J)+R_1(3J)\}_{(0,\,0)}-\tfrac{1}{2}\{P_1(J)+R_1(3J)\}_{(0,\,1)} = \Delta G_1''(0)-\alpha_1''(M+\tfrac{1}{4}); \quad M=2J+5J^2. \quad (5)$$

These combinations for four low values of M are included in Fig. 2, and clearly substantiate the line obtained from the infra-red data, rather than one which would extrapolate 1.6 cm^{-1} higher.

To demonstrate the true nature of this discrepancy, the quantities $\Delta G_i(v)$ have been determined directly from the measured centers of bands in the β system[18] for values of v ranging from 4 to 14. These data have then been used to calculate the function $\Delta G_i'(v)=\Delta G_i(v)-1875.000+28.000v$, which would be linear in v if $\omega_e x_e$ were the last nonzero coefficient in the usual representation of $G(v)$ as a power series in $(v+\frac{1}{2})$. The values thus calculated are indicated by the circles in Fig. 3, while the dotted curves show the $\Delta G_i'(v)$ calculated from the equation of Jenkins, Barton, and Mulliken. One observes that though Fig. 3 suggests a very high accuracy of measurements, the dotted curves, which fit the experimental points very well over the range in v for which they were determined, show a behavior for $v<4$ which has its basis not in reality, but in the nature of a cubic equation. In fact it is easy to see that the points between $v=0$ and 14 cannot be conveniently represented with the aid of the usual type of vibrational energy expression; hence it seems best to fit the vibrational levels in the region where their behavior is normal, i.e., out to $v=10$, with a cubic equation in $(v+\frac{1}{2})$. The equations:

$$\begin{aligned} G_1(v) &= 1904.03\,(v+\tfrac{1}{2})-13.97\,(v+\tfrac{1}{2})^2 \\ &\qquad -0.00120\,(v+\tfrac{1}{2})^3 \\ G_2(v) &= 1903.68\,(v+\tfrac{1}{2})-13.97\,(v+\tfrac{1}{2})^2 \\ &\qquad -0.00120\,(v+\tfrac{1}{2})^3 \end{aligned} \quad (6)$$

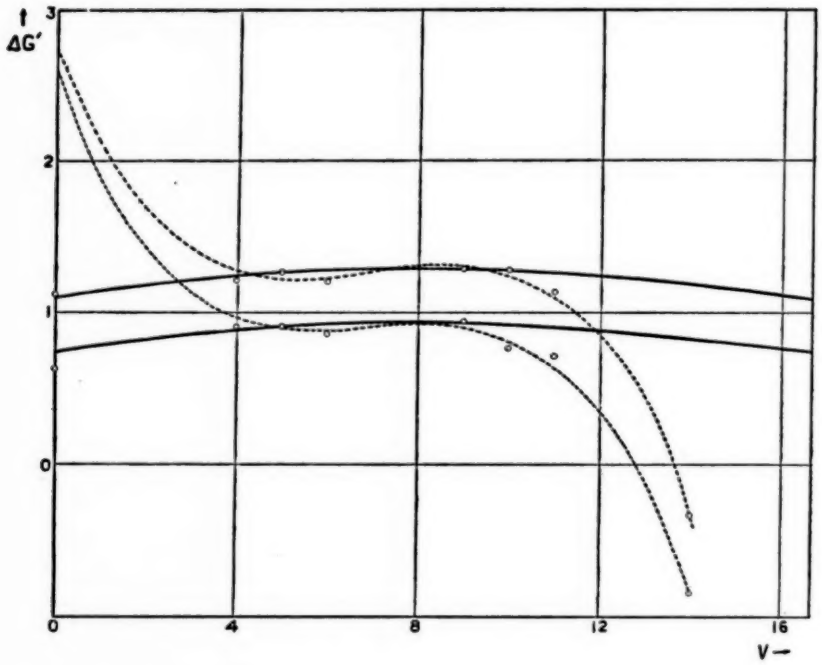

FIG. 3. The dependence of the reduced vibrational term spacing, $\Delta G_i'(v)$, on the vibrational quantum number. The dotted curve corresponds to the equation of Barton, Jenkins, and Mulliken, determined from the β bands alone, the full curves to Eqs. (6) of the text, and the circles to experimental values from the β system and the infra-red (the points for $V=0$ are from the infra-red data).

correspond to the full lines of Fig. 3. Beyond $v=10$, it appears that some change in the bonding is setting in, a situation not uncommon in diatomic molecules, but one which one would hardly anticipate for such low vibrational levels of the ground state of a stable chemical molecule.

Rotational energy

For the determination of the rotational constants, it is first convenient to employ Eqs. (2), and then to make certain, with the aid of the more exact Eq. (1), that the use of the approximate expressions has been suitable. Accordingly, the usual combinations, $\Delta_2 T_i(J, v)$, have been calculated, and are given in the fourth and fifth columns of Table I. In the approximation of Eqs. (2), these are related to the rotational constants as follows:

$$\Delta_2 T_i(J, v)/2(2J+1) = B^*_{vi} + 3D^*_{vi}/2 + 2D^*_{vi}(J+\tfrac{1}{2})^2. \quad (7)$$

Hence the left side of Eq. (7) should be a linear function of $(J+\frac{1}{2})^2$; such appeared to be the case upon plotting the experimental data, and the rotational constants were therefore determined by fitting an equation of the form of (7) to them by the method of least squares. Since our combinations extend only to $J=21\frac{1}{2}$, and several are missing in the $^2\Pi_{3/2}$ sub-band, we have also treated by the same method the combinations for the ground vibrational state given by Schmid, Koenig, and Farkas,[1b] from the γ system. These data appear to be considerably less accurate than ours; in particular, the combinations for $J<10\frac{1}{2}$ show so much scatter that they have been rejected. Treated in this fashion, the infra-red data give:

$$B^*_{01}=1.6696\ \text{cm}^{-1};\ B^*_{02}=1.7200\ \text{cm}^{-1};$$
$$B^*_{11}=1.6525\ \text{cm}^{-1};\quad B^*_{12}=1.7015\ \text{cm}^{-1}.$$

The electronic data for the ground state give:

$$B^*_{01}=1.6705\ \text{cm}^{-1};\quad B^*_{02}=1.7279\ \text{cm}^{-1};$$
$$D^*_{01}=0.53\times10^{-6}\ \text{cm}^{-1};$$
$$D^*_{02}=-10.06\times10^{-6}\ \text{cm}^{-1}.$$

The infra-red data, particularly for the $^2\Pi_{3/2}$ state, do not cover a wide enough range in

$(J+\frac{1}{2})^2$ to give significant values of the quantities D^*_{vi}, although they do confirm the sign difference given by the electronic data. On the other hand, the slopes are very small, and for low values of J the infra-red combinations prove more consistent. With these facts in mind we have chosen the following values for the rotational constants:

$$B_0=1.6959\ \text{cm}^{-1};\quad B_1=1.6770\ \text{cm}^{-1};\quad D_0=-4.8\times10^{-6}\ \text{cm}^{-1}.$$

When the above values of B_v are plotted against v, together with those determined in the region of $v=6$ to 13 from the β bands,[1a] it is found that they are all very well fitted by a straight line which differs but slightly from the one originally determined from these electronic data alone. The best line, extrapolated to $v=-\frac{1}{2}$, then gives $B_e=1.7046\ \text{cm}^{-1}$, and gives $\alpha=0.01777\ \text{cm}^{-1}$ as its slope, the latter in reasonable agreement with the values of α_i determined from the infra-red data alone by Eqs. (4).

The values of B_v calculated by Schmid, Koenig, and Farkas,[1b] however, fall consistently above this line, a circumstance which seems to be due both to their method of treating their data, and to the large scatter shown by their combinations for low J. This viewpoint is confirmed by the fact that their combinations for $J>10\frac{1}{2}$ in the ground vibrational state give a value for B_0, when treated by our method, which is in essential agreement with the infra-red value.

In order to verify the correctness of this method of analysis, the rotational levels have been calculated out to $J=42\frac{1}{2}$ by Eq. (1), by using $B_v=1.6959\ \text{cm}^{-1}$, $A=124.2\ \text{cm}^{-1}$, and $D_v=0$. It is then found that $\Delta_2T_i(J,v)/2(2J+1)$ is neither a constant nor even precisely linear in $(J+\frac{1}{2})^2$. However this departure from linearity, out to $J=42\frac{1}{2}$ in any case, is too small to be of significance when compared with the experimental scatter of points, and this function appears to be adequately represented by:

$$\Delta_2T_i(J,v)/2(2J+1)=B_v+3D_v/2+(-1)^ik_1+\{2D_v+(-1)^{i+1}k_2\}(J+\tfrac{1}{2})^2. \quad (8)$$

The quantities k are positive constants which for this particular choice of B_v and A, which corresponds to the ground vibrational state, are:

$$k_1=0.0243\ \text{cm}^{-1};\quad k_2=6.78\times10^{-6}\ \text{cm}^{-1}.$$

These may be compared with the experimental values:

$k_1=0.0252\ \text{cm}^{-1}$ (infra-red)
$k_1=0.0287\ \text{cm}^{-1}$ (γ bands);
$k_2=5.3\times10^{-6}\ \text{cm}^{-1}$ (γ bands).

The form of Eq. (8) shows that our analysis with Eqs. (2) and (3) has been essentially correct, and the agreement of the observed and calculated k's would appear to be adequate.

Finally the molecular constants for the ground state of NO may be summarized as:

$$\omega_{e1}=1904.03\ \text{cm}^{-1}\qquad B_e=1.7046\ \text{cm}^{-1}$$
$$\omega_{e2}=1903.68\ \text{cm}^{-1}\qquad \alpha=0.0178\ \text{cm}^{-1}$$
$$\omega_ex_e=13.97\ \text{cm}^{-1}\qquad I_e=16.423\times10^{-40}\ \text{g cm}^2$$
$$\omega_ey_e=-0.00120\ \text{cm}^{-1}\qquad r_e=1.1508\text{A}$$
$$D_0=-5\times10^{-6}\ \text{cm}^{-1}.$$

In conclusion, we wish to express our appreciation to Professor E. F. Barker, at whose suggestion this problem has been investigated, for his continued interest and helpful discussions; and to the Physics Department of the University of Michigan for the use of their excellent infra-red equipment. One of us (E. H. E.) is pleased to acknowledge his special indebtedness to the National Research Council.

Isotope Shift in Magnesium

JOHN P. VINTI
Worcester Polytechnic Institute, Worcester, Massachusetts
(Received September 26, 1939)

A theoretical investigation is made to see whether nuclear motion alone can account for observed fine structure in magnesium, especially for the lines $3\,^1S_0-3\,^1P_1$, $3\,^1S_0-3\,^3P_1$, $3\,^1P_1-3\,^1D_2$, $3\,^3P-3\,^3D$, and the limit of the series $3\,^1P_1-n\,^1D_2$. Both by calculation with explicit radial functions and by the choice of theoretical parameters to fit observed shifts, it is shown that the values of the core-valence parameters occurring in the theory are not at all negligible, so that a two-electron model would not be permissible. Calculations with explicit radial functions give correct signs for the specific shifts of all these lines except for the limiting shift of $3\,^1P_1-n\,^1D_2$. In the case of the line $3\,^1P_1-3\,^1D_2$ the correct sign is obtained only when one takes into account the perturbation of $(3s)$ $(3d)$ $^1D_2$ by $(3p)^2\,^1D_2$; however, greater accuracy in the solution of the perturbation problem could not improve the agreement very much as long as the present radial functions are used. The total shift of any member of $3\,^3P-3\,^3D$ comes out much smaller than any of the other total shifts, in agreement with Meissner's observation of the sharpness of its members. A test of the theory independent of the use of explicit radial functions is carried out by adjusting the theoretical parameters so as to give the observed shifts of the five lines mentioned. According to the theory, all these parameters are essentially positive; the necessary values of the parameters do indeed all turn out to be positive, provided that the value of Jackson and Kuhn is accepted in preference to that of Fisher for the shift of the resonance line. The shift of the line $3\,^1P_1-5\,^1S_0$ and the sharpness of the lines $3\,^3P-4\,^3S$ afford independent evidence that Fisher's value is incorrect, or else that nuclear motion is not the sole cause of the shift in the resonance line $3\,^1S_0-3\,^1P_1$. There also arises an inconsistency unless the perturbation of $(3s)$ $(3d)$ $^1D_2$ by $(3p)^2\,^1D_2$ is taken into account. The necessary values of the parameters are shown by the estimate of corresponding f values to be reasonable both as to their absolute and as to their relative values. With certain acceptable assumptions, it is shown that if the shifts in Mg are due to nuclear motion alone, then three relations may be deduced connecting the specific shifts. These are: (1) the specific shifts of the resonance line $3\,^1S_0-3\,^1P_1$ and of any member of $3\,^3P-(3p)^2\,^3P$ must be equal; (2) (for any members) the sum of the specific shifts of the lines $3\,^3D-(3p)$ $(3d)$ ^3D and $3\,^3P-3\,^3D$ must equal the sum of the specific shifts of the lines $(3p)^2\,^3P-(3p)$ $(3d)$ ^3D and $3\,^1S_0-3\,^1P_1$; (3) a complicated quadratic relation involving the specific shifts of the five lines $3\,^1S_0-3\,^1P_1$, $3\,^1S_0-3\,^3P_1$, $3\,^1P_1-3\,^1D_2$, $3\,^3P-3\,^3D$, and $(3p)^2\,^3P-(3p)$ $(3d)$ ^3D, as well as the interaction parameter α for $3\,^1D_2$. With the use of known shifts, including the Jackson-Kuhn value for the resonance line, these relations lead to the prediction (for any member) of total shifts of 0.035 cm^{-1} for λ2778 to $2784=3\,^3P-(3p)^2\,^3P$, of 0.027 cm^{-1} for λ3890 to $3900=(3p)^2\,^3P-(3p)$ $(3d)$ ^3D, and of 0.061 cm^{-1} for λ2810 to $2812=3\,^3D-(3p)$ $(3d)$ ^3D. It is concluded that the quantum-mechanical theory of nuclear motion, without the assumption of non-Coulomb nuclear fields or of nuclear spins, gives a good qualitative explanation of fine structure in magnesium. It appears that a measurement of the shifts of lines λ2778 to 2784, λ3890 to 3900, and λ2810 to 2812 would furnish the best quantitative test.

INTRODUCTION

MAGNESIUM is known to occur in three isotopes, 24, 25, and 26, with relative abundances very close to 7 : 1 : 1. Various experimenters[1] have investigated the fine structure[2] of Mg I. Before the investigations of Meissner[1] all lines that showed fine structure were found to have two components only. Using the method of atomic beams, Meissner found, for most of the lines showing structure, three components that were practically equally spaced, the lowest frequency component being the most intense in each case and the two much weaker components of higher frequency being of about equal intensity. Meissner's results, together with the abundance ratios, point strongly to this fine structure as being purely a mass effect, i.e., as arising purely from nuclear motion and not from nuclear fields differing for each isotope or from nuclear spin. We may identify the main component in each case as due to isotope 24, and the two weaker components as due to isotopes 25 and 26, the order probably being 24, 25, 26; there seems to be no evidence of splitting due to nuclear spin even in the case of isotope 25.

For the series $3\,^1P_1-n\,^1D_2$ Meissner found $\nu_{26}-\nu_{24}$ to be $+0.0831$ cm^{-1} for $n=3$ and $+0.056$ cm^{-1} for the limit $n=\infty$; the latter figure may

[1] R. F. Bacher and R. A. Sawyer, Phys. Rev. **47**, 587 (1935); D. A. Jackson and H. Kuhn, Proc. Roy. Soc. **A154**, 679 (1936); R. A. Fisher, Phys. Rev. **51**, 381 (1937); K. W. Meissner, Ann. d. Physik **31**, 505 (1938).

[2] The expression "fine structure" is used in the present paper to denote, without assumption as to origin, any nonelectric nonmagnetic splitting of a singlet line or of any member of a set of multiplet lines.

be regarded as the shift of a "line" $3\,^1P-3\,^2S$ (Mg II). He also found each member of $3\,^3P-3\,^3D$ and of $3\,^3P-4\,^3S$ to be sharp, so that the shifts must be very small in these cases. Bacher and Sawyer[1] found a shift of $+0.083$ cm^{-1} for the intercombination line $3\,^1S_0-3\,^3P_1$; since in those cases where Bacher and Sawyer and Meissner investigated the same lines, the shift found by Bacher and Sawyer agrees rather well with Meissner's $\nu_{26}-\nu_{24}$, we may attribute this to $\nu_{26}-\nu_{24}$. For the resonance line $3\,^1S_0-3\,^1P_1$ Fisher[1] found a shift of $+0.066$ cm^{-1} and Jackson and Kuhn[1] found $+0.033$ cm^{-1}.

Besides the work of Meissner, the general facts that no nonzero nuclear spins have been detected for elements of both even atomic number and even mass number[3] and that non-Coulomb nuclear fields have thus far been found to be of possible importance only in heavy atoms,[3] apparently leave no explanation for the shifts in Mg except nuclear motion. In this paper we shall investigate, as completely as current theory allows, whether nuclear motion does fully account for the shifts above mentioned. We shall consider especially the shifts of the lines $3\,^1S_0-3\,^1P_1, 3\,^1S_0-3\,^3P_1, 3\,^1P_1-3\,^1D_2, 3\,^3P-3\,^3D$, and $3\,^3P-3\,^2S$ (Mg II); we shall also be able from the above observed shifts to predict, without the use of special radial wave functions, the shifts of the line $3\,^3P-(3p)^2\,^3P$ discovered by Bowen and Millikan[4] and of the lines $(3p)^2\,^3P-(3p)(3d)\,^3D$ and $3\,^3D-(3p)(3d)\,^3D$ discovered by Paschen.[5]

General Theory

Let H_0 and E_0 be the energy operator and a corresponding energy for a ν-electron atom, the nucleus being supposed fixed. Then the effect of nuclear motion can be expressed exactly by the addition to H_0 of a term[6]

$$G\equiv(2M)^{-1}(\sum_{i=1}^{\nu}\mathbf{p}_i)^2,$$

where M is the nuclear mass and $\mathbf{p}_i$ the momentum of the ith electron relative to the nucleus. We shall write $G\equiv N+\sigma$, where

$$N\equiv(2M)^{-1}\sum_{i=1}^{\nu}\mathbf{p}_i^2, \quad \text{and} \quad \sigma\equiv M^{-1}\sum\sum_{i>j}\mathbf{p}_i\cdot\mathbf{p}_j,$$

the summations being extended over all the electrons, 12 in the case of Mg I. N is called the "normal" term and σ the "specific" term. Suppose now that one knows the energy E_0 and the wave function of a given state for the case of a fixed nucleus ($M=\infty$); then the problem becomes one in perturbation theory, since G is small compared to H_0. Before considering the perturbation problem, however, we may mention that the effect of the term N alone can always be given exactly[6] (spin-orbit forces being left out of account): *viz.*, replace E_0 by $E_0(1+m/M)^{-1}$, where m denotes the electronic mass. This statement follows from the fact that the potential energy V is homogeneous of degree -1; i.e., $V(\xi x_1\cdots\xi z_\nu)=\xi^{-1}V(x_1\cdots z_\nu)$. Thus if $\psi(x_1\cdots z_\nu)$ satisfies the wave equation with electron mass m and energy E_0, one finds on making the transformation $x_k=\xi x_k'$ that $\psi(\xi x_1'\cdots\xi z_\nu')$ satisfies the equation with electron mass $m\xi$ and energy $E_0\xi$. Then since the effect of N is to add $1/M$ to $1/m$, we must put $\xi=M/(m+M)=(1+m/M)^{-1}$. Thus if σ were negligible, we should have, letting E denote the total energy corresponding to H_0+N: $E=E_0-(m/M)E$, so that the part of the observed total energy due to N would be given exactly by $-(m/M)E$.

In the perturbation problem let us consider only the case of LS coupling, and suppose that the unperturbed wave functions make H_0 and the operators corresponding to S, L, J, and M_J diagonal. There arises a question about the degeneracy due to M_J; this difficulty is at once resolved, however, since both N and σ commute with the operators corresponding to S, L, J, and M_J. Thus N and σ are already almost diagonal with respect to the unperturbed wave functions, having no components between unperturbed states of different S, L, J, or M_J (or of different S, L, M_L, or M_S if that representation is the starting one); they may have components between states which, in an approximation in which H_0 is not diagonal, can perturb each other. They have no components between states of equal energy, so that the perturbation theory

[3] H. A. Bethe and R. F. Bacher, Rev. Mod. Phys. **8**, 82 (1936). Cf. pp. 217 and 225.
[4] I. S. Bowen and R. A. Millikan, Phys. Rev. **26**, 150 (1925).
[5] F. Paschen, Ann. d. Physik **12**, 509 (1932).
[6] D. S. Hughes and C. Eckart, Phys. Rev. **36**, 694 (1930).

for nondegenerate systems may be applied at once. In the first order we have the familiar result that each state simply gets an additional energy equal to $\bar{N}+\bar{\sigma}$, where the bar denotes the diagonal element with respect to the unperturbed wave function. It is easily seen that the second approximation in each case leads to a correction which is smaller by a factor of the order m/M.

The term $\bar{N}$ can easily be calculated by use of the virial theorem for a Coulombian system. Since $N=(m/M)T$, where T is the operator for the kinetic energy of the electrons, we have $\bar{N}=(m/M)\bar{T}$; the virial theorem tells us that, spin-orbit forces being neglected, $\bar{T}=-E_0$, so that $\bar{N}=-(m/M)E_0$. The spin-orbit restriction means that in this approximation $\bar{N}$ has the same value for all J values of a given multiplet. We have here a check on our neglect of higher approximations in the perturbation problem: with spin-orbit neglect, an exact theory gives $-(m/M)E$ and first-order theory gives $-(m/M)E_0$ for the correction due to N; the difference is entirely negligible. We may thus feel safe in applying first-order theory also for the effect of σ.

We should now show that $\bar{\sigma}$ (as well as $\bar{N}$) has the same value for all J and M_J of a given multiplet, at least to the approximation that we shall use for our wave functions. This independence is physically reasonable, since dependence on M_J would indicate something like a Zeeman effect due to nuclear motion and dependence on J would be expected only for a perturbation like a spin-orbit interaction. To show it, suppose we start with a system of approximate wave functions, linear combinations of determinants, which form an orthonormal system and make the operators for S, L, M_L, and M_S diagonal. If there are any important configuration interactions, this system of functions is supposed to take that fact into account. Now suppose an operator K commutes with an angular momentum $\mathbf{P}$, where the eigenvalues of $\mathbf{P}^2$ are $P(P+1)h^2/4\pi^2$ and those of P_z are $M_P h/2\pi$. Then not only is K diagonal in a representation in which $\mathbf{P}^2$ and P_z are diagonal, but the diagonal components of K in such a representation are independent of M_P.[7] Now it is easily shown that σ or N commutes with any component of $\mathbf{L}$ or $\mathbf{S}$, where $\mathbf{L}$ denotes the total orbital angular momentum and $\mathbf{S}$ the total spin angular momentum. Thus we must obtain the same $\bar{\sigma}$ for all M_L and M_S of a given multiplet. Then, performing a unitary transformation to the $SLJM_J$ scheme, we easily prove that the same $\bar{\sigma}$ results for all J and M_J of the multiplet. The same argument applies to $\bar{N}$, so that the procedure for $\bar{N}$, which led to a value independent of J or M_J, is consistent with such a system of wave functions.

The above discussion covers the cases where configuration interaction is or is not negligible, and shows that in either case we may use SLM_LM_S functions rather than $SLJM_J$ functions. For the cases where configuration interaction is negligible, we shall use the Slater[8] method of diagonal sums, so that in such cases we need not find even the SLM_LM_S functions. All that we shall then need will be diagonal elements of σ with respect to certain of the determinants (slm_lm_s functions) corresponding to the multiplet.

The Matrix Elements

Let $A_\rho(r, \theta, \phi, \sigma_z)$ denote the total function for the ρth orbit, the product of the space function $a_\rho(r, \theta, \phi)$ and the spin function $\delta_\rho(\sigma_z)$; the functions a_ρ are supposed to form an orthonormal set. Let U be the normalized determinantal wave function corresponding to the configuration $A_1, A_2, \cdots A_r \cdots A_t \cdots A_v$ and U' that corresponding to $A_1, A_2, \cdots A_{r'} \cdots A_{t'} \cdots A_v$, so that U and U' differ by two orbits. Then, since

$$\sigma = M^{-1}\sum_{i>j}\sum \mathbf{p}_i \cdot \mathbf{p}_j,$$

and since $(a_\rho|\,\mathbf{p}\,|a_\mu)=0$ unless $l_\mu - l_\rho = \pm 1$,[9] we have:[10]

$$(U|\,\sigma\,|U) = -M^{-1}\sum_{\mu>\rho}\sum |(a_\mu|\,\mathbf{p}\,|a_\nu)|^2\delta_{\mu\rho}, \tag{1}$$

$$(U|\,\sigma\,|U') = M^{-1}[(a_r|\,\mathbf{p}\,|a_{r'})\cdot(a_t|\,\mathbf{p}\,|a_{t'})\delta_{rr'}\delta_{tt'} - (a_r|\,\mathbf{p}\,|a_{t'})\cdot(a_t|\,\mathbf{p}\,|a_{r'})\delta_{rt'}\delta_{tr'}]. \tag{2}$$

In these equations $\delta_{\mu\rho}$, e.g., is a Kronecker delta on the spins of the μth and ρth orbits; in

[7] E. U. Condon and G. S. Shortley, *The Theory of Atomic Spectra* (Cambridge University Press, 1935), p. 49.

[8] J. C. Slater, Phys. Rev. **34**, 1293 (1929).

[9] This relation holds even if a_μ and a_ρ correspond to different central fields.

[10] J. C. Slater, Phys. Rev. **38**, 1115 (1931). Reference 7, p. 173.

Eq. (1) the summations are over all occupied orbits; throughout the paper we abbreviate the scalar product of a complex vector $\mathbf{C}$ and its complex conjugate $\mathbf{C}^*$ to $|\mathbf{C}|^2$. $(U|\sigma|U')$ is the only type of nondiagonal matrix element that we shall need, and we shall need it only in the case where configuration interaction is allowed for. In listing values of $(U|\sigma|U)$ and of $\bar{\sigma}$ we shall omit an additive term which pertains only to the neon-like core and is thus common to all spectral terms, therefore canceling out when we take differences to find shifts of lines.

We now need general formulas for the one-electron matrix elements of momentum $(nlm_l|\mathbf{p}|n'l'm_l')$. We adopt the Condon and Shortley[11] convention for the signs of the angle functions, so that the usual formulas for angular momentum operators acting on the angle functions hold for all m_l; this makes for convenience in examining wave functions for angular momentum properties in those cases where they have to be written down explicitly. We next use the formulas of Bethe[12] for the result of $\partial/\partial x$, $\partial/\partial y$, and $\partial/\partial z$ on the product of the normalized angle function and any function of the radius r, realizing that the Bethe angle function $Y_B(l, m_l)$ and the Condon-Shortley angle function $Y_C(l, m_l)$ are connected by the relation $Y_B=(-1)^{m_l}Y_C$. We of course find the selection rules $\Delta l=\pm 1$ for the matrix elements of any component of momentum, $\Delta m_l=\pm 1$ for those of p_x and p_y, and $\Delta m_l=0$ for those of p_z. We also obtain the following formulas, from which, because of the Hermitian property of the matrix of $\mathbf{p}$, all the nonvanishing matrix elements of $\mathbf{p}$ may be found:

$$\begin{aligned}
&(n, l, m_l|p_x|n', l-1, m_l\mp 1)\\
&\quad=\pm(i/2)C_l[(l\pm m_l-1)(l\pm m_l)]^{\frac{1}{2}}\\
&\qquad\qquad\times F(n, l; n', l-1)\\
&(n, l, m_l|p_y|n', l-1, m_l\mp 1)\\
&\quad=(\tfrac{1}{2})C_l[(l\pm m_l-1)(l\pm m_l)]^{\frac{1}{2}}\\
&\qquad\qquad F(n, l; n', l-1) \quad (3)\\
&(n, l, m_l|p_z|n', l-1, m_l)\\
&\qquad=-iC_l(l^2-m_l^2)^{\frac{1}{2}}F(n, l; n', l-1),
\end{aligned}$$

where

$$C_l\equiv[(2l+1)(2l-1)]^{-\frac{1}{2}}$$

and

$$F(n, l; n', l-1)\equiv(h/2\pi)\int_0^\infty R(nl)\Big\{dR(n, l-1)/dr - [(l-1)/r]R(n, l-1)\Big\}r^2dr,$$

$R(nl)$ being the radial function for the orbit nl, so normalized that

$$\int_0^\infty R^2r^2dr=1.$$

Eqs. (3) lead at once to Eqs. (4), which are all that we need for the case in which configuration interaction plays no role:

$$\begin{aligned}
&|(n, l, m_l|\mathbf{p}|n', l-1, m_l)|^2\\
&\qquad=C_l^2(l^2-m_l^2)F(n, l; n', l-1)\\
&|(n, l, m_l|\mathbf{p}|n', l-1, m_l\mp 1)|^2\\
&\quad=(\tfrac{1}{2})C_l^2(l\pm m_l-1)(l\pm m_l)F^2(n, l; n', l-1). \quad (4)
\end{aligned}$$

Eqs. (4) agree with the expressions developed by Bartlett and Gibbons[13] by a somewhat easier but less straightforward method. We have outlined the above derivation because we need Eqs. (3) as well as Eqs. (4), when we come to treat perturbed levels. At this point a change of units is useful; one easily shows that:

$$\begin{aligned}
F(n, l; n', l-1)&=(h/2\pi a_0)J(n, l; n', l-1)\\
&=(2mRy)^{\frac{1}{2}}J(n, l; n', l-1), \quad (5)
\end{aligned}$$

where

$$J(n, l; n', l-1)\equiv\int_0^\infty R(nl)\left[\frac{dR(n, l-1)}{dr} - \frac{l-1}{r}R(n', l-1)\right]r^2dr,$$

where a_0 is the Bohr radius, Ry the Rydberg energy, and r is the radius expressed in units of a_0; because of this change of units $R(r)$ in Eq. (5) has a functional form different from $R(r)$ in Eq. (3).

Formulas for the Specific Shift for Cases in which Configuration Interaction Is Negligible

We proceed to calculate $\bar{\sigma}$ in terms of the integrals $J(n, l; n', l-1)$ for those spectral terms

[11] Reference 7, p. 52.
[12] H. A. Bethe, *Handbuch der Physik*, Vol. 24, No. 1, p. 558.
[13] J. H. Bartlett, Jr. and J. J. Gibbons, Jr., Phys. Rev. 44, 538 (1933). There is an error in their formula for their $C(l, l-1)$, consisting of an interchange of subscripts.

for which configuration interaction may be neglected; for our present problem of magnesium this means all terms arising from 3-quantum orbits except $(3s)(3d)\ ^1D_2$ and $(3p)^2\ ^1D_2$. We use the Slater diagonal sum method and Eqs. (1), (4), and (5), and we write the formulas without the term common to all spectral terms.

For $(3s)^2\ ^1S$ and $3s\ ^2S$(MgII) the wave functions are single determinants corresponding respectively to the configurations $3s^+\ 3s^-$ and $3s^{\pm}$. (Superscript signs denote m_s values and subscripts where necessary denote m_l values.) The value of $\bar{\sigma}$ for $(3s)^2\ ^1S$ comes out double that for $3s\ ^2S$, which is

$$-M^{-1}\sum_{m_l=-1}^{+1}|(2p_{m_l}|\mathbf{p}|3s)|^2=-2(m/M)RyJ^2(2p,3s).$$

The configuration $(3s)(3p)$ will serve to illustrate the use of the diagonal sum method. Noting that $3s^+\ 3p_1^+$ belongs only to the triplet, one has for $3\ ^3P$:

$$\bar{\sigma}=-M^{-1}[\sum_{m_l=-1}^{+1}|(2p_{m_l}|\mathbf{p}|3s)|^2+\sum_{n=1}^{3}|(3p_1|\mathbf{p}|ns)|^2]$$

$$=-2(m/M)Ry[J^2(2p,3s)+\tfrac{1}{3}\sum_{n=1}^{3}J^2(3p,ns)].$$

One also notes that $\Sigma m_s=\Sigma m_l=0$ for each of $3s^+\ 3p_0^-$ and $3s^-\ 3p_0^+$, and that these relations hold for no other choices of the m_s's and m_l's; thus each of these determinants belongs to the singlet with $M_S=M_L=0$ and to the triplet with $M_S=M_L=0$. The diagonal sum rule then tells us that the sum of the $\bar{\sigma}$'s for the singlet and the triplet is given by evaluating the sum in Eq. (1) for each of these determinants and adding the results. This sum turns out to be:

$$-4(m/M)Ry[J^2(2p,3s)+\tfrac{1}{3}\sum_{n=1}^{2}J^2(3p,ns)].$$

By difference we obtain for $3\ ^1P$:

$$-2(m/M)Ry[J^2(2p,3s)+\tfrac{1}{3}\{\sum_{n=1}^{2}J^2(3p,ns)-J^2(3p,3s)\}].$$

For $(3s)(3d)$ the results for the singlet and the triplet come out equal, perturbation by $(3p)^2$ being left out of account. This result, which is $-2(m/M)Ry[J^2(2p,3s)+(\frac{2}{5})J^2(3d,2p)]$, we can accept only for the triplet, which is unperturbed by $(3p)^2$. For $(3p)^2$, with perturbation of the ^1S by $(3s)^2\ ^1S$ and of the ^1D by $(3s)(3d)\ ^1D$ left out of account, the same value is obtained for the ^3P, the ^1S, and the ^1D, *viz.*

$$-4/3(m/M)Ry\sum_{n=1}^{2}J^2(3p,ns);$$

this result is acceptable for the ^3P, since it is unperturbed. For $(3p)(3d)$ the values of $\bar{\sigma}$ are

$$-2(m/M)Ry[\tfrac{1}{3}\sum_{n=1}^{2}J^2(3p,ns)+\tfrac{2}{5}J^2(3d,2p)+\eta J^2(3d,3p)],$$

where for ^1P, ^3P, ^1D, ^3D, ^1F, ^3F the values of η are, respectively, $-1/15$, $1/15$, $\frac{1}{5}$, $-\frac{1}{5}$, $-\frac{2}{5}$, $\frac{2}{5}$. Since $(3p)(3d)\ ^3D$ is of odd parity, it is not perturbed by $(3s)(3d)\ ^3D$, so that the above formula may be considered acceptable for the ^3D.

The Specific Shift of $3\ ^1D_2$

There is good evidence that the level $(3s)(3d)\ ^1D_2$ is rather strongly perturbed by the level $(3p)^2\ ^1D_2$. The singlet lies well below the triplet, and the work of Bacher[14] indicates that the exchange integral which should give the singlet-triplet separation (if there were no perturbation) has such a sign as to put the singlet above the triplet. Furthermore, on computing the effect of the level $(3p)^2\ ^1D_2$ on $(3s)(3d)\ ^1D_2$, Bacher finds that such a perturbation puts the singlet below the triplet, in fact about 2200 cm^{-1} below as compared with the observed 1550 cm^{-1}.[15]

We must thus find a wave function for $(3s)(3d)\ ^1D$ that will allow for admixture of $(3p)^2\ ^1D$, and calculate the corresponding specific shift. Such a wave function may be written in the form:

$$\Psi=(1+|\alpha|^2)^{-\frac{1}{2}}(\psi_1+\alpha\psi_2), \qquad (6)$$

where ψ_1 and ψ_2 are normalized wave functions for $(3s)(3d)\ ^1D$ and $(3p)^2\ ^1D$, respectively, that do not take account of configuration interaction. The quantity α is a coefficient that will have an absolute value less than 1 for the perturbed $(3s)(3d)\ ^1D$ and an absolute value greater than 1

[14] R. F. Bacher, Phys. Rev. **43**, 264 (1933).
[15] R. F. Bacher, Phys. Rev. **56**, 385 (1939).

for the perturbed $(3p)^2\ ^1D$; the factor involving α is prefixed for normalization. The usual diagonalizing process leads to the equations for α:

$$\begin{aligned}(H_{11}-E)+H_{12}\alpha&=0\\ H_{21}+(H_{22}-E)\alpha&=0,\end{aligned}\tag{7}$$

where H_{11}, H_{22}, H_{12}, and H_{21} are matrix elements of H_0 with respect to ψ_1 and ψ_2. The corresponding secular equation is:

$$\begin{vmatrix}H_{11}-E & H_{12}\\ H_{21} & H_{22}-E\end{vmatrix}=0,\tag{8}$$

the roots of which give the energies of the two perturbed ^1D's.

At this point we must decide on what radial functions to use for $3s$, $3p$, and $3d$. The only available functions are those given by Bacher.[14] We write them below with slight corrections in the normalizations and with the constant exponentials in the 3d function expressed numerically; also our R's are such that

$$\int_0^\infty R^2r^2dr=1.$$

The unit of length is the Bohr radius a_0.

$$\begin{aligned}R(3s)&=(2.8191)^{-1}(-e^{-0.95r}r^2\\ &\qquad+11.96e^{-3.92r}r-6.86e^{-11.70r}),\\ R(3p)&=(2.3526)^{-1}(e^{-1.00r}r^2-10.43e^{-3.90r}r),\\ R(3d)&=-10^{-3}(52.155e^{-0.70r}r^2\\ &\qquad+7.0691e^{-0.35r}r^2).\end{aligned}\tag{9}$$

Since these functions are admittedly none too accurate, we shall not use them in a straightforward way to calculate α, but shall determine the quantities involved as much as possible by the use of experimental data. By the usual spectral theory one has for the energy of $(3s)(3d)\ ^3D$, which is unperturbed by $(3p)^2$, the expression $F_1-\frac{1}{5}R_b$, and for H_{11} the expression $F_1+\frac{1}{5}R_b$, where F_1 is a constant that does not concern us, and R_b is one of Bacher's integrals, $\frac{1}{5}R_b$ being the usual singlet-triplet exchange integral. Using $R_b=+10{,}190$ cm^{-1} as determined from the above radial functions and the observed energy of $(3s)(3d)\ ^3D=-13{,}715$ cm^{-1}, the ionization limit being taken as the zero, we obtain $H_{11}=-9639$ cm^{-1}. Again, from the Slater theory for p^2, we have $H_{22}=F_2+(1/25)R_e$, and the energy of $(3p)^2\ ^3P$ (which is unperturbed by $(3s)(3d)$) $=F_2-(\frac{1}{5})R_e$. F_2 is a constant that does not concern us, and R_e, one of Bacher's integrals, comes out $+29{,}940$ cm^{-1} with the above radial functions; equating $F_2-(\frac{1}{5})R_e$ to the observed energy of $(3p)^2\ ^3P$, *viz.* -3819 cm^{-1}, we find $H_{22}=+3367$ cm^{-1}. For E we use the observed value for $(3s)(3d)\ ^1D$, *viz.* $-15{,}269$ cm^{-1}. With these values for H_{11}, H_{22}, and E, Eq. (8) gives $|H_{12}|=10{,}240$ cm^1. Direct calculation of H_{12} with the same choice of constant phases for ψ_1 and ψ_2 that we later use and the same choice of signs for the radial functions as in Eqs. (9) leads to a positive real value for H_{12}; thus $H_{12}=+10{,}240$ cm^{-1}, so $H_{21}=H_{12}$, and α comes out real. Eqs. (7) now readily give $\alpha=-0.550$. From Eq. (6) we have:

$$\begin{aligned}\bar{\sigma}\equiv(\Psi|\sigma|\Psi)&=(1+\alpha^2)^{-1}[(\psi_1|\sigma|\psi_1)\\ &\quad+\alpha^2(\psi_2|\sigma|\psi_2)+\alpha(\psi_1|\sigma|\psi_2)+\alpha(\psi_2|\sigma|\psi_1)].\end{aligned}\tag{10}$$

Also, one easily verifies by applying the proper angular momentum operators that:

$$\begin{aligned}\psi_1&=2^{-\frac{1}{2}}(U_1-U_2)\\ \psi_2&=U_3,\end{aligned}\tag{11}$$

where U_1, U_2, and U_3 are the normalized determinants corresponding, respectively, to $3s^+3d_2^-$, $3s^-3d_2^+$, and $3p_1^+\ 3p_1^-$. From Eqs. (11), (1), and (2) we obtain:

$$\begin{aligned}(\psi_1|\sigma|\psi_1)&=-M^{-1}[\sum_{m_l}|(2p_{m_l}|\mathbf{p}|3s)|^2\\ &\qquad+\sum_{m_l}|(3d_2|\mathbf{p}|2p_{m_l})|^2],\end{aligned}\tag{12a}$$

$$(\psi_2|\sigma|\psi_2)=-2M^{-1}\sum_{n=1}^{2}|(3p_1|\mathbf{p}|ns)|^2,\tag{12b}$$

$$\begin{aligned}(\psi_1|\sigma|\psi_2)=(\psi_2|\sigma|\psi_1)^*&=2^{\frac{1}{2}}M^{-1}(3s|\mathbf{p}|3p_1)\\ &\quad\cdot(3d_2|\mathbf{p}|3p_1).\end{aligned}\tag{12c}$$

Eqs. (12a) and (12b), by the use of Eqs. (4) and (5), and Eq. (12c), by the use of Eqs. (3) and (5), can be expressed as:

$$\begin{aligned}(\psi_1|\sigma|\psi_1)&=-2(m/M)Ry[J^2(2p,3s)\\ &\qquad+(2/5)J^2(3d,2p)],\\ (\psi_2|\sigma|\psi_2)&=-4/3(m/M)Ry\sum_{n=1}^{2}J^2(3p,ns),\\ (\psi_1|\sigma|\psi_2)+(\psi_2|\sigma|\psi_1)&=(8)(15)^{-\frac{1}{2}}(m/M)Ry\\ &\qquad\times J(3p,3s)J(3d,3p).\end{aligned}\tag{13}$$

Equations (10) and (13) then give for the perturbed $3\,{}^1D$:

$$\bar{\sigma} = -2(m/M)Ry(1+\alpha^2)^{-1}[J^2(2p, 3s) + (2/5)J^2(3d, 2p) + (2/3)\alpha^2\sum_{n=1}^{2} J^2(3p, ns) - 4(15)^{-\frac{1}{2}}\alpha J(3p, 3s)J(3d, 3p)]. \quad (14)$$

We now collect in Table I the formulas already obtained for the specific shift; we here list the formulas for the quantity k, where $\bar{\sigma} \equiv -2(m/M) \times Ryk$. In the case of $3s\,{}^2S$(Mg II) we put a prime on the $3s$ to indicate that it would be desirable to use a different $R(3s)$ in this case in computing $J(2p, 3s)$. We also include $4\,{}^3S$ and $5\,{}^1S$ in the table for later purposes.

Numerical Calculations

Suppose we have a line due to the transition $A \rightarrow B$. Let the total energy of state A be E_A, its electronic kinetic energy T_A, term value τ_A, the normal shift of an isotope of mass M (as compared with a nucleus of infinite mass) $N_A(M)$, the specific shift (as compared with that of $M=\infty$) $\sigma_A(M)$; also let $N_A(26) - N_A(24) \equiv \delta N_A$ and $\sigma_A(26) - \sigma_A(24) \equiv \delta\sigma_A$. Now, using the definition of N and the virial theorem and putting the energy difference equal to the term value difference with reversed sign, we have:

$$N_A(M) - N_B(M) = (m/M)(T_A - T_B) = (m/M)(E_B{}^0 - E_A{}^0) = (m/M)(\tau_A - \tau_B). \quad (15)$$

Also, using $\bar{\sigma} \equiv -2(m/M)Ryk$, we have

$$\sigma_A(M) - \sigma_B(M) = -2(m/M)Ry(k_A - k_B). \quad (16)$$

Now, expressing both ν's and E's in cm^{-1}, we have:

$$E_A(26) - E_A(24) = \delta N_A + \delta\sigma_A, \quad \nu_{26} = E_A(26) - E_B(26),$$

etc., from which

$$\Delta\nu \equiv \nu_{26} - \nu_{24} = \delta(N_A - N_B) + \delta(\sigma_A - \sigma_B). \quad (17)$$

TABLE I. *Formulas for the specific shifts in terms of the integrals $J(n, l; n', l-1)$.*

Term	k (in $\bar{\sigma} = -2(m/M)Ryk$)
$3s\,{}^2S$(Mg II)	$J^2(2p, 3s')$
$(3s)^2\,{}^1S$	$2J^2(2p, 3s)$
$(3s)(3p)$	$J^2(2p, 3s) + (1/3)\left[\sum_{n=1}^{2} J^2(3p, ns) + \eta J^2(3p, 3s)\right]$, where $\eta = +1$ for ${}^3P$ and -1 for ${}^1P$.
$(3s)(3d)\,{}^3D$	$J^2(2p, 3s) + (2/5)J^2(3d, 2p)$
$(3s)(3d)\,{}^1D$	$(1+\alpha^2)^{-1}\left[J^2(2p, 3s) + (2/5)J^2(3d, 2p) + (2/3)\alpha^2\sum_{n=1}^{2} J^2(3p, ns) - 4(15)^{-\frac{1}{2}}J(3p, 3s)J(3d, 3p)\right]$
$(3p)^2\,{}^3P$	$(2/3)[J^2(3p, 1s) + J^2(3p, 2s)]$
$(3p)(3d)$	$1/3\sum_{n=1}^{2} J^2(3p, ns) + (2/5)^{-1}J^2(3d, 2p) + \eta J^2(3d, 3p)$, where the values of η are given below*
$(3s)(4s)\,{}^3S$	$J^2(2p, 3s) + J^2(2p, 4s)$
$(3s)(5s)\,{}^1S$	$J^2(2p, 3s) + J^2(2p, 5s)$

* ${}^1P = -1/15$, ${}^3P = 1/15$, ${}^1D = 1/5$, ${}^3D = -1/5$, ${}^1F = -2/5$, and ${}^3F = 2/5$.

TABLE II. *Uncorrected values of the J's, calculated from radial functions.*

$nl; n', l-1$	$J'(n, l; n', l-1)$	$J'^2(n, l; n', l-1)$
$2p3s$	-0.2606	0.0679
$3p1s$	0.3911	0.1529
$3p2s$	-0.2911	0.0848
$3p3s$	0.2918	0.0851
$3d2p$	0.1148	0.01319
$3d3p$	0.4700	0.2209
$2p1s$	-3.125	
$2p2s$	-1.014	

Eqs. (15) and (16) give:

$$(\Delta\nu)_N \equiv \delta(N_A - N_B) = (1/26 - 1/24)(1838)^{-1}(\tau_A - \tau_B) = (\tau_B - \tau_A)/573{,}460 \text{ cm}^{-1}, \quad (18)$$

$$(\Delta\nu)_\sigma \equiv \delta(\sigma_A - \sigma_B) = -(1/26 - 1/24)(1838)^{-1}2Ry(k_A - k_B) = 0.3827(k_A - k_B) \text{ cm}^{-1}. \quad (19)$$

To compute the k's we must compute the integrals $J(n, l; n', l-1)$; to do this we must have radial functions for $1s$, $2s$, and $2p$, besides those for $3s$, $3p$, and $3d$ given in Eqs. (9). Morse, Young, and Haurwitz[16] have obtained such functions for Mg^{++} by a variational method; we shall use their functions, thus making the assumption that the core functions are not appreciably affected by the presence of electrons in the M shell. They are:

$$\begin{aligned} R(1s) &= 2(\mu a)^{\frac{3}{2}}e^{-\mu a r}, \\ R(2s) &= 2(\mu^5/3N_2)^{\frac{1}{2}}(e^{-\mu r}r - 3A/\mu e^{-\mu b r}), \\ R(2p) &= 2(\mu^5 c^5/3)^{\frac{1}{2}}e^{-\mu c r}r, \end{aligned} \quad (20)$$

where $a = 3.21$, $\mu a = 11.75$, $b = 3.00$, $\mu b = 10.96$, $2c\mu = 7.55$, and $2\mu = 7.31$. Also $A = (a+b)^3/(1+a)^4$ and $N_2 = 1 - 48A/(1+b)^4 + 3A^2/b^3$. The parameter A is so chosen that $R(2s)$ is orthogonal to $R(1s)$. The Bohr radius a_0 is the unit of length and the functions are so normalized that

$$\int_0^\infty R^2 r^2 dr = 1.$$

However, our above $R(3s)$ is not quite orthogonal to $R(1s)$ or to $R(2s)$ nor $R(3p)$ to $R(2p)$. Since our fundamental equations (1) and (2) for the matrix elements are true only if the single electron functions form an orthonormal set, we shall have to correct for this lack of orthogonality. We denote values of $J(n, l; n', l-1)$ calculated from Eq. (5) with the use of Eqs. (9) and (20), and thus uncorrected for this lack of orthogonality, by adding primes as superscripts. Some elementary integrations then lead to Table II for $J'(n, l; n', l-1)$.

To make the corrections for lack of orthogonality, note that we start from slm_lm_s functions in the form of determinants; since the value of a determinant is not changed by adding a constant times a given row to another row, we may subtract from the $3p$ function enough of the $2p$ to produce orthogonality of $3p$ to $2p$ and from the $3s$ enough of the $1s$ and the $2s$ to produce orthogonality of $3s$ to $1s$ and $2s$. Let us denote the corresponding normalized orthogonalized radial functions by $R^0(3p)$ and $R^0(3s)$. Then, using these latter functions, the others being

[16] Morse, Young, and Haurwitz, Phys. Rev. **48**, 948 (1935).

TABLE III. *Corrected values of the J's, calculated from radial functions.*

$n, l; n', l-1$	$J(n, l; n', l-1)$	$J^2(n, l; n', l-1)$
$2p3s$	−0.2772	0.0768
$3p1s$	0.4011	0.1609
$3p2s$	−0.2812	0.0791
$3p3s$	0.2879	0.0829
$3d2p$	0.1148	0.01319
$3d3p$	0.4689	0.2199
$J^2(3p, 1s)+J^2(3p, 2s)=0.2399$		

unchanged, we shall have a right to apply the fundamental analysis resulting in Table I. We find:

$$R(3p)=c_1[R(3p)+\rho_1 R(2p)],$$
$$R(3s)=c_2[R(3s)+\rho_2 R(1s)+\rho_3 R(2s)],$$

where

$$c_1=1.0001,\quad c_2=1.0002,\quad \rho_1=-0.00984,$$
$$\rho_2=-0.001531,\quad \text{and}\quad \rho_3=0.02102.$$

The corrected J's are then easily expressed in terms of the uncorrected J's (including those for $2p\,1s$ and $2p\,2s$, for which reason we have inserted the values of the latter in Table II). The corrected J's are given in Table III; Tables I and III together give numerical values for the k's, listed in Table IV. In Table IV the value of k in the case $(3s)(3d)\,{}^1D$ is given for several values of α. The value $\alpha=0$ corresponds to no interaction with $(3p)^2\,{}^1D$ and the value $\alpha=-0.550$ to the interaction that we have actually found. It is seen that interaction increases the value of k. Since, however, our solution of the interaction problem may be somewhat in error, it is of interest also to know what is the largest value that interaction can give to k. This cannot be found by varying α arbitrarily and thus finding the maximum k, since only values $|\alpha|\leqq 1$ correspond to the term that we call $(3s)(3d)\,{}^1D$. Furthermore our analysis shows that α must be negative, and a simple calculation shows that k increases monotonically as α varies from 0 to -1; however, a value as large as 1 for $|\alpha|$ would undoubtedly be a good deal too large, since it would give equal importance to both configurations.

Using values of k from Table IV, observed term values [17] τ, and Eqs. (18) and (19), we obtain Table V below, giving a comparison of observed[18] and calculated total shifts and observed and calculated specific shifts for all lines arising from 3-quantum configurations for which the shifts have been measured. The observed specific shifts are obtained by subtracting the normal shifts (as calculated from Eq. (18)) from the observed total shifts. In regard to the line $3\,{}^3P-3\,{}^3D$ it is well to mention that Meissner was able to resolve this line so as to obtain the members corresponding to the triplet structure, but was unable to obtain any further resolution; the figure 0 is accordingly entered for $(\Delta\nu)_{\text{obs}}$ for this line. The high resolution which Meissner was able to obtain, as indicated by his success with the singlets and the small probable errors which he gives, leads one to believe that it must actually be zero at least to two decimal places. The line $3\,{}^1S-S\,{}^3P_1$ is an intercombination line, depending for its existence on departure from LS coupling; there is thus some question as to the applicability of the theory in this case, but since intercombination lines in Mg are weak compared to permitted lines, the departure from LS coupling is probably small, so we include this line also in our table. It may be noted also that values of $(\Delta\nu)_c$ calculated from values of k obtained by neglecting the core-valence J's, and using only $J(3p, 3s)$ and $J(3d, 3p)$, disagree markedly with the calculated values of $(\Delta\nu)_c$ in Table V. (In some cases they would lead to better agreement, in others to worse.) We may therefore conclude that a two-electron model is not permissible for calculating isotope shift in magnesium; any agreement thus obtained with experiment would be quite misleading.

A comparison of columns (5) and (6) of Table V shows that for the five lines calculated the calculated $\Delta\nu$ has the right order of magnitude for all but the first and last lines, being too small by a factor of about 2 for the first line and about $2\frac{1}{2}$ for the last line; it is interesting to note that the calculated $\Delta\nu$ for $3\,{}^3P-3\,{}^3D$, all members of which are sharp, comes out much smaller than the other $\Delta\nu$'s. A more severe test is obtained by comparing columns (3) and (7) for the specific

TABLE IV. *Values of k in $\bar{\alpha}\equiv -2(m/M)Ry\ k$, calculated from radial functions.*

TERM	k	
$3s\,{}^2S$(MgII)	0.0768	
$(3s)^2\,{}^1S$	0.1537	
$(3s)(3p)^3P$	0.1844	
$(3s)(3p)^1P$	0.1292	
$(3s)(3d)^3D$	0.0821	
$(3s)(3d)^1D$	$(1+\alpha^2)^{-1}\left[\begin{matrix}0.0821-0.1394\alpha\\ +0.1599\alpha^2\end{matrix}\right]$	
	0.0821	(for $\alpha=0$)
	0.1591	(for $\alpha=-0.550$)
	0.1970	(for $\alpha=-1$)

[17] The term values are taken from Bacher and Goudsmit, *Atomic Energy States*, except in the cases of $(3p)^2\,{}^2P$ and $(3p)(3d)\,{}^3D$, which are taken from Paschen, reference 5. The center of gravity is used for triplet levels.

[18] In the column for observed shifts, M=Meissner, F=Fisher, JK=Jackson and Kuhn, BS=Bacher and Sawyer, the references being given in footnote 1.

TABLE V. *A comparison of observed shifts with shifts calculated from radial wave functions.*

LINE	λ IN A	$(\Delta\nu)_{\sigma\text{CALC}}$ CM^{-1}	$(\Delta\nu)_N$ CM^{-1}	$(\Delta\nu)_{\text{CALC}}$ CM^{-1}	$(\Delta\nu)_{\text{OBS}}$ CM^{-1}	$(\Delta\nu)_{\sigma\text{OBS}}$ CM^{-1}
$3\,^1P-3s\,^2S$(MgII)		−0.0200	0.0464	0.0264	0.056(M) 0.066(F)	0.010 0.005(F)
$3\,^1S_0-3\,^1P_1$	2852	−0.0094	0.0611	0.0517	0.033(JK)	−0.028(JK)
$3\,^1S_0-3\,^3P_1$	4571	0.0118	0.0382	0.0499	0.083(BS)	0.045
$3\,^3P-3\,^3D$	3829 to 3838	−0.0392	0.0455	0.0063	0(M)	−0.045
$3\,^1P_1-3\,^1D_2$	8807	−0.0180 ($\alpha=0$) 0.0114 ($\alpha=-0.55$) 0.0236 ($\alpha=-1$)	0.01980	0.0018 ($\alpha=0$) 0.0312 ($\alpha=-0.55$) 0.0434 ($\alpha=-1$)	0.0831(M)	0.0633
$3\,^3P-(3p)^2\,^3P$	2778 to 2784		0.0627			
$(3p)^2\,^3P-(3p)(3d)\,^3D$	3890 to 3900		0.0448			
$3\,^3D-(3p)(3d)\,^3D$	2810 to 2812		0.0620			
$3\,^3P-4\,^3S$	5167 to 5184		0.0337		0(M)	−0.0337
$3\,^1P_1-5\,^1S_0$	5711		0.0305		0.0543(M)	0.0238

shifts alone. Even then, however, the sign comes out correct for all the lines but the first, provided that we accept the Jackson-Kuhn value for $3\,^1S_0-3\,^1P_1$, and we shall see that there is evidence for their value rather than Fisher's. In the case of the first "line" $3\,^2S$(Mg II)$\rightarrow 3\,^1P$, for which the sign of the specific shift comes out wrong, we may attribute at least part of the discrepancy to the error made in using the same radial function for the $3s'$ of $3s\,^2S$(Mg II) as for the $3s$ in $(3s)(3p)$. In the case of the line $3\,^1P_1-3\,^1D_2$, it is seen that perturbation of $(3s)(3d)$ by $(3p)^2$ must be taken into account to get the correct sign for the specific shift, but that greater accuracy in the solution of the interaction problem cannot lead to a good numerical agreement, i.e., with the radial functions above used.

ANOTHER TEST OF THE THEORY

The test of the theory just given depends on the use of explicit radial functions, which are probably not very accurate. There is another method of testing the theory which does not depend on such explicit use of radial functions. We may calculate what values of the J^2's are necessary to give the observed shifts and then test the reasonableness of the J^2's by finding what f values they give.

Let us introduce the abbreviations $J^2(2p, 3s')\equiv b_0$, $J^2(2p, 3s)\equiv b_1$, $J^2(3p, 1s)+J^2(3p, 2s)\equiv b_2$, $J^2(3p, 3s)\equiv b_3$, $J^2(3d, 2p)\equiv b_4$, $J^2(3d, 3p)\equiv b_5$, $J^2(2p, 4s)\equiv b_6$, $J^2(2p, 5s)\equiv b_7$, and let us denote the specific shifts of the lines $3\,^1P-3s\,^2S$(Mg II), $3\,^1S_0-3\,^1P_1$, $3\,^1S_0-3\,^3P_1$, $3\,^3P-3\,^3D$, $3\,^1P_1-3\,^1D_2$, $3\,^3P-(3p)^2\,^3P$, $(3p)^2\,^3P-(3p)(3d)\,^3D$, $3\,^3D-(3p)(3d)\,^3D$, $3\,^3P-4\,^3S$, and $3\,^1P_1-5\,^1S_0$ by s_0, s_1, s_2, s_3, s_4, s_5, s_6, s_7, s_8, and s_9, respectively. (Of these s_5, s_6, and s_7 are not yet known, but as we wish to predict them we include equations for them also). Then, putting $0.3827\equiv\gamma$ for short, we find from Eq. (19) and Table I:

$$b_0-b_1-(\tfrac{1}{3})b_2+(\tfrac{1}{3})b_3=s_0/\gamma, \quad (21.0)$$

$$-b_1+(\tfrac{1}{3})b_2-(\tfrac{1}{3})b_3=s_1/\gamma, \quad (21.1)$$

$$-b_1+(\tfrac{1}{3})b_2+(\tfrac{1}{3})b_3=s_2/\gamma, \quad (21.2)$$

$$-(\tfrac{1}{3})b_2-(\tfrac{1}{3})b_3+(\tfrac{2}{5})b_4=s_3/\gamma, \quad (21.3)$$

$$(1+\alpha^2)^{-1}[b_1+(\tfrac{2}{5})b_4+(\tfrac{2}{5})\alpha^2b_2-(4\alpha)(15)^{-\frac{1}{2}}(b_3b_5)^{\frac{1}{2}}]-b_1-(\tfrac{1}{3})b_2+(\tfrac{1}{3})b_3=s_4/\gamma, \quad (21.4)$$

$$-b_1+(\tfrac{1}{3})b_2-(\tfrac{1}{3})b_3=s_5/\gamma, \quad (21.5)$$

$$-(\tfrac{1}{3})b_2+(\tfrac{2}{5})b_4-(\tfrac{1}{5})b_5=s_6/\gamma, \quad (21.6)$$

$$-b_1+(\tfrac{1}{3})b_2-(\tfrac{1}{5})b_5=s_7/\gamma, \quad (21.7)$$

$$-(\tfrac{1}{3})b_2-(\tfrac{1}{3})b_3+b_6=s_8/\gamma, \quad (21.8)$$

$$-(\tfrac{1}{3})b_2+(\tfrac{1}{3})b_3+b_7=s_9/\gamma. \quad (21.9)$$

We evaluate b_1, b_2, b_3, b_4, b_5 from Eqs. (21.0) to (21.4). Eqs. (21.1) and (21.2) at once give $b_3=\frac{3}{2}(s_2-s_1)/\gamma=0.286$, provided the Jackson-Kuhn value is used for s_1. To go further we have to make an assumption about b_0; if we assume as before that $R(3s')=R(3s)$, then $b_0=b_1$, and we

can evaluate the rest of the b's. Eqs. (21.0) and (21.1) then give $b_1=-(s_0+s_1)/\gamma$. The Jackson-Kuhn value for s_1 then gives $b_1=0.047$, while the Fisher value gives -0.039. Since the b's must all be positive, this fact appears to be against the Fisher value, unless one is willing to admit that nuclear motion is not the only factor producing shift in the resonance line $3\,{}^1S_0-3\,{}^1P_1$. It is true, of course, if one takes into account that b_0 may differ somewhat from b_1, that the value of b_1 deduced from Fisher's s_1 might conceivably be increased from -0.039 to a positive value. But there is other evidence against Fisher's value, independent of any assumption about b_0. If one subtracts Eq. (21.8) from Eq. (21.9) and Eq. (21.1) from Eq. (21.2), one obtains:

$$(s_9-s_8)/\gamma=(\tfrac{2}{3})b_3+b_7-b_6$$
$$(s_2-s_1)/\gamma=(\tfrac{2}{3})b_3.$$

Now very probably[19] $J^2(2p, 5s)<J^2(2p, 4s)$, so that $b_7<b_6$; thus we must have $s_9-s_8<s_2-s_1$. Now $s_9-s_8=0.058$ cm^{-1}, while $s_2-s_1=0.040$ cm^{-1} with Fisher's s_1 and 0.073 cm^{-1}, with the Jackson-Kuhn s_1. We again reach the conclusion that *if Fisher's value for the shift of the resonance line is correct, then such a shift cannot be due to nuclear motion alone.* Since other evidence in Mg I points against such a conclusion, we prefer to decide tentatively in this paper for the Jackson-Kuhn value for s_1. We can also see that Eqs. (21.1) to (21.4) are not compatible if $\alpha=0$: if we put $\alpha=0$ in Eq. (21.4) and subtract it from Eq. (21.3), we obtain $(\frac{2}{3})b_3=(s_4-s_3)/\gamma$, while by subtracting Eq. (21.1) from Eq. (21.2) we obtained $(\frac{2}{3})b_3=(s_2-s_1)/\gamma$. Thus $\alpha=0$ would require that $s_4+s_1=s_3+s_2$; Table V gives $s_3+s_2=0$ and $s_4+s_1=0.035$ cm^{-1} with the Jackson-Kuhn value for s_1, and 0.068 cm^{-1} with the Fisher value. Thus the observed shifts point directly to the interaction of $(3s)(3d)\,{}^1D$ with $(3p)^2\,{}^1D$ as being very important. We now readily finish solving Eqs. (21.0) to (21.4), using $\alpha=-0.550$, obtaining Table VI for the values of $J^2(nl; n', l-1)$ necessary to account for the observed shifts. The magnitude of the core-valence J^2's again shows that a two-electron model would not be permissible.

Up to this point we have made no assumption whatever as to whether the various electrons move in different central fields or all move in the same central field. If we now assume that they all move in the same central field with potential energy $V(r)$, we have (Appendix I):

$$J(n, l; n', l-1)=(\tfrac{1}{2})[\epsilon(n', l-1)-\epsilon(nl)]\times r(nl; n', l-1), \quad (22)$$

where

$$r(n, l; n'l')\equiv\int_0^\infty R(nl)R(n'l')r^3dr,$$

the unit of length being a_0 and where $\epsilon(nl)$ is the energy of the electron in the orbit nl, expressed in Rydberg units. This assumption of the same central field for each electron was made by Slater[8] in his paper on complex spectra and is approximately borne out by Hartree's calculations. The various electrons according to the Hartree method move in only slightly different fields; our ϵ's are thus essentially the energies which would be given by the Hartree method. We may thus look on $\epsilon(nl)$ as the energy which would be required to remove the nl electron from the atom, if exchange were not operative. If the above assumption as to central fields were not made, Eq. (22) would have to contain an additive term proportional to

$$\int_0^\infty[V_{nl}(r)-V_{n',\,l-1}(r)]R(nl)R(n'l-1)r^3dr;$$

we may regard Hartree's calculations as showing the unimportance of this term. However, this assumption about central fields is used only in this section in judging the reasonableness of the J^2's and is not used in the previous direct calcula-

TABLE VI. *Values of the J^2's calculated from observed shifts, assuming $R(3s')=R(3s)$ and the Jackson-Kuhn value for the resonance line.*

$nl; n', l-1$	$J(nl; n', l-1)$	$J^2(nl; n', l-1)$
$2p3s$		0.047
$3p1s$		$J^2(3p, 1s)+J^2(3p, 2s)=0.208$
$3p2s$		
$3p3s$	0.535	0.286
$3d2p$		0.118
$3d3p$	0.351	0.123

[19] See Eq. (26) below; although $|\epsilon(2p)-\epsilon(5s)|>|\epsilon(2p)-\epsilon(4s)|$, f values fall off so rapidly that $|f(2p\to5s)|\ll|f(2p\to4s)|$, so that $J^2(2p, 5s)<J^2(2p, 4s)$. Considerations of overlapping of $2p$ with $4s$ or with $5s$ also lead to the conclusion that $r^2(2p, 5s)\ll r^2(2p, 4s)$, so that $J^2(2p, 5s)<J^2(2p, 4s)$. (See Eq. (22) below.)

tions with wave functions or in the section where we predict shifts for other lines.

Now, using atomic units, with $l'=l\pm1$, we have:[20]

$$f(nl\to n'l')\equiv(1/3)(2l'+1)^{-1}[\epsilon(nl)-\epsilon(n'l')]\times\sum_{m_l m_{l'}}\sum|(nlm_l|\mathbf{r}|n'l'm_{l'})|^2, \quad (23)$$

$$=(1/3)(2l'+1)^{-1}\max(l,l')\times[\epsilon(nl)-\epsilon(n'l')]r^2(nl;n'l'). \quad (24)$$

Thus

$$f(nl\to n',l-1)=(1/3)l(2l-1)^{-1}\times[\epsilon(nl)-\epsilon(n',l-1)]r^2(nl;n',l-1). \quad (25)$$

Comparison of Eqs. (25) and (22) leads to the relation:

$$f(nl\to n',l-1)=(4/3)[\epsilon(nl)-\epsilon(n',l-1)]^{-1}\times l(2l-1)^{-1}J^2(nl;n',l-1). \quad (26)$$

The ϵ's can be estimated for $1s$, $2s$, and $2p$ from x-ray data, and for $3s$, $3p$, and $3d$ from term values in Mg I and Mg II; the details are given in Appendix II. The results are $\epsilon(1s)=-96.0$, $\epsilon(2s)=-4.58$, $\epsilon(2p)=-3.65$, $\epsilon(3s)=-0.764$, $\epsilon(3p)=-0.299$, $\epsilon(3d)=-0.106$. Using these values for the ϵ's, the J^2's in Table VI, and Eq. (26), we obtain Table VII for the f values.

Note that the (3, 3) f values are of the same order of magnitude and are large compared to the (3, 2) f values, which are all of the same order, being in turn large compared to the (3, 1) f value. These relative values are to be expected and help to show the reasonableness of the f's. For an actual comparison with experimental data we must remember that these f values are for the system of one electron moving in the effective Hartree field of the rest of the Mg atom, and as such could not be directly compared with f values in Mg I, even if the latter were known. They may, however, be compared for order of magnitude with f values in Na I. In Na I, theoretical calculations by Trumpy[21] and by Prokofjew[21] give 0.98 for $f(3p\to3s)$, while various experiments[21] give values ranging from 0.97 to 1.16; according to the Kuhn-Reiche sum rule we should expect a value less than 1. For $f(3d\to3p)$ calculations by Prokofjew[21] give 0.832 and for $f(2p\to3s)$ calculations by Sugiura[22] give -0.043. These theoretical calculations are all based on radial functions obtained by numerical integration, the field being chosen with the aid of a W. K. B. modified Bohr quantum condition so as to reproduce observed term values; as such they are probably quite reliable. We see that our f values are of the correct order of magnitude, with $f(3p\to3s)$ and $f(3d\to3p)$ both ~1, with $f(3p\to3s)>f(3d\to3p)$ as in Na I, and with $f(2p\to3s)$ about half that for Na I; the parallelism with Na f values is remarkable. Thus we have a confirmation of the reasonableness of the J^2's and the consequent likelihood of the essential correctness of the theory.

TABLE VII. *f values calculated from J^2's that give the observed shifts.*

$nl, n', l-1$	$f(nl\to n', l-1)$
$2p3s$	-0.022
$3p1s$	<0.0029
$3p2s$	<0.065
$3d2p$	0.0296
$3p3s$	0.820
$3d3p$	0.566

PREDICTIONS OF THE SHIFTS OF OTHER LINES

Equations (21) are capable of yielding still other interesting results. Comparison of Eqs. (21.5) and (21.1) gives $s_5=s_1$ as a requirement of the theory; this result is independent of any assumption as to the relative magnitudes of b_0 and b_1. In words, if the shifts in Mg are due to nuclear motion alone, then the specific shifts of the resonance line $3\,^1S_0-3\,^1P_1$ and of any member of $3\,^3P-(3p)^2\,^3P$ must be equal. Also, if one tries to solve Eqs. (21.1), (21.2), (21.3), (21.6), and (21.7) for b_1, b_2, b_3, b_4, b_5, one finds that the determinant of the coefficients of the b's vanishes, so that these equations are not independent; one readily finds that $s_7+s_3=s_6+s_1$. Thus, nuclear motion alone being effective, the sum of the specific shifts of the lines $3\,^3D-(3p)(3d)\,^3D$ and $3\,^3P-3\,^3D$ must equal the sum of the specific shifts of the lines $(3p)^2\,^3P-(3p)(3d)\,^3D$

[20] H. A. Bethe, *Handbuch der Physik*, Vol. 24, No. 1, p. 435.

[21] Cf. S. A. Korff and G. Breit, Rev. Mod. Phys. **4**, 499 (1932) for a tabulation of f values with references.

[22] Y. Sugiura, Phil. Mag. **4**, 495 (1927). This f value corresponds to a line forbidden by the Pauli principle, but was calculated by Sugiura for a check of his f values by the Kuhn-Reich sum rule.

and $3\,^1S_0-3\,^1P_1$. Suppose now that one tries to solve Eqs. (21.1), (21.2), (21.3), (21.4), and (21.6) for b_1, b_2, b_3, b_4, b_5; one readily solves for b_3 and b_5 and for b_4 and b_2 in terms of b_1. One then inserts these values of b_2, b_3, b_4, b_5 into Eq. (21.4) to solve for b_1, but b_1 at once cancels out, leaving the general relation:

$$(1+\alpha^2)(s_4-s_2)+s_1=s_3-2\alpha[(s_2-s_1)^2+2(s_2-s_1)(s_3-s_6)]^{\frac{1}{2}}. \quad (27.3)$$

The other relations are:

$$s_5=s_1, \quad (27.1)$$

$$s_7+s_3=s_6+s_1. \quad (27.2)$$

Thus of the seven equations (21.1) to (21.7) only four are independent. The relations (27) are independent of any assumption as to the relative magnitude of b_0 and b_1; they do depend on: (1) having the same radial function for a given 3-quantum orbit in all configurations involving two 3-quantum electrons, (2) having LS coupling, (3) having the perturbation of $(3s)(3d)$ by $(3p)^2$ as the only important perturbation. Eq. (27.3) is an equation quadratic in the specific shifts of all the lines $3\,^1S_0-3\,^1P_1$, $3\,^1S_0-3\,^3P_1$, $3\,^3P-3\,^3D$, $3\,^1P_1-3\,^1D_2$, and $(3p)^2\,^3P-(3p)(3d)\,^3D$. Using the Jackson-Kuhn value for s_1 and the value $\alpha=-0.550$, we obtain from Eqs. (27): $s_5=-0.028$ cm^{-1}, $s_6=-0.018$ cm^{-1}, and $s_7=-0.001$ cm^{-1}. The corresponding normal shifts are 0.063 cm^{-1}, 0.045 cm^{-1}, and 0.062 cm^{-1}, respectively, leading to total shifts of 0.035 cm^{-1}, 0.027 cm^{-1}, 0.061 cm^{-1} for any member of the sets of lines λ2778 to $2784=3\,^3P-(3p)^2\,^3P$, λ3890 to $3900=(3p)^2\,^3P-(3p)(3d)\,^3D$, and λ2810 to $2812=3\,^3D-(3p)(3d)\,^3D$, respectively. It appears that measurement of the shifts of these lines would afford the best quantitative test of the idea that nuclear motion is alone responsible for fine structure in magnesium.

The author wishes to express his gratitude to Professor Breit for the original suggestion of this problem and for valuable advice during the investigation.

Appendix I

To show that

$$\int_0^\infty R(nl)\left[\frac{dR(n',l-1)}{dr}-\frac{(l-1)}{r}R(n',l-1)\right]r^2dr = \tfrac{1}{2}[\epsilon(n',l-1)-\epsilon(nl)]\int_0^\infty R(nl)R(n',l-1)r^2dr,$$

we resort to the following argument. With a_0 as the unit of length and the Rydberg constant as the unit of energy, with $S(nl)\equiv rR(nl)$, and with the superscript primes denoting differentiation with respect to r, we have:

$$S''(nl)+[\epsilon(nl)-V-l(l+1)/r^2]S(nl)=0, \quad (I)$$

$$S''(n'l')+[\epsilon(n'l')-V-l'(l'+1)/r^2]S(n'l')=0. \quad (II)$$

Multiply (I) by $rS(n'l')$, (II) by $rS(nl)$, take the difference, express $S(n'l')S''(nl)-S''(n'l')S(nl)$ as $(d/dr)[S(n'l')S'(nl)-S'(n'l')S(nl)]$, integrate from $r=0$ to $r=\infty$, put

$$\int_0^\infty S(n'l')S'(nl)dr=-\int_0^\infty S(nl)S'(n'l')dr,$$

and then replace the S's by the R's. The result is:

$$2\int_0^\infty R(nl)\frac{dR(n'l')}{dr}r^2dr=[\epsilon(n'l')-\epsilon(nl)]\int_0^\infty R(nl)R(n'l')r^2dr+[l(l+1)-l'(l'+1)-2]\int_0^\infty R(nl)R(n'l')rdr. \quad (III)$$

If now in (III) we put $l'=l-1$, we at once obtain the desired relation.

Appendix II: Estimates of the ϵ's

To estimate the ϵ's for $1s$, $2s$, and $2p$ we take $-\epsilon$ as corresponding, respectively, to the term values of the x-ray absorption limits K, $L_{\rm I}$, and a mean of $L_{\rm II}$ and $L_{\rm III}$, without making corrections to "reduced" term values, these corrections being small. From Ase[23] we have the K-absorption limit at 9.496A and from Skinner and Johnston[24] we have the $L_{\rm I}$ limit at 62.0 volts and the $L_{\rm II}$ and $L_{\rm III}$ limits at 49.5 and 49.2 volts. We obtain $\epsilon(1s)=-96.0$, $\epsilon(2s)=-4.58$, and $\epsilon(2p)=-3.65$.

For the 3-quantum orbits the ϵ's can be estimated from term values in Mg I and Mg II. E.g. for the $3d$, the value of $\epsilon(3d)$ as determined from the configuration $(3s)(3d)$, which is the only configuration in our problem involving $3d$, must correspond to a mean of the singlet and triplet term values; the mean must be taken in order to avoid the effect of exchange, since these ϵ's are supposed to be Hartree energies. Also, for the singlet, in order to avoid the effect of perturbation by $(3p)^2$, one should use the value before deduced, *viz.* 9639 cm^{-1}, corresponding to no perturbation by $(3p)^2$. On averaging this with the triplet term value, one obtains $-\epsilon(3d)=11{,}677$ cm$^{-1}=0.106$ *Ry*.

For the $3p$, the singlet-triplet mean for $(3s)(3p)$ gives 33,201 cm^1. One can also obtain a value from the $(3p)^2\,^1D$, which if unperturbed by $(3s)(3d)$ we saw before would have a term value of -3367 cm^{-1}; we wish to include the effect of this configuration because it occurs in our perturbed $(3s)(3d)\,^1D$. By adding -3367 cm^{-1} to 121, 267 cm^{-1}, the term value of $3s\,^2S$ of Mg. II, one obtains the work required to strip the atom to the neon-like core; then on subtracting from this the term value 85, 537 cm^{-1} of $3p\,^2P$ in Mg II, one obtains the network to remove a $3p$ electron from

[23] See M. Siegbahn, *Spektroskopie der Roentgenstrahlen*, second edition (Springer, 1931), p. 265.

[24] H. W. B. Skinner and J. E. Johnston, Proc. Roy. Soc. **A161**, 420 (1937).

$(3p)^2\,{}^1D$, leaving another $3p$ electron behind; this procedure gives 32,363 cm^{-1}. The mean of these values from $(3s)(3p)$ and $(3p)^2$ gives $-\epsilon(3p)=32{,}782\ cm^{-1}=0.299\ Ry$.

For the $3s$, the configurations $(3s)^2$ and $3s$ give at once 61,672 cm^{-1} and 121,267 cm^{-1}, respectively, there being no exchange correction to be made in these cases. For $(3s)(3p)$ we add the singlet-triplet mean 33,201 cm^{-1} to 121,267 cm^{-1} to find the work to strip down to the core, and subtract from this the term value 85,537 cm^{-1} of $3p\,{}^2P$ in Mg II, to find the net work required to remove the $3s$, leaving behind the $3p$; this gives 68,931 cm^{-1}. A similar procedure for $(3s)(3d)$, with the use of the above 11,677 cm^{-1} for the singlet-triplet mean term value, leads to 83,167 cm^{-1}. The deviation of the value computed from the configuration $3s$ (alone) from the other three values illustrates the error probably made in putting $R(3s')=R(3s)$. However, a mean of the four values gives $-\epsilon(3s)=83{,}759\ cm^{-1}=0.764Ry$.

DECEMBER 1, 1939 PHYSICAL REVIEW VOLUME 56

The Dielectric Constants of Ammonia, Nitrogen, and Carbon Dioxide at Ultra-High Frequency

GERALD W. FOX AND ALDEN H. RYAN*
Physics Laboratory, Iowa State College, Ames, Iowa

(Received September 14, 1939)

The heterodyne beat method has been used to determine the dielectric constants of nitrogen, carbon dioxide, and ammonia at a frequency of 56 megacycles in the temperature range of 22°C to 45°C. The method proved to be entirely satisfactory showing that the techniques customarily applied in making measurements at the lower frequencies are applicable in the ultra-high frequencies as well. The dielectric constants of nitrogen and ammonia at 56 megacycles agree with the values found at low frequencies. In the case of carbon dioxide, an anomaly was observed, the value of the constant rising from its normal value to a maximum at about 39°C and then decreasing. This variation is briefly discussed.

INTRODUCTION

WITH the growing use of the ultra-high frequencies in applied physics, redetermination of the dielectric constants of gases appears desirable at these frequencies. The purpose of the present investigation was twofold: (1) To determine whether the heterodyne beat method could be used successfully at frequencies up to 56 megacycles per second. (2) To determine the dielectric constant of three typical gases (nitrogen, ammonia, and carbon dioxide) at a frequency around 56 mc, as a preliminary to future work at still higher frequencies.

EXPERIMENTAL METHOD

In the heterodyne method, two oscillators are used, one of fixed frequency, and one whose frequency depends in part on a condenser to which the material under study can be admitted. As this capacity is altered, the frequency of the circuit of which it is a part changes and this shift appears as a change in the beat note between the two oscillators.

Hector and Schultz[1] pointed out the experimental difficulties of this method. These are: to maintain the frequency stability of the fixed oscillator; to prevent synchronization of the two oscillators when the beat frequency approaches zero; and to prevent changes in the frequency of the variable oscillator, except as produced by admitting the material to the condenser.

In the present apparatus, the first difficulty was reduced by using a crystal-controlled oscillator, operating on a frequency of 14.18 mc. A second stage quadrupled this to 56.76 mc. The crystal was a Bliley B5 low drift crystal, and for further stability, it was enclosed in a crystal oven.

The second difficulty was eliminated by thoroughly shielding both oscillators and their batteries, and by coupling the oscillators very weakly to the detector by radiation. The use of high frequency reduced synchronization, since the beat frequency change was much larger than

* Now Westinghouse Research Fellow, East Pittsburgh, Pennsylvania.

[1] L. G. Hector and H. L. Schultz, Physics **7**, 133–136 (1936).

is possible at lower frequencies. No trace of synchronism was observed.

The third difficulty was reduced by using a tube especially designed for high frequencies (the RCA 955) in an electron coupled circuit. In addition, care was exercised to maintain the oscillator at constant temperature, and a buffer stage was used for isolation.

After detection, the beat note was amplified by a two-stage audio-amplifier and was then measured by comparing it with a calibrated audio-frequency, using a cathode-ray oscilloscope to indicate zero beat.

The test condenser was made of two concentric cylinders, supported on Pyrex tubing in such a way that the fixed capacity (not affected by admitting the gas) was minimized. In addition, the cylindrical construction tended to prevent deformation of the condenser by the change of pressure on admitting the gas. The condenser and a one-liter flask, used as a reservoir for the gas, were placed in a metal box for electrical shielding and to improve the temperature control of the condenser.

A remote control system was used to tune the oscillators and open the stopcock which admitted gas to the condenser, so that the operator could sit before the cathode-ray oscilloscope and maintain a continuous check on the behavior of the apparatus during the entire course of a reading which required about forty-five seconds. All readings were rejected in which the beat note did not remain constant after taking the reading. Very few readings, aside from those taken as trials while the apparatus was coming to equilibrium, were rejected.

The difference between atmospheric pressure and the pressure in the condenser after admitting the gas was measured on a mercury manometer, which could be read by means of a lens arrangement to one-tenth of a millimeter. Atmospheric pressure was obtained from a standard mercury barometer.

Readings were made over a range of temperature from room up to about 45°C. The temperature was maintained at any point within 0.05°C and was read on a precision mercury thermometer, graduated directly in tenths of a degree, which was hung close to the condenser.

The nitrogen was taken from a tank furnished by the Ohio Chemical and Manufacturing Company, who guaranteed a purity of 99.9 percent. Attempted further purification of the gas produced no change in the results and the rest of the readings were taken using the gas directly from the tank.

The carbon dioxide was obtained from a tank supplied by Pure Carbonic, Inc., who guaranteed it to have a purity of 99.95 percent. It was used directly, after an attempt to purify it further produced no change in the results.

The ammonia was taken from a tank furnished by the Barrett Company, and was also used directly.

Results

The directly observed data were the change in beat note between the two oscillators, the gas temperature and its pressure. The dielectric constant at the observed temperature and pressure was computed from the beat note by means of the equation given by Hector and Schultz:[1] $\epsilon-1=2(R+1)\Delta f/F$, where ϵ is the dielectric constant, $R=c/C$ is the ratio of the capacity not affected by the gas to the effective capacity of the test condenser, Δf is the change in the beat note, and F is the original frequency of the oscillator. The more complete form of the equation given by Hector and Schultz was not used, since the difference between results computed by either equation was less than the random experimental error.

The ratio R of stray to effective capacity was obtained by measuring the frequency of the oscillator when the test condenser was connected and when it was disconnected. This method is subject to a slight error, because it is not possible to disconnect the test condenser without changing to some extent the stray capacity of the circuit. Also, a part of the stray capacity is in the condenser itself. However, calculation showed the effect of this error to be small enough to be disregarded.

The ratio R was measured at a temperature of 22°C. At higher temperatures, its value was slightly different, because of expansion of the apparatus (primarily the test condenser). The effect of the change in temperature upon R was calculated, and each reading was corrected. The validity of this procedure is shown by the fact

TABLE I. *Values of* $\epsilon-1$ *at 56.72 mc.*

DATE	TEMP.	$(\epsilon-1)\times10^7$ NTP	$(\epsilon-1)\times10^7$ CORR.	NO. OF READINGS
		Nitrogen		
May 28	22.70	5,848	5,847	10
April 17	23.00	5,774	5,768	10
April 10	23.50	5,883	5,874	6
June 3	25.50	5,883	5,874	5
May 8	26.50	5,786	5,761	12
May 17	27.25	5,791	5,760	14
May 27	27.50	5,851	5,818	7
June 2	30.01	5,820	5,772	10
May 25	30.10	5,843	5,794	5
May 23	30.70	5,863	5,811	11
June 3	33.70	5,890	5,820	5
June 5	35.11	5,894	5,815	6
June 5	37.21	5,913	5,822	6
June 5	40.66	5,933	5,821	6
June 4	46.05	5,924	5,780	7
			Mean 5,808	Total 120
		Ammonia		
May 19	27.30	68,488	68,466	10
May 20	27.60	68,348	68,314	10
May 20	28.28	68,087	68,049	10
				Total 30
		Carbon Dioxide		
April 16	22.36	9,894	9,891	10
May 15	23.00	10,005	9,999	8
April 15	23.45	9,962	9,953	10
May 28	25.22	10,001	9,982	10
May 27	26.14	10,058	10,033	10
May 27	28.85	10,075	10,034	12
May 5	29.30	10,080	10,036	13
May 25	30.48	10,161	10,101	5
May 25	32.30	10,288	10,226	6
May 30	34.55	10,263	10,183	6
May 30	37.31	10,312	10,220	5
June 1	38.10	10,366	10,269	5
June 1	38.99	10,368	10,266	6
May 30	38.98	10,373	10,265	9
May 30	40.80	10,311	10,198	5
May 31	42.55	10,272	10,149	5
May 31	44.20	10,257	10,124	7
June 1	47.20	10,324	10,167	8
June 4	47.33	10,215	10,062	6
				Total 147

that the dielectric constant of nitrogen, which should show no variation with temperature, was the same throughout the temperature range. Consequently, the corrections, when applied to the other gases, can be considered equivalent to a check of the gas against nitrogen. The readings taken at 56.72 mc are given in Table I. The third column is $\epsilon-1$ at zero degrees centigrade and one atmosphere pressure. The next column gives the preceding reading corrected for the change in R.

As expected, there is no variation with temperature for nitrogen. The decrease in the dielectric constant of ammonia is to be expected from the effect of its moment. On the other hand, the variation with temperature of the dielectric constant of carbon dioxide is quite unexpected. It will be noted that $\epsilon-1$ appears to increase with temperature to a maximum at about 30°C, and then decreases toward the value it had at 22°C.

To check this, a series of readings at 28.36 mc was taken on nitrogen and carbon dioxide over the same temperature range. The results are given in Table II. The same anomaly still appears in the carbon dioxide data.

To facilitate comparison of the data, Figs. 1 and 2 are given, showing in graphical form the data tabulated above.

DISCUSSION OF RESULTS

It is evident from the data that the heterodyne beat method can be used successfully at ultra-high frequencies. The random errors (due primarily to oscillator instability) are small, amounting to an average deviation from the mean of less than one-half of one percent for the readings on nitrogen. For carbon dioxide and ammonia, the average deviation of each reading

TABLE II. $\epsilon-1$ *at 28.36 mc.*

DATE	TEMP.	$(\epsilon-1)\times10^7$ NTP	$(\epsilon-1)\times10^7$ CORR.	NO. OF READINGS
		Nitrogen		
June 13	22.82	5,779	5,769	10
June 14	25.00	5,823	5,783	7
June 14	27.17	5,850	5,788	10
June 14	30.33	5,840	5,740	5
June 15	30.77	5,944	5,839	10
June 14	33.27	5,901	5,766	7
June 15	34.98	5,876	5,820	7
June 15	37.55	5,981	5,794	7
June 15	40.42	5,991	5,770	7
June 15	43.20	6,040	5,786	6
			Mean 5,786	Total 76
		Carbon Dioxide		
June 19	26.52	9,990	9,963	6
June 19	29.00	10,170	10,128	7
June 17	30.50	10,133	10,082	6
June 19	33.05	10,285	10,219	7
June 19	35.40	10,297	10,217	6
June 17	37.70	10,346	10,252	10
June 17	38.60	10,234	10,135	9
June 18	39.80	10,169	10,062	7
June 18	40.68	10,112	10,000	8
June 18	43.28	10,090	9,962	7
June 18	44.93	10,159	10,022	6
June 18	47.30	10,162	10,010	6
				Total 85

from the mean of that series of readings was less than one-third of one percent. This degree of accuracy compares favorably with that obtained by other observers at lower frequencies.

A distinction must be made between relative accuracy and absolute accuracy. While the relative accuracy of this kind of work can be made quite high, the absolute accuracy is limited by the accuracy of calibration of the apparatus. In the present work, a study of the sources of error indicates that the values of $\epsilon-1$ can be relied upon to one percent, and the relative values (for example, the variation of the dielectric constant of carbon dioxide with temperature) to one-half percent.

There appears to be no change in the dielectric constant of these gases with frequency up to 56 megacycles. The values obtained for the dielectric constant of nitrogen and ammonia at 56.72 mc agree with the results of previous

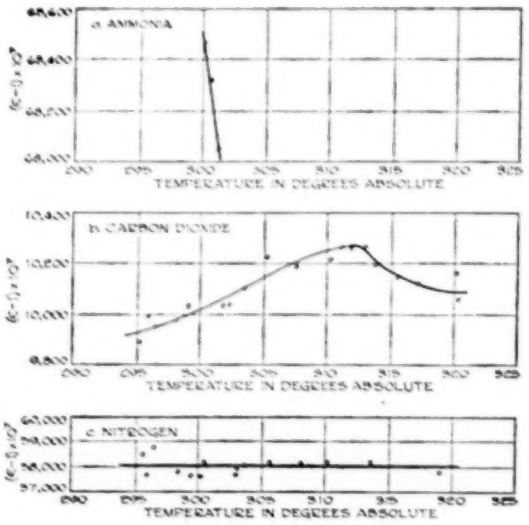

FIG. 1. Dielectric constant of ammonia, carbon dioxide, and nitrogen at 56 mc.

observations as well as those results agree among themselves. The dielectric constant of CO_2, while showing an anomalous variation with temperature, seems to be approaching the normal value at both ends of the curves of Figs. 1 and 2. Furthermore, the values of the dielectric constants of nitrogen and carbon dioxide measured at 56.72 mc were the same, within experimental error, as when measured at 28.36 mc.

It is unlikely that the variation of the dielectric constant of CO_2 with temperature is due to experimental error. Identical technique was used on all the gases, and any effect originating in the apparatus would have shown in the data taken on the other gases. Since the only modification made in changing gases was to remove one tank and substitute another, any experimental error must be laid to the valve on the CO_2 tank or to some impurity in the gas. The former hypothesis is unlikely, since a different valve was used for some of the readings, and also because any contamination originating in the valve would tend to "clean up" during the course of removing gas from the tank over a period of two months. The possibility of an impurity in the gas itself is also remote, in view of its guaranteed purity. In any case, the results require that the concentration of the impurity increase with temperature up to a certain point, and then decrease, which is improbable. It was possible to reproduce results at any temperature within experimental error, which is inconsistent with the idea of an impure gas.

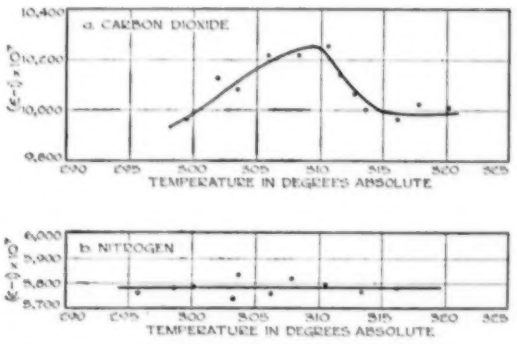

FIG. 2. Dielectric constant of carbon dioxide and nitrogen at 28 mc.

A study of the literature shows that very few determinations of the dielectric constant of CO_2 have covered the same temperature range reported in the present investigation. Only Jona,[2] v. Braunmuhl,[3] and Watson and his co-workers in 1931[4] and 1934[5] have determined the dielectric constant of this gas at more than one temperature between 20 and 45°C, where most of the present work was done.

[2] M. Jona, Physik. Zeits. **20**, 14–20 (1919).
[3] H. J. v. Braunmuhl, Physik. Zeits. **28**, 141–148 (1927).
[4] Watson, Rao and Ramaswamy, Proc. Roy. Soc., London **A132**, 569–585 (1931).
[5] Watson, Rao, Ramaswamy, Proc. Roy. Soc., London **A143**, 558–588 (1934).

Jona's data show a sharp rise in the dielectric constant to a maximum at about 27°C, followed by a steady decline to a temperature of 79.9°C, from which point the value of $\epsilon-1$ remained fairly constant to a temperature of 152.6°C. However, since he had only four points between 20°C and 80°C, and since his values of $\epsilon-1$ are far too high, his evidence must not be considered too seriously.

Braunmuhl's data show an effect very similar to that reported here. He made eleven determinations between 19.8°C and 63°C, which form a curve of nearly the same shape as that shown in Fig. 1, the maximum falling at about 37°C.

Watson and his co-workers in 1931[4] made eight determinations of the dielectric constant of CO_2 between 22.2°C and 26.6°C, which seem to show a downward trend with temperature. The same observers in 1934 made twelve determinations between 20.1°C and 29.2°C, which show no definite trend.

It seems that the effect must be regarded as resulting from some change in the structure of the molecule. This conclusion is supported by several other lines of evidence involving the specific heat of CO_2, its viscosity and thermal diffusion measurements and measurements of its electric moment.

McCrea[6] first pointed out that the specific heat of CO_2 could not be explained on the basis of either a linear or a triangular model, taken alone. He advanced the theory that the stimulation of a particular molecular vibration at a certain frequency caused a change from a linear to a triangular form. According to Fowler[7] recent measurements have removed some of the discrepancy noted by McCrea. Nevertheless, the agreement between theory and experiment is not yet completely satisfactory.

[6] W. H. McCrea, Proc. Camb. Phil. Soc. **23**, 890–900 (1927).
[7] R. H. Fowler, *Statistical Mechanics*, 2nd edition (Macmillan, New York), p. 97.

Ibbs and Wakeman[8] from their results on thermal diffusion of mixtures of gases containing CO_2, and from their results on the viscosity of CO_2, have concluded that the molecule may take two forms, a linear one which exists at low temperatures, and a bent one which exists at high temperatures. They have found similar evidence in the work of other observers in this field.

More recently, Van Cleave and Maass[9] have deduced from their measurements that the viscosity of CO_2 has a point of inflection at 12°C, indicating a change in form, and that the molecule has a small electric moment.

The results of measurements of the electric moment of CO_2 are very divergent. As Zahn and Miles[10] pointed out, different observers agree on the moment of CO within a few percent, but disagree on the moment of CO_2 by a hundred percent or more. The most reliable results are taken to be those of Zahn,[11] Watson *et al.*,[5] and Stuart,[12] all of whom report a zero or very small moment for CO_2. Nevertheless, it is noteworthy that, in general, the observers who reported a large moment for CO_2 took readings at and above room temperature, while those who reported a small moment took readings both above and below room temperature. This difference might be expected, if the dielectric constant of CO_2, has an abnormally high value slightly above room temperature, as the present work seems to indicate.

It is planned to continue this work at still higher frequencies and over a wider range of temperature.

[8] T. L. Ibbs and A. C. R. Wakeman, Proc. Roy. Soc., London **A134**, 613–642 (1932).
[9] A. B. Van Cleave and O. Maass, Can. J. Research **B13**, 140–148 (1935).
[10] C. T. Zahn and J. B. Miles, Phys. Rev. **32**, 497–504 (1928).
[11] C. T. Zahn, Phys. Rev. **27**, 455–459 (1926).
[12] H. A. Stuart, Zeits. f. Physik **47**, 457–478 (1928).

The Paramagnetic Susceptibility of Copper-Nickel and Zinc-Nickel Alloys

MARY A. WHEELER
*Yale University, New Haven, Connecticut**

(Received October 11, 1939)

Alloys of nickel were prepared with 0 to 60 percent copper or 0 to 30 percent zinc. Their susceptibilities above their Curie temperatures were measured as a function of the temperatures using a Weiss-Foëx magnetic balance at a field of 11,000. Plots of $1/\chi$ against T showed that the Curie-Weiss law holds only in restricted ranges of temperature, the curve becoming concave towards the T axis at high temperatures, especially for the alloys of low nickel content. The susceptibility at a given temperature decreases less rapidly than linearly with percent copper or zinc added. These results are discussed from the points of view of the Heisenberg and the Bloch models.

THE theory of the strong paramagnetism of the ferromagnetic metals and alloys above their Curie points is still in an unsatisfactory state. In general these substances have a region some distance above their Curie points in which the reciprocal of the susceptibility, $1/\chi$, is a linear function of $(T-\theta_p)$, where θ_p is the paramagnetic Curie temperature, while in the region immediately above the Curie point there is a strong curvature. The molecular field theory of Pierre Weiss explains this linearity on a phenomenological basis by the assumption of a "molecular field" in addition to the externally applied field. The attempts to place the molecular field on a theoretical basis were unsatisfactory until Heisenberg showed that the exchange force between the electronic spins in an incomplete inner shell, such as the 3*d* electrons of nickel, would introduce just such a term. Numerous calculations based on the Heisenberg model have proved the difficulty of determining the actual value of this term. Opechowski[1] has carried out a series development, which incorporates preceding results of Heisenberg, and which leads to contradictory results with successive approximations, showing that the convergence is too slow for this method to be reliable. P. R. Weiss and J. H. Van Vleck[2] applied the Bethe-Peierls method devised for order-disorder transitions. From their calculations a nearly linear relation is found to exist between $1/\chi$ and T over some ranges of temperature but this linearity is accidental and of limited range.

All calculations based on the Heisenberg model are necessarily approximations. This is due to the nature of the model itself which assumes that the electrons responsible for the ferromagnetism are permanently attached to their atoms, thus neglecting any transfer of electrons from atom to atom. Stoner,[3] in the alternative method of attack, has used the Bloch modal and treats the 3*d* as well as the 4*s* electrons in nickel, for example, as collective electrons, belonging to the metal as a whole. Similarly Mott[4] has explained the ferromagnetic saturation moment of nickel (0.6 Bohr magneton) by assuming that the 4*s* energy band is so broadened that it overlaps the 3*d* band, and in consequence the outer ten electrons in nickel are divided between the 3*d* and the 4*s* bands in such a way that on the average there is 0.6 electron per atom in the 4*s* band and 0.6 electron per atom missing from the 3*d* band. The ferromagnetic moment below the Curie point and the paramagnetic moment above it are then due to the holes in the 3*d* band; the 4*s* electrons cannot contribute magnetic moment because of the great width of the band. Mott adds to this a neat explanation of the change of Curie point and of atomic moment of nickel when alloyed with another metal, such as copper or zinc, which has its 3*d* shell full and one or two 4*s* electrons besides. The 3*d* band is much narrower than the 4*s* band and thus the density of

* This work was done during a leave of absence from Vassar College as Faculty Fellow, 1937–8.

[1] W. Opechowski, Physica **4**, 181 (1937).

[2] P. R. Weiss and J. H. Van Vleck, Phys. Rev. **55**, 673 (1939).

[3] E. C. Stoner, *Magnetism and Matter* (Methuen and Company, London, 1934), p. 431.

[4] N. F. Mott and H. Jones, *The Theory of the Properties of Metal and Alloys* (Oxford University Press, 1936), p. 192.

energy states is much greater. It follows that, on the formation of alloys of nickel, the 4*s* electrons supplied by copper or zinc will tend to fall into the holes in the 3*d* band of the alloy until the 3*d* band is full. This will occur at 60 percent copper or 30 percent zinc. This theory is supported by the ferromagnetic properties of these alloys. Sadron[5] has shown, if some extrapolation is allowed, that the saturation moment per nickel atom and likewise the Curie temperature decrease in proportion to the copper or zinc added, reaching zero at 60 percent copper or 30 percent zinc. Later we shall see that this support is not so complete as is usually supposed.

The paramagnetic susceptibility above the Curie point also must depend upon the distribution of electrons between 3*d* and 4*s* states. Stoner[6] has carried out this analysis. He finds the observed curvature in the $1/\chi - T$ curve directly above the Curie point consistent with this theory. A linear relation holds at high temperatures because the energy changes fixed by the band structure are relatively less important. Deviations from the Curie-Weiss law in this region may still be explained by a change in the band form or in the number of electrons in the band.

Presumably the actual explanation is somewhere between these two extreme hypotheses and it is accordingly more difficult to formulate. It may be argued that the Heisenberg model is better than the Bloch model in nickel. The reason is that the 3*d* electrons, which alone are responsible for ferromagnetism in nickel, are rather firmly attached to their atoms. The fact that nickel has an atomic saturation moment of 0.6 Bohr magneton may mean that 60 percent of the nickel atoms are momentarily in the configuration $3d^9 4s$ and 40 percent in $3d^{10}$. In the alloy there may be a redistribution of the nickel atoms between these configurations. Analyses so far completed fail to include properly fluctuations of atoms between possible configurations. Since the calculations based on the Heisenberg model necessarily neglect the energy associated with the transfer of electrons, results derived from this model may be expected to be in error. The calculated susceptibility will probably be too high.

Another possible error in the results calculated from either model may be attributed to the neglect of the influence of the orbital motion of electrons upon the magnetic susceptibility. In all known cases except that of pyrrhotite the orbital momentum must be nearly quenched at room temperature because the gyromagnetic ratio is almost 2, which would be the value for the electron spin alone. The mechanism for the quenching of this orbital momentum is unexplained on the Heisenberg model. It may be possible that at higher temperatures the orbital momentum might make a contribution to the susceptibility. Since the gyromagnetic ratio is nearly the same for the various metals and their alloys the crystalline field is probably unimportant. The Bloch model explains the quenching as a result of the wandering of electrons from atom to atom. It may also be noted that an antiferromagnetic coupling between the orbital angular momenta may be present and cause such a quenching;[7] this is not considered in any of the theories.[8]

In view of the theoretical uncertainties reviewed above it seemed worth while to carry out precise measurements on the susceptibilities of nickel-copper and nickel-zinc alloys above their Curie points. Copper forms a complete series of solid solutions with nickel and zinc is also very soluble in nickel, the solubility limit lying at 30 percent. In both cases there is only a small change in the lattice constant.[9] Copper and zinc immediately succeed nickel in the periodic table. Thus an atom of nickel in either series of alloys is in a situation very similar to that in the pure metal except that each atom of copper has added one extra electron to the alloy and each atom of zinc has added two. With increasing dilution of nickel and greater average separation between nickel atoms both the ferromagnetic coupling between the 3*d* electronic spins and the antiferromagnetic coupling of their orbital angular momenta should decrease, and temperature changes dependent upon these factors might be especially apparent.

The paramagnetic susceptibility of copper-

[5] C. Sadron, Ann. de physique **17**, 371 (1932).
[6] E. C. Stoner, Proc. Roy. Soc. **A165**, 372 (1938).

[7] A. Sommerfeld and H. A. Bethe, *Handbuch der Physik*, second edition, Vol. 24, No. 2, p. 613.
[8] An excellent review of this subject by J. H. Van Vleck is soon to appear in Ann. de l'Institut Henri Poincaré.
[9] S. Holgersson, Ann. d. Physik **79**, 35 (1926); J. Schramm, Zeits. f. Metallkunde **30**, 122 (1938).

nickel alloys above their Curie points has already been investigated. The most consistent results are those of Alder[10] and Gustafsson.[11] Alder measured the values of the susceptibility from −190°C to 750°C and found at all temperatures a decrease in susceptibility as the percent of copper increased, with certain unexplained irregularities. Gustafsson repeated this work but did not find the irregularities previously noted. His measurements extended from room temperature to 450°C. In the present investigation this range has been extended to 800°C, and results compared with similar measurements on zinc-nickel alloys. Since this work was undertaken, the magnetic properties of zinc-nickel have been reported by Schramm.[12] Quantitative comparison is difficult because of the form of the published data.

Preparation of Alloys

The alloys were prepared from the purest metals obtainable. The base material was Baker's C. P. nickel, purified further by the rotating cathode method of Fink. This material was prepared by Lawrence Ott in 1931 and has been used in other investigations in this laboratory. This was alloyed with Hilger electrolytic copper, 99.995 percent pure, containing oxygen as the chief impurity. The zinc used was prepared for spectrographic analysis by the New Jersey Zinc Co. and was of 99.999 percent purity. The copper alloys were melted in magnesia crucibles under hydrogen at atmospheric pressure, then pounded to hasten homogenizing, and annealed at a temperature of 900°C for a week. It was very important that homogenizing should be complete since even slight segregations of nickel atoms would cause a large error. As the zinc alloys could not be made in an open crucible, owing to the high volatility of zinc, the zinc and nickel were sealed under a pressure of 10^{-5} mm or less in a small tube of fused silica and annealed at a temperature of 1000°C for a week so that the zinc completely diffused through the nickel. It was impossible to melt these alloys under these conditions due to the low softening point of the container. Spectrographic test for silicon gave negative results.

The homogeneity of the 15 percent copper alloy was tested in two ways, magnetically and microscopically. Specimens of the same melt were polished, etched and examined microscopically by Dr. R. M. Brick of the Department of Metallurgy, after two, five, and seven days homogenizing. No inhomogeneity could be detected even in the two-day sample. The abruptness of the transition at the Curie temperature has been shown by Marian[13] to be a proof of homogeneity. The transition becomes more abrupt as length of time for homogenizing is increased until a limit is reached when most of the change occurs within from 5 to 20° for copper alloys between 0 and 12 percent, 30 to 60° for 12 to 35 percent copper, and over 60° for alloys with more than 35 percent copper. For this 15 percent alloy the corresponding range in the specimen annealed for two days was 35°, for the one annealed for seven days was 15°. Therefore the magnetic method of test was more sensitive than the microscopic and was used subsequently for all alloys with a Curie point above room temperature. In each case it was found that the transition took place within the temperature limits just quoted from Marian.

The mean composition of these alloys reported was determined by chemical analysis. In different parts of the copper-nickel melt the composition as cast differed by as much as 1 percent for the 15 percent alloy and 2 percent for the 60 percent alloy. The zinc-nickel was of much more uniform composition, the greatest deviation being 0.5 percent for the 9 percent alloy.

The 13 percent copper sample of the copper-nickel series was supplied by Dr. R. M. Bozorth of the Bell Laboratories. This was synthesized from Mond nickel (0.03 percent Fe) and Hilger spectroscopically pure copper.

Magnetic Measurements

A Weiss-Foëx translation balance with a large Weiss magnet was used for the magnetic measurements. The furnace used was similar to one described by Foëx and Forrer[14] and the temperatures were measured by a Chromel-alumel thermocouple calibrated by the melting points of Bi and Sn as indicated by the change of sus-

[10] M. Alder, Thèse, Zurich (1916).
[11] G. Gustafsson, Ann. d. Physik **28**, 121 (1937).
[12] J. Schramm, Zeits. f. Metallkunde **30**, 327 (1938).
[13] V. Marian, J. de phys. et rad. [7] **8**, 313 (1937).
[14] G. Foëx and R. Forrer, J. de phys. et rad. [6] **7**, 180 (1926).

TABLE I. *Mass susceptibilities of* CuNi *alloys. The results on two different specimens are given for each alloy.*

T(°K)	$\chi\times10^6$	$1/\chi\times10^{-4}$
13.0 percent Cu by weight		
599	51.85	1.929
635	36.50	2.740
695	25.01	3.998
743	19.98	5.005
816	15.06	6.640
879	12.63	7.918
899	12.04	8.306
973	10.28	9.728
995	9.75	10.26
1071	8.33	12.00
518	225.15	.4441
563	80.64	1.240
582	61.99	1.613
633	36.26	2.759
680	26.77	3.736
712	22.51	4.442
789	16.30	6.135
833	14.30	6.993
952	10.64	9.398
1084	8.45	11.84
15.0 percent Cu by weight		
558	72.63	1.377
575	57.92	1.727
633	32.81	3.048
669	25.98	3.849
721	20.30	4.926
808	14.76	6.775
854	12.87	7.770
913	11.24	8.897
983	9.83	10.17
1054	8.77	11.40
593	50.65	1.974
600	45.94	2.177
640	33.39	2.995
691	24.57	4.070
741	19.20	5.208
789	15.96	6.266
890	12.08	8.278
939	10.85	9.217
22.7 percent Cu by weight		
471	81.65	1.225
484	69.09	1.447
487	63.22	1.582
497	55.40	1.805
511	48.41	2.066
533	37.96	2.634
547	32.75	3.053
554	32.39	3.087
582	26.01	3.845
596	23.37	4.279
602	23.48	4.259
629	20.53	4.871
645	18.29	5.467
701	14.93	6.698
754	12.79	7.819
518	42.66	2.344
550	31.89	3.136
602	22.62	4.421
626	19.53	5.120
654	17.69	5.653
660	16.22	6.165
689	15.02	6.658
722	13.54	7.386
729	13.36	7.485
766	11.84	8.446
792	10.98	9.107
855	9.47	10.56
882	8.96	11.16
933	8.24	12.14
971	7.71	12.97
28.7 percent Cu by weight		
475	31.58	3.167
500	25.69	3.893
561	17.33	5.770
573	16.46	6.075
612	13.73	7.283
642	12.37	8.084
693	10.77	9.285
753	9.17	10.91
809	8.10	12.34
876	7.07	14.15
957	6.26	15.98
429	52.46	1.906
454	39.89	2.507
483	29.14	3.432
534	20.34	4.916
580	15.94	6.274
625	13.35	7.491
668	11.36	8.803
724	9.78	10.22
765	8.87	11.27
37.0 percent Cu by weight		
331	53.30	1.876
380	28.84	3.467
397	25.24	3.962
442	17.97	5.565
489	13.53	7.391
539	10.97	9.116
573	9.82	10.18
609	8.81	11.36
657	7.63	13.10
687	7.13	14.02
751	6.31	15.85
412	21.31	4.693
483	13.80	7.246
550	10.37	9.643
607	8.66	11.55
641	7.97	12.54
688	7.18	13.93
721	6.73	14.85
775	6.08	16.44
840	5.52	18.11
876	5.26	19.02
941	4.87	20.54
970	4.73	21.14
49.6 percent Cu by weight		
293	11.78	8.489
346	8.45	11.84
404	6.83	14.65
439	6.26	15.96
446	6.16	16.24
496	5.35	18.70
565	4.71	21.24
584	4.55	21.97
654	4.12	24.25
690	4.03	24.83
735	3.79	26.47
749	3.71	26.92
806	3.53	28.32
852	3.37	29.67
911	3.22	31.02
293	11.37	8.79
345	8.10	12.34
396	6.93	14.43
447	5.95	16.79
501	5.18	19.32
563	4.51	22.17
606	4.29	23.33
650	3.97	25.21
703	3.78	26.46
747	3.57	27.98
827	3.31	30.21
897	3.15	31.74
948	3.05	32.79
60.9 percent Cu by weight		
295	3.30	30.25
341	3.01	33.17
382	2.78	35.94
439	2.58	38.76
480	2.52	39.64
530	2.43	41.18
580	2.35	42.45
627	2.31	43.26
635	2.30	43.52
728	2.20	45.39
810	2.12	47.08
294	3.27	30.61
345	2.95	33.92
399	2.68	37.30
447	2.58	38.68
504	2.43	41.07
557	2.35	42.54
612	2.27	44.05
655	2.23	44.82
709	2.18	45.87
757	2.13	47.04
819	2.07	48.40
857	2.04	48.97
900	2.01	49.85
976	1.97	50.84

TABLE II. *Mass susceptibilities of* ZnNi *alloys. The results on two different specimens are given for each alloy.*

T(°K)	$\chi\times10^6$	$1/\chi\times10^{-4}$	T(°K)	$\chi\times10^6$	$1/\chi\times10^{-4}$	T(°K)	$\chi\times10^6$	$1/\chi\times10^{-4}$
5.1 percent Zn by weight			*17.0 percent Zn by weight*			*26.2 percent Zn by weight*		
677	43.69	2.289	445	26.38	3.791	293	9.09	11.00
709	33.47	2.988	487	19.80	5.051	346	7.54	13.26
722	31.42	3.183	554	14.51	6.892	398	6.53	15.31
779	22.70	4.405	603	12.40	8.065	443	5.96	16.79
816	19.45	5.141	646	10.83	9.234	505	5.28	18.93
863	16.27	6.146	692	9.75	10.25	563	4.85	20.62
902	14.65	6.826	743	8.69	11.50	594	4.65	21.52
926	13.66	7.321	806	7.64	13.09	669	4.26	23.45
993	11.70	8.547	849	7.16	13.97	723	4.06	24.62
			905	6.74	14.83	848	3.72	26.87
			935	6.56	15.24	904	3.59	27.84
						959	3.51	28.51
656	51.22	1.952	406	37.65	2.656	293	9.14	10.93
690	38.63	2.589	423	32.51	3.076	347	7.49	13.35
716	31.59	3.166	452	25.55	3.914	394	6.67	14.99
769	23.41	4.272	497	18.74	5.336	468	5.75	17.39
790	21.53	4.645	558	14.37	6.959	518	5.23	19.11
833	18.21	5.491	572	13.52	7.396	593	4.66	21.47
864	16.37	6.109	654	10.47	9.551	687	4.15	24.09
890	15.06	6.640	688	9.55	10.47	739	3.97	25.17
914	14.09	7.097	693	9.37	10.67	817	3.75	26.66
951	12.80	7.812				843	3.68	27.18
						911	3.54	28.22
						974	3.44	29.10
9.1 percent Zn by weight			*21.2 percent Zn by weight*			*29.7 percent Zn by weight*		
590	46.68	2.145	295	32.60	3.067	293	5.22	19.14
626	32.52	3.075	363	18.88	5.297	327	5.02	19.92
658	27.65	3.617	419	13.95	7.168	371	4.61	21.69
687	22.29	4.486	479	11.00	9.091	396	4.36	22.93
744	18.11	5.522	545	8.79	11.38	441	4.12	24.24
749	17.17	5.824	600	7.80	12.82	502	3.84	26.01
818	14.06	7.112	642	7.11	14.07	582	3.55	28.14
847	12.74	7.849	688	6.59	15.18	645	3.40	29.38
855	12.54	7.974	742	6.08	16.45	698	3.31	30.24
902	11.27	8.873	782	5.80	17.25			
954	10.13	9.872	823	5.55	18.00			
957	10.07	9.930	885	5.17	19.33			
991	9.51	10.52	962	4.90	20.41			
1001	9.38	10.66						
518	132.45	0.7553	294	33.13	3.018	293	5.14	19.44
536	92.50	1.081	309	27.06	3.695	345	4.66	21.45
558	65.27	1.532	312	26.48	3.776	449	3.97	25.18
570	58.11	1.721	338	21.64	4.621	510	3.69	27.06
604	39.49	2.532	366	18.04	5.543	554	3.54	28.26
625	33.11	3.020	383	16.28	6.143	610	3.42	29.21
650	28.27	3.537	476	11.06	9.042	664	3.25	30.77
679	23.88	4.188	514	9.80	10.21	745	3.11	32.18
702	21.23	4.710	517	9.60	10.42	835	2.99	33.44
729	19.08	5.241	592	8.04	12.44	900	2.91	34.38
751	17.31	5.777	683	6.71	14.89	957	2.86	34.94
784	15.61	6.406	689	6.72	14.88			
			765	6.05	16.54			
			832	5.62	17.80			
			883	5.32	18.81			
			947	5.03	19.88			

ceptibility. As only relative susceptibilities were obtained by this method, absolute values were found by comparison with a standard of pure gold of known mass susceptibility $(0.145\pm0.001)\times10^{-6}$.

For these measurements the specimens were sealed into silica tubes under a pressure of 10^{-6} mm to prevent change of composition due to diffusion and oxidation. After a measurement at a high temperature a repetition of one at a low temperature was made as a test for any permanent change which might have occurred in

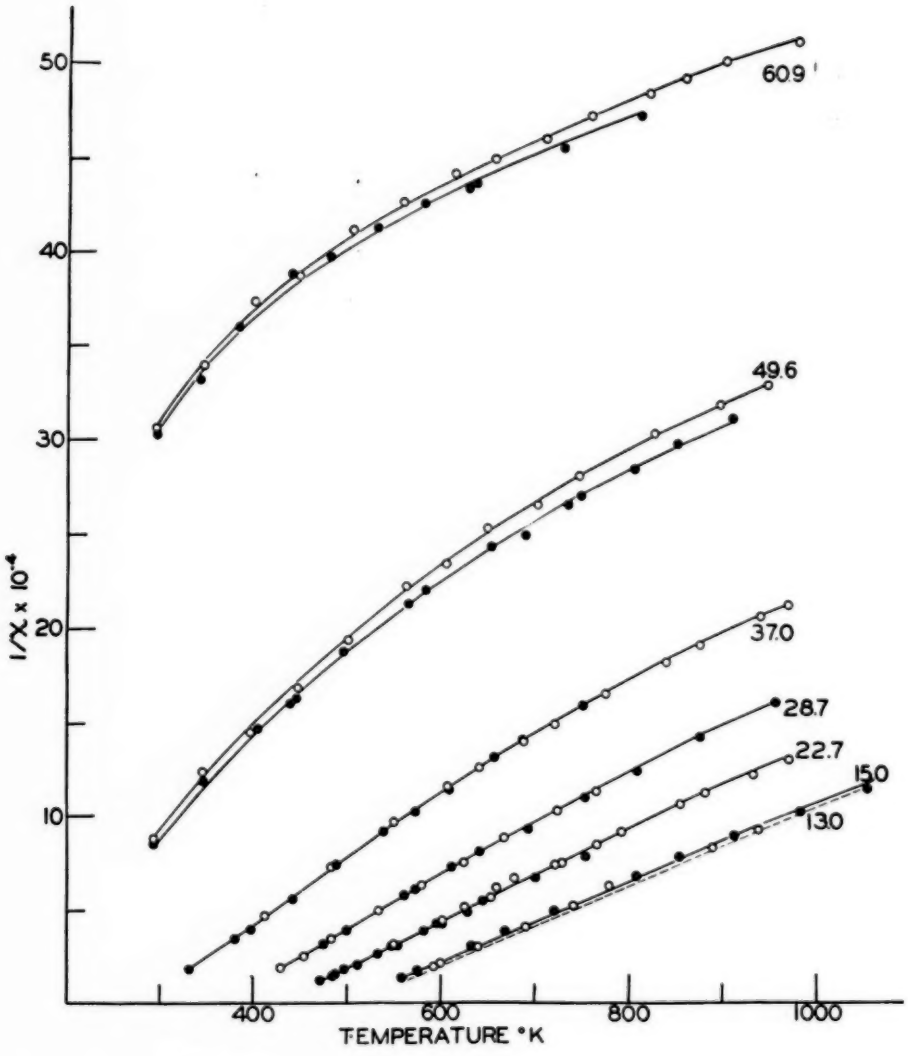

FIG. 1. Reciprocals of mass susceptibilities of CuNi alloys plotted against the temperatures for various percents of copper.

the specimen. When a run had been completed the container was cracked open, the specimen removed, and the susceptibility of the silica measured separately.

To prove the absence of ferromagnetic impurity (e.g., undissolved nickel) the susceptibility was measured at several values of the magnetic field between 3000 and 15,000, at both room and higher temperatures, and in no case was there a deviation from proportionality between susceptibility and field. Subsequently measurements of susceptibility *versus* temperature were taken at a fixed field of 11,350.

DISCUSSION OF RESULTS

Tables I and II give the data, T and χ, and the calculated values of $1/\chi$ for the copper and zinc alloys, respectively. These results are presented graphically in Figs. 1–4, a separate curve being drawn for each specimen in Figs. 1 and 2. Gustafsson's values for copper-nickel at the corresponding temperatures are plotted for comparison in Fig. 3; for each temperature his points (crosses) lie slightly higher than the curves obtained here.

These results show, in the first place, that the Curie-Weiss law holds only within restricted

ranges of temperature. When measurements could be obtained in the neighborhood of the Curie point, the curves become convex towards the T axis as is usual. At high temperatures, on the other hand, the curves become concave towards the T axis, especially for the alloys of low nickel content. The second important result is that the susceptibility at a given temperature decreases less rapidly than linearly with the addition of copper or zinc. Thus extrapolation to zero moment at 60 percent copper or 30 percent zinc is not justified. If the percent copper or zinc were plotted against average moment per nickel atom instead of moment per gram of alloy the general shape of the curves would be the same although the absolute value of the slope would decrease more rapidly with increase of copper or zinc.

In the preceding discussion of the $1/\chi - T$ curves based on the Bloch model it was mentioned that the Curie-Weiss law ought to hold best at high temperatures. Thus the curvature found for these alloys at high temperatures is not predicted by this theory. One cause for a deviation from the Curie-Weiss law could be a change in the form of the energy band at the high temperatures, due to a change in the lattice constant. When the temperature is raised and the lattice expands the band becomes narrower, causing an increase in susceptibility. The coefficient of thermal expansion of the copper-nickel alloys, at least, is known to obey the law of mixtures, increasing from the value for nickel proportionately to the percent copper added. Thus this effect would be greater in the alloys of high copper content. This is just what is found: the susceptibility at high temperatures is larger than that predicted by the Curie-Weiss law, particularly for alloys high in copper or zinc. It may be doubted, however, in view of the small total change in lattice constant, whether any such secondary effect could be important.

A second possible cause for a deviation from the theoretical curve would be a change in the number of electrons in the band. It may be possible that at higher temperatures and lower nickel contents the 4s electrons do not so readily

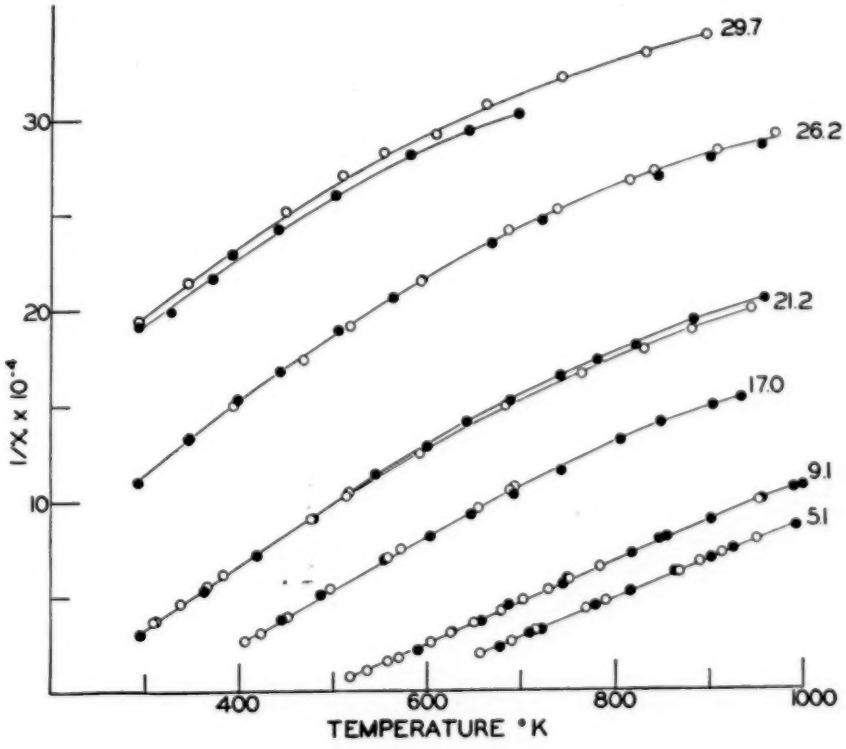

FIG. 2. Reciprocals of mass susceptibilities of ZnNi alloys plotted against the temperatures for various percents of zinc.

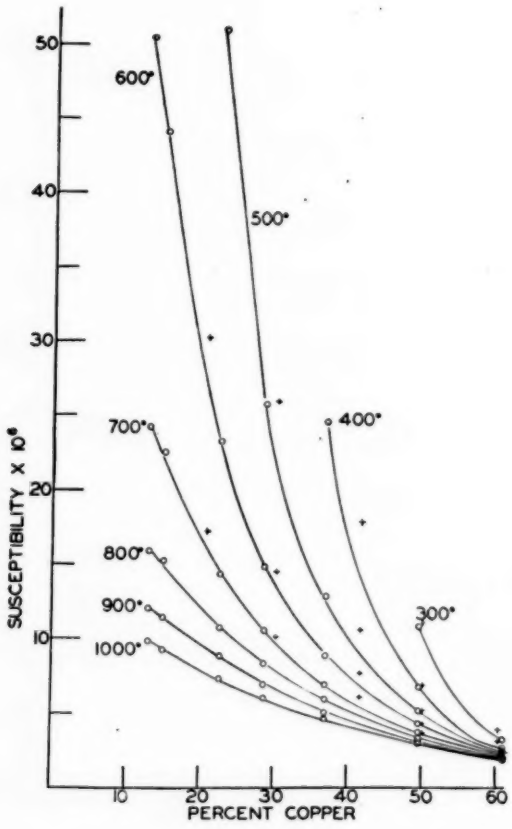

FIG. 3. Mass susceptibilities *versus* percent copper by weight for various temperatures. Gustafsson's values are indicated by crosses.

fall into the holes in the 3*d* band, with the result that in such cases the susceptibility is abnormally increased.

The second experimental result, that the susceptibility drops more slowly than in proportion to the copper or zinc content, contradicts the predictions of the Curie-Weiss law, $\chi = C/(T-\theta_p)$. By this theory in its simple form both C and θ_p are proportional to the number of paramagnetic atoms. Thus the susceptibility should decrease more rather than less rapidly than is required by a linear relation between χ and percent composition. This suggests again that the 4*s* electrons do not inevitably fill the empty spaces in the 3*d* shell, particularly at high copper and zinc content. This is difficult to reconcile with the Bloch model without special modifications. In fact the exchange interaction between the electronic spins should decrease with increased separation of the nickel atoms, resulting in a decreased value of θ and therefore a decreased susceptibility.

As yet the Heisenberg model also has not been sufficiently developed to explain either of these results satisfactorily. It should be emphasized that a linear relation between $1/\chi$ and T is not necessarily predicted by this theory. A small excess susceptibility at the high temperatures could be explained by a redistribution of the nickel atoms from d^{10} to d^9 configurations. This is, of course, comparable to the scattering of an electron from a *d* to an *s* band in the Bloch model, and is equally incalculable. Anomalous increase of susceptibility at high temperatures might also be qualitatively explained by unquenching of orbital momenta.

No predictions have been made from this point of view about the variation of the susceptibility with the percent copper or zinc added. If only the nickel atoms contribute magnetic moment, these results indicate that there may be a redistribution of the nickel atoms between the d^{10} and d^9 states with alloying. If the orbital moment is quenched due to an antiferromagnetic coupling this would decrease as the average distance between the nickel atoms increased. An added susceptibility would then result from the magnetic contribution of the orbital momenta in the alloys of low nickel content. On the other hand, as mentioned before, the ferromagnetic coupling of the electronic spins would also decrease with increased separation of the nickel atoms, causing a decrease in θ and with it a decrease in the susceptibility. Any change in the antiferromagnetic coupling or in the spin-orbit coupling would cause the gyromagnetic ratio to differ from 2. Sucksmith[15] found a g value of 1.9 at room temperature for copper-nickel alloys with Curie points around -10°C, which shows that the influence of the orbital momenta is not important just above the Curie point. Similar measurements on alloys with lower Curie points would be very illuminating as the orbital momenta are more apt to be liberated at temperatures well above the Curie point.

A comparison of the susceptibilities for the two sets of specimens shows that an alloy with a

[15] W. Sucksmith, Helv. Phys. Acta **8**, 205 (1935).

certain percent zinc corresponds most closely to the alloy with twice that percent copper. The ratio of the susceptibility of the zinc alloy to that of the corresponding copper alloy is always greater than unity but is never greater than 1.5. In general, it is higher for the alloys of low percent nickel. In other words, any factor which causes an increase in susceptibility is stronger in zinc alloys than in copper alloys having the same number of excess electrons.

No corrections for the diamagnetism of the core or for temperature independent paramagnetism were made. The atomic moment was not calculated because of the inadequacies of the Curie-Weiss law. These results agree with Gustafsson's in showing no sudden changes of slope such as were found by Alder.

The ferromagnetic Curie point was above room temperature in a few cases so that it could be measured and compared with the paramagnetic Curie point.[16] For the 15 percent copper alloy the temperature of the ferromagnetic Curie point was measured for the sample annealed for two days and for one annealed for five days. The transition from ferromagnetic to paramagnetic state was not only more gradual for the two-day sample, as already mentioned, but the value of θ_f at the point of inflection was higher for the two-day sample. The value of θ_p was the same within experimental error.

In conclusion it should be repeated that the explanation of these results is necessarily incomplete because neither the Bloch nor the Heisenberg model adequately describes the state of the alloy, and because many factors have had to be neglected in the calculations.

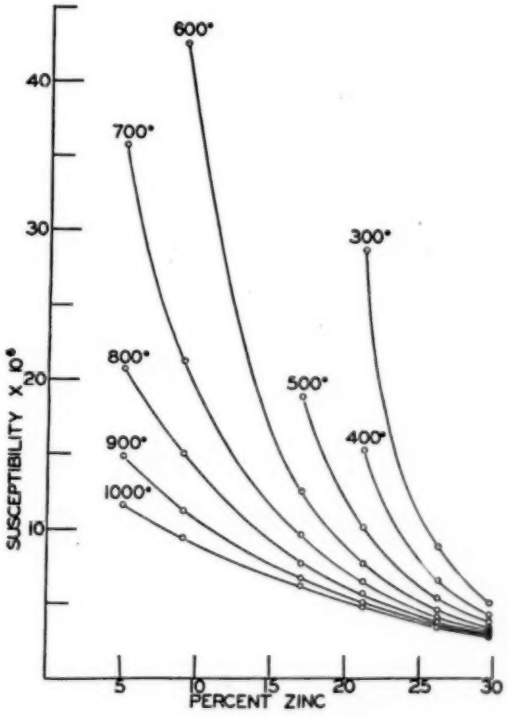

FIG. 4. Mass susceptibilities *versus* percent zinc by weight for various temperatures.

This work was done while I was a guest in the Sloane Physics Laboratory. The zinc used was the gift of Professor W. E. Milligan of the Hammond Metallurgical Laboratory of Yale. I am especially grateful to Professor L. W. McKeehan for valuable advice and encouragement and to Professor J. H. Van Vleck of Harvard for suggesting the problem and for helpful criticism.

	θ_f	θ_p		θ_f	θ_p
[16] 13 percent Cu	488°K	508°K	5 percent Zn	532	560
15 percent Cu	474	500	9 percent Zn	457	487
23 percent Cu	394	420			
29 percent Cu	351	370			

The Quantum-Mechanical Basis of Statistical Mechanics

EDWIN C. KEMBLE
Harvard University, Cambridge, Massachusetts

(Received September 6, 1939)

Von Neumann's macroscopic entropy definition is not wholly satisfactory because (*a*) it rests on an unsatisfactory characterization of macroscopic variables, (*b*) it fails to make satisfactory connection with the Nernst heat theorem, (*c*) it is based on an unsatisfactory definition of thermal equilibrium, (*d*) it is not applicable to microscopic systems. It is proved that if two systems initially in independent states are placed in thermal contact and isolated, the sum of their microscopic entropies cannot decrease, but will in general increase. This theorem is a substitute for the usual rule regarding the increase in entropy of a single isolated system. Appreciable departures from the canonical state are shown to have a vanishingly small probability in the case of a system subjected to the thermostat experimental procedure described in a preceding paper.

IN a preceding paper[1] (hereafter referred to as (I)) I have outlined a new quantum-mechanical approach to statistical mechanics and a closely related modification of thermodynamic theory. In this article I shall consider more fully the existing status of the basic problems of statistical mechanics and shall formulate with greater care the two fundamental theorems mentioned in the foregoing paper, supplying at the same time the requisite detailed proofs. The proof of one of these theorems (derivation of canonical ensemble) lacks complete mathematical rigor, but I believe it will be found convincing nevertheless.

THE MACROSCOPIC STATISTICAL DEFINITION OF ENTROPY

The fundamental thesis of this paper and the one which precedes it is that by using a refined operational definition of thermal equilibrium it is possible to justify v. Neumann's *microscopic* entropy definition and so to avoid difficulties which arise in connection with his *macroscopic* entropy definition. Since relatively few physicists in this day of specialization are familiar with these newer entropy definitions, a preliminary discussion of the not wholly satisfactory macroscopic definition of entropy is in order.

The macroscopic conception of entropy had its origin in the Bohr theory which assumed that every free atom and molecule spends practically all its time in one or another of the allowed stationary states, or energy levels, transitions between which take place discontinuously. The transitions, or jumps, from one stationary state to another were assumed to obey simple statistical laws like those governing the atomic disintegrations in radioactivity. With this picture the state of a perfect gas could be described by giving the number of molecules in each energy level, or stationary state. Using classical statistics and the Boltzmann-Planck method of counting complexions one readily "derives" the entropy formula

$$S=-kN\sum_n w_n \ln (w_n/g_n) \qquad (1)$$

for a gas composed of N molecules, where w_n is the fractional population of the nth stationary state of an individual molecule and g_n is its statistical weight. This expression for the entropy, when suitably modified to take into account the Fermi-Dirac statistics, or the Einstein-Bose statistics, as the case may be, gives a very satisfactory description of the thermal behavior of the various kinds of "gases" to which it can be applied. If one assumes that the fraction of molecules jumping from the state n to the state m per unit time is $A_{nm}g_m$, while the fraction jumping in the reverse direction is $A_{nm}g_n$ it follows that

$$dw_n/dt=-\sum_m A_{nm}(w_n g_m - w_m g_n). \qquad (2)$$

Here A_{nm} is a transition probability characteristic of the pair of states n and m. It is assumed to vanish unless the energies of these states are sensibly the same. On the basis of Eq. (2) Pauli

[1] "Fluctuations, Thermodynamic Equilibrium, and Entropy," Phys. Rev. **56**, 1013 (1939).

proved the "H theorem"[2]

$$dS/dt \geqq 0, \tag{3}$$

in which the equality sign holds only if $w_n : g_n = w_m : g_m$, the systems under discussion being isolated.

In order to extend the above method to thermodynamic systems of the most general kind and put the theory on a modern quantum-mechanical basis, Pauli proposed[2] that we interpret the expression (1) as the entropy, not of a single sample of gas, but of a Gibbsian ensemble of N independent identical sample gaseous systems—identifying w_n and g_n with the fractional population and statistical weight of the nth state of any of the complete systems. The fundamental problem of statistical mechanics would then be solved if we could show that Eq. (2) is valid under the conditions to which (1) is to be applied. Now unfortunately Eq. (2) does not follow directly from the rules of quantum mechanics although Dirac[3] has given a fairly satisfactory derivation for the radiative transitions of a single atom. To validate (2) for his own purpose Pauli found it necessary to introduce an approximate Hamiltonian H_0 with a complete orthonormal system of eigenfunctions $\chi_1, \chi_2, \cdots \chi_\nu, \cdots$. These functions were then united into groups with which the indices n and m of Eq. (2) were correlated. g_n was identified with the number of orthogonal functions in the nth group. The different states in each group cover a small range of energies and were assumed to be indistinguishable from the point of view of macroscopic measurements. The individual functions, or states, correspond to the cells in phase space of the Planck theory, while the groups correspond to the "macroscopic states" of the same theory. It will be useful for the development of an intuitive understanding of the present theory to apply the term "macrocell" to each of these groups. Corresponding to each macrocell there is a linear manifold of functions and hence each cell can be regarded as a division of function space.

Pauli found it necessary to make certain plausible assumptions both with regard to matrix elements of the perturbing potential $H-H_0$ and with regard to the initial state of the system under investigation. The assumption regarding the initial state is an "hypothesis of elementary chaos" applied to the elements of the statistical matrix in a representation based on the χ functions. On this basis he was able to set up a formal proof of Eq. (2). Considerable difficulties arise, however, when one attempts to give a more rigorous form to Pauli's argument.[4] Moreover the limitation to chaotic initial states is a serious one.

The concept of macroscopic entropy was further developed by von Neumann.[5] His contributions were of a twofold character. First of all he gave a refined form to the definition of the macrocell. Each of these linear manifolds is assumed to consist of the simultaneous eigenfunctions of a set of so-called "macroscopic variables." These are commuting operators the measurement of which corresponds closely to the macroscopic, or classical, measurements we are actually able to perform on the gross systems envisaged in ordinary thermodynamic discussion. Thus the maximum information about a system which is obtainable by predictive macroscopic measurement is assumed to assign it to a mixture of wave functions which belong to a common macrocell.

The macrocells can be set up in a variety of ways according to the type of measurements one has in mind. Von Neumann chooses to use a two-dimensional array in which all the cells in any one row have a common energy range which does not overlap the range of any other. Using the notation of Gibbs we may conveniently refer to such a row of equal-energy cells as an "ergodic shell." Let us specify each macrocell by a pair of subscripts ν and a, of which the latter indicates the particular ergodic shell to which the cell belongs. Let $s_{\nu a}$ denote the number of linearly independent wave functions, i.e., the statistical

[2] W. Pauli, Jr., Sommerfeld Festschrift, *Probleme der Moderne Physik* (Leipzig, 1928), p. 30.

[3] P. A. M. Dirac, Proc. Roy. Soc. **A114**, 243 (1927). In the present paper we can neglect the perturbative influence of radiation on the thermodynamic system by including the radiation in the system from the beginning after the manner of Dirac.

[4] These are illustrated in the section on "Quantum Statistical Mechanics" in the present writer's book, *Fundamental Principles of Quantum Mechanics* (New York, 1937).

[5] J. v. Neumann, Gött. Nachr. 273–291 (1927); Zeits. f. Physik **57**, 30–70 (1929). Cf. also W. Pauli and M. Fierz, Zeits. f. Physik **106**, 572 (1938).

weight, of the cell ν, a and let $G_a = \sum_\nu s_{\nu a}$ denote the total statistical weight of the ergodic shell a. Consider a pure state ensemble of isolated systems with wave function ψ_t which develops in time according to the Schrödinger equation. Let ψ_0 be the initial form of ψ_t. We denote by $x_{\nu a}$ the square of the norm of the projection[6] of ψ_t on the macrocell ν, a. This is the probability that measurement of a system in the pure state ψ_t will assign it to the given macrocell. We will call this quantity the "fractional population" of the cell ν, a for an ensemble in the state ψ_t. The expression for the macroscopic entropy of a system which belongs to such an ensemble becomes (cf. Eq. (1))

$$S_{\text{mac}}(\psi_t) = -k\sum_a\sum_\nu x_{\nu a} \ln (x_{\nu a}/s_{\nu a}). \qquad (4)$$

Von Neumann compares the above expression with the corresponding expression for the macroscopic entropy of a modified ensemble to which he applies the term "microcanonical." This modified ensemble is a mixture defined by an explicit statistical operator,[7] and so constructed that the relative population density $x_{\nu a}/s_{\nu a}$ of each cell of the original ensemble is replaced by the average population density of all the cells of the same ergodic shell. Thus, if $u_a = \sum_\nu x_{\nu a}$ denotes the original fractional population of the entire shell a, we make the substitution $x_{\nu a} \to u_a s_{\nu a}/G_a$. If the new ensemble were restricted to a single ergodic shell, it would be a very close analog of the microcanonical ensemble of Gibbs, which has a uniform density-in-phase over an ergodic shell in classical phase-space. Since, however, the new ensemble is not restricted to a single ergodic shell, we prefer to speak of it as a *uniformized ensemble*. Let $\bar{S}_{\text{mac}}(\psi_t)$ denote the corresponding macroscopic entropy for a single system. It has the value

$$\bar{S}_{\text{mac}}(\psi_t) = \bar{S}_{\text{mac}}(\psi_0) = -k\sum_a u_a \ln (u_a/G_a). \qquad (5)$$

Since ψ_t changes in time, the "populations" $x_{\nu a}$ and entropy $S_{\text{mac}}(\psi_t)$ also change, but the u_a's and $\bar{S}_{\text{mac}}(\psi_t)$ are constant.

We are now in a position to discuss the two theorems which form the second part of v. Neumann's contribution to our subject. For the validity of each theorem it is necessary to assume that with few exceptions the eigenvalues of the exact Hamiltonian operator are nondegenerate, that there are no cases—or at most an insignificantly small number—where the energy difference of one pair of levels in an ergodic shell is equal to the energy difference of another pair in the same shell, and finally that *the statistical weight of each macrocell is large compared with the number of cells in the corresponding ergodic shell.* Another important assumption will be mentioned after the primary content of the theorems has been stated.

The first theorem, which we shall call theorem A, is analogous to the Boltzmann-Pauli H-theorem for isolated systems (cf. Eq. (3)). The first part of this theorem consists in a proof that $\bar{S}_{\text{mac}}(\psi_0)$ forms an upper bound for $S_{\text{mac}}(\psi_t)$ in the case of an isolated system.[8] Von Neumann then shows that the long time average of the difference $\bar{S}_{\text{mac}}(\psi_0) - S_{\text{mac}}(\psi_t)$ is—at least with rare exceptions—a negligibly small quantity. This means that moments at which $S_{\text{mac}}(\psi_t)$ is appreciably less than $\bar{S}_{\text{mac}}(\psi_0)$ are so rare that if at any particular moment $\bar{S}_{\text{mac}}(\psi_0) - S_{\text{mac}}(\psi_t)$ is not small, it follows that the chance is very great that in a short time $S_{\text{mac}}(\psi_t)$ will increase and return to the neighborhood of $\bar{S}_{\text{mac}}(\psi_0)$. This proposition is evidently an equivalent of the classical H theorem but superior in form to Eq. (3) since it avoids the familiar paradox connected with the

[6] Let the macrocell ν, a consist of all linear combinations of the $s_{\nu a}$ wave functions $\omega_{1\nu a}, \omega_{2\nu a}, \omega_{3\nu a}, \cdots$. The projection of ψ_t on the macrocell is then defined as

$$\sum_\lambda (\psi_t, \omega_{\lambda\nu a})\omega_{\lambda\nu a},$$

where the sum ranges from $\lambda = 1$ to $\lambda = s_{\nu a}$. The quantity $x_{\nu a}$ is explicitly

$$x_{\nu a} = \sum_\lambda |(\psi_t, \omega_{\lambda\nu a})|^2.$$

The symbol (,) denotes a Hermitian scalar product.

[7] Every quantum-mechanical state can be defined either by a statistical matrix ϱ, or by a statistical operator V. Using the notation of Eq. (1) of the preceding paper, we define the statistical operator V corresponding to the statistical matrix ϱ by the equation

$$V = \Sigma_s w_s P_{\psi_s}$$

where P_{ψ_s} is the projection operator which, when applied to any function $F(x)$ yields the projection of F on ψ_s, *viz.*, $(F, \psi_s)\psi_s$. The statistical matrix ϱ is computed from V just as we compute the matrix of any physical quantity from the corresponding operator.

[8] One obtains $\bar{S}_{\text{mac}}(\psi_0)$ if he maximizes $S_{\text{mac}}(\psi_t)$, regarded as a function of the independent variables $x_{\nu a}$, subject to the conditions

$$\Sigma_\nu x_{\nu a} = u_a = \text{Const.}$$

reversibility of the time coordinate in the mechanical equations of motion.[9]

Von Neumann's second theorem—we call it theorem *B*—has to do with the relation between the expectation value $\bar{\alpha}_t$ of any macroscopically observable quantity α for the pure state ψ_t and the expectation value $\bar{\alpha}^{(u)}$ of the same quantity for the corresponding uniformized ensemble. It states that the time average of $[\bar{\alpha}^{(u)}-\bar{\alpha}_t]^2$ is small compared with $[\bar{\alpha}^{(u)}]^2$. This means that the time averages of the macroscopically measurable properties of any pure state ensemble differ negligibly from the corresponding properties of the appropriate steady state of maximum macroscopic entropy. Now the classical ergodic hypothesis and the less drastic quasi-ergodic hypothesis were assumptions used to justify the replacement of the time averages of the properties of an isolated system by statistical averages over the corresponding microcanonical ensemble.[10] Since theorem *B* reaches essentially the same goal, it may be called a *quantum-mechanical form of the ergodic theorem.*

Both theorems, while proved initially for arbitrary pure state ensembles, must hold equally for arbitrary mixed state ensembles. They have the important advantage that they avoid Pauli's assumption that the initial state is chaotic. They do require, however, the assumption that the matrix connecting the system of eigenfunctions of the exact Hamiltonian with any convenient system of simultaneous eigenfunctions of the macroscopic variables shall be chaotic. Von Neumann proves by an averaging process that the vast majority of conceivable forms for this unknown matrix are chaotic. This means that the assumption is an exceedingly mild one.

[9] Cf. e.g., P. and T. Ehrenfest, *Enzyklop. d. Math. Wiss.* (Leipzig, 1912), Bd. IV, Heft 32; J. H. Jeans, *Dynamical Theory of Gases* (Cambridge, 1916), pp. 65, 193–5; G. Jager, *Die kinetische Theorie der Gase und Flüssigkeiten*, pp. 374–5, in Geiger and Scheel's *Handbuch d. Physik*, Band IX (Berlin, 1926). This paradox persists in the quantum mechanics since the equations of motion in matrix form and the Schrödinger equation have the same properties with respect to the reversal of the time coordinate as the dynamical equations of classical theory.

[10] Cf. e.g., P. and T. Ehrenfest, reference 9; P. S. Epstein, "Critical Appreciation of Gibbs' Statistical Mechanics," esp. p. 477, in *A Commentary on the Scientific Writings of J. Willard Gibbs* (New Haven, 1936), Vol. II.

Objections to the Identification of Thermodynamic Entropy with Macroscopic Entropy

These results seem at first sight to be quite satisfactory. They give a mathematical and physical explanation of the approach of thermal equilibrium in isolated systems which can hardly fail to provoke admiration. Since the ergodic theorem and the *H* theorem have long been regarded as the two fundamental theorems of statistical mechanics the derivation of such theorems based on the macroscopic statistical definition of entropy suggests that we forthwith identify the macroscopic entropy of Eq. (4)—or the more general expression which parallels (4) when the state under consideration is a mixed one—with the thermodynamic entropy and consider that we have formulated a logical quantum-mechanical basis for the second law of thermodynamics. There are a number of difficulties, however, in the way of making such an interpretation of von Neumann's work.

(*a*) First among the difficulties felt by the writer is a dissatisfaction with von Neumann's characterization of macroscopic measurements and the corresponding macroscopic variables. He postulates that the macroscopic variables are all simultaneously measurable, i.e., that the corresponding operators all commute. This implies, as von Neumann shows, that a predictive[11] macroscopic measurement shall sharply separate states belonging to different ergodic shells. Now these shells are either uniquely defined, or have boundaries which vary with the precise procedure used in making the energy measurement. The first hypothesis implies a quantum structure in function space (Hilbert space) which we can hardly take seriously, since it rests on a mathematically convenient postulate unsupported by experimental evidence and opposed to all our intuitions. The second hypothesis implies that not *all* macroscopic variables are correlated with non-overlapping cells, although the macroscopic

[11] By a predictive measurement we mean one which sorts the systems measured into groups, or ensembles, each of which has a unique value of the measured variable. Von Neumann does not use the terms "predictive measurement" and "retrospective measurement" introduced by the writer (cf. my book, *Fundamental Principles of Quantum Mechanics* (New York, 1937), Section 41c.), but the above statement is merely a translation of what he does say into slightly different language.

state of a system can be adequately described in terms of one or more sets of macroscopic variables whose cells do not overlap. This assumption would destroy the uniqueness of the entropy definition. It also leads to the disturbing conclusion that by making successive predictive macroscopic energy measurements using procedures involving different ergodic shell systems we should be able to make a microscopic, or quasi-microscopic, predictive energy measurement. Either assumption is on the face of it irreconcilable with the method which we actually do use for the measurement of macroscopic energies, *viz.*, the reading of a thermometer combined with a calorimetric study of heat capacity.

The truth is that actual measurements cannot be divided into two sharply defined classes which we can designate as macroscopic and microscopic. The cruder measurements which we call macroscopic do not divide function space into linear manifolds and cannot be associated with rigorously commuting dynamical variables, although the lack of commutability is of little importance for most purposes because these measurements do not greatly disturb the measured system and because they have so little precision that a small disturbance does not make much difference.

(*b*) My second difficulty comes from an unwillingness to accept the discrepancy between the von Neumann theory and the quasi-empirical type of applied statistical mechanics set forth in the standard treatise of Fowler.[12]

Of course Fowler's procedure is frankly *ad hoc*, but it derives strength from the fact that it gives satisfactory answers to the questions customarily dealt with in the statistical theory of matter. It is primarily adapted to the treatment of samples of matter, such as gases and crystals, which are composed of many weakly interacting subsystems. The Bohr picture of such a system was one in which each subsystem, each molecule in the case of a gas, occupied at every moment a definite quantized stationary state. The state of the complete system could then be described by specifying the fraction of molecules of each type in each of its private stationary states. This model is adapted by Fowler to the language of wave mechanics and to the Pauli principle. It is then used to construct a supposed quantum-mechanical equivalent of the microcanonical ensemble of Gibbs which serves for the computation of the properties of thermal equilibrium. The Fowler microcanonical state is a collection of equally populated microscopic states of equal energy—if energy be calculated with omission of interaction terms between the different molecules. Each microscopic state corresponds to one member of a set of orthogonal eigenfunctions of an approximate Hamiltonian operator H_0 with a common energy eigenvalue.

The Darwin-Fowler method of determining average values for such a microcanonical state depends fundamentally on the very great degeneracy of the approximate Hamiltonian H_0, which is built up by adding the private Hamiltonians of the individual molecules. From the model and the method Fowler derives as a statistical definition of the entropy of a state of thermal equilibrium the expression

$$S = k \ln C, \tag{6}$$

where C is the number of linearly independent eigenfunctions of H_0 with the common energy E (statistical weight of E). This definition is not unrelated to that of von Neumann, for the macroscopic entropy of a uniformized state restricted to a single ergodic shell a as defined by (5) is $k \ln G_a$, so that we have only to identify the number of linearly independent wave functions in a von Neumann ergodic shell with the number of linearly independent functions in a Fowler microcanonical state in order to bring the two definitions into agreement. Actually both methods require for their validity that the entropy be not too small. Fowler, however, is clever enough to apply (6) right down to the absolute zero of temperature, where C normally goes to zero, carrying the entropy with it. It is by this extrapolation of his formula out of the range of its derivation that he is able to give such a satisfactory account of the Nernst heat theorem and the chemical constants of various gases. The extrapolation also receives support from the widespread intuitive agreement of physicists concerning two related propositions, *viz.*, that entropy is a measure of disorder, and that at

[12] R. H. Fowler, *Statistical Mechanics* (Cambridge, England, and New York, second edition, 1936).

the absolute zero every system must occupy its lowest possible energy level.

On the other hand, the von Neumann theory requires that the statistical weight G_0 of the innermost ergodic shell shall be large, like all the others, and so makes the macroscopic entropy of the equilibrium state of least energy a large number. The assumption that G_0 is large is, in fact, a denial either of the validity of our ordinary conception of the absolute zero, or else of the possibility of attaining temperatures indefinitely close to that zero.

(*c*) A third difficulty lies in the fact that the use of a microcanonical model for the state of thermodynamic equilibrium implies that thermodynamic equilibrium is to be obtained experimentally by the procedure α described in the preceding paper (I). Von Neumann's rejection of the microscopic definition of entropy was due to his acceptance of the operational definition α. My reasons for preferring the procedure β, in which the system is placed for a long time in a heat bath with measured temperature, are sufficiently explained in (I).

(*d*) Finally, there is the objection[13] that the macroscopic definition of entropy is not applicable to microscopic systems, because we cannot set up macrocells for microscopic systems, which have very large statistical weights, but which contain only experimentally indistinguishable pure states.

The Microscopic Statistical Definition of Entropy

The microscopic entropy is defined by Eq. (5) of the foregoing paper (I). We denote this quantity by the symbol S_{mic}, dropping the subscript on occasion when no ambiguity will result. It is immediately evident from the discussion of microscopic entropy in (I) that none of the objections (*a*), (*b*), (*d*) applies to it. To see how it works out in the neighborhood of the absolute zero we need the expression for S_{mic} in the case of a system in thermal equilibrium at the temperature T. For such states we make the hypothesis to be verified hereafter that the statistical matrix ϱ referred to a system of eigenfunctions of the exact Hamiltonian has the form specified by the right-hand member of Eq. (3) of (I). Thus ϱ is diagonal in this scheme of representation and the diagonal elements are

$$r_j \equiv \rho(j,j) = e^{-\gamma E_j}/\sum_m e^{-\gamma E_m} = e^{-E_j/kT}/\sum_m e^{-E_m/kT}. \quad (7)$$

For convenience we take the zero level of energy to be the lowest energy level of the system. Let g_0 denote the statistical weight of the lowest level. It is evident at once that

$$\lim_{T\to 0} r_j = \frac{1}{g_0}\delta_{E_j,0}.$$

Hence

$$\lim_{T\to 0} S_{\text{mic}} = -kg_0\left[\frac{1}{g_0}\ln\frac{1}{g_0}\right] = k \ln g_0.$$

Thus the microscopic entropy is identical with Fowler's entropy at the absolute zero. This means that objection (*c*) does not apply to this definition.

We continue the justification of the definition by discussing in detail the interaction between two quantum-mechanical systems A and B and its effect on their microscopic entropies. Every statistical matrix ϱ_{A+B} for the united system $A+B$ generates corresponding statistical matrices ϱ_A and ϱ_B for the parts A and B taken separately. Hence one can compute separately the microscopic entropies of A, B, and $A+B$.[14] It turns out that the entropy of the united system is not equal to the sum of the entropies of the parts except under special conditions.

Let $\varphi_1, \varphi_2, \cdots \varphi_n, \cdots$ denote a complete orthonormal system of functions in the coordinate space of the system A. Let $\chi_1, \chi_2, \cdots \chi_m, \cdots$ denote a similar system of functions in the coordinate space of the system B. Then the system of product functions $\Phi_{nm} \equiv \varphi_n\chi_m$ is complete and orthonormal in the coordinate space of the united system $A+B$. Let us assume that the united system is in a state P sufficiently definite to give it a specific statistical matrix ϱ_{A+B} whose typical element in the Φ_{nm} scheme is $\rho_{A+B}(nm, n'm')$. Then ϱ_{A+B} describes the sta-

[13] See preceding paper (I).

[14] A sudden alteration in the Hamiltonian of the united system corresponding to the insertion or withdrawal of an insulating membrane to break or make thermal contact between A and B does not change ϱ_{A+B} abruptly and so produces no discontinuous alteration in the entropies.

tistical properties of a quasi-infinite ensemble of united systems $A+B$ prepared like the original pair. Such an ensemble will include within itself an ensemble of systems A and another of systems B. The statistical properties of the former are described by a matrix ϱ_A defined by[15]

$$\rho_A(n, n') = \sum_m \rho_{A+B}(nm, n'm), \tag{8}$$

while the properties of the latter are described by the matrix

$$\rho_B(m, m') = \sum_n \rho_{A+B}(nm, nm'). \tag{9}$$

By proper choice of the two systems of functions $\varphi_1, \varphi_2, \cdots$ and $\chi_1, \chi_2, \cdots$ the matrices ϱ_A and ϱ_B can always be made diagonal. Let us assume that such a choice has been made. Then the microscopic entropies of A, B, and $A+B$ are as follows:

$$S_A = -k\sum_n \rho_A(n, n) \ln \rho_A(n, n), \tag{10a}$$

$$S_B = -k\sum_m \rho_B(m, m) \ln \rho_B(m, m), \tag{10b}$$

$$S_{A+B} = -k \text{ Spur } \varrho_{A+B} \ln \varrho_{A+B}. \tag{11}$$

It is easy to see that a *sufficient* condition for the equality of S_A+S_B and S_{A+B} is that ϱ_{A+B} have the product form required by the equation

$$\rho_{A+B}(nm, n'm') = \rho_A(n, n')\rho_B(m, m')$$
$$= [\sum_m \rho_{A+B}(nm, n'm)][\sum_n \rho_{A+B}(nm, nm')]. \tag{12}$$

In this case the diagonalization of ϱ_A and ϱ_B carries with it the diagonalization of ϱ_{A+B}. From Eq. (11) we obtain

$$\begin{aligned} S_{A+B} &= -k\sum_n\sum_m \rho_A(n, n)\rho_B(m, m) \\ &\quad \times \ln \rho_A(n, n)\rho_B(m, m) \\ &= -k\sum_n [\rho_A(n, n) \ln \rho_A(n, n) \\ &\quad + \sum_m \rho_B(m, m) \ln \rho_B(m, m)] \\ &= S_A + S_B. \end{aligned} \tag{13}$$

We next prove that in general

$$S_{A+B} \leqq S_A + S_B. \tag{14}$$

For this purpose it is convenient to use Klein's lemma[16] which states that the sum $\sum_\kappa \rho(\kappa, \kappa) \ln \rho(\kappa, \kappa)$ for any statistical matrix ϱ is a maximum in a representation in which ϱ is diagonal. Let S_{A+B}' denote the entropy which the united system would have in a state Q whose statistical matrix ϱ_{A+B}' is derived from ϱ_{A+B} by discarding all off-diagonal elements in a representation which diagonalizes ϱ_A and ϱ_B. Then

$$S_{A+B}' = -k\sum_m\sum_n \rho_{A+B}(nm, nm) \times \ln \rho_{A+B}(nm, nm) \geqq S_{A+B}. \tag{15}$$

Let S_{A+B}'' in turn denote the entropy of the united system $A+B$ in a second hypothetical state, say R, whose statistical matrix ρ_{A+B}'' is given by

$$\rho_{A+B}''(nm, n'm') = \rho_A(n, n')\rho_B(m, m') = \rho_A(n, n)\rho_B(m, m)\delta_{n, n'}\delta_{m, m'}. \tag{16}$$

The state R conforms to the special hypothesis of Eq. (12), so that

$$S_{A+B}'' = S_A + S_B. \tag{17}$$

In order to prove that S_{A+B}'' is not less than S_{A+B}' let us seek the maximum entropy of $A+B$ for all forms of ϱ_{A+B} which are diagonal in n and m and satisfy the conditions

$$\begin{aligned} \sum_m \rho_{A+B}(nm, nm) &= \rho_A(n, n), \\ \sum_n \rho_{A+B}(nm, nm) &= \rho_B(m, m), \end{aligned} \tag{18}$$

where the right-hand members are fixed for all values of n and m. Let $u(nm)$ denote the typical diagonal element of the matrix $\mathbf{u}$ which gives the desired maximum. Let $d\rho(nm)$ denote the increment $\rho_{A+B}(nm, nm) - u(nm)$. Introducing a double series of Lagrangian multipliers λ_n, γ_m for the double series of conditions (18) as well as a multiplier α for the condition Spur $\rho_{A+B}=1$, we locate the desired maximum by the equation

$$\sum_m\sum_n [\ln u(nm) + 1 - \alpha - \lambda_n - \gamma_m] d\rho(nm) = 0.$$

The coefficient of each $d\rho(nm)$ must vanish for proper choices of α, λ_n, and γ_m, so that $\mathbf{u}$ must have the form

$$u(nm, n'm') = u(nm)\delta_{n, n'}\delta_{m, m'} = \exp(\alpha + \lambda_n + \gamma_m - 1)\delta_{n, n'}\delta_{m, m'}.$$

With the aid of Eqs. (18) one can readily evaluate

[15] J. v. Neumann, *Math. Grundlagen d. Quantummechanik* (Berlin, 1932) (referred to hereafter as *M. G. Q.*) p. 226.

[16] O. Klein, Zeits. f. Physik **72**, 767 (1931); J. v. Neumann, *M. G. Q.*, p. 202; W. M. Elsasser, Phys. Rev. **52**, 991 (1937).

λ_n, γ_m and show that

$$u(nm)=\rho_A(n,n)\rho_B(m,m). \tag{19}$$

The expansion of S_{A+B} about the "point" defined by (19) begins with the terms

$$S_{A+B}=-k\{\sum_n\sum_m u(nm)\ \ln\ u(nm) + u(nm)^{-1}[d\rho(nm)]^2+\cdots\}.$$

Since the diagonal elements $u(nm)$ are essentially positive, the second-order terms show that (19) must give a maximum. In the absence of any other stationary point we conclude that $\varrho_{A+B}=\mathbf{u}=\varrho_{A+B}''$ must give an absolute maximum entropy subject to the conditions (18). Thus the entropy of the state R is not less than S_{A+B}'. The inequality (15) and Eq. (17) now yield the desired inequality

$$S_{A+B}\leqq S_A+S_B. \tag{20}$$

The equality sign applies only if (*a*) ϱ_{A+B} is diagonal in the same matrix scheme as ϱ_A and ϱ_B, and if (*b*) the diagonal elements of ϱ_{A+B} are identical with those of ϱ_{A+B}''. Both of these conditions are contained in the single equation (12), which is therefore a *necessary* as well as a sufficient condition for the relation

$$S_{A+B}=S_A+S_B \tag{21}$$

to subsist.

Equation (12) also forms a necessary and sufficient condition for the *independence* of the states of A and B. Here the statement that the states are independent is intended to signify that ϱ_{A+B} contains no information such that a measurement of some property of A can affect our expectation of the result of a subsequent measurement of a property of B.

For brevity we confine ourselves here to the proof of the necessity of the condition. Let us suppose to begin with that A and B are known to be in pure states with the respective wave functions ψ_A and ψ_B. Such states are necessarily independent in the above sense. As v. Neumann[17] has shown, it follows that the united system is also in a pure state with the wave function $\psi_A(x_A)\psi_B(x_B)$. Let us next suppose that A is in a mixed state with the probability w_{As} of the wave function $\psi_{As}=\sum_n c_{ns}\varphi_n(x_A)$ while B is in an independent mixed state with the probability w_{Bt} of the wave function $\psi_{Bt}=\sum_m d_{mt}\chi_m(x_B)$. The condition of independence demands that the united system have the probability $W_{st}=w_{As}w_{Bt}$ of the wave function $\Psi_{st}=\sum_n\sum_m c_{ns}d_{mt}\Phi_{mn}$. Consequently [cf. Eq. (1) of (I)]

$$\rho_{A+B}(nm,\ n'm')=\sum_s\sum_t w_{As}w_{Bt}c_{ns}d_{mt}(c_{n's})^*(d_{m't})^* =\rho_A(n,n')\rho_B(m,m')$$

as was to be proved.[18]

The ordinary time-dependent Schrödinger wave equation is applicable to systems which are either isolated or subject to external influence only through the variation of classical parameters which enter into its Hamiltonian function. We shall speak of such systems as *insulated* since they can receive energy only as reversible work. The effect of the passage of time on the statistical matrix of an insulated system is to produce a canonical transformation

$$\varrho(t+\Delta t)=e^{-iH\Delta t/\hbar}\varrho(t)e^{iH\Delta t/\hbar}, \tag{22a}$$

$$i\hbar\frac{d\varrho}{dt}=\mathbf{H}\varrho-\varrho\mathbf{H}, \tag{22b}$$

with respect to which Spur $\varrho\ln\varrho$ is invariant. Thus the microscopic entropy of an insulated system is constant in time. The apparent conflict between this theorem and the thermodynamic principle of the increase of entropy has been the fundamental difficulty with the microscopic definition of entropy. If a system is composed of two parts, say A and B, which do not interact, the theorem is readily seen to apply to each part. However, if the two parts interact due to a mutual energy term in the Hamiltonian of the united system, it is no longer possible to apply Eqs. (22a) and (22b) to the separate parts. Hence we cannot expect S_A+S_B to be constant in time.

It is not easy to trace the changes of S_A+S_B in time under these circumstances, for ϱ does not remain diagonal in a fixed coordinate system. In

[17] J. v. Neumann, reference 15, p. 228.

[18] If the states of A and B are independent a corresponding ensemble of united systems would be obtained by arbitrary pair formation from independent ensembles of the A species and the B species. If the states of A and B are dependent the corresponding ensemble of united systems is based on a specific pairing of the A and B systems which it contains. It *suffices* to insure the independence of the two states that the experiments from which our information about A is built up are entirely independent of the experiments which have given us our information about B.

the special case that A and B are initially in independent states, however, so that $S_A(t_0)+S_B(t_0)=S_{A+B}(t_0)$, it follows from the relation (20) that S_A+S_B can never decrease below its initial value. It must then increase at least temporarily, or remain constant. Let us examine the consequences of the assumption that it remains constant. The first of these is that Eq. (12) must hold for a range of values of t. Hence

$$\frac{d}{dt}\rho_{A+B}(nm, n'm') = \rho_B(m, m')\frac{d}{dt}\rho_A(n, n') + \rho_A(n, n')\frac{d}{dt}\rho_B(m, m'). \quad (23)$$

By Eq. (22b)

$$i\hbar\frac{d}{dt}\rho_{A+B}(nm, n'm') = \sum_{\nu,\mu}[H(nm, \nu\mu)\rho_{A+B}(\nu\mu, n'm') - \rho_{A+B}(nm, \nu\mu)H(\nu\mu, n'm')]. \quad (24)$$

But

$$i\hbar\frac{d}{dt}\rho_A(n, n') = \sum_m i\hbar\frac{d}{dt}\rho_{A+B}(mm, n'm) = \sum_{m,\nu,\mu}[H(nm, \nu\mu)\rho_{A+B}(\nu\mu, n'm) - \rho_{A+B}(nm, \nu\mu)H(\nu\mu, n'm)], \quad (25)$$

$$i\hbar\frac{d}{dt}\rho_B(m, m') = \sum_{n,\nu,\mu}[H(nm, \nu\mu)\rho_{A+B}(\nu\mu, nm') - \rho_{A+B}(nm, \nu\mu)H(\nu\mu, nm')]. \quad (26)$$

Eliminating the time derivatives from Eqs. (23), (24), (25) and (26), we obtain

$$\begin{aligned}&\sum_{\nu,\mu}[H(nm, \nu\mu)\rho_{A+B}(\nu\mu, n'm') - \rho_{A+B}(nm, \nu\mu)H(\nu\mu, n'm')]\\ &= \rho_B(m, m')\sum_{r,\nu,\mu}[H(nr, \nu\mu)\rho_{A+B}(\nu\mu, n'r) - \rho_{A+B}(nr, \nu\mu)H(\nu\mu, n'r)]\\ &\quad + \rho_A(n, n')\sum_{s,\nu,\mu}[H(sm, \nu\mu)\rho_{A+B}(\nu\mu, sm') - \rho_{A+B}(sm, \nu\mu)H(\nu\mu, sm')]. \quad (27)\end{aligned}$$

Let us next eliminate the elements of ϱ_{A+B} from Eq. (27) by means of Eq. (12) and give ϱ_A and ϱ_B diagonal form. (*Some* choice of the two systems of basic coordinate functions $\varphi_n, \cdots$ and $\chi_m, \cdots$ will always make these matrices diagonal at the moment under consideration.) In this way we derive

$$\begin{aligned}&H(nm, n'm')[\rho_A(n', n')\rho_B(m', m') - \rho_A(n, n)\rho_B(m, m)]\\ &= \rho_B(m, m)\delta_{m,m'}[\rho_A(n', n') - \rho_A(n, n)]\times\sum_r H(nr, n'r)\rho_B(r, r)\\ &\quad + \rho_A(n, n)\delta_{n,n'}[\rho_B(m', m') - \rho_B(m, m)]\times\sum_s H(sm, sm')\rho_A(s, s). \quad (28)\end{aligned}$$

This equation shows that if our initial hypothesis that S_A+S_B is constant in time obtains for all choices of $\varrho_A(t_0)$ and $\varrho_B(t_0)$ it is *necessary* as well as sufficient that the Hamiltonian matrix $\mathbf{H}$ of the united system shall be resolvable into the sum of two parts, one diagonal in m and the other diagonal in n. This is exactly the form of $\mathbf{H}$ characteristic of the absence of physical interaction between A and B. To be sure Eq. (28) shows that other forms of $\mathbf{H}$ are compatible with Eq. (23) if the matrices ϱ_A, ϱ_B satisfy relations of the form

$$\rho_A(n', n')\rho_B(m', m') = \rho_A(n, n)\rho_B(m, m). \quad (29)$$

It is improbable, however, that such relations can hold throughout an interval of time when there is an interaction term in $\mathbf{H}$. In any case the necessary correlation of ϱ_A, ϱ_B, and $\mathbf{H}$ would be such an unusual occurrence that we can safely dismiss it as of no practical importance.

We are thus led to the following double conclusion. If the initial states of the two systems A and B at t_0 are independent, whether they interact or not, for positive values of Δt,

$$S_A(t_0+\Delta t)+S_B(t_0+\Delta t) \geqq S_A(t_0)+S_B(t_0). \quad (30)$$

If they interact,

$$S_A(t_0+\Delta t)+S_B(t_0+\Delta t) > S_A(t_0)+S_B(t_0) \quad (31)$$

in practically every case.

These rules take the place of the classical principle of the increase of entropy due to irreversible processes occurring within a single isolated system.[19] The increase in S_A+S_B is not

[19] Cf. section on "The Principle of Entropy Increase" in (I).

monatonic in time for an indefinite period, however, for both S_A and S_B depend on a superposition of oscillatory terms. After the initial phase relationships are lost the entropies may be expected to oscillate irregularly about long time average values.

Since these conclusions may be disagreeable to readers thoroughly imbued with the thermodynamic notion that the entropy of any complete system must equal the sum of the entropies of its parts, we pause to consider the significance and credibility of the fundamental inequality

$$S_{A+B} < S_A + S_B,$$
$$\text{if} \qquad \rho_{A+B}(nm, n'm') \neq \rho_A(n, n')\rho_B(m, m'). \quad (32)$$

First of all it should be remembered that the equality (21) applies instead of (32) whenever the systems A and B have no interaction and when we have no information correlating probabilities for one system with probabilities for the other. It also applies to a high degree of approximation if the united system $A+B$ is a member of a Gibbs canonical ensemble (canonical state) and if the mutual energy of A and B can be neglected in comparison with the individual energies, as in ordinary thermal contact. This is a consequence of the fact that $e^{-(E_{An}+E_{Bm})/kT} = e^{-E_{An}/kT} e^{-E_{Bm}/kT}$. But the canonical state is the state of thermal equilibrium and in classical thermodynamics it is customary to regard the energy of any sample of matter as the sum of the energies of its parts. Moreover, in thermodynamics the entropy is defined only for systems in thermal equilibrium, or capable of being brought into thermal equilibrium by the introduction of suitable constraints. Thus it becomes apparent that the principle of the additivity of entropy in thermodynamics is ordinarily confined to cases in which Eq. (21) is valid. So far as I know the only exception to this rule is in the attempt to refer the onset of thermal equilibrium for isolated systems to the principle of the increase of entropy, where one imagines a system with non-uniform temperature divided into small volume elements, neglects the departure from thermal equilibrium inside each element, and identifies the entropy of the complete system with the sum of the entropies of the elements. The validity of this procedure is open to question even from the classical standpoint and the device is eliminated in the modified thermodynamics of (I). We conclude that the relation (32) does *not* bar an identification of S_{mic} with the entropy of suitably formulated phenomenological thermodynamics. In fact this relation affords the basis for the statistical derivation of the second law at the end of (I).

Additional light on (21) and (32) is thrown by a further consideration of the quasi-subjective character of ϱ and $S(\varrho)$ remarked in (I). The wave function ψ and the statistical matrix ϱ are the ingredients of recipes for the prediction of the results of statistical measurements made upon appropriate Gibbsian ensembles of identical systems. Due to the discontinuous changes in ψ and ϱ which accompany all measurements and changes in information these mathematical quantities cannot be regarded as descriptions of objective reality, but must be interpreted as descriptions of information.[20]

One should note, however, that in most cases ϱ embodies hypothetical, or potential information rather than actual information. One of the purposes of the present paper is to show that if we carry an ensemble of systems through the operation β for creating thermodynamic equilibrium we fix—to all intents and purposes—a state with a unique ϱ whose general characteristics are known. Ordinarily, on the other hand, we do not know enough about the state of a system to fix a definite corresponding ψ or ϱ. The relation between our actual information and the hypothetical information required to specify a ψ or ϱ is similar to the relation between actual information and the maximum conceivable information contained in the classical specification of phase in the statistical mechanics of Gibbs.

The application of the subjective point of view to microscopic entropy leads to the interpretation of $S_{\text{mic}}(\varrho)$ as a measure of the information discarded in creating a mixed state ensemble with matrix ϱ from its pure state components. It can also be regarded as an inverse measure of the information regarding the behavior of an arbi-

[20] Some physicists, in spite of the Einstein, Podolsky, and Rosen controversy, still object to this essentially subjective interpretation [Cf. e.g., H. P. Robertson, J. App. Phys. **9**, 190 (1938)]. I have no desire to thrust a world-philosophy on the reader, but offer this interpretation of ψ and ϱ as the only one which seems to square with practice. If anyone can discover a definite additional scientific meaning for ψ and ϱ, I have no objection, but hope they will bring it forward soon.

trary individual system in the ensemble which becomes available from complete information regarding the statistical behavior of the ensemble as a whole.

From this point of view Eq. (21) is reasonable because the mental act of uniting a system A with an independent system B neither adds nor subtracts from our information regarding either system. In the general case, however, ϱ_{A+B} contains information regarding the correlation of measurements of A with simultaneous measurements of B. This information is not contained in the pair of matrices ϱ_A, ϱ_B. Hence the sum of the entropies of A and B is greater than the entropy of $A+B$. The contrast between the behavior of S_{A+B} and S_A+S_B when two independent systems are placed in thermal contact and insulated is due to the substitution of correlational information for information that in the beginning had to do only with one system or the other.

An "Operational Derivation" of the Canonical Ensemble

We are now ready to attack the fundamental problem of our theory, *viz.*, the verification of the statement—used up to this point as a postulate—that a Gibbsian ensemble of identical systems subjected to the physical operation β described in (I) will be converted into a canonical ensemble with temperature T. Actually we must content ourselves with setting up an arbitrary but neutral scheme of probabilities based on group integration from which it appears that the probability of an appreciable deviation from the canonical state in an ensemble of systems subjected to the operation β can be made as small as desired by increasing the heat capacity of the thermostat B relative to that of the system A and by making the period of interaction very long. Since the quantum mechanics itself is an induction based on a finite number of observations—and hence, strictly speaking, a plausible hypothesis rather than a certainty—our failure to devise an airtight compulsive proof need not be disturbing.

The process β involves the interaction of an ensemble of systems A with a corresponding ensemble of thermostats B for a long time. Let H_A, H_B, and H denote the respective Hamiltonian operators for the separate systems A, B and the united interacting system $A+B$. Here $H=H_A+H_B+H'$, where H' is a small mutual energy term. Let φ_n, χ_m, ψ_κ denote typical eigenfunctions of H_A, H_B, and H, respectively. Let E_{An}, E_{Bm}, W_κ be the corresponding eigenvalues. The matrix $\mathbf{U}$ which performs the transformation from the $\varphi_n\chi_m$ scheme to the ψ_κ scheme is defined by

$$\psi_\kappa=\sum_n\sum_m\varphi_n\chi_m U(nm,\kappa). \tag{33}$$

$\mathbf{U}$ will transform the statistical matrix ϱ_{A+B} in a scheme based on the $\varphi_n\chi_m$ functions into the corresponding matrix ω_{A+B} in a scheme based on the ψ_κ functions, and vice versa, according to the familiar rules

$$\omega_{A+B}(\kappa,\kappa')=\sum_n\sum_m\sum_{n'}\sum_{m'}U^{-1}(\kappa,nm)\times\rho_{A+B}(nm,n'm')U(n'm',\kappa'), \tag{34}$$

$$\rho_{A+B}(nm,n'm')=\sum_\kappa\sum_{\kappa'}U(nm,\kappa)\times\omega_{A+B}(\kappa,\kappa')U^{-1}(\kappa',n'm'). \tag{35}$$

Although the hypothesis is unessential we may assume that initially ϱ_{A+B} has the direct product form of Eq. (12) and corresponding to independent initial states for A and B. The matrix elements $\omega_{A+B}(\kappa,\kappa')$ connecting different exact energy levels W_κ, $W_{\kappa'}$ contain the time factors $\exp[2\pi i(W_{\kappa'}-W_\kappa)t/h]$. Since the system B is macroscopic and (as we shall suppose) confined to a container, we may assume that the Hamiltonian H is free from all exact symmetry except that due to the permutation of like particles.[21] This means that so long as we include in the systems of wave functions φ_n, χ_m, ψ_κ only those with allowed types of permutation symmetry we can neglect degeneracy in H and assume that none of the off-diagonal elements of ω_{A+B} are constant. Let $f_{\kappa'\kappa}$ denote the quantity $2\pi(W_{\kappa'}-W_\kappa)/h$. Then

$$\rho_A(n,n')=\sum_n\rho_{A+B}(nm,n'm)$$
$$=\sum U(nm,\kappa)U^{-1}(\kappa,\nu\mu)\rho_A{}^0(\nu,\nu')\rho_B{}^0(\mu,\mu')\times U(\nu'\mu',\kappa')e^{if_{\kappa'\kappa}t}U^{-1}(\kappa',n'm). \tag{35}$$

[21] Throughout this discussion we follow the apparently universal custom of disregarding permutations of like particles some of which belong to A and some to B. In other words we disregard our inability to distinguish between elementary particles which belong to A and others which belong to B. To take this distinction into account would involve difficulties which are believed to be purely formal.

Here the summation is to be extended over all values of all indices except n and n'.

The theory hinges on the character of the matrix $\mathbf{U}$ which, in turn, depends on the operators H and H'. These operators will, of course, change radically as we pass from one physical problem to another. Since the definition of these operators is based on the assumption that the systems A and B are isolated from the rest of the universe it is evident that H and H' are subject to variation with the way in which we idealize the given physical systems in order to satisfy the isolation postulate. Moreover, there is a strong idealization of the experimental situation in supposing that we can ever secure an ensemble of macroscopic systems $A+B$ with identical Hamiltonian functions. We can be confident, however, that if the desired theorems hold for practically all such ideal ensembles they will hold also for such approximations to the ideal as we are actually able to construct.

In any case our information regarding $\mathbf{U}$ is meager and wholly insufficient to fix its form. For this reason we can make no progress without employing a calculus of probabilities similar to that used by v. Neumann. The procedure is to average over all possible forms of $\mathbf{U}$ consistent with our *a priori* (experimental) information, with a type of average which favors no particular form of matrix. Having determined a $\mathbf{U}$-average for ϱ_A in this way, we shall examine the probable departures from the average by estimating the average squares of the deviations of the matrix elements from their means. These anomalies turn out to be extremely small so that we can use $[\rho_A(n, n')]_{U-\text{av}}$ in place of $\rho_A(n, n')$ for practical purposes. The reader will find a partial justification of this somewhat arbitrary procedure at the end of the section on thermodynamic equilibrium in the preceding paper (I).

The only information available regarding $\mathbf{U}$ beyond the fact of its unitary character comes from what we know or can infer about the magnitude of the interaction energy H'. Our first task is to give mathematical form to our rather vague information about H'. Usually H' comes out of the interface energy of the systems A and B at their surface of contact. Although surface tension phenomena often give a means of measuring the interface energy, it is so small that it is customary to neglect it entirely in most thermodynamic theory.[22] On the other hand, H' is the instrument with which B stirs A. A large interaction energy means a good thermal contact and effective stirring. Hence it behooves us not to place an excessively low estimate on the possible measured values of H'.

Now $|U(nm, \kappa)|^2$ is the probability that a system $A+B$ initially in the pure state ψ_κ will go over into the state $\varphi_n\chi_m$ when the appropriate measurement is made. If this probability is not zero, the discrepancy between the initial exact energy W_κ and the final measured approximate energy, $E_{nm}=E_{An}+E_{Bm}$, is to be accounted for by H'. Thus the average value of H' for the state ψ_κ, say ϵ_κ, determines the value of $W_\kappa-E_{nm}$ at which the Fourier coefficients $U(nm, \kappa)$ tend to have their maximum absolute values, while the root mean square of $H'-\epsilon_\kappa$ controls the range of values of $W_\kappa-E_{nm}$ for which the quantities $|U(nm, \kappa)|^2$ are not negligibly small.

At this point we postulate that the systems A and B which make up our initial ensemble conform to the restrictions inherent in the definition of the process β given in (I). More specifically we make the following detailed assumptions. (a_1) The system B is a truly macroscopic one with energy levels whose average spacing is much smaller than any other energy interval we shall want to consider. (a_2) Each system B has been subjected to prolonged thermometric study by means of a thermometer which can be considered to form part of the system. This study has shown the system to be in a state of macroscopic thermal equilibrium with a temperature τ on the extrapolated gas scale. This temperature measurement will be treated as a form of approximate energy measurement.[23] It will fix the average energy of the systems B in the ensemble, say $\bar{E}_B$. The corresponding energy uncertainty ΔE_B, will

[22] It is one of the tacit postulates of thermodynamic theory that the manipulation used in making thermal contact between a thermodynamic system and a heat bath shall be such as to produce a negligible increase in the total energy.

[23] A gas thermometer registers a short time average of the kinetic energy of translation of the gas. By keeping the thermometer under observation for a long time we fix the long time average kinetic energy of translation, which is a monatonic function of the energy of the complete system B. When the heat capacity of B is large the perturbation of its energy due to the temperature reading itself can be neglected.

be approximately equal to the product of the heat capacity, C_B, and the probable error of the temperature measurement, $\Delta\tau$. (a_3) The energy of each system A in the ensemble is assumed to be sufficiently well known and sufficiently small so that we can neglect it in comparison with that of the companion system B. This means that we postulate our right to identify $\bar{E}_B$ and ΔE_B, respectively, with the corresponding quantities $\bar{W}$ and ΔW for the ensemble of united systems. (a_4) Finally we suppose that if ψ_κ has an energy, W_κ, which is a reasonable energy in view of the information regarding $\bar{W}$ and ΔW, the expectation value of H' and the standard deviation of H' from its expectation value, calculated for ψ_κ, are both small compared with the uncertainty in the total energy, but very large compared with the spacing of the energy levels of $A+B$ near $\bar{W}$.

Let us now express ϵ_κ, i.e., the expectation value of H' for ψ_κ, and the corresponding standard deviation, say D_κ, in terms of W_κ, the energies E_{nm}, and the elements of $\mathbf{U}$. Elementary manipulation yields $\epsilon_\kappa \equiv (H'\psi_\kappa, \psi_\kappa) = (H\psi_\kappa - H_0\psi_\kappa, \psi_\kappa) = W_\kappa - (H_0\psi_\kappa, \psi_\kappa)$, where H_0 denotes H_A+H_B. Hence

$$\sum_n \sum_m E_{nm} |U(nm, \kappa)|^2 = W_\kappa - \epsilon_\kappa = \bar{H}_0. \quad (36)$$

Similarly

$$D_\kappa^2 \equiv ([H'-\epsilon_\kappa]^2\psi_\kappa, \psi_\kappa) = ([W_\kappa - \epsilon_\kappa - H_0]^2\psi_\kappa, \psi_\kappa)$$
$$= \sum_n \sum_m (W_\kappa - \epsilon_\kappa - E_{nm})^2 |U(nm, \kappa)|^2. \quad (37)$$

The assumptions (a_4) can now be given definite mathematical form by specifying definite upper and lower bounds for ϵ_κ and D_κ^2. Thus we write

$$\bar{\epsilon} - \epsilon' < W_\kappa - \sum_n \sum_m E_{nm} |U(nm, \kappa|^2 < \bar{\epsilon} + \epsilon', \quad \kappa = 0, 1, 2, 3, \cdots \quad (38)$$

$$\bar{D} - D' < \sum_n \sum_m (W_\kappa - \epsilon_\kappa - E_{nm})^2 \times |U(nm, \kappa)|^2 < \bar{D} + D', \quad \kappa = 0, 1, 2, 3, \cdots \quad (39)$$

The inequalities (38) and (39) create restrictions imposed on $\mathbf{U}$. In addition there are the familiar relations which express its unitary character, *viz.*,

$$\sum_n \sum_m |U(nm, \kappa)|^2 = 1, \quad \kappa = 0, 1, 2, \cdots \quad (40)$$

$$\sum_\kappa |U(nm, \kappa)|^2 = 1, \quad n, m = 0, 1, 2, \cdots \quad (41)$$

$$\sum_n \sum_m U(nm, \kappa) U(nm, \kappa')^* = 0, \quad \kappa \neq \kappa' = 0, 1, 2, \cdots \quad (42)$$

$$\sum_\kappa U(nm, \kappa) U(n'm', \kappa)^* = 0. \quad (n, m) \neq (n', m') = 0, 1, 2, \cdots \quad (43)$$

The problem is now to evaluate the mean value of $\rho_A(n, n')$ for large values of t by averaging the right-hand member of Eq. (35) over all forms of the matrix $\mathbf{U}$ consistent with the restrictions (38) to (43). In making such an average we must introduce a set of independent parameters which fix the form of $\mathbf{U}$ and assign *a priori* probabilities to different ranges of these parameters. We should like to do this so as to favor no one form of $\mathbf{U}$ over another. The method of group integration[24] used by von Neumann[5] affords an apparently unique means to this end.

To avoid setting up an element of volume in a parameter space of infinitely many dimensions we introduce a succession of approximations in each of which the matrices $\mathbf{U}$ are limited to a finite number of rows and columns, σ, besides being subjected to the inequalities (38) and (39).[25] Volume can be defined in the parameter space of the $\sigma \times \sigma$ element unitary matrices so that volumes are invariant to transformations induced in the parameter space by members of the group. Volume integration over this parameter space then gives a method of averaging functions of the elements of the matrix $\mathbf{U}$ which has the required neutral character. Volume integrals can be identified with probabilities when the volume element is properly normalized. If the averages of the functions we are interested in, due to volume integration over the part of parameter space which lies within the limits imposed by Eqs. (38) and (39), approach satisfactory limits as σ becomes infinite, we can identify the limits with the desired averages over the group of infinite matrices $\mathbf{U}$.

It is neither necessary nor feasible to carry this procedure through in rigorous detail. In fact some preliminary computations which need not be

[24] Cf. F. D. Murnaghan, *The Theory of Group Representations* (Baltimore, 1938), Chapter VIII.

[25] The allowed rows and columns may be chosen to include all energy levels W_κ, E_{nm}, for which $|W_\kappa - \bar{W}|$ and $|E_{nm} + \bar{\epsilon} - \bar{W}|$ are less than appropriate upper bounds. A slight modification of (39) is necessary for levels W_κ which are very close to the limits.

reproduced here suggest that the condition (39) does not restrict the values of $|U(nm, \kappa)|^2$ for large values of $(W_\kappa - \epsilon_\kappa - E_{nm})^2$ strongly enough to insure the success of the limiting process. Hence it is likely that we ought to replace the obvious and simple condition (39) by a more powerful one, such as the postulate that

$$\exp\left[\left(\frac{H'-\epsilon_\kappa}{\Delta W}\right)^2\right]-1 = \left(\frac{H'-\epsilon_\kappa}{\Delta W}\right)^2+\frac{1}{2}\left(\frac{H'-\epsilon_\kappa}{\Delta W}\right)^4+\cdots$$

is to have a small expectation value. This postulate leads to the double inequality

$$P-p<\sum_n\sum_m\left\{\exp\left[\left(\frac{W_\kappa-\epsilon_\kappa-E_{nm}}{\Delta W}\right)^2\right]-1\right\} \times|U(nm, \kappa)|^2<P+p, \quad \kappa=0, 1, 2, \cdots \quad (44)$$

where P and p are positive constants small in comparison with unity. It is convenient to choose p small in comparison with P. The condition (44) acts like (39), but restricts the higher moments of $(H'-\epsilon_\kappa)$, as well as the standard deviation, D_κ. It is in as good accord with our *a priori* information about H' as the condition (39).

Giving ϵ' in Eq. (38) a value small in comparison with $\bar{\epsilon}$ we can replace ϵ_κ in Eq. (44) by $\bar{\epsilon}$ with very slight error. Let $\zeta(nm, \kappa)$ denote the energy difference $E_{nm}+\bar{\epsilon}-W_\kappa$. Let $g_\sigma(nm, \kappa)$ denote the group average value of $|U(nm, \kappa)|^2$ for a finite value of σ large enough to include a nonvanishing element $U(nm, \kappa)$. Then

$$P-p<\sum_n\sum_m\left\{\exp\left[\left(\frac{\zeta(nm, \kappa)}{\Delta W}\right)^2\right]-1\right\} \times g_\sigma(nm, \kappa)<P+p, \quad \kappa=0, 1, 2, \cdots. \quad (45)$$

It follows that g_σ must approach zero rapidly as $\zeta(nm, \kappa)$ becomes large. The set of values of $g_\sigma(nm, \kappa)$ for fixed values of κ and σ form a distribution of unity over the energy levels E_{nm} in the neighborhood of $E_{nm}=W\kappa-\bar{\epsilon}$ which is confined by (45) to a narrow range independent of the value assigned to σ. There seems no reason to doubt that as σ becomes infinite the averages $g_\sigma(nm, \kappa)$ will approach limiting values $G(nm, \kappa)$ which conform to the conditions

$$P-p<\sum_n\sum_m\left\{\exp\left[\left(\frac{\zeta(nm, \kappa)}{\Delta W}\right)^2\right]-1\right\} \times G(nm, \kappa)<P+p, \quad \kappa=0, 1, 2, \cdots \quad (46)$$

$$-\epsilon'<\sum_n\sum_m\zeta(nm, \kappa)G(nm, \kappa)<\epsilon', \quad \kappa=0, 1, 2, \cdots \quad (47)$$

$$\sum_n\sum_m G(nm, \kappa)=1, \quad \kappa=0, 1, 2, \cdots \quad (48)$$

$$\sum_\kappa G(nm, \kappa)=1. \quad n, m=0, 1, 2, \cdots \quad (49)$$

We accordingly adopt the condition (44) in place of (39), giving to P and p small values which turn out not to be crucial.

The quantity $G(nm, \kappa)$ plays a very important part in our theory. It represents the group-integration average of $|U(nm, \kappa)|^2$. It is a function of E_{nm} and W_κ defined thus far only for discrete values of the arguments. We assume that the discrete points can be fitted by interpolation to a smooth continuous function $\bar{G}(\zeta+W-\bar{\epsilon}, W)=G(\zeta, W)$. We also assume that if W is held fast the resulting function of ζ has a single maximum near $\zeta=0$ and fades exponentially [cf. (46)] to zero as $|\zeta|$ increases. Its general form must resemble that of an error curve.

However we define the breadth of the peak formed by the curve $G(\zeta, W)$ for constant W, it will be of the order of magnitude $P^1\Delta W$. This is the standard deviation of ζ obtained from (46) and (48) by neglecting p in comparison with P and discarding higher order terms in the expansion of the exponential function. By postulate (a_4) it is large compared with the average spacing of the energy levels W_κ, or E_{nm}, near $\bar{W}$. Hence we can introduce a function $u(E_{nm})=u(\zeta+W-\bar{\epsilon})$ to represent the density of the energy levels in the neighborhood of $E=E_{nm}$ and replace the sums in (46), (47), (48) by integrals. Thus

$$P-p<\int\{\exp[(\zeta/\Delta W)^2]-1\}G(\zeta, W) \times u(\zeta+W-\bar{\epsilon})d\zeta<P+p, \quad (49)$$

$$-\epsilon'<\int\zeta G(\zeta, W)u(\zeta+W-\bar{\epsilon})d\zeta<\epsilon', \quad (50)$$

$$\int G(\zeta, W)u(\zeta+W-\bar{\epsilon})d\zeta=1. \quad (51)$$

Although u increases rapidly with ζ we can treat it as a constant over the narrow range of values of ζ required for effective convergence of the above integrals. Making this approximation and the special assumption that $G(\zeta, W)$ has the form $Ae^{-(\zeta/a)^2}$, it is easy to verify that the "half-breadth" a is $P^{\frac{1}{2}}\Delta W(2+P)^{\frac{1}{2}}/(1+P)$ in satisfactory agreement with our previous estimate of the order of magnitude of the breadth of the peak.

We can now return to the fundamental Eq. (35). Our first task is to show that group integration over the entire group of $\sigma\times\sigma$ element unitary matrices (referred to hereafter as the σ-group), or over the portion of that group which satisfies (38) and (44), eliminates most of the terms of the right-hand member of Eq. (35).

Every matrix $\mathbf{U}$ of the σ-group can be written in the form $\mathbf{U}=\mathbf{FA}$, where $\mathbf{F}$ is a diagonal unitary matrix and the diagonal elements of $\mathbf{A}$ are real and positive.[24] The matrix $\mathbf{F}=\|e^{i\varphi_p}\delta_{p,q}\|$ is specified by the phase angles φ_p of its diagonal elements. (For our present purpose it is convenient to revert to a single indexing notation for the matrix elements.) The matrix $\mathbf{A}$ can be specified by $\sigma^2-\sigma$ parameters $\alpha_1, \alpha_2, \cdots$. The φ's and α's together constitute a complete set of independent parameters for the matrices $\mathbf{U}$. The volume element in the parameter space of the σ-group has the general form $V(\varphi_1, \varphi_2, \cdots \alpha_1, \alpha_2, \cdots)d(\varphi)d(\alpha)$.

Consider the transformation

$$\mathbf{U}\rightarrow\mathbf{U}'=\mathbf{QU}=\mathbf{QFA},$$

where $\mathbf{Q}$ is a diagonal unitary matrix $\|e^{i\theta_p}\delta_{p,q}\|$. $\mathbf{U}'$ can be written in the standard form $\mathbf{F}'\mathbf{A}$ if we define $\mathbf{F}'$ as the diagonal unitary matrix $\|e^{i(\varphi_p+\theta_p)}\delta_{p,q}\|$. Thus the above matrix transformation induces the transformation

$$\varphi_p\rightarrow\varphi_p'=\varphi_p+\theta_p,\quad \alpha_s\rightarrow\alpha_s'=\alpha_s,\quad p, s=0, 1, 2, \cdots$$

in parameter space. Since the volume element is invariant of every such transformation[24] $V(\varphi, \alpha)$ must actually be independent of the parameters $\varphi_1, \varphi_2, \cdots$. This means that equal ranges of the φ's are "equally probable."

The restrictions (38) and (44) cut down the allowed ranges of the α's, but not those of the φ's. Hence the formation of the group average of the right-hand member of Eq. (35) involves integration over all values of the φ's from 0 to 2π. The result for one term is proportional to

$$\int U(nm,\kappa)U^{-1}(\kappa,\nu\mu)U(\nu'\mu',\kappa')U^{-1}(\kappa',n'm)d(\varphi)$$

$$=A(nm,\kappa)A^{-1}(\kappa,\nu\mu)A(\nu'\mu',\kappa')A^{-1}(\kappa',n'm)$$

$$\times\int\exp\left[i(\varphi_{nm}+\varphi_{\nu'\mu'}-\varphi_{\nu\mu}-\varphi_{n'm})\right]d(\varphi)$$

$$=(2\pi)^{-1}\left[\delta_{\nu',\nu}\delta_{\mu',\mu}\delta_{n',n}+\delta_{\nu',n'}\delta_{\mu',m}\delta_{\nu,n}\delta_{\mu,m}\right]$$

$$\times A(nm,\kappa)A^{-1}(\kappa,\nu\mu)A(\nu'\mu',\kappa')A^{-1}(\kappa',n'm).$$

Let us indicate the limiting group average for infinite σ by $[\ ]_U$. It follows from the above and Eq. (35) that

$$[\rho_A(n,n')]_U=[1-\delta_{n,n'}]\rho_A{}^0(n,n')\textstyle\sum_m\rho_B{}^0(m,m)$$
$$\times\textstyle\sum_{\kappa,\kappa'}[\,|U(nm,\kappa)|^2\,|U(n'm,\kappa')|^2]_U e^{if_{\kappa'\kappa}t}$$
$$+\delta_{n,n'}\textstyle\sum_{\nu,\mu}\rho_A{}^0(\nu,\nu)\rho_B{}^0(\mu,\mu)$$
$$\times\textstyle\sum_{m,\kappa,\kappa'}[U(nm,\kappa)U^{-1}(\kappa,\nu\mu)U(\nu\mu,\kappa')$$
$$\times U^{-1}(\kappa',nm)]_U e^{if_{\kappa'\kappa}t}. \quad (52)$$

As t increases the initial phase relationships between the terms of the above equation will be lost and interference between the different oscillatory terms will cause $[\rho_A(n,n')]_U$ to hover around the time average obtained by dropping all terms for which $f_{\kappa',\kappa}\neq 0$. Let us suppose that it requires a time t' for the phases of the different terms to become thoroughly mixed up. Then the probability that $[\rho_A(n,n')]_U$, or $\rho_A(n,n')$, lies in a given range at an arbitrarily chosen time $t>t'$ is not to be distinguished from the long time average of this probability. Let us denote the time average of the $\mathbf{U}$-average by $[\ ]_{U,t}$. Thus we write

$$[\rho_A]_{U,t}=\lim_{\tau\rightarrow\infty}\left\{\frac{1}{\tau}\int_0^\tau[\rho_A]_U dt\right\}.$$

We propose to show that

$$\left[\{\rho_A(n,n')-[\rho_A(n,n')]_{U,t}\}^2\right]_{U,t}$$

is so small that the probability of any appreciable discrepancy between $\rho_A(n,n')$ and $[\rho_A(n,n')]_{U,t}$ is negligible, provided that we choose $t>t'$. Thus we can identify $[\rho_A]_{U,t}$ with the matrix σ

of the ultimate state of thermal equilibrium.* We reserve for the present the discussion of the time t' required for the approximate attainment of thermal equilibrium.

Neglecting accidental degeneracy we identify the condition $f_{\kappa'\kappa}\neq 0$ with $\kappa'\neq\kappa$. The time average of Eq. (52) is then

$$[\rho_A(n,n')]_{U,t}=(1-\delta_{n,n'})\rho_A{}^0(n,n')\sum_m\rho_B{}^0(m,m)\times\sum_\kappa[|U(nm,\kappa)|^2|U(n'm,\kappa)|^2]_U+\delta_{n,n'}\sum_{\nu,\mu}\rho_A{}^0(\nu,\nu)\rho_B{}^0(\mu,\mu)\times\sum_{m,\kappa}[|U(nm,\kappa)|^2|U(\nu\mu,\kappa)|^2]_U. \quad (53)$$

The maximum value of $[|U(nm,\kappa)|^2]_U$, i.e., of $G[\zeta(nm,\kappa),W_\kappa]$, must be of the order of magnitude of the reciprocal of the number of levels in the energy range defined by the breadth of the peak of the curve $G(\zeta,W_\kappa)$. This order of magnitude is $[u(W_\kappa-\bar{\epsilon})P^{\frac{1}{2}}\Delta W]^{-1}$. By hypothesis $P^{\frac{1}{2}}\Delta W$ is very large compared with the average spacing of the energy levels $u(W_\kappa-\bar{\epsilon})^{-1}$. Hence the maximum and all other values of $[|U(nm,\kappa)|^2]_U$ must be very small compared with unity. In fact we can make them as small as we please by increasing the heat capacity of the thermostat, for this increases the energy level density u without affecting our estimate of the uncertainty of the perturbing energy H'.

Since $|U(nm,\kappa)|^2$ is essentially positive, the probability of any value much greater than the average must be extremely small. Hence we can say that any value of $|U(nm,\kappa)|^2$ which is not extremely small compared with unity must be extremely improbable. It follows that to assign a specific value to $|U(\nu\mu,\kappa')|^2$ which is not excessively improbable will not appreciably affect the probability that the square of the absolute value of some other element $U(nm,\kappa)$ lies in a given and not very improbable range. For if we fix the value of $U(\nu\mu,\kappa')$ or $|U(\nu\mu,\kappa')|^2$ the problem of choosing the remaining elements of the matrix $\mathbf{U}$ is defined by a set of equations similar to (38), (40)–(44) and very insensitive to the choice of $U(\nu\mu,\kappa')$ so long as $|U(\nu\mu,\kappa')|$ is small. Eq. (40), for example, goes over into

$$(\textstyle\sum_n\sum_m)'|U(nm,\kappa)|^2=1-\delta_{\kappa,\kappa'}|U(\nu\mu,\kappa')|^2\leqq 1,$$

where $(\sum_n\sum_m)'$ denotes a sum over all sets of values of n and m with the omission of ν,μ when $\kappa=\kappa'$. We conclude that to an approximation that can be made as good as we please by increasing the heat capacity of B, the group-integration probabilities of various values for the different matrix elements are *independent*. Hence we can replace $[|U(nm,\kappa)|^2|U(n'm,\kappa)|^2]_U$ by

$$[|U(nm,\kappa)|^2]_U[|U(n'm,\kappa)|^2]_U \leqq G[\zeta(nm,\kappa),W_\kappa]G[\zeta(n'm,\kappa),W_\kappa] \quad \text{if } n\neq n'.$$

The off-diagonal elements of $[\rho_A]_{U,t}$ are now given to a close approximation by

$$[\rho_A(n,n')]_{U,t}=\rho_A{}^0(n,n')\sum_m\rho_B{}^0(m,m)\times\sum_\kappa G[\zeta(nm,\kappa),W_\kappa]G[\zeta(n'm,\kappa),W_\kappa]. \quad n\neq n' \quad (54)$$

But $G[\zeta(n'm,\kappa),W_\kappa]$ can be made smaller than an arbitrarily small positive quantity α by giving B a sufficiently large heat capacity. Hence (54) yields the inequality

$$|[\rho_A(n,n')]_{U,t}|<|\rho_A{}^0(n,n')|\alpha\times\sum_m\rho_B{}^0(m,m)\sum_\kappa G[\zeta(nm,\kappa),W_\kappa]=\alpha|\rho_A{}^0(n,n')|. \quad n\neq n'.$$

This means that the off-diagonal elements of $[\rho_A]_{U,t}$ *are negligible.*

Equation (53) gives the following expression for the typical *diagonal* element of $[\rho_A]_{U,t}$:

$$[\rho_A(n,n)]_{U,t}=\sum_\nu\sum_\mu\rho_A{}^0(\nu,\nu)\rho_B{}^0(\mu,\mu)\times\sum_m L(E_{nm},E_{\nu\mu}). \quad (55)$$

Here $L(E_{nm},E_{\nu\mu})$ denotes

$$\sum_\kappa[|U(nm,\kappa)|^2|U(\nu\mu,\kappa)|^2]_U,$$

or its equivalent,

$$\sum_\kappa G[\zeta(nm,\kappa),W_\kappa]G[\zeta(\nu\mu,\kappa),W_\kappa].$$

Since $G[\zeta(nm,\kappa),W_\kappa]$ approaches zero rapidly as $|\zeta(nm,\kappa)|$ becomes larger than $P^{\frac{1}{2}}\Delta W$, every term in the sum $L(E_{nm},E_{\nu\mu})$ must be vanishingly small unless for *some* values of κ the quantities $\zeta(nm,\kappa)=E_{nm}+\bar{\epsilon}-W_\kappa$ and $\zeta(\nu\mu,\kappa)=E_{\nu\mu}+\bar{\epsilon}-W_\kappa$ are *simultaneously* small. This condition is satisfied only when $E_{nm}-E_{\nu\mu}=E_m+E_n-E_{\nu\mu}$ is small. Thus, if

$$L(E_{nm},E_{\nu\mu})=M(E_m+E_n-E_{\nu\mu},E_{\nu\mu}),$$

* Cf. Eq. (2) of (I).

the function $M(z, E_{\nu\mu})$ so defined, with $z=E_m+E_n-E_{\nu\mu}$, will be negligibly small outside a range of values of z of the order of magnitude of $P^{\frac{1}{2}}\Delta W$.

Using the same device as in Eqs. (49), (50), (51) we replace the sum

$$\sum_m L(E_{nm}, E_{\nu\mu})=\sum_m M(E_m+E_n-E_{\nu\mu}, E_{\nu\mu})$$

by an integral. In making this substitution we can identify the energy level density of the system B with the energy level density of the united system, since the heat capacity of A is supposed to be negligible compared with that of B. Thus

$$\sum_m L(E_{nm}, E_{\nu\mu})=\int_{-\infty}^{+\infty} u(E)M(E+E_n-E_{\nu\mu}, E_{\nu\mu})dE$$
$$=\int_{-\infty}^{+\infty} u(z-E_n+E_{\nu\mu})M(z, E_{\nu\mu})dz. \quad (56)$$

Before applying this expression it is necessary to introduce a suitable assumption regarding the character of the density function $u(E)$. It *suffices* for our purpose to postulate that $u(E)$ increases as an exceedingly high power of the energy, at least in the neighborhood of $E=\bar{W}$. This familiar assumption is readily verified for the case that B is an ideal monatomic gas. It is equivalent to the more directly useful postulate that near $\bar{W}$ $u(E)=u(\bar{W})\exp[\lambda(E-\bar{W})/\bar{W}]$, where λ is a large positive number.

To justify the above assumption more fully and gain insight into the range of energies for which it should hold we resort to a physical interpretation of $u(E)$ based on a well-known entropy definition used in the classical statistical mechanics of macroscopic systems. According to this definition the entropy of a macroscopic system with energy E is identical up to an arbitrary additive constant with $k\ln\Phi(E)$, where $\Phi(E)$ is the extension-in-phase inside the ergodic surface $H(p, q)=E$ in the Gibbs phase-space. Jordan[26] has given a proof that this definition can be carried over into the quantum-statistical mechanics of macroscopic systems if we replace $\Phi(E)$ by the number of energy levels J of energy less than, or equal to, E. We can identify $J(E)$ with

$$\int_0^E u(y)dy.$$

Let $S_c(E)$ denote the entropy as thus defined and let T be the thermodynamic temperature corresponding to the energy E. Since $dS_c/dE=T^{-1}$ and $J=Ae^{S_c/k}$, where A is a constant,

$$u(E)=dJ/dE=(J/k)dS_c/dE=J/kT$$
$$=A\{\exp[S_c(E)/k]\}/kT. \quad (57)$$

Let $\xi\equiv E-\bar{W}$. Expanding $S_c(E)$ in powers of ξ and denoting the temperature corresponding to $\bar{W}$ by τ, we obtain

$$S_c(E)=S_c(\bar{W})+\xi/\tau+(\xi^2/2)\left[\frac{d}{dE}\left(\frac{1}{T}\right)\right]_{E=\bar{W}}$$
$$+\cdots=S_c(\bar{W})+\xi/\tau-\xi^2/(2C\tau^2)+\cdots.$$

Here C is the heat capacity of the system at $E=\bar{W}$. It follows that we can approximate $S_c(E)$ closely by the first two terms of the above series provided that $|\xi|\ll 2C\tau$. Since $2C\tau$ is of the order of magnitude of the energy $\bar{W}$, the above condition will be easily satisfied over an energy range of the order of magnitude of the energy uncertainty ΔW in the case of the system $A+B$ we have under consideration. This range is much wider than that required for effective convergence of the integral (56). Hence we can replace $u(E)$ in (56) by

$$u(E)=(A/k\tau)\exp[S_c(\bar{W})/k+\xi/k\tau]$$
$$=u(\bar{W})e^{\xi/k\tau}. \quad (58)$$

In combining (58) with (56) we note that $\xi=E-\bar{W}=z-E_n+E_{\nu\mu}-\bar{W}$. Then

$$\sum_m L(E_{nm}, E_{\nu\mu})=u(\bar{W})\exp[-(E_n+\bar{W}-E_{\nu\mu})/k\tau]$$
$$\times\int_{-\infty}^{+\infty} e^{z/k\tau}M(z, E_{\nu\mu})dz.$$

It is to be observed that E_n enters *only* through the factor $e^{-E_n/k\tau}$.

Equation (55) now yields

$$[\rho_A(n, n)]_{U,t}=\exp[(\psi_A-E_n)/k\tau], \quad (59)$$

[26] P. Jordan, *Stat. Mech. auf Quantentheor. Grundlage* (Braunschweig, 1933), Chap. 2, §3.

where Ψ_A is a function of $\bar{W}$, or τ, defined by

$$e^{\Psi_A/k\tau}=\sum_\nu\sum_\mu \rho_A{}^0(\nu,\nu)\rho_B{}^0(\mu,\mu)u(\bar{W})$$
$$\times\exp\left[(E_{\nu\mu}-\bar{W})/k\tau\right]\int_{-\infty}^{+\infty} e^{z/k\tau}M(z,E_{\nu\mu})dz. \quad (60)$$

It is not actually necessary to use (60) to fix Ψ_A since this can be done by means of the normalization condition

$$\sum_m[\rho_A(n,n)]_{U,t}$$
$$=\exp\left[\psi_A/k\tau\right]\sum_n \exp\left[-E_n/k\tau\right]=1. \quad (61)$$

$[\varrho_A]_{U,t}$ is thus shown to be a diagonal matrix of the type which characterizes a canonical ensemble with modulus $\Theta=k\tau$. Our derivation is independent of the initial states of the systems A and B provided that the conditions (a_1) to (a_4) are satisfied. The reader will easily convince himself that it goes through equally well if the initial states of A and B are not independent. This concludes the first part of our proof that the operation β can be considered to create a canonical ensemble.

It remains to examine the anomalies in the matrix ϱ_A, i.e., the quantities

$$\Delta(n,n')\equiv[|\rho_A(n,n')-[\rho_A(n,n')]_{U,t}|^2]_{U,t}$$
$$=[|\rho_A(n,n')|^2]_{U,t}-|[\rho_A(n,n')]_{U,t}|^2. \quad (62)$$

These fluctuations can be considered negligible if the elements of Δ satisfy the inequality

$$\Delta(n,n')\ll|[\rho_A(n,n)]_{U,t}|^2. \quad (63)$$

If they *are* negligible, it means as we have previously remarked, that the chance that the operation β will produce a state which departs appreciably from the canonical one is negligible.

Consider the general expression for $|\rho_A(n,n')|^2$. This is the formidable sum

$$|\rho_A(n,n')|^2=\sum\rho_A{}^0(\nu,\tilde{\nu})\rho_B{}^0(\mu,\tilde{\mu})\rho_A{}^0(\tilde{\nu}',\nu')$$
$$\times\rho_B{}^0(\tilde{\mu}',\mu')U(nm,\kappa)U^{-1}(\kappa,\nu\mu)U(\tilde{\nu}\tilde{\mu},\tilde{\kappa})$$
$$\times U^{-1}(\tilde{\kappa},n'm)U^{-1}(\kappa',nm')U(\nu'\mu',\kappa')$$
$$\times U^{-1}(\tilde{\kappa}',\tilde{\nu}'\tilde{\mu}')U(n'm',\tilde{\kappa}')$$
$$\times\exp\left[i(f_{\tilde{\kappa}\kappa}-f_{\tilde{\kappa}'\kappa'})t\right]. \quad (64)$$

The sum is to be extended over the fourteen indices m, m', κ, $\tilde{\kappa}$, κ', $\tilde{\kappa}'$, ν, $\tilde{\nu}$, μ, $\tilde{\mu}$, ν', $\tilde{\nu}'$, μ', $\tilde{\mu}'$.

Formation of the time average eliminates all terms except those for which

$$f_{\tilde{\kappa}\kappa}-f_{\tilde{\kappa}'\kappa'}=(W_{\tilde{\kappa}}-W_\kappa-W_{\tilde{\kappa}'}+W_{\kappa'})/\hbar. \quad (65)$$

Assuming incommensurability of energy values to be the rule, this condition implies that either

$$\tilde{\kappa}=\kappa,\quad \tilde{\kappa}'=\kappa'; \quad (65a)$$

or

$$\tilde{\kappa}=\tilde{\kappa}',\quad \kappa=\kappa'. \quad (65b)$$

Writing $U(nm,\kappa)$ in the form $\exp[i\varphi_{nm}]A(nm,\kappa)$ as before, we see that the group average of the product of the eight elements of $\mathbf{U}$ and $\mathbf{U}^{-1}$ will vanish unless

$$\varphi_{nm}-\varphi_{\nu\mu}+\varphi_{\tilde{\nu}\tilde{\mu}}-\varphi_{n'm}-\varphi_{nm'}+\varphi_{\nu'\mu'}$$
$$-\varphi_{\nu'\tilde{\mu}'}+\varphi_{n'm'}\equiv 0. \quad (66)$$

This implies that the indices of the positive and negative terms are equal in pairs. There are twenty-four ways of pairing these terms and in all forty-eight ways of satisfying the conditions (65) and (66). Each way gives rise to a separate set of terms contributing to the time and group average of $|\rho_A(n,n')|^2$.

Let us first deal with the typical diagonal element $[|\rho_A(n,n)|^2]_{U,t}$. In this case (66) is reduced to

$$-\varphi_{\nu\mu}+\varphi_{\tilde{\nu}\tilde{\mu}}+\varphi_{\nu'\mu'}-\varphi_{\tilde{\nu}'\tilde{\mu}'}\equiv 0. \quad (67)$$

There are just two ways of satisfying this requirement, *viz.*,

$$\nu,\mu=\tilde{\nu},\tilde{\mu},\quad \nu',\mu'=\tilde{\nu}',\tilde{\mu}'; \quad (67a)$$

and

$$\nu,\mu=\nu',\mu',\quad \tilde{\nu},\tilde{\mu}=\tilde{\nu}',\tilde{\mu}'. \quad (67b)$$

To make the group average of the product

$$U(nm,\kappa)U^{-1}(\kappa,\nu\mu)U(\tilde{\nu}\tilde{\mu},\tilde{\kappa})U^{-1}(\tilde{\kappa},nm)$$
$$\times U^{-1}(\kappa',nm')U(\nu'\mu',\kappa')U^{-1}(\tilde{\kappa}',\tilde{\nu}'\tilde{\mu}')U(nm',\tilde{\kappa}')$$

as large as possible this product should be reduced to four pairs of conjugate complex quantities. The desired reduction is obtained if, and only if, we unite the conditions (65a) and (67a). Let $S_1(n,n)$ denote the sum of the contributions to $[|\rho_A(n,n)|^2]_{U,t}$ from terms in which this method of pairing indices is used.

$$S_1(n,n)=\sum\rho_A{}^0(\nu,\nu)\rho_B{}^0(\mu,\mu)\rho_A{}^0(\nu',\nu')$$
$$\times\rho_B{}^0(\mu',\mu')[|U(nm,\kappa)|^2|U(\nu\mu,\kappa)|^2$$
$$\times|U(nm',\kappa')|^2|U(\nu'\mu',\kappa')|^2]_U, \quad (68)$$

where the sum is extended over all indices except n. This expression differs from $|[\rho_A(n,n)]_{U,t}|^2$ only in the substitution of

$$[|U(nm,\kappa)|^2|U(\nu\mu,\kappa)|^2|U(nm',\kappa')|^2 \times|U(\nu'\mu',\kappa')|^2]_U$$

for

$$[|U(nm,\kappa)|^2|U(\nu\mu,\kappa)|^2]_U \times[|U(nm',\kappa')|^2|U(\nu'\mu',\kappa')|^2]_U.$$

Due to the approximate independence of the probability systems of different matrix elements these two expressions can be considered equivalent. Consequently in the special case of Eq. (62) where $n'=n$ the largest of the four sets of terms in

$$[|\rho_A(n,n)|^2]_{U,t} \text{ is canceled by } |[\rho_A(n,n)]_{U,t}|^2.$$

The set of terms in $[|\rho_A(n,n)|^2]_{U,t}$ obtained by combining (65a) and (67b) is

$$\begin{aligned}S_2(n,n)=\sum&|\rho_A{}^0(\nu,\nu')|^2|\rho_B{}^0(\mu,\mu')|^2\\ &\times[|U(nm,\kappa)|^2|U(nm',\kappa')|^2\\ &\times U^{-1}(\kappa,\nu\mu)U(\nu'\mu',\kappa)\\ &\times U(\nu\mu,\kappa')U^{-1}(\nu'\mu',\kappa')]_U. \quad (69)\end{aligned}$$

We wish to prove that $S_2(n,n)$ is very small compared with $S_1(n,n)$. To this end we first derive the lemma

$$\rho(a,a)\rho(b,b)\leqslant|\rho(a,b)|^2. \quad (70)$$

Using the notation of Eq. (1) of (I) with the abbreviation $c_{as}=(\psi_s,\varphi_a)$,

$$\begin{aligned}\rho(a,a)\rho(b,b)&=\sum_{s,s'}w_sw_{s'}|c_{as}|^2|c_{bs'}|^2\\ &=\sum_s w_s{}^2|c_{as}|^2|c_{bs}|^2+\sum_{s'>s}w_sw_{s'}\\ &\quad\times[|c_{as}|^2|c_{bs'}|^2+|c_{bs}|^2|c_{as'}|^2];\\ |\rho(a,b)|^2&=\sum_{s,s'}w_sw_{s'}c_{as}(c_{bs})^*(c_{as'})^*c_{bs'}\\ &=\sum_s w_s{}^2|c_{as}|^2|c_{bs}|^2\\ &\quad+\sum_{s'>s}w_sw_{s'}[c_{as}(c_{bs})^*(c_{as'})^*c_{bs'}\\ &\quad+(c_{as})^*c_{bs}c_{as'}(c_{bs'})^*].\end{aligned}$$

Since $|c_{as}c_{bs'}-c_{as'}c_{bs}|^2\geqq0$,

$$|c_{as}|^2|c_{bs'}|^2+|c_{bs}|^2|c_{as'}|^2\geqq c_{as}c_{bs'}(c_{bs})^*(c_{as'})^*+c_{bs}c_{as'}(c_{as})^*(c_{bs'})^*.$$

The inequality (70) is now immediate and

$$\begin{aligned}S_1(n,n)\geqslant\sum&|\rho_A{}^0(\nu,\nu')|^2|\rho_B{}^0(\mu,\mu')|^2\\ &\times[|U(nm,\kappa)|^2|U(nm',\kappa')|^2|U(\nu\mu,\kappa)|^2\\ &\times|U(\nu'\mu',\kappa')|^2]_U. \quad (71)\end{aligned}$$

Both of the sums in (69) and (71) extend over all indices except n. Comparing the right-hand members of (69) and (71) we note that, since the average phase angle of $U^{-1}(\kappa,\nu\mu)U(\nu'\mu',\kappa)\times U(\nu\mu,\kappa')U^{-1}(\nu'\mu',\kappa')$ is almost zero, the former must be very much smaller than the latter. Thus $S_2(n,n)$ is negligible in comparison with $S_1(n,n)$ and $|[\rho_A(n,n)]_{U,t}|^2$. A similar argument carries through for the other two sets of terms so that the condition (63) is fulfilled insofar as concerns the diagonal elements of Δ.

Finally we turn to the off-diagonal terms. To get a maximum contribution we fulfill the conditions (65) and (66) so as to make all terms real and positive and at the same time retain a maximum number of terms. To this end we avoid pairing fixed phase angles in (66) with variable phase angles. We can do no better than combine (65a) and (67a) with the condition $m=m'$. The resulting set of terms is identical with the right-hand member of (68) except for the insertion of a factor $\delta_{m,m'}$ in each which eliminates the summation over m'. It follows that this maximum set of terms is vanishingly small compared with $S_1(n,n)$ and $|[\rho_A(n,n)]_{U,t}|^2$. Therefore the condition (63) must be satisfied with respect to off-diagonal as well as diagonal terms. This completes our justification of the physical operation β as a proper one for generating a canonical ensemble of systems A.

The reader will note in conclusion that the thermodynamic temperature of the ensemble of systems A as defined at the end of (I) is identical with the measured thermodynamic temperature τ of the thermostat ensemble.

The Time Distribution of So-Called Random Events

ARTHUR RUARK
University of North Carolina, Chapel Hill, North Carolina
(Received October 9, 1939)

It is shown that in a sequence of random events, the expected distribution of interval-sizes in a run of given duration differs from the Bateman distribution when the counting rate is different from the average one. The formula for "local" size-distribution to be expected for such a run is derived by the use of Bayes' theorem. It is pointed out that this theorem is useful in discussing the properties of any statistical system which is known to be in a condition differing from the idealized equilibrium state.

1. Description of a Fluctuation Problem of Very General Type

IN analyzing the results of some counting experiments the writer encountered a statistical problem which appears to have an interest far transcending its immediate applications. It is in fact an instance of the following general problem:

A physical system governed by statistical laws is described by a number of variables a, b, $\cdots$, etc., both independent and dependent. If the system were in equilibrium they would take the values $\bar{A}$, $\bar{B}$, etc. In actuality the system fluctuates around the equilibrium state. In a particular experiment we find that a takes the deviant value A; or more accurately, we determine the probability αdA that a lies in the range A to $A+dA$. We inquire, what can be inferred as to the probabilities βdB, γdC, etc., that the variables b, c, etc. lay in ranges dB, dC, etc. at the time of the experiment?

Questions of this kind arising in the statistical mechanics of gases might be attacked by solving the Boltzmann differential equation for the velocity-distribution function, subject to the restriction $a=A$, but we want to point out that when the functions β, γ, etc. do not yield to direct attack, another method is available, namely, the use of Bayes' theorem of *a posteriori* probabilities. For example, if there are just two variables a and b to consider, this theorem states:

(Unconditional chance that a lies in dA)
$\times$(Chance that b lies in dB when we know that a lies in dA)
=(Unconditional chance that b lies in dB)
$\times$(Chance that a lies in dA when we know that b lies in dB).

The importance of such problems lies in the fact that their solution gives us a closer understanding of the conditions existing in the fluctuant states which are always encountered in nature. We proceed to the problem in radioactive fluctuations which led to these remarks. It will be solved by Bayes' theorem, for attempts to proceed otherwise yielded no valuable results.

2. A Problem in the Distribution of Random Events

A distribution of events is said to be random in time if the chance that one of them occurs in time dt is a constant, fdt. Bateman's formula gives the chance W_n that n events will occur in time t, namely,

$$W_n=(ft)^n e^{-ft}/n! \tag{1}$$

Then the chance that an interval between two events will exceed t is

$$W_0=e^{-ft}. \tag{2}$$

In deriving (1), all values of n up to "infinity" are supposed to be possible, and the understanding is that the formula shall be applied to a hypothetical situation,—that in which similar counting experiments, each of duration t, have been accumulated in "unlimited numbers." Similarly, (2) is a mathematical idealization referring to a single run of "unlimited duration." Here we shall discuss the physical situation encountered in studying long runs of events, whose distribution may be expected to conform roughly to the predictions of Eq. (2). Suppose we arrange an apparatus which does two things. It records the number of particles, n, given out by a constant radioactive source in a long time D, let us

say 5000 seconds. Also, as each particle arrives, the instrument decides automatically whether the interval which has elapsed since the arrival of the preceding particle is greater than or less than a chosen value T (let us say one second). If the interval is greater than T, it is counted on a recording dial, so that at the end of the run we also know P, the number of intervals between events which exceed the value T. At this stage the best estimate we can make as to the average counting rate f is n/D,[1] but let us continue to record the total number of events, until f is known with very high accuracy. We shall assume for the present that f is exactly known, discussing later the consequences of the fact that f is really subject to statistical error. Now the problem we want to solve is this:

The average counting rate is f and a certain run has yielded n counts in time D. n is *not* equal to the expected value fD. What is the distribution function $G(t)$ replacing (2) during the interval D?[2]

3. The Solution

Figure 1 represents a chronograph sheet showing the events which arrived in the run of duration D. $G(T)$ is the chance that an interval between adjacent events, picked at random from the run, will be longer than T (and less than D, of course), when it is known that exactly n events arrived during the run. Bayes' theorem then says:

(Unconditional chance there are n events in the run) $\times G(T) =$ (Unconditional chance an interval picked at random from the run will be longer than T and less than D) $\times$ (Chance that n events occur in the run, when it is known that an interval picked at random from the run is longer than T and less than D).

The words "picked at random" are defined to mean that in the selection each interval has an equal chance of being picked. For example, they might be assigned labels, and the labels could be thrown into an urn, after which one label would be drawn. In evaluating the unconditional chance in the right-hand member we must remember that all the intervals considered are less than D; for this subclass of intervals it is easy to show[3] that the probability of a length between T and D is $(e^{-fT}-e^{-fD})/(1-e^{-fD})$. Calling the last factor in Bayes' theorem φ, we have

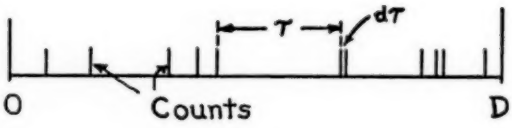

FIG. 1.

$$G(T)=\frac{e^{-fT}-e^{-fD}}{1-e^{-fD}}\cdot\frac{\varphi}{(fD)^n e^{-fD}/n!}. \qquad (3)$$

In getting φ, we must remember the exact conditions: an interval I has already been picked out at random and has turned out to have a length between T and D, as shown in Fig. 1. An interval satisfying these conditions belongs to a subclass different from the subclass considered above, and the chance that its length lies in a range $d\tau$ is

$$e^{-f\tau}fd\tau/(e^{-fT}-e^{-fD}). \qquad (4)$$

A slight approximation will now be made. When fD is large we can afford to neglect the cases in which I is the first or the last interval in the run. These end intervals are each bounded by a single count, for the chance is zero that a count occurs exactly at time zero or at time D. Leaving these two intervals out of consideration, the very fact that we have picked an interior interval assures us that the run contains at least two counts, namely, the ones which initiate and terminate I. We are interested, then, in the chance that the two stretches outside I, which have a total length of $D-\tau$, shall contain just $(n-2)$ counts in all. This chance is just the same as though the intervals were contiguous, namely

$$[f(D-\tau)]^{n-2}e^{-f(D-\tau)}/(n-2)! \qquad (5)$$

Taking the product of (4) and (5), and integrat-

[1] Strictly speaking, it is $(n+1)/D$, as Meixner has shown. See reference 5.

[2] The law replacing Eq. (1) can be worked out from that replacing Eq. (2). See Ruark and Devol, Phys. Rev. **49**, 355 (1936); especially p. 356.

At first sight it seems that the problem we have set up differs from the general ones discussed above. The only difference is that we are seeking the integrated distribution $G(t)$ while $(dG/dt)dt$ is the chance that an interval lies between t and $t+dt$; this corresponds to βdB in the discussion above.

[3] A. Ruark and L. Devol, Phys. Rev. **49**, 355 (1936); see Section A-1.

ing over τ, we get

$$\varphi \cong \frac{[f(D-T)]^{n-1}}{(e^{f(D-T)}-1)(n-1)!}; \quad n=2, 3, \cdots; \tag{6}$$

$$G \cong \frac{1}{1-e^{-fD}} \cdot \frac{n}{fD} \cdot \left(1-\frac{T}{D}\right)^{n-1}; \quad n=2, 3, \cdots. \tag{7}$$

Here the approximation sign is used because of the simplification introduced above.[4] Neglecting the first fraction we rewrite (7) in the form

$$G \cong \frac{n}{fD}\left(1-\frac{T}{D}\right)^{n-fD-1} \cdot \left(1-\frac{fT}{fD}\right)^{fD}. \tag{7'}$$

Here the last factor approximates e^{-fT} very closely, so the first two factors show the effect of a known fluctuation in counting rate on the probability than an interval has a length greater than T. The first factor increases with n but the second decreases, and the rapidity of its fall depends on T. Either factor may predominate, depending on the value of T. It is easy to explain this physically. Suppose we have a set of counts, fD in number, which obey Eq. (2) very closely. We insert an extra count at random. By choosing fT large enough, we can make it certain that the total duration of the intervals shorter than T is large compared to the total duration of those longer than T. In such a case, there is a large probability that the extra count will fall into an interval shorter than T, splitting it into two still shorter ones and thereby decreasing the fraction of the intervals which are longer than T. The opposite conclusion is reached when fT is chosen very small. Detailed analysis shows that when fT is unity we are at the border between the two cases and G is insensitive to changes of n.

We next consider the influence of the fact that f itself is not accurately known. Suppose f has been determined by taking ν counts over a time t which is much longer than D. Meixner[5] showed that the chance f lies in df is

$$((ft)^{\nu}/\nu!)e^{-ft}tdf. \tag{8}$$

With this weight-factor the average of (7') over all values of f[6] is found to be

$$\bar{G} = \frac{t}{\nu}\frac{n}{D}\left(1-\frac{T}{D}\right)^{n-1}. \tag{9}$$

The expected number of intervals, $\bar{P}$, having length greater than T is therefore $n\bar{G}$. One wishes also to know the standard deviation of the numbers P_1, P_2, etc. encountered in a series of runs. A direct attempt to evaluate this standard deviation leads to a result so complicated that it is useless, but when $(n-fD)$ is a small fraction of fD we can get a useful approximation.[7] Dropping the restriction that the counts must occur in a time D, we ask for the probability that in a run of n counts, P of the intervals are longer than T.

This is merely

$$W(n, P) = C_p{}^n e^{-fTP}(1-e^{-fT})^{n-P}. \tag{10}$$

On this simple basis, considering a large group of runs, the fractional standard deviation of P is $[(1-e^{-fT})/ne^{-fT}]^{\frac{1}{2}}$, and in applications this may be replaced by $\{[1-(P/n)]/P\}^{\frac{1}{2}}$.

To summarize: if we deal with a limited portion of a random distribution and find that the local counting rate is higher or lower than the average, the length-distribution law of the intervals differs from Eq. (2), and the expected local form of this distribution is given by Eq. (7), which is fundamental in the sense that it determines the expected local values of all properties of the sequence of events.

[4] Therefore Eq. (7) really gives the chance that an *interior interval* is greater than T when there are n counts in the run. The accurate formula for G can be obtained, but the situation is complex, so we prefer to work with (7).

[5] J. Meixner, Ann. d. Physik **30**, 665 (1937).

[6] Equation (7) can be averaged over f with the aid of a formula on p. 243 of Whittaker and Watson, *Modern Analysis*, fourth edition. The result is a series which converges uniformly for all physically possible values of its variable, and in fact very rapidly when ν is large.

[7] This has already been used in the doctoral dissertation of Dr. Mary W. Hodge, not yet published.

LETTERS TO THE EDITOR

Prompt publication of brief reports of important discoveries in physics may be secured by addressing them to this department. Closing dates for this department are, for the first issue of the month, the eighteenth of the preceding month, for the second issue, the third of the month. Because of the late closing dates for the section no proof can be shown to authors. The Board of Editors does not hold itself responsible for the opinions expressed by the correspondents.

Communications should not in general exceed 600 words in length.

Mass and Stability of C^{14}

The question of the radioactivity of C^{14} has not finally been settled. McMillan[1] observed a long period activity from targets in Berkeley which he suggested might be due to a common contaminant, probably carbon. Bonner and Brubaker[2] from cloud-chamber observations of the slow neutron reaction $N^{14}+n \rightarrow C^{14}+H^1$ concluded that the mass of C^{14} is 14.00767 which renders it unstable by 0.17 Mev. It should be possible to check this value by the reaction $C^{13}+D^2 \rightarrow C^{14}+H^1$ and also the reaction $B^{11}+He^4 \rightarrow C^{14}+H^1$. The former of these was studied by bombarding carbon targets with 3-Mev deuterons from a cyclotron and observing the range of the protons evolved. The protons from C^{13} should have a greater range than those from C^{12} and hence be easily distinguished. With an Aquadag target (supposedly pure Acheson graphite) a group of range 82.0 cm is found superposed on a longer range group which was traced to occluded nitrogen. A spectroscopically pure target gave no longer range group but a single group ending at 81.1 cm ($\pm$2.0 cm). The yield is small but definite and was found in each of eight separate runs which are consistent with one another. This group is ascribed to the reaction $C^{13}+D^2 \rightarrow C^{14}+H^1$ and yields an energy change value of +8.21 Mev. The mass of C^{14} deduced is 14.00775 $\pm$0.00025. The number of protons was compared with that from $C^{12}+D^2 \rightarrow C^{13}+H^1$ and found to correspond to a cross section one-half as great.

Some unpublished experiments made two years ago in which a boron target was bombarded by both polonium and ThC′ alpha-particles gave groups at 42.1 and 97.6 cm in the forward direction which can be ascribed to the $B^{11}+He^4 \rightarrow C^{14}+H^1$ reaction. The energy change values are +0.62 and +0.70 Mev, respectively. If the mean value of 0.66 ($\pm$0.30) Mev is taken the value 14.00797 ($\pm$0.00035) is deduced for C^{14} which agrees reasonably with the previous value. It is likely that the ranges found with natural sources would be shorter than the true ranges so that the slightly higher value found here is reasonable. The suggested value for C^{14}, combining the two sets of data, is 14.00780$\pm$0.00020. This means that C^{14} should be unstable, emitting an electron with an energy of 300,000 ev. A thin-walled counter was used to look for activity from the targets but no such easily absorbable beta-rays could be found in numbers sufficiently great to warrant claiming their detection. It is likely that C^{14} has a half-life of several years in which case a total of twelve hours bombardment with 0.5 microampere of deuterons would not produce a detectable activity.

I wish to thank Mr. W. L. Davidson, Jr., for assistance in running the cyclotron and much invaluable activity.

ERNEST POLLARD

Sloane Physics Laboratory,
Yale University,
New Haven, Connecticut,
November 14, 1939.

[1] Edwin McMillan, Phys. Rev. **49**, 875 (1936).
[2] T. W. Bonner and W. M. Brubaker, Phys. Rev. **49**, 778 (1936).

The Radioactivity of Mn^{56}

We have attempted to measure the γ-rays from Mn^{56} by counting the electrons ejected from a thin lamina in the Wilson cloud chamber. These electrons fit an energy group having an extrapolated end-point between 1.50 and 1.75 mc^2, indicating a γ-ray line of 600–700 kev. There is, however, marked straggling out to about 3.90 mc^2, which may indicate a γ-ray line at about 1.7 Mev. These findings agree with those of Dunworth,[1] except that the interpretation of the flat distribution between 1.75 and 3.90 mc^2 is not clear. It is possible that there are other lines between the two mentioned.

That such might be the case is suggested by the results obtained by other workers. If one examines the curves published by Seaborg and Livingood[2] and by Langer, Mitchell and McDaniel,[3] it is seen the γ-ray background is high compared to the measured β-ray intensity. There are three possible explanations of this: (a) the number of quanta per disintegration is large, (b) there are very many electrons (presumably of low energy) that are not being detected by the counting system, or (c) some combination of the above two possibilities.

Our measurements of the β-ray spectrum indicate that (c) is the most likely.

R. H. BACON
E. N. GRISEWOOD
C. W. VAN DER MERWE

Department of Physics,
New York University,
Washington Square College,
New York, New York,
November 17, 1939.

[1] J. V. Dunworth, Nature **143**, 1065 (1939).
[2] G. T. Seaborg and J. J. Livingood, Phys. Rev. **54**, 397 (1938).
[3] Langer, Mitchell and McDaniel, Phys. Rev. **56**, 422 (1939).

Radioactive Isotopes of Indium from Alpha-Bombardment of Silver

Further investigation[1] of the radioactivity produced in silver when it is bombarded with 16-Mev alpha-particles shows that the activity consists primarily of two periods having half-lives of 20 minutes and 65 minutes. These two periods decay by positron emission and have been chemically identified as indium. The possible radioactive indium isotopes are In^{110} and In^{112}. Cadmium isotopes which might be produced are stable.

The 20-minute period is undoubtedly the same as that first reported by Lawson and Cork[2] who used Cd+d and assigned it to In^{111}. A definite assignment of this period was difficult at the time because of several possible indium isotopes and the lack of experimental data. Barnes[3] produced the same activity by Cd+p but had no reason for changing its assignment. The fact that the 20-minute indium period is produced by Ag+α definitely assigns it to In^{112} formed by the reaction $Ag^{109}(\alpha, n)$ In^{112}.

The 72-second period has been observed from In+fast neutrons[2] and In+γ[4] and assigned to In^{112}. We have looked for such a period produced by Ag+α and could not find it. To check the possibility that this period might be due to In^{114} we have bombarded Cd with α-particles where In^{114} would be produced in the reaction Cd^{111} (α, p) In^{114}. The chemical separation required only two minutes, but no activity was observed. The 72-second period is not produced by slow neutrons[2] on indium which is further evidence that it cannot be due to In^{114}. There remains the possibility that this period is due to In^{111} produced by an $n-3n$ or $\gamma-2n$ reaction. In^{111} would be allowed by the proton and deuteron reactions in which the 72-second period has been observed.

The 65-minute indium period has also been observed by Barnes[3] in Cd+p and assigned tentatively to In^{110}. Our alpha-particle data from the reaction Ag^{107} (α, n) In^{110} verifies his assignment. The absence of the 65-minute period with the reaction Cd+d also indicates that In^{110} produces this period.

Two other weaker activities were observed in the reaction Ag+α; one of about 9 hours and another weaker one of 2–3 days. A 9.4-hour period is characteristic of gallium produced by Cu^{63} (α, n) Ga^{66}. The intensity observed was consistent with the copper impurity in the fine silver (99.95 percent). In the chemical procedure some gallium was added to the solution and the gallium and indium precipitated as hydroxides. This precipitate was dissolved in 6n HCl and the gallium separated from the indium by extraction with ether. The gallium fraction showed half-lives of 60 minutes and 9.4 hours characteristic of Cu+α and the indium precipitate had activities of 65 minutes and a 9.4-hour period greatly reduced in intensity indicating that the separation by the ether extraction was not complete. By comparing the relative intensities from pure copper and that of our silver, it was evident that one could detect less than 1 part in 10,000 of copper in silver.

A long bombardment of Ag by α-particles gives an additional weak period of 2–3 days half-life. This has not been chemically identified and since the intensity of this period is less than that of any of the other activities observed, it also may be due to an impurity. However, it may be identical with the 2.7-day indium period found by Barnes[3] and Cork[5] and assigned by the former to an isomeric state of In^{112}.

L. D. P. King
W. J. Henderson

Purdue University,
Lafayette, Indiana,
November 10, 1939.

[1] King, Henderson and Risser, Phys. Rev. **55**, 1118 (1939).
[2] J. L. Lawson and J. M. Cork, Phys. Rev. **52**, 531 (1937).
[3] S. W. Barnes, Phys. Rev. **56**, 414 (1939).
[4] W. Bothe and W. Gentner, Zeits. f. Physik **106**, 236 (1937).
[5] J. M. Cork and J. L. Lawson, Phys. Rev. **56**, 291 (1939).

Air Mass Effect on Cosmic-Ray Intensity

Blackett[1] has suggested that the "temperature effect" of the cosmic rays is due to the vertical shift of the layer in which the mesotrons are formed and has further suggested that it may be possible to correlate cosmic-ray data with the structure of depressions. Data obtained with a Carnegie, Model C cosmic-ray meter loaned to us by A. H. Compton indicate a noticeable change in intensity at the fronts separating different air masses.

The data were obtained while the meter was on board the *M. S. Northland* traveling between Seattle and Juneau, Alaska, in the process of investigating the latitude effect. The location of the fronts was obtained from the Seattle airport office of the U. S. Weather Bureau. Of the twelve fronts investigated, three were cold fronts, one was warm, and eight were occlusions. The cold fronts gave changes of from 2.9 percent to 5 percent; the warm front gave a change of 2 percent, while the occlusions gave changes of from 1.7 percent to 2.5 percent. The changes took place over a space of from one to three hours. Two further cases of fluctuation were noticed, one accompanying an influx of warm moist air aloft, the other representing a zone of transition which contained no definite front.

The explanation of such an effect follows at once from Blackett's suggestion. If z is the height of mesotron formation and L the mean range, then the fractional change in intensity is given by:

$$dI = -\frac{dz}{L}.$$

In a private communication from A. H. Compton, we learn that recent experiments of Rossi and of Schein show that $L \sim 9$ km whereas z is not less than 20 km. Using the value of $L = 9$ km and the observed values for dI, we find that dz is from 200 m to 400 m.

If we connect the formation of the mesotrons with a layer of given density, then the vertical shift of this layer at the passage of a front will be given by:

$$dz = \frac{RT}{Mg} \ln\left(\frac{PT_0}{P_0T}\right),$$

where T_0 is the absolute temperature of the layer before passage of the front and T the temperature after, P_0 and P are the corresponding pressures, M the molecular weight of air, R the gas constant, and g the acceleration of gravity. Unfortunately there were no data available at heights as great as 20 km. However, data by J. Bjerknes[2] and J.

Bjerknes and Palmen[3] for a height of 14 to 16 km indicate that at a warm front $T_0/T=1.05$ and $P/P_0=1.01$ giving

$$dz=400 \text{ m},$$

whereas at a cold front $T_0/T=0.866$, while $P/P_0=0.970$, giving

$$dz=-1 \text{ km}.$$

One would expect the disturbance to be smaller at higher altitudes giving dz of the order of magnitude required by the observations.

DONALD H. LOUGHRIDGE
PAUL GAST

University of Washington,
Seattle, Washington,
November 10, 1939.

[1] P. M. S. Blackett, Phys. Rev. **54**, 973 (1938).
[2] J. Bjerknes, Geofys. Pub. **9**, No. 9 (1933).
[3] J. Bjerknes and E. Palmen, Geofys. Pub. **12**, No. 2 (1937).

Rotational and Alternating Hysteresis Losses in Electrical Sheet Steel

A method of measuring alternating hysteresis loss involving the use of small disks has been recently developed by Brailsford,[1] who used it to determine the variation of this loss with magnetization for four electrical sheet steels. Previously, he had measured[2] the rotational hysteresis loss of the same samples so that he was able to draw a curve showing the ratio of the two losses as a function of the magnetization. This curve has been reproduced in Fig. 1.

The writer has used this method of measuring rotational hysteresis loss in investigating the behavior of several transformer sheet steels. The rotational loss curves of these materials were similar to the ones shown in the references, but differed in some details. The alternating losses were also measured, but not by the disk method; instead, the hysteresis loops were measured for the same steels with Epstein strips (25 cm by 3 cm), half of them cut along the rolling direction and the other half at right angles to it. Since there is little preferred orientation of the grains in hot rolled sheets, from which the samples were obtained, there is not much variation of the loss characteristics with direction. Hence, the loss found by combining equal numbers of strips cut along the two directions can be considered to be the correct average loss for the material and to be strictly comparable with the average alternating loss as found by Brailsford, who measured these loss curves in several directions and then used their mean.

The relationship between rotational and alternating hysteresis losses was found by the writer to be not nearly so simple as that indicated by Brailsford's work. The ratio between the two losses is plotted in Fig. 1 for three different steels. Samples A and B contained from 2.5 to 3.0 percent of silicon while C contained from 3.5 to 4.0 percent. After hot rolling, B and C were pickled and given an alkaline surface treatment. The material was about 13 mils thick and was tested in the annealed condition. Although the general trend is the same in the two cases, the three curves for the most part lie definitely below the range in which all of Brailsford's points fall (as indicated by the broken lines). The reason for this discrepancy seems to be that

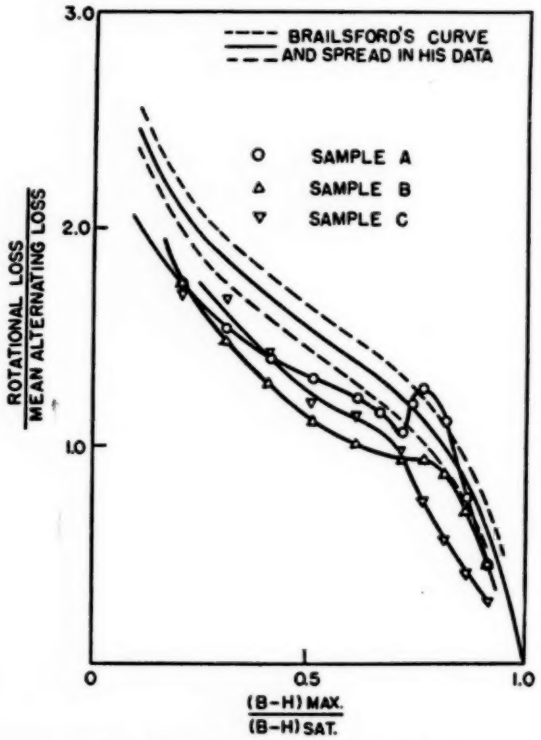

FIG. 1. Ratio of rotational to mean alternating loss as a function of magnetization.

two entirely different methods were used to measure the alternating hysteresis loss. Since the disk method of determining alternating loss has not been checked against a standard method, which must be done before the former can be accepted as reliable, the discrepancy can probably be attributed to errors associated with the measurements upon the disks. This is somewhat more likely than that the difference between the two sets of results should be due to differences in the behavior of the two groups of materials, which are of the same general nature, although coming from different sources. However, this possibility cannot be excluded.

Another interesting feature of the curves A, B and C is that they are not nearly so smooth as the ones that can be drawn through the points shown in Brailsford's paper, and they also differ considerably among themselves. This is all due to the differences in the details of the rotational loss curves themselves. Whether the discrepancy between the two sets of results is real or not, these curves indicate that the scatter of the experimental points is greater than that previously found. This means that one type of loss cannot be calculated from the other type on the basis of a smoothed ratio curve with anything like the accuracy that would appear to be possible from a consideration of Brailsford's average curve.

L. P. TARASOV

Research Laboratory,
General Electric Company,
Schenectady, New York,
October 11, 1939.

[1] F. Brailsford, J.I.E.E. **84**, 399 (1939).
[2] F. Brailsford, J.I.E.E. **83**, 566 (1938).

Multiple Scattering of Fast Electrons: A Correction

In a letter to the editor of *The Physical Review*[1] which we published recently concerning the multiple scattering of electrons in carbon and lead, an error was made in giving the weight of the carbon scatterer used. The correct value is 0.57 g/cm², instead of the value of 0.75 g/cm² which was given previously. In Table I are given the

TABLE I. *Experimental and theoretical average values of* $H\rho\theta$.

	EXP. $\langle H\rho\theta\rangle_{Av}$ GAUSS CM DEG.	THEOR. $\langle H\rho\theta\rangle_{Av}$ GAUSS CM DEG.
C, 0.57 g/cm²	1.60×10^5	1.87×10^5
Pb, 0.072 g/cm²	1.56×10^5	2.38×10^5

numerical values of the average $H\rho\theta$ (measured in projection), which may be of convenience, and which were not given explicitly in our previous letter. The averages given include all the tracks observed; no attempt was made in this case to distinguish between the Gaussian part of the distribution and the single or plural scattering tail. The theoretical values given are those calculated by means of the formula of E. J. Williams.[2] The formula which he designates as (37) in his text is the particular one which we have used. According to our understanding this formula takes into account the contribution due to the single scattering tail, and is therefore the appropriate one to use in comparison with our experimental values.

N. L. OLESON
K. T. CHAO
J. HALPERN
H. R. CRANE

University of Michigan,
Ann Arbor, Michigan,
November 10, 1939.

[1] N. L. Oleson, K. T. Chao, J. Halpern and H. R. Crane, Phys. Rev. **56**, 482 (1939).
[2] E. J. Williams, Proc. Roy. Soc. **A169**, 531 (1939).

A Report on the Development of the Electron Supermicroscope at Toronto

In a previous paper,[1] the construction of a magnetic electron microscope of high resolving power was described and some of the preliminary photographs were reproduced. From these a resolving limit of 200A was inferred. During the past year, the apparatus has undergone considerable refinement in an attempt to increase the facility of operation and to obtain an estimate of the practical limit of the resolving power for various types of specimens.

A vacuum camera has been constructed which enables the plate to be introduced into the recording chamber through an "air-lock" without breaking the vacuum in the whole system. The time required to change plates has been reduced from 35 minutes to 5 minutes by this arrangement. This camera effects a further saving of time in that it enables the operator to record a number of images on a single large plate. The number of photographs per plate may be varied from 3 to 34 (3 in.×2 in. to ¼ in.×2 in.) according to the requirements of the type of work in progress.

The technique of preparing specimen-holders and mounting specimens has been refined to ensure that any preparation less than 3000A in thickness will be unaffected by the electron bombardment. The time required for the preparation is approximately the same as the time required to carry out the corresponding technique in light microscopy. During the past month the authors have prepared more than 300 specimens of a variety of types, and have taken over 500 electron microphotographs of approximately 60 specimens selected from those prepared. The results of this work will be published in the near future in the periodicals devoted to the particular types of problems involved.

The magnetic lens, which was described in the paper referred to above, has been fitted with a new type of pole-piece assembly which ensures a more precise axial symmetry in the magnetic field produced. The images which have been obtained with this new lens show considerable improvement over those obtained with the previous type.

As a result of a thorough investigation into the method of alignment, it has been established that the proper control of the illuminating system is the most important factor in the production of images of high quality. An illuminating pencil of large angular aperture with correspondingly high intensity and small depth of focus has been found most suitable for visual observation of the images, while an illuminating pencil of small angular aperture and correspondingly low intensity, but large depth of focus, has been found most suitable for the successful photographic recording of the images.

The resolving limit of the instrument is now estimated to be better than 60A. This limit appears to be imposed,

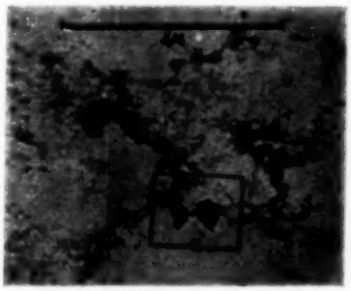

FIG. 1. Electron microphotograph of colloidal gold. Electron-optical magnification 12,700. Total magnification 45,000.

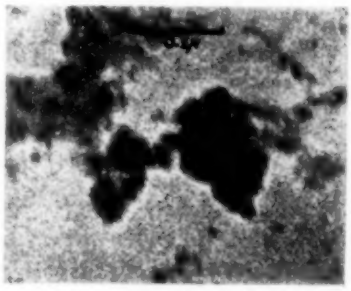

FIG. 2. Portion of Fig. 1. Total magnification 180,000.

to a great extent, by the nature of the specimens rather than by instrumental factors. Fig. 1 is an electron microphotograph of a test object consisting of colloidal gold deposited on a collodion membrane 200Å in thickness. The electron-optical magnification was 12,700. In order to make visible to the eye all the details present on the negative and in order to overcome difficulties of reproduction, the photograph has been enlarged, by optical means, to a total magnification of 45,000. The indicated part of this photograph has been enlarged to a total magnification of 180,000 and is shown in Fig. 2. The separations of the smaller particles and the sharpness of the edges of the larger particles allows a resolving power of better than 60Å to be inferred.

E. F. Burton
J. Hillier
A. Prebus

Department of Physics,
University of Toronto,
Toronto, Canada,
November 13, 1939.

[1] A. Prebus and J. Hillier, Can. J. Research **A17**, 49–63 (1939).

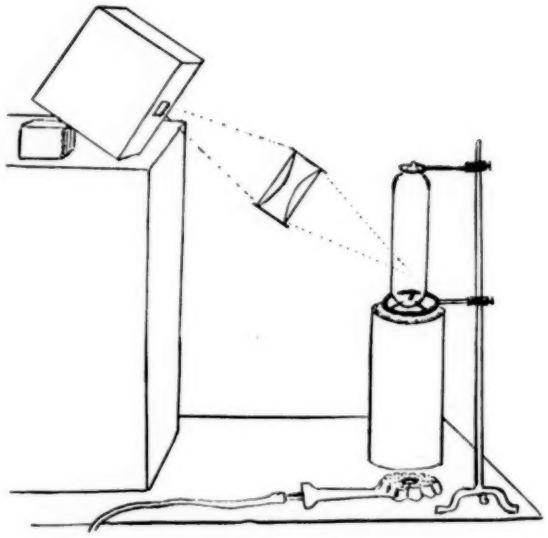

FIG. 1. Arrangement of apparatus to show resonance radiation of sodium.

Lecture Demonstration of Resonance Radiation of Sodium

The phenomenon of resonance radiation is of such fundamental importance in connection with the theory of atomic spectra that some method of demonstrating it to a large audience is much to be desired. The earlier methods which I have employed—small glass bulbs containing the vapor of sodium, illuminated by a sodium flame, are not well suited for the lecture table, as the images of the flame seen reflected from the spherical surface of the bulb are so bright that one sees the fainter cone of resonance radiation with difficulty, except from certain rather restricted directions.

The recent development of the sodium arc as a commercial lamp, and the invention of a glass capable of resisting the action of sodium vapor at a high temperature, have made it possible to demonstrate the resonance radiation of the vapor to a large audience. Small sodium arc lamps are coming into use for spectroscopic purposes in most laboratories, and the large cylindrical bulbs which are employed for the street lamps make ideal resonance bulbs. With the cylindrical container and a properly directed light beam, none of the rays reflected from the glass reach the audience, and the resonance phenomena can be seen from all directions.

Through the courtesy of Mr. L. J. Buttolph, of the General Electric Vapor Lamp Company, I was furnished with a highly exhausted cylindrical bulb of sodium resisting glass, charged with a suitable amount of metallic sodium. This bulb measures 6×24 cm and is mounted vertically above a chimney made of thick asbestos paper, heated from below by a ring gas burner of the type employed in gas stoves. The chimney is about 13 cm in diameter and 30 cm in length. The glass cylinder should be supported from below by an iron ring furnished with three thin metal rods as shown in Fig. 1. This arrangement is made to give a minimum obstruction to the upward flow of hot air along the side of the bulb. The sodium "lab-arc," as furnished by the Vapor Lamp Company is housed, together with the transformer, in a small metal box, with a sliding panel on one side perforated by a wide slit. This can be removed and a panel of asbestos paper perforated by a 2-cm square hole put in its place. The lamp is mounted in an inclined position as shown in Fig. 1. Its rays shoot down from the square window at an angle of about 30° and fall on a large short focus condensing lens which focuses the rays on the cylinder as shown. It is obvious that the reflected rays are thrown down upon the table by this arrangement instead of going off at all angles as is the case with a spherical bulb.

The gas burner is now lighted, the numerous small flames being turned down low at the start. When first trying the experiment it is well to check the temperature of the hot air stream flowing over the bulb with a thermometer. It is best not to let it rise above 350° C which is about the maximum temperature that can be measured with a mercury thermometer. If sodium condenses on the walls in the region where the resonance phenomena are to appear, the deposit can be wiped out by brushing the wall of the tube with the flame of a Bunsen burner. When the temperature reaches 130° the path of the rays through the vapor is marked by a faint yellow luminosity which increases rapidly in brightness as the temperature rises. The region outside of the luminous cone of light will now be observed to glow with a fainter yellow light. This is the secondary resonance radiation, excited by the primary radiation from the illuminated cone of vapor. At the same time the luminous cone retreats towards the front wall of the tube, the vapor becoming so dense at 300° that the radiations capable of exciting resonance are all absorbed and re-emitted laterally within a short distance from the point of entry. An image of the rectangular aperture is now seen on the wall of the tube where the radiations from the lamp enter and at 350° this image is as sharply

defined as if formed on a sheet of paper. Moreover it is nearly as bright as if formed on a white surface if the sodium lamp is operated at a lower temperature so as to give narrow lines. If it is desired to show this, it can be readily done by allowing the lamp to cool, and then starting it again with the resonance tube at 300. One-half of the square image of the lamp's window is then covered with a strip of white paper, or better with a piece of mica which has been "smoked" with the white oxide formed by burning a short piece of magnesium wire or ribbon.[1] The square patch of luminosity is of course invisible if viewed through the tube from behind, owing to the inability of its radiation to penetrate the vapor. The close equality of intensity of the images on the vapor and on white paper shows, however, that very little true absorption of light occurs, and that most of the energy is re-emitted. It is important to employ a bulb of clear glass. The lightly frosted bulbs used in most of the lamps are unsuitable, but Mr. Buttolph has agreed to supply bulbs similar to mine, highly exhausted and charged with sodium ready for use, through the W. M. Welch Company, 1515 Sedgwick Street, Chicago, Illinois.

R. W. Wood

Johns Hopkins University,
Baltimore, Maryland,
November 13, 1939.

[1] See *Physical Optics*, 3rd edition, p. 595.

THE AMERICAN INSTITUTE OF PHYSICS

INCORPORATED

ADMINISTRATIVE STAFF

HENRY A. BARTON, *Director*

MADELINE M. MITCHELL, *Publications Manager*

Office: 175 Fifth Avenue, New York, New York

JOURNALS

THE PHYSICAL REVIEW

REVIEWS OF MODERN PHYSICS

JOHN T. TATE, *Editor*

J. W. BUCHTA, *Assistant Editor*

JOURNAL OF APPLIED PHYSICS

ELMER HUTCHISSON, *Editor*

THE JOURNAL OF THE OPTICAL SOCIETY OF AMERICA

THE REVIEW OF SCIENTIFIC INSTRUMENTS

F. K. RICHTMYER, *Editor*

JOURNAL OF THE ACOUSTICAL SOCIETY OF AMERICA

FLOYD A. FIRESTONE, *Editor*

THE JOURNAL OF CHEMICAL PHYSICS

HAROLD C. UREY, *Editor*

JOSEPH E. MAYER, *Assistant Editor*

THE AMERICAN PHYSICS TEACHER

DUANE ROLLER, *Editor*

GOVERNING BOARD

For The American Physical Society:

JOHN T. TATE, *Chairman*
University of Minnesota

GEORGE B. PEGRAM, *Secretary*
Columbia University

KARL T. COMPTON
Massachusetts Institute of Technology

For The Optical Society of America:

E. C. CRITTENDEN
National Bureau of Standards

A. C. HARDY
Massachusetts Institute of Technology

W. B. RAYTON
Bausch & Lomb Optical Company

For The Acoustical Society of America:

FLOYD A. FIRESTONE
University of Michigan

HARVEY FLETCHER
Bell Telephone Laboratories

WALLACE WATERFALL
The Celotex Corporation

For The Society of Rheology:

WHEELER P. DAVEY
Pennsylvania State College

MELVIN MOONEY
United States Rubber Products, Inc.

R. L. PEEK, JR.
Bell Telephone Laboratories

For The American Association of Physics Teachers:

PAUL E. KLOPSTEG
Central Scientific Company

FREDERIC PALMER, JR.
Haverford College

F. K. RICHTMYER
Cornell University

The American Institute of Physics is a membership corporation of which five societies are the founding members. These five societies are the principal national societies devoted to pure and applied physics in America. Their names, and those of their representatives who form the Governing Board of the Institute, are given above. The principal work of the Institute is the publication of journals sponsored by the societies or by itself. The names and the editors of the journals are also listed above.

The broad purpose of the Institute is to represent, in all matters of wide or common interest, the five thousand or more members and subscribers associated with the Founder Societies and the journals. It aims to advance the science and profession of physics, and to promote cooperation between pure research, the applied sciences and the industries. To achieve these aims, it is greatly in need of an endowment and is empowered by law to administer grants and funds of any kind.

CONTENTS

PHYS. REV. 56 (1939) DECEMBER 1

Experimental Test of Sakowsky's Theory of Cosmic-Ray Fine Structure . . . . H. S. RIDNER 1069

World-Wide Variations on the Earth's Magnetic Field and the Intensity of Cosmic Radiation . . . . . O. GODART 1074

Scattering of Protons by Protons. III . N. P. HEYDENBURG, L. R. HAFSTAD AND M. A. TUVE 1078

Deuteron-Deuteron, Proton-Helium, and Deuteron-Helium Scattering . . . . . N. P. HEYDENBURG AND R. B. ROBERTS 1092

Nuclear Isomerism in Zinc . . . . . J. W. KENNEDY, G. T. SEABORG AND E. SEGRÈ 1095

Some Features of an Electrostatic Generator and Ion Source for High Voltage Research . . . . . I. A. GETTING, J. B. FISK AND H. VOOT 1098

Search for a Short Range Group of Protons in the D—D Reaction . . . . . F. E. MYERS, R. D. HUNTOON, C. G. SHULL AND C. M. CRENSHAW 1104

Binding Energy of H^3 . . . . . FREDERICK W. BROWN 1107

Spectra of Y V and Zr VI . . . . . F. W. PAUL AND W. A. RENNE 1110

Fundamental Rotation-Vibration Band of Nitric Oxide . R. H. GILLETTE AND EUGENIE H. EYSTER 1113

Isotope Shift in Magnesium . . . . . JOHN P. VINTI 1120

Dielectric Constant of Ammonia, Nitrogen, and Carbon Dioxide at Ultra-High Frequency . . . . . GERALD W. FOX AND ALDEN H. RYAN 1133

Paramagnetic Susceptibility of Copper-Nickel and Zinc-Nickel Alloys . . MARY A. WHEELER 1137

Quantum-Mechanical Basis of Statistical Mechanics . . . . . EDWIN C. KEMBLE 1146

Time Distribution of So-Called Random Events . . . . . ARTHUR RUARK 1165

Letters to the Editor:

Mass and Stability of C^4 . . . . . ERNEST POLLARD 1168

Radioactivity of Mn^{55} . . . . . R. H. BACON, E. N. GREENWOOD AND C. W. VAN DER MERWE 1168

Radioactive Isotopes of Indium from Alpha-Bombardment of Silver . . . . . L. D. P. KING AND W. J. HENDERSON 1169

Air Mass Effect on Cosmic-Ray Intensity . . . . . DONALD H. LOUGHRIDGE AND PAUL GAST 1169

Banded and Alternating Hysteresis Loops in Electrical Sheet Steel . . . . . L. P. TARASOV 1170

Multiple Scattering of Fast Electrons: A Correction . . . . . N. L. OLESON, K. T. CHAO, J. HALPERN AND H. R. CRANE 1171

Report on the Development of the Electron Supermicroscope at Toronto . . . . . E. F. BURTON, J. HILLIER AND A. PRESTON 1171

Lattice Demonstration of Resonance Radiation of Sodium . . . . . R. W. WOOD 1172

LANCASTER PRESS, INC., LANCASTER, PA.